

Development of Molecularly Imprinted Polymer-based sensing platforms for health and environmental applications

Citation for published version (APA):

Caldara, M. (2023). *Development of Molecularly Imprinted Polymer-based sensing platforms for health and environmental applications*. [Doctoral Thesis, Maastricht University]. Maastricht University. <https://doi.org/10.26481/dis.20231122mc>

Document status and date:

Published: 01/01/2023

DOI:

[10.26481/dis.20231122mc](https://doi.org/10.26481/dis.20231122mc)

Document Version:

Publisher's PDF, also known as Version of record

Please check the document version of this publication:

- A submitted manuscript is the version of the article upon submission and before peer-review. There can be important differences between the submitted version and the official published version of record. People interested in the research are advised to contact the author for the final version of the publication, or visit the DOI to the publisher's website.
- The final author version and the galley proof are versions of the publication after peer review.
- The final published version features the final layout of the paper including the volume, issue and page numbers.

[Link to publication](#)

General rights

Copyright and moral rights for the publications made accessible in the public portal are retained by the authors and/or other copyright owners and it is a condition of accessing publications that users recognise and abide by the legal requirements associated with these rights.

- Users may download and print one copy of any publication from the public portal for the purpose of private study or research.
- You may not further distribute the material or use it for any profit-making activity or commercial gain
- You may freely distribute the URL identifying the publication in the public portal.

If the publication is distributed under the terms of Article 25fa of the Dutch Copyright Act, indicated by the "Taverne" license above, please follow below link for the End User Agreement:

www.umlib.nl/taverne-license

Take down policy

If you believe that this document breaches copyright please contact us at:

repository@maastrichtuniversity.nl

providing details and we will investigate your claim.

**Development of Molecularly Imprinted
Polymer-based sensing platforms for health
and environmental applications**



Interreg



Co-funded by
the European Union

Meuse – Rhine (NL – BE – DE)

The research work presented in this thesis was conducted at the Sensor Engineering department, Faculty of Science and Engineering, Maastricht University.

The research work presented in this thesis was supported by the European Regional Development Fund through the Saber Print project, funded by the Interreg VA Deutschland-Nederland program, grant number 144277. Part of the work presented was also supported by the Interreg Euregion Meuse-Rhine, project “Food Screening EMR” (EMR159), funded by the European Regional Development Fund of the European Union.

ISBN:

Cover Design: Manlio Caldara

Layout: ProefschriftMaken

Printing: ProefschriftMaken

© 2023 by Manlio Caldara

All rights reserved

No part of this publication may be reproduced, stored in a retrieval system, or transmitted in any form or by any means, electronic, mechanical, photocopying, recording or otherwise, without the prior permission in writing from the author.

Development of Molecularly Imprinted Polymer-based sensing platforms for health and environmental applications

DISSERTATION

to obtain the degree of Doctor at Maastricht University,
on the authority of the Rector Magnificus,
Prof. dr. Pamela Habibović
in accordance with the decision of the Board of Deans,
to be defended in public
on Wednesday 22 November 2023 at 16:00 hours

by

Manlio Caldara

Supervisors:

Dr. Bart van Grinsven

Prof. dr. Thomas J. Cleij

Co-supervisor:

Dr. Kasper Eersels

Assessment Committee:

Prof. dr. Romano Orrù (Chair)

Dr. Matthew B. Baker

Prof. dr. Wim Deferme (Hasselt University)

Dr. Carmen López Iglesias

Prof. dr. Patrick Wagner (KU Leuven University)

Table of Contents

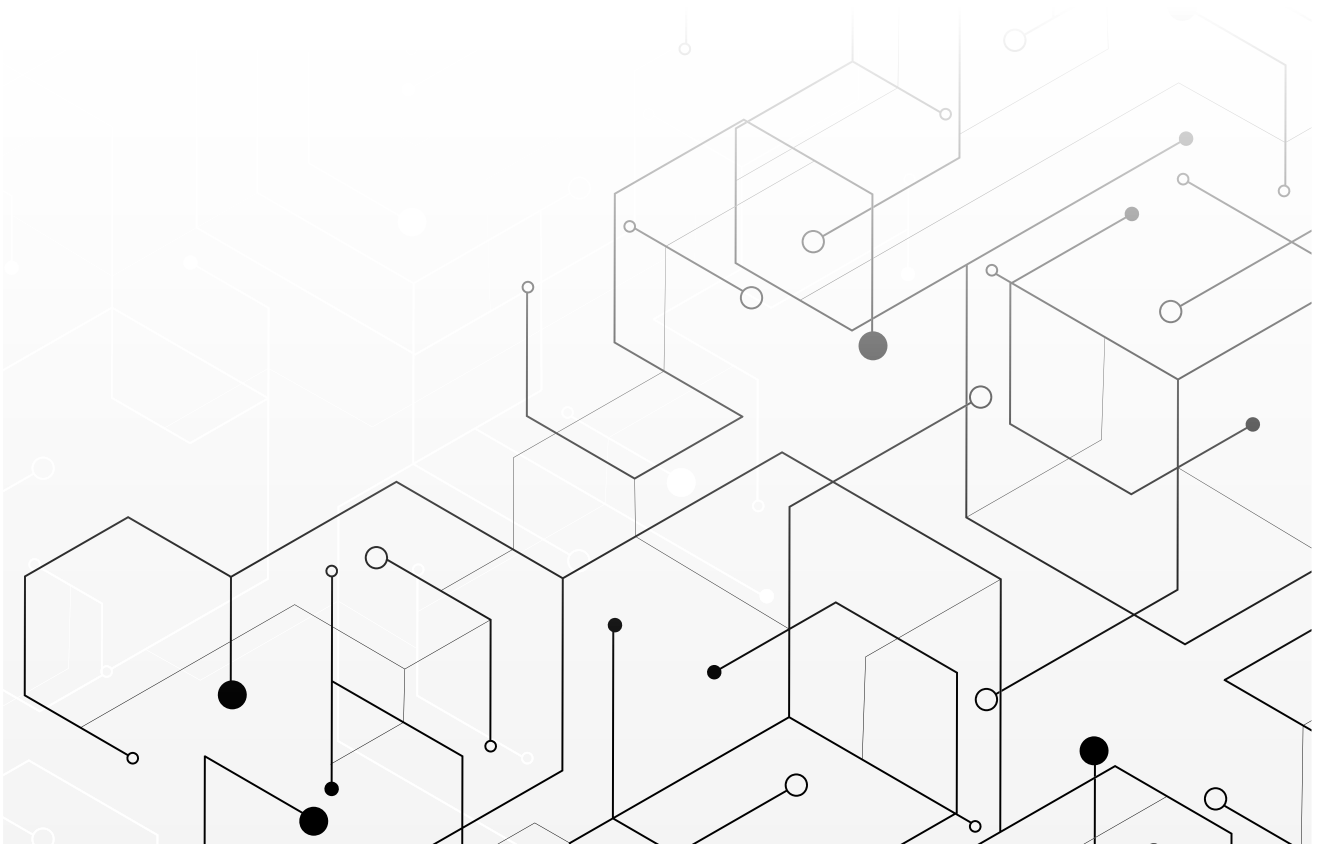
Chapter 1	9
Introduction	9
Introduction to Biosensors	10
Biological Sensing Elements	11
Molecularly Imprinted Polymers	15
Imprinted Polymer-based Sensing Platforms	18
Aims and Outlines	20
References Chapter 1	22
Preface to Chapter 2	32
Chapter 2	33
Recent Advances in Molecularly Imprinted Polymers for Glucose Monitoring: From Fundamental Research to Commercial Application	33
Introduction	35
Production Methods of MIPs for Glucose Detection	40
Readout Technologies Employed for MIP-Based Glucose Detection	49
Promising MIP-Based Technologies for Glucose Sensing	55
Conclusions	58
References Chapter 2	59
Preface to Chapter 3	72
Chapter 3	73
Thermal Detection of Glucose in Urine Using a Molecularly Imprinted Polymer as a Recognition Element	73
Introduction	75
Materials and Methods	79
Results and Discussion	82
Conclusions	95
References Chapter 3	96
Preface to Chapter 4	100
Chapter 4	101
A Molecularly Imprinted Polymer-Based Thermal Sensor for the Selective Detection of Melamine in Milk Samples	101
Introduction	103

Materials and Methods	105
Results and Discussion	108
Conclusions	116
References Chapter 4	117
Preface to Chapter 5.....	122
Chapter 5	123
Deposition Methods for the Integration of Molecularly Imprinted Polymers (MIPs) in Sensor Applications	123
Abstract	124
Introduction	125
Mechanical MIP deposition	128
Electrochemical MIP deposition	136
Chemical deposition	143
Vacuum deposition methods	146
Conclusion and future outlook	148
References Chapter 5	149
Preface to Chapter 6.....	168
Chapter 6	169
Dipstick sensor based on molecularly imprinted polymer-coated screen-printed electrodes for the single-shot detection of glucose in urine samples - From fundamental study towards point-of-care application	169
Abstract	170
Introduction	171
Materials and Methods	173
Results and Discussion	176
Conclusions	182
References Chapter 6	183
Chapter 7	189
Conclusion and Outlook.....	189
References Chapter 7	193
Summary	194
Summary (in Dutch).....	197
Impact.....	199

References Impact paragraph 202
Curriculum Vitae 203
List of Publications 204

Chapter 1

Introduction



Introduction to Biosensors

Biosensors are analytical devices that make use of a biological or biomimetic recognition element in conjunction with a transducer to detect and quantify a specific analyte (Figure 1.1).[1] Biosensing devices can detect a wide range of targets in a rapid, sensitive, and selective manner,[2] making them a critical tool in a large variety of fields such as clinical diagnostics,[3] environmental monitoring,[4] drug analysis[5] and food safety.[6]

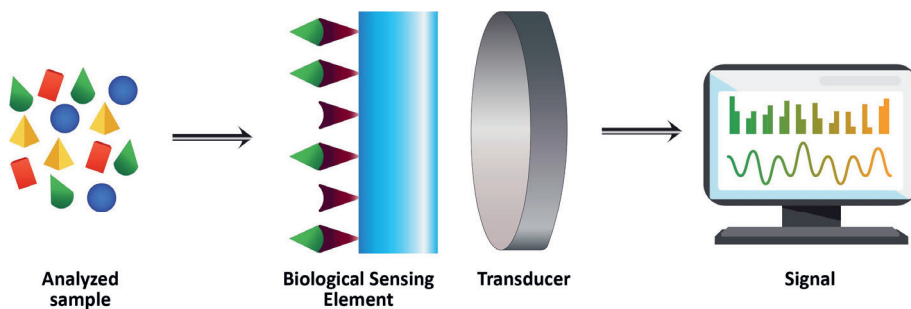


Figure 1.1 Graphical illustration of a biosensor's various elements as well as the recognition event that occurs in biosensor devices.

Biosensors can be engineered to detect a wide variety of analytes, including macromolecules such as proteins, bacteria, viruses and nucleic acids, as well as small molecules or even ions.[7] One of the key components of a biosensor is the recognition/receptor element, also known as biological sensor element; this element is able to recognise and thus bind to the target analyte, resulting in the generation of a signal that is then recorded and converted into a tangible signal from an appropriate transducer element. The recognition elements employed for the fabrication of bio sensing devices can be subdivided into two main categories: natural and synthetic receptors.[8,9] These receptor elements are able to interact with the target analyte and subsequently produce a tangible signal. The binding event is converted by the transducer into an electrical, optical, thermal or electrochemical signal, which is then amplified and analysed.[10]

Because of their ability to detect low concentrations of analytes with high specificity and sensitivity, the use of biosensors has grown rapidly in recent years and has allowed the monitoring and/or early diagnosis of critical infections and diseases (such as COVID-19 or diabetes).[11–13] As a result, biosensors for different applications, including point-of-care testing, environmental monitoring, food quality control, and industrial process monitoring are in continuous demand in order to fulfil fundamental public needs.[14] Novel biosensors are constantly evolving, with new technologies and methods being developed to improve their performance, lower their cost, and broaden their applicability in a variety of settings.[15]

Biological Sensing Elements

The core component of a biosensor device is represented by the receptor element, which is then connected to an appropriate transducer technology. These receptors can be either natural or synthetic,[8,16,17] with both having their advantages and disadvantages in respect to the other.

Natural receptors

The most often employed receptor elements are natural recognition elements. Examples include, enzymes, antibodies, and nucleic acids, which are used every day by millions of people for immediate monitoring of various diseases, conditions, and contaminations.[18–21] The most used enzymatic biosensor is certainly represented by the glucometer, a device that uses a combination of an enzyme, usually glucose oxidase (GOx), deposited onto an electrode surface and an amperometric transducer.[22] More specifically, the enzyme GOx is able to catalyse the oxidation of glucose, when this reaction takes place, it produces a tangible signal that can then be measured electrochemically by a transducer to allow the quantification of glucose in the analysed sample. Based on the indirect or direct nature of the signal and on the presence or less of mediators three different generations of glucometers have been developed and commercialized in the last few years (Figure 1.2).[23] Many other enzyme-based biosensors have been developed in recent decades and are widely used for various applications, such as food safety monitoring,[24] pollutant detection,[25] and monitoring of various industrial processes.[26,27] However, the most important enzymatic sensors certainly are the electrochemical enzymatic glucose sensors, due to the ever-increasing interest from the scientific communities in developing new and more user-friendly technologies for the detection of the sugar in physiological samples.

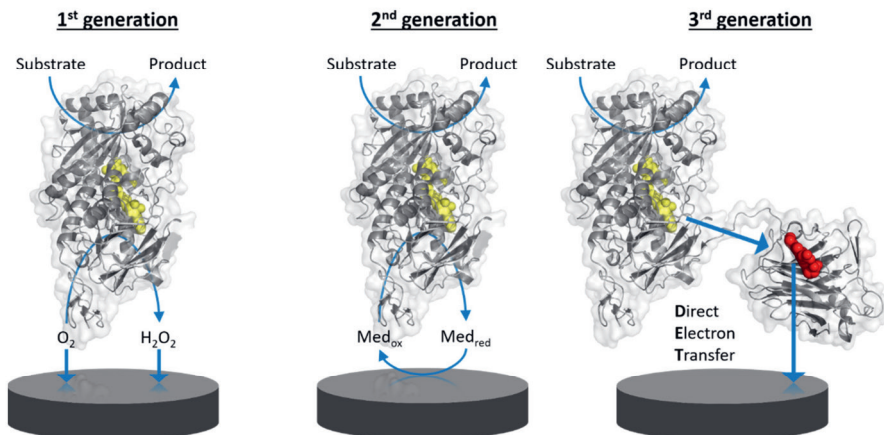


Figure 1.2 Graphical representation of the working principle of the three different generations of enzyme-based amperometric biosensors. Figure reproduced with permission from ref. [23] Copyright 2021, MDPI.

Another category of natural recognition elements that has seen an increasing interest worldwide in the past years is that of antibodies.[28,29] Antibody-based biosensors, also called immunosensors, exploit the well-known recognition mechanism between antigen and antibody, resulting in a high-affinity interaction which generates a measurable signal.[30] In the immediate aftermath of the COVID-19 crisis, rapid tests based on antibodies capable of targeting the viral antigens of the virus have proven to be crucial for the detection of these viral infections and thus provide a very valuable tool against the still pressing crisis caused by the pandemic of COVID-19 and its variants.[31]

Many other immunosensors targeting a broad range of targets are available on the market and are regularly used for various applications, such as: clinical diagnosis, environmental analysis, food analysis, etc. Immunosensors have been used for many years and are now considered validated and reliable means of analysis in these application fields. For example, an immunosensor for melamine detection in milk samples is employed in one of our works (**Chapter 4**) [32] to confirm the presence/absence of melamine in the milk sample tested. Overall, natural receptors are valuable sensing elements successfully employed in biosensors, they have allowed us to face challenging and problematic societal issues and they still represent an important component in most commercial devices for health and environmental monitoring.[16] However, they also suffer from limitations related to costs, production time, as well as stability in harsh environments due to their innate nature.[33]

Several studies on the stability of GOx, for example, have shown that this enzyme is highly unstable when exposed to high temperature or extreme pH,[34] thus limiting the shelf-life of the biosensor as a whole. Another significant drawback correlated to enzymes and thus enzymatic biosensors is represented by their incompatibility with sterilization procedures. In addition, drawbacks related to antibodies and therefore immunosensors are linked to ethical issues raised for production and testing of monoclonal antibodies by making use of animals.[35,36] Moreover, several immunosensor-based assays require the storing of these biosensors in controlled temperature and conditions,[37] thus limiting the accessibility of the product from the end-user.

Despite these limitations, natural receptors such as enzymes and antibodies are still extensively used in biosensors, especially in applications requiring high specificity and sensitivity. In recent years, the development of synthetic receptors, such as aptamers, metal organic frameworks (MOFs), and molecularly imprinted polymers (MIPs), resulted in alternatives that can overcome some of the above-mentioned limitations of their natural counterparts and permit for the sensing of an even broader range of target analytes.[38–40]

Synthetic receptors

Synthetic receptors, such as natural receptors, are designed and engineered to recognize and bind target analytes with high specificity and affinity. Instead of their natural counterparts, these receptors can be employed, as sensing elements in biosensor devices. Synthetic receptors provide several advantages over natural receptors, including lower cost, greater stability, and the possibility to be specifically tailored to recognize a broader range of target analytes, next to that their production does not require the use of living biological material.[41,42]

One class of synthetic receptors are aptamers, these are short, single-stranded DNA/RNA molecules or oligopeptides capable of binding to a variety of targets.[43,44] Aptamers are created through a process known as SELEX, which stands for systematic evolution of ligands via exponential enrichment; in this

process, an aptamer for a specific target is carefully selected from a library of oligo nucleotides.[45] These synthetic receptors have numerous advantages over enzymes and antibodies, including low cost and the ability to be engineered for multiple targets and thus applications thanks to the SELEX process.[46,47] In fact, different works have reported aptasensors for a large variety of small molecules (e.g. adenosine,[48,49] toxins[50]) but also larger entities, such as proteins, like thrombin,[51] and even bacteria.[52,53] One of the main drawbacks associated to aptamers is their susceptibility in certain environments, they can be degraded by nucleases and present a low thermal stability, which can affect their rebinding properties, especially in biological media.[54]

Another type of synthetic receptor that is gaining popularity in biosensing applications is metal-organic frameworks (MOFs).[55] MOFs are synthetic materials formed by metal ions or clusters that form a porous and crystalline network.[56] These networks allow for interaction with analytes, resulting in changes in optical, electrical, or mechanical properties of the MOF.[57] The detection of small molecules such as volatile organic compounds (VOCs) is one example of the use of MOFs as sensing elements in biosensors; more specifically, a fluorescent MOF-based sensor has been developed for the detection of ammonia gas.[58] MOFs have also been used in conjunction with GOx to detect glucose. The enzyme catalyses the formation of hydrogen peroxide, which reacts with a dye in the MOF material, resulting in an observable colour change.[59] Despite their numerous potential benefits, metal-organic frameworks (MOFs) have a few drawbacks that should be considered. In several cases, these synthetic receptors do not display good stability in aqueous solutions or at variable pH values,[60,61] limiting the spectrum of applications of MOFs-based biosensing devices. Furthermore, the metal ions utilized in their synthesis or the release of organic ligands during their degradation may make these materials potentially toxic.[62,63] This can represent an important limitation for different biomedical applications, such as the development of wearable or invasive MOF-based technology. Lastly, another important class of synthetic receptors that could overcome most of the above-mentioned issues related to natural and synthetic sensing elements are molecularly imprinted polymers or MIPs.

Using Molecularly Imprinted Polymers (MIPs) as recognition elements in sensing applications can offer several advantages. These materials provide excellent selectivity and specificity for a target analyte, allowing it to be detected even in complex sample matrices. MIPs are extremely stable and robust, making them ideal for a wide range of applications and hostile conditions. Furthermore, MIPs are inexpensive and easy to manufacture in large quantities, making them an appealing alternative for commercial sensor development. Their adaptability allows them to be tailored to individual analytes, increasing sensitivity and affinity.

However, despite the advantages, there are some challenges associated with MIP-based sensors. The synthesis of MIPs can be challenging and require optimization of polymerization conditions and template removal to achieve the desired rebinding capabilities. During synthesis, imprinting bias can occur, resulting in differences in recognition site distribution and affinity, which can affect the reproducibility of MIP-based sensors. Furthermore, MIPs compete with other thoroughly validated recognition elements, such as antibodies or enzymes. While MIPs have distinct advantages, the increasing availability of alternative recognition elements may have an impact on their adoption in the sensing sector.

As a result, extensive commercial implementation of MIP-based sensors will likely require standardization and validation methods to ensure consistent and trustworthy devices, which may prove

challenging in particular industries. Finally, the distinct advantages of using MIPs as recognition elements, such as selectivity, stability, cost-effectiveness, and customizability, make them an attractive option for sensing applications. Despite obstacles and potential competition, increasing prospects and continual developments in MIP-based sensor development hold significant potential for solving different sensing challenges across multiple industries. MIPs can be further established as valuable recognition elements in sensing through standardization attempts, promoting their widespread use in a variety of application fields.

Molecularly Imprinted Polymers

Molecularly imprinted polymers (MIPs) are a type of synthetic receptor created through a process known as molecular or polymer imprinting.[64] MIPs are typically formed by polymerizing one or more functional monomers around a template molecule, which is then removed from the polymeric network, leaving behind a cavity, which is complementary in shape, size, and chemical functionalities to the target molecule (**Figure 1.3**).[65,66] The resulting polymeric material can be used as a biomimetic sensing element to detect the target molecule both qualitatively and quantitatively.[67]

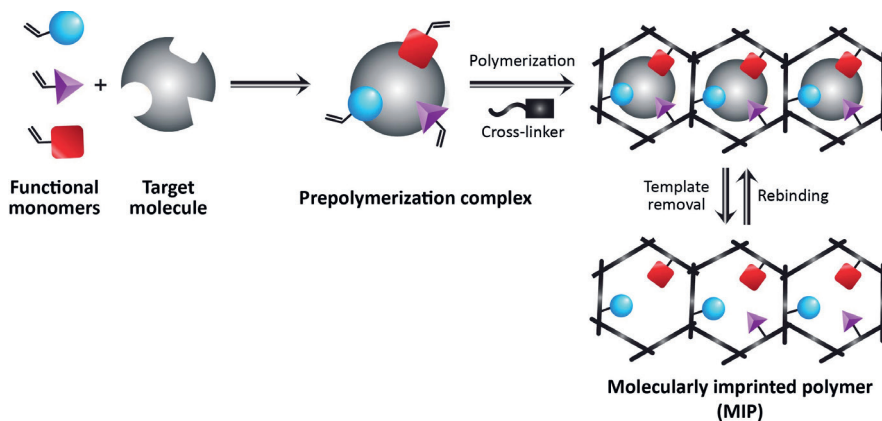


Figure 1.3 Graphical representation of synthesis, extraction and rebinding steps involved in the molecular imprinting process.

The reagents used for the polymerization reaction are (usually) functional monomer(s), a cross linker molecule and a polymerization initiator. To obtain the best rebinding capabilities, a careful selection of these reagents used for the MIPs production is needed.[68] The functional monomers provide the interaction with the template molecule via different non-covalent bonds, such as hydrophobic interactions, van der Waals forces and hydrogen bonding. For this reason, selecting an appropriate functional monomer is crucial to obtain a highly selective MIP for a determined target.[69] The most used functional monomers for the synthesis of these functional materials are methacrylic acid (MAA), acrylamide (AAM) and acrylic acid (AA) due to their capability of forming hydrogen bonds with the template molecule.[70] Other monomers frequently utilized for MIPs synthesis are styrene,[71] vinyl pyridine[72] and 2-hydroxyethyl methacrylate (HEMA).[73] These monomers are mostly used to obtain MIP particles via thermal or UV-initiated polymerization reactions. When the imprinted polymers is formed using an electropolymerization approach, different monomers are usually employed. Between these, pyrrole is the most popular, due to its favourable electrochemical properties that allow rapid formation of a polypyrrole film at relatively low potentials.[74] Other monomers employed for the production of electropolymerized MIPs (eMIPs) are aniline, thiophene, 3-aminophenol and their derivatives.[75] In **Figure 1.4** the chemical structures of the most commonly employed monomers can be seen.

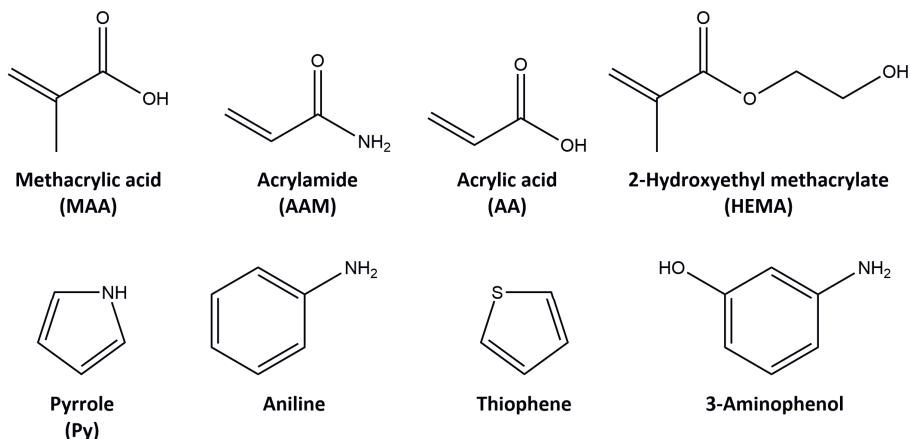


Figure 1.4 Chemical structures of commonly used monomers for MIPs production.

MIPs can be manufactured using a variety of polymerization techniques. Bulk polymerization is the most basic approach. In this process, the monomer(s), cross-linker and template are mixed together in a small amount of porogenic solvent. Polymerization is then triggered with UV light or thermally to generate a solid block of polymer, which will then undergo an extraction process to remove the template from the polymeric network.[76] Another fabrication method is surface imprinting. This approach employs a soft lithography process to fabricate imprinted polymer layers. In this method, a template immobilized on a solid surface is placed on another substrate containing the pre-polymer mixture. After polymerization, the two substrates are separated and the result is a thin functionalized imprinted film, also known as surface imprinted polymers or SIPs.[77,78] Many other techniques have been investigated in recent years and are still being studied by researchers worldwide to improve scalability while maintaining reliability during the polymer production. For example, techniques such as precipitation polymerization and emulsion polymerization, are commonly used to obtain more homogeneous MIP particles with a high surface area.[79,80] Other novel and promising approaches make use of the so-called solid-phase synthesis[81] or photopolymerization techniques, such as the reversible addition–fragmentation chain transfer (RAFT) living polymerization approach.[82]

A key advantage of MIPs as receptor elements is that they can be engineered to recognize a target molecule in complex matrices such as physiological fluids or various foods and liquids. In fact, unlike other types of recognition elements, these polymeric materials are known to be highly resistant and stable under a broad range of extreme and variable conditions.[83] Due to these advantageous characteristics, MIPs have found applications in a wide range of areas, including biosensors, chromatography, drug delivery, and environmental monitoring.[84] However, there are a few drawbacks associated with the manufacturing of MIPs and MIP-based devices that still need to be addressed to unlock the full potential of these sensing elements. One challenge is the possibility of non-specific binding from other molecules in the sample matrix, which could be limited by accurate tuning of reagents and their molar ratio.[85] Another essential step involved in the fabrication of these devices is the deposition method used to integrate these polymeric materials in different substrates.[86] As previously stated, in order to manufacture a biosensor device, the recognition element must be integrated onto an appropriate substrate, which is then in contact with a transducer capable of

converting the biological/chemical binding event into a tangible signal. In the case of MIPs, the integration process of these materials in various substrates is still in its early stages.[87] However, many researchers are developing fast and reproducible methods to fabricate devices with little batch-to-batch variation, bringing MIP-based platforms closer to commercialization than ever before.[87,88]

Imprinted Polymer-based Sensing Platforms

The field of molecular imprinting has made astonishing progress in the last few decades by widening up the range of possible target analytes and therefore increasing the fields of application for these receptor elements.[76] However, these materials do not possess output ability of their own and therefore need to be integrated in a substrate and coupled to an appropriate transducer element.[88] Obviously, the selected substrate will therefore condition the transducer chosen to convert the binding event. Imprinted polymeric materials can be subdivided in Molecularly Imprinted Polymers (MIPs) and Surface Imprinted Polymers (SIPs). While they both share the same concept of imprinting a molecule into a polymer matrix, they mainly differ in their imprinting strategy and their physical form. MIPs can be shaped in various forms depending on the polymerization technique employed, while SIPs are thin films that need to be synthesized directly onto a solid substrate (Figure 1.5).[77] The transducer technologies that are frequently associated with MIPs and SIPs can be divided into electrochemical, optical, mass-sensitive and thermal devices.[89]

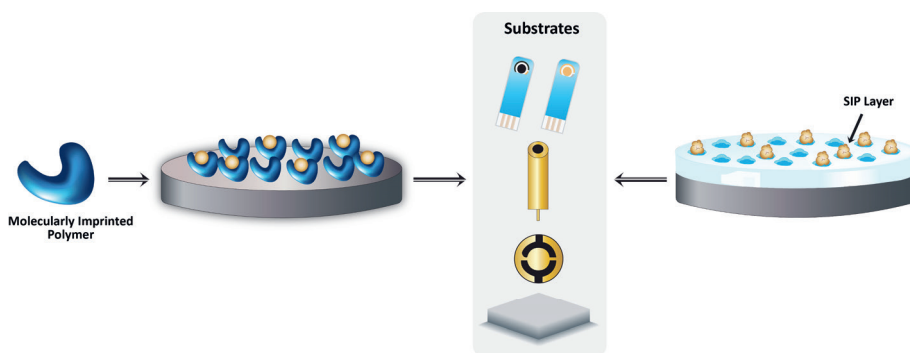


Figure 1.5 Graphical representation of MIPs- and SIPs-based platforms and some examples of commonly used substrates as solid supports for imprinted polymers.

One of the most attractive categories of MIP-based sensors is certainly represented by MIP-based electrochemical sensors.[90] These platforms make use of electrochemical techniques, such as potentiometry, amperometry, voltammetry and electrochemical impedance spectroscopy. The most commonly used substrates in point-of-care devices are represented by different types of electrodes, with growing attention given to miniaturized platforms using flexible, low-cost screen-printed electrodes (SPEs).[91] Unsurprisingly, electrode platforms are the preferred substrates for electrochemical transducers, due to their conductivity and compatibility with electronics. Most MIP-electrochemical sensors are obtained via “*in situ*” polymerization onto an electrode surface and are employed for the electrochemical detection of several analytes.[75,92] The technique employed usually involves the electropolymerization of one or more monomers on the surface[93] or require a previous modification of the surface in order to allow the growth of the polymeric material onto it.[94,95]. Though many of these sensors have successfully demonstrated notable sensitivity and selectivity, these fabrication processes require many steps that need to be optimized and that could lead to high cost and poorly reproducible methods.

MIP-based optical sensing platforms are based on the change in optical properties of MIPs upon binding with the target molecule. In these sensors, MIP films are typically synthesized on substrates such as

functionalized glass,[96–98] ITO electrodes,[99] or plastic optical fibres[100,101] to produce MIP-functionalized optical platforms. Fluorescence, absorption, surface-enhanced Raman spectroscopy (SERS), and surface plasmon resonance (SPR) are among the optical techniques used by these platforms for different applications.[102,103]. The combination of MIPs and optical transducers allows for the creation of label-free, real-time sensing platforms. However, as with MIP-electropolymerized films, further optimization and standardization of polymer film synthesis is required to improve the reproducibility and reliability of these sensors.

Another readout approach used in combination with imprinted polymers is based on the detection of surface mass loading in, e.g. quartz crystal microbalances (QCM).[64,104] The resonance frequency of the crystals will change due to mass loading on their surface. This frequency change is proportional to the mass of the target molecule, allowing for quantitative detection of the target molecule.[105,106] The benefit of using the QCM technique is the ability to detect a large number of different analytes with little regard for other physical properties. The substrates for this readout technology are represented by specific electrodes for these transducers, also known as QCM electrodes,[107] onto which the imprinted polymers are coated.

Another readout technology, known as the "heat-transfer method" (HTM), has emerged in the last decade[108] and has been successfully used in conjunction with imprinted polymers.[109,110] The HTM is a thermal sensing platform that has gained popularity in recent years and has recently been used to detect bacteria and small organic molecules using surface-imprinted polymers and MIPs.[111–115] In short, the method can detect changes in thermal resistance across a liquid-solid interface using MIPs/SIPs as the receptor layer deposited between the two.[108] The thermodynamic properties of the receptor layer are altered when a target analyte is added to the liquid phase and is able to bind to the receptor, changing the thermal conduction at the solid to liquid interface.[116] The overall change is then recorded after exposing the receptor layers to increasing concentrations of the target, allowing for a quantitative analysis of the sample introduced. The substrates used for receptor layer deposition are made of thermally conductive materials, which greatly benefits the sensor's overall response. For example, polished aluminium chips,[113,117] thermocouples,[118] or screen-printed electrodes[119,120] are common substrates. In recent years, an intriguing proof of principle involving the use of a double readout technology (HTM and EIS) has been achieved by modifying the HTM setup with a gold wire to allow the impedimetric analysis.[111]

Aims and Outlines

This thesis is a collection of peer-reviewed published chapters that investigates the development of MIP-based sensing platforms for clinical diagnostics and food safety analysis.

A literature review on advances in molecularly imprinted polymers for glucose monitoring is presented in **Chapter 2**. This chapter aims to answer the question: *What are the recent innovations in MIP-based glucose sensors and what challenges need to be addressed to develop a valid commercial alternative to a field predominantly occupied by enzymatic glucose sensors?* This chapter provides an overview and a critical evaluation of the various production methods of glucose-MIPs, as well as the diverse readout technologies used in conjunction with MIP-based sensors, from both an academic and a commercial standpoint. Furthermore, potential promising approaches in terms of manufacturing and transducers used are discussed. In addition, potential future approaches and obstacles are outlined, which the MIP-sensing field may encounter in an attempt to penetrate the commercial market for glucose sensing.

One promising readout technology for glucose detection highlighted in **Chapter 2** is the so-called “Heat-Transfer Method” (HTM). As a result, in **Chapter 3**, the question to be answered is: *Would a MIP-based platform coupled with an HTM transducer be suitable for glucose recognition in a complex matrix such as urine?* Until now, the HTM method has never been used to detect a critical biomarker, such as glucose, in clinically relevant samples. In this study, MIP particles were synthesized using a bulk polymerization method and a dummy template approach. Then, the optimized MIP particles were deposited onto an aluminium substrate-polyvinyl chloride (Al-PVC) via micro-contact deposition to fabricate a thermally conductive receptor layer. Finally, a real-life sample analysis in glucose-spiked human urine samples demonstrated promising linearity and sensitivity, making the developed low-cost platform very appealing for commercial applications and follow-up research.

One of the key advantages of MIPs as synthetic recognition elements is that they are able to recognize a target in matrices where other recognition elements may suffer. Therefore, **Chapter 4** targets the research question: *Can the same production process exploited in Chapter 3 be used for the development of a MIP-HTM platform for the individuation of melamine-adulterated milk samples?* In the previous chapter the thermal MIP-based platform in combination with HTM was successfully employed for rebinding analysis in untreated human urine samples. A field of application that could greatly benefit from this advantageous feature is food safety analysis. For example melamine is an adulterant molecule that has received increased attention as a result of its misuse in milk products, which has resulted in serious health issues worldwide. In **Chapter 4**, the fabrication process of the platform employed in the previous chapter was applied to manufacture a thermal MIP-based platform targeting melamine in a different complex matrix, such as milk.

Though two low-cost MIP-based platforms were successfully produced using a simple mechanical MIP deposition onto an Al-PVC substrate, this methodology is not easily scalable, severely limiting the sensors' potential. As a result, **Chapter 5** presents a literature review focusing on the various deposition methods used for the integration of imprinted polymers in sensor applications. The deposition of these polymers in various substrates to create a MIP-based platform is a critical step that can have a significant impact on the sensor's reliability, batch-to-batch variation, and thus its commercial potential. Different deposition methodologies are critically evaluated in this chapter, with the versatility and limiting factors of each approach discussed. This chapter tackles the research question: *What are the*

different deposition methods employed to integrate MIPs in sensing platforms and what are the most suitable deposition processes for the development of commercial MIP-based devices?

One of the most interesting novel deposition approaches discussed in **Chapter 5** involves the mixing of MIP particles with graphitic ink and the direct screen-printing of the mixture to obtain a screen-printed electrode (SPE) functionalized with MIP particles as recognition element (MIP-SPE). Using this approach allows for the preparation of functionalized MIP-SPE platforms in a cost-effective, reproducible and easily scalable manner. In **Chapter 6**, this innovative approach is explored by using bulk MIP particles synthesized and optimized in **Chapter 3** in order to obtain the first MIP-SPE platform for glucose detection with this deposition methodology. Moreover, the developed MIP-SPE sensor has proven to be suitable for the quantitative analysis of glucose in buffer solutions and urine samples with two different readout technologies, HTM and EIS. Thanks to the possibility of using this sensor with a handheld SPE connector and a commercial impedance analyser in a dipstick configuration, this would allow for the single-shot, non-invasive analysis of the glucose concentration in physiological samples. The question to be answered in this chapter is: *Is it possible to utilise a screen-printing deposition method to integrate bulk MIP particles onto SPEs and would this platform be able to quantify glucose in urine samples with two different readout technologies?*

References Chapter 1

1. D’Orazio, P. Biosensors in Clinical Chemistry. *Clin. Chim. Acta* 2003, 334, 41–69, doi:10.1016/S0009-8981(03)00241-9.
2. Wanekaya, A.K.; Chen, W.; Mulchandani, A. Recent Biosensing Developments in Environmental Security. *J. Environ. Monit.* 2008, 10, 703, doi:10.1039/b806830p.
3. Justino, C.I.L.; Duarte, A.C.; Rocha-Santos, T.A.P. Critical Overview on the Application of Sensors and Biosensors for Clinical Analysis. *TrAC - Trends Anal. Chem.* 2016, 85, 36–60, doi:10.1016/j.trac.2016.04.004.
4. Dennison, M.J.; Turner, A.P.F. Biosensors for Environmental Monitoring. *Biotechnol. Adv.* 1995, 13, 1–12, doi:10.1016/0734-9750(94)00020-D.
5. Yu, D.; Blankert, B.; Viré, J.; Kauffmann, J. Biosensors in Drug Discovery and Drug Analysis. *Anal. Lett.* 2005, 38, 1687–1701, doi:10.1080/00032710500205659.
6. Alocilja, E.C.; Radke, S.M. Market Analysis of Biosensors for Food Safety. *Biosens. Bioelectron.* 2003, 18, 841–846, doi:10.1016/S0956-5663(03)00009-5.
7. Ding, J.; Qin, W. Recent Advances in Potentiometric Biosensors. *TrAC - Trends Anal. Chem.* 2020, 124, 115803, doi:10.1016/j.trac.2019.115803.
8. Manhas, J.; Edelstein, H.I.; Leonard, J.N.; Morsut, L. The Evolution of Synthetic Receptor Systems. *Nat. Chem. Biol.* 2022, 18, 244–255, doi:10.1038/s41589-021-00926-z.
9. Lavigne, J.J.; Anslyn, E. V. Sensing A Paradigm Shift in the Field of Molecular Recognition: From Selective to Differential Receptors. *Angew. Chemie Int. Ed.* 2001, 40, 3118–3130, doi:10.1002/1521-3773(20010903)40:17<3118::AID-ANIE3118>3.0.CO;2-Y.
10. Antunez, E.E.; Martin, M.A.; Voelcker, N.H. Porous Silicon-Based Sensors for Protein Detection. In *Porous Silicon for Biomedical Applications*; Santos, H.A.B.T.-P.S. for B.A. (Second E., Ed.; Elsevier, 2021; pp. 359–395 ISBN 978-0-12-821677-4.
11. Laghrib, F.; Saqrane, S.; El Bouabi, Y.; Farahi, A.; Bakasse, M.; Lahrach, S.; El Mhammedi, M.A. Current Progress on COVID-19 Related to Biosensing Technologies: New Opportunity for Detection and Monitoring of Viruses. *Microchem. J.* 2021, 160, 105606, doi:10.1016/j.microc.2020.105606.
12. Haleem, A.; Javaid, M.; Singh, R.P.; Suman, R.; Rab, S. Biosensors Applications in Medical Field: A Brief Review. *Sensors Int.* 2021, 2, 100100, doi:10.1016/j.sintl.2021.100100.
13. Alsalameh, S.; Alnajjar, K.; Makhzoum, T.; Al Eman, N.; Shakir, I.; Mir, T.A.; Alkattan, K.; Chinnappan, R.; Yaqinuddin, A. Advances in Biosensing Technologies for Diagnosis of COVID-19. *Biosensors* 2022, 12, 898, doi:10.3390/bios12100898.
14. Naresh, V.; Lee, N. A Review on Biosensors and Recent Development of Nanostructured Materials-Enabled Biosensors. *Sensors* 2021, 21, 1109, doi:10.3390/s21041109.

15. Kabay, G.; DeCastro, J.; Altay, A.; Smith, K.; Lu, H.; Capossela, A.M.; Moarefian, M.; Aran, K.; Dincer, C. Emerging Biosensing Technologies for the Diagnostics of Viral Infectious Diseases. *Adv. Mater.* 2022, 34, 2201085, doi:10.1002/adma.202201085.
16. Turner, A.P.F. Biosensors--Sense and Sensitivity. *Science* (80-.). 2000, 290, 1315–1317, doi:10.1126/science.290.5495.1315.
17. Roberts, A.; Mahari, S.; Gandhi, S. Biological/Synthetic Receptors (Antibody, Enzyme, and Aptamer) Used for Biosensors Development for Virus Detection. In *Advanced Biosensors for Virus Detection*; Elsevier, 2022; pp. 113–131 ISBN 9780128244944.
18. Dincer, C.; Bruch, R.; Costa-Rama, E.; Fernández-Abedul, M.T.; Merkoçi, A.; Manz, A.; Urban, G.A.; Güder, F. Disposable Sensors in Diagnostics, Food, and Environmental Monitoring. *Adv. Mater.* 2019, 31, 1806739, doi:10.1002/adma.201806739.
19. Kevadiya, B.D.; Machhi, J.; Herskovitz, J.; Oleynikov, M.D.; Blomberg, W.R.; Bajwa, N.; Soni, D.; Das, S.; Hasan, M.; Patel, M.; et al. Diagnostics for SARS-CoV-2 Infections. *Nat. Mater.* 2021, 20, 593–605, doi:10.1038/s41563-020-00906-z.
20. Ferri, S.; Kojima, K.; Sode, K. Review of Glucose Oxidases and Glucose Dehydrogenases: A Bird's Eye View of Glucose Sensing Enzymes. *J. Diabetes Sci. Technol.* 2011, 5, 1068–1076, doi:10.1177/193229681100500507.
21. Yoo, E.-H.; Lee, S.-Y. Glucose Biosensors: An Overview of Use in Clinical Practice. *Sensors* 2010, 10, 4558–4576, doi:10.3390/s100504558.
22. Nery, E.W.; Kundys, M.; Jeleń, P.S.; Jönsson-Niedziółka, M. Electrochemical Glucose Sensing: Is There Still Room for Improvement? *Anal. Chem.* 2016, 88, 11271–11282, doi:10.1021/acs.analchem.6b03151.
23. Schachinger, F.; Chang, H.; Scheiblbrandner, S.; Ludwig, R. Amperometric Biosensors Based on Direct Electron Transfer Enzymes. *Molecules* 2021, 26, 4525, doi:10.3390/molecules26154525.
24. Kaur, K.; Kaushal, P. Enzymes as Analytical Tools for the Assessment of Food Quality and Food Safety. In *Advances in Enzyme Technology*, First Edition; Elsevier, 2019; pp. 273–292 ISBN 9780444641144.
25. Rebollar-Pérez, G.; Campos-Terán, J.; Ornelas-Soto, N.; Méndez-Albores, A.; Torres, E. Biosensors Based on Oxidative Enzymes for Detection of Environmental Pollutants. *Biocatalysis* 2016, 1, 118–129, doi:10.1515/boca-2015-0010.
26. Serna Cock, L.; Zetty Arenas, A.M.; Ayala Aponte, A. Use of Enzymatic Biosensors as Quality Indices: A Synopsis of Present and Future Trends in The Food Industry. *Chil. J. Agric. Res.* 2009, 69, 270–280, doi:10.4067/s0718-58392009000200017.
27. Vojinović, V.; Cabral, J.M.S.; Fonseca, L.P. Real-Time Bioprocess Monitoring. *Sensors Actuators B Chem.* 2006, 114, 1083–1091, doi:10.1016/j.snb.2005.07.059.
28. Miura, D.; Asano, R. Biosensors: Immunosensors. In *Encyclopedia of Sensors and Biosensors*; Elsevier, 2023; pp. 298–314.

29. Kimura, H.; Asano, R. Strategies to Simplify Operation Procedures for Applying Labeled Antibody-Based Immunosensors to Point-of-Care Testing. *Anal. Biochem.* 2022, 654, 114806, doi:10.1016/j.ab.2022.114806.
30. Amiri, M.; Arshi, S.; Saberi, R.S. Recent Advances in Immunosensors for Healthcare. In *The Detection of Biomarkers*; Elsevier, 2022; pp. 335–368 ISBN 9780128228593.
31. Yüce, M.; Filiztekin, E.; Özkaya, K.G. COVID-19 Diagnosis —A Review of Current Methods. *Biosens. Bioelectron.* 2021, 172, 112752, doi:10.1016/j.bios.2020.112752.
32. Caldara, M.; Lowdon, J.W.; Royackers, J.; Peeters, M.; Cleij, T.J.; Diliën, H.; Eersels, K.; van Grinsven, B. A Molecularly Imprinted Polymer-Based Thermal Sensor for the Selective Detection of Melamine in Milk Samples. *Foods* 2022, 11, 2906, doi:10.3390/foods11182906.
33. Kozitsina, A.; Svalova, T.; Malysheva, N.; Okhokhonin, A.; Vidrevich, M.; Brainina, K. Sensors Based on Bio and Biomimetic Receptors in Medical Diagnostic, Environment, and Food Analysis. *Biosensors* 2018, 8, 35, doi:10.3390/bios8020035.
34. O'malley, J.J.; Ulmer, R.W. Thermal Stability of Glucose Oxidase and Its Admixtures with Synthetic Polymers. *Biotechnol. Bioeng.* 1973, 15, 917–925, doi:10.1002/bit.260150509.
35. Gray, A.; Bradbury, A.R.M.; Knappik, A.; Plückthun, A.; Borrebaeck, C.A.K.; Dübel, S. Animal-Free Alternatives and the Antibody Iceberg. *Nat. Biotechnol.* 2020, 38, 1234–1239, doi:10.1038/s41587-020-0687-9.
36. Gray, A.C.; Sidhu, S.S.; Chandrasekera, P.C.; Hendriksen, C.F.M.; Borrebaeck, C.A.K. Animal-Friendly Affinity Reagents: Replacing the Needless in the Haystack. *Trends Biotechnol.* 2016, 34, 960–969, doi:10.1016/j.tibtech.2016.05.017.
37. Zheng, Y.; Li, J.; Zhou, B.; Ian, H.; Shao, H. Advanced Sensitivity Amplification Strategies for Voltammetric Immunosensors of Tumor Marker: State of the Art. *Biosens. Bioelectron.* 2021, 178, 113021, doi:10.1016/j.bios.2021.113021.
38. Motherwell, W.B.; Bingham, M.J.; Six, Y. Recent Progress in the Design and Synthesis of Artificial Enzymes. *Tetrahedron* 2001, 57, 4663–4686, doi:10.1016/S0040-4020(01)00288-5.
39. Çorman, M.E.; Ozcelikay, G.; Cetinkaya, A.; Kaya, S.I.; Armutcu, C.; Özgür, E.; Uzun, L.; Ozkan, S.A. Metal-Organic Frameworks as an Alternative Smart Sensing Platform for Designing Molecularly Imprinted Electrochemical Sensors. *TrAC Trends Anal. Chem.* 2022, 150, 116573, doi:10.1016/j.trac.2022.116573.
40. Kuah, E.; Toh, S.; Yee, J.; Ma, Q.; Gao, Z. Enzyme Mimics: Advances and Applications. *Chem. - A Eur. J.* 2016, 22, 8404–8430, doi:10.1002/chem.201504394.
41. Bell, T.W.; Hext, N.M. Supramolecular Optical Chemosensors for Organic Analytes. *Chem. Soc. Rev.* 2004, 33, 589–598, doi:10.1039/b207182g.
42. Cieplak, M.; Kutner, W. Artificial Biosensors: How Can Molecular Imprinting Mimic Biorecognition? *Trends Biotechnol.* 2016, 34, 922–941, doi:10.1016/j.tibtech.2016.05.011.

43. Jayasena, S.D. Aptamers: An Emerging Class of Molecules That Rival Antibodies in Diagnostics. *Clin. Chem.* 1999, 45, 1628–1650, doi:10.1093/clinchem/45.9.1628.
44. O’Sullivan, C.K. Aptasensors – the Future of Biosensing? *Anal. Bioanal. Chem.* 2002, 372, 44–48, doi:10.1007/s00216-001-1189-3.
45. Luo, X.; Xia, J.; Jiang, X.; Yang, M.; Liu, S. Cellulose-Based Strips Designed Based on a Sensitive Enzyme Colorimetric Assay for the Low Concentration of Glucose Detection. *Anal. Chem.* 2019, 91, 15461–15468, doi:10.1021/ACS.ANALCHEM.9B03180.
46. Iliuk, A.B.; Hu, L.; Tao, W.A. Aptamer in Bioanalytical Applications. *Anal. Chem.* 2011, 83, 4440–4452, doi:10.1021/ac201057w.
47. Zhou, J.; Rossi, J. Aptamers as Targeted Therapeutics: Current Potential and Challenges. *Nat. Rev. Drug Discov.* 2017, 16, 181–202, doi:10.1038/nrd.2016.199.
48. Liu, Z.; Yuan, R.; Chai, Y.; Zhuo, Y.; Hong, C.; Yang, X.; Su, H.; Qian, X. Highly Sensitive, Reusable Electrochemical Aptasensor for Adenosine. *Electrochim. Acta* 2009, 54, 6207–6211, doi:10.1016/j.electacta.2009.05.057.
49. Fu, B.; Cao, J.; Jiang, W.; Wang, L. A Novel Enzyme-Free and Label-Free Fluorescence Aptasensor for Amplified Detection of Adenosine. *Biosens. Bioelectron.* 2013, 44, 52–56, doi:10.1016/j.bios.2012.12.059.
50. Nguyen, P.-L.; Sekhon, S.S.; Ahn, J.-Y.; Ko, J.H.; Lee, L.; Cho, S.-J.; Min, J.; Kim, Y.-H. Aptasensor for Environmental Monitoring. *Toxicol. Environ. Health Sci.* 2017, 9, 89–101, doi:10.1007/s13530-017-0308-2.
51. Deng, B.; Lin, Y.; Wang, C.; Li, F.; Wang, Z.; Zhang, H.; Li, X.-F.; Le, X.C. Aptamer Binding Assays for Proteins: The Thrombin Example—A Review. *Anal. Chim. Acta* 2014, 837, 1–15, doi:10.1016/j.aca.2014.04.055.
52. Majdinasab, M.; Hayat, A.; Marty, J.L. Aptamer-Based Assays and Aptasensors for Detection of Pathogenic Bacteria in Food Samples. *TrAC Trends Anal. Chem.* 2018, 107, 60–77, doi:10.1016/j.trac.2018.07.016.
53. Liu, M.; Yue, F.; Kong, Q.; Liu, Z.; Guo, Y.; Sun, X. Aptamers against Pathogenic Bacteria: Selection Strategies and Apta-Assay/Aptasensor Application for Food Safety. *J. Agric. Food Chem.* 2022, 2022, 5498, doi:10.1021/acs.jafc.2c01547.
54. Yu, Y.; Liang, C.; Lv, Q.; Li, D.; Xu, X.; Liu, B.; Lu, A.; Zhang, G. Molecular Selection, Modification and Development of Therapeutic Oligonucleotide Aptamers. *Int. J. Mol. Sci.* 2016, 17, 358, doi:10.3390/ijms17030358.
55. Du, L.; Chen, W.; Zhu, P.; Tian, Y.; Chen, Y.; Wu, C. Applications of Functional Metal-Organic Frameworks in Biosensors. *Biotechnol. J.* 2021, 16, 1900424, doi:10.1002/biot.201900424.
56. Rowsell, J.L.C.; Yaghi, O.M. Metal-Organic Frameworks: A New Class of Porous Materials. *Microporous Mesoporous Mater.* 2004, 73, 3–14, doi:10.1016/j.micromeso.2004.03.034.

57. Meek, S.T.; Greathouse, J.A.; Allendorf, M.D. Metal-Organic Frameworks: A Rapidly Growing Class of Versatile Nanoporous Materials. *Adv. Mater.* 2011, 23, 249–267, doi:10.1002/adma.201002854.
58. Goel, P.; Singh, S.; Kaur, H.; Mishra, S.; Deep, A. Low-Cost Inkjet Printing of Metal–Organic Frameworks Patterns on Different Substrates and Their Applications in Ammonia Sensing. *Sensors Actuators B Chem.* 2021, 329, 129157, doi:10.1016/j.snb.2020.129157.
59. Jing, W.; Kong, F.; Tian, S.; Yu, M.; Li, Y.; Fan, L.; Li, X. Glucose Oxidase Decorated Fluorescent Metal–Organic Frameworks as Biomimetic Cascade Nanozymes for Glucose Detection through the Inner Filter Effect. *Analyst* 2021, 146, 4188–4194, doi:10.1039/d1an00847a.
60. Bunzen, H. Chemical Stability of Metal-organic Frameworks for Applications in Drug Delivery. *ChemNanoMat* 2021, 7, 998–1007, doi:10.1002/cnma.202100226.
61. Yu, Z.; Cao, X.; Wang, S.; Cui, H.; Li, C.; Zhu, G. Research Progress on the Water Stability of a Metal–Organic Framework in Advanced Oxidation Processes. *Water, Air, Soil Pollut.* 2021, 232, 18, doi:10.1007/s11270-020-04953-9.
62. Zhao, W.; Deng, J.; Ren, Y.; Xie, L.; Li, W.; Wang, Q.; Li, S.; Liu, S. Antibacterial Application and Toxicity of Metal–Organic Frameworks. *Nanotoxicology* 2021, 15, 311–330, doi:10.1080/17435390.2020.1851420.
63. Kumar, P.; Anand, B.; Tsang, Y.F.; Kim, K.H.; Khullar, S.; Wang, B. Regeneration, Degradation, and Toxicity Effect of MOFs: Opportunities and Challenges. *Environ. Res.* 2019, 176, 108488, doi:10.1016/j.envres.2019.05.019.
64. Haupt, K.; Mosbach, K. Molecularly Imprinted Polymers and Their Use in Biomimetic Sensors. *Chem. Rev.* 2000, 100, 2495–2504, doi:10.1021/cr990099w.
65. Piletsky, S.A.; Panasyuk, T.L.; Piletskaya, E. V.; Nicholls, I.A.; Ulbricht, M. Receptor and Transport Properties of Imprinted Polymer Membranes - A Review. *J. Memb. Sci.* 1999, 157, 263–278, doi:10.1016/S0376-7388(99)00007-1.
66. Advincula, R.C. Engineering Molecularly Imprinted Polymer (MIP) Materials: Developments and Challenges for Sensing and Separation Technologies. *Korean J. Chem. Eng.* 2011, 28, 1313–1321, doi:10.1007/s11814-011-0133-2.
67. Mahony, J.O.; Nolan, K.; Smyth, M.R.; Mizaikoff, B. Molecularly Imprinted Polymers - Potential and Challenges in Analytical Chemistry. *Anal. Chim. Acta* 2005, 534, 31–39, doi:10.1016/j.aca.2004.07.043.
68. Kaabi, F.B.H.; Pichon, V. Different Approaches to Synthesizing Molecularly Imprinted Polymers for Solid-Phase Extraction. *LCGC North Am.* 2007, 25, 732–739.
69. Wei, S.; Mizaikoff, B. Recent Advances on Noncovalent Molecular Imprints for Affinity Separations. *J. Sep. Sci.* 2007, 30, 1794–1805, doi:10.1002/jssc.200700166.
70. Kryscio, D.R.; Peppas, N.A. Critical Review and Perspective of Macromolecularly Imprinted Polymers. *Acta Biomater.* 2012, 8, 461–473, doi:10.1016/j.actbio.2011.11.005.

71. Awokoya, K.N.; Batlokwa, B.S.; Moronkola, B.A.; Chigome, S.; Ondigo, D.A.; Tshentu, Z.; Torto, N. Development of a Styrene Based Molecularly Imprinted Polymer and Its Molecular Recognition Properties of Vanadyl Tetraphenylporphyrin in Organic Media. *Int. J. Polym. Mater. Polym. Biomater.* 2013, 63, 107–113, doi:10.1080/00914037.2013.769255.
72. Piscopo, L.; Prandi, C.; Coppa, M.; Sparnacci, K.; Laus, M.; Laganà, A.; Curini, R.; D'Ascenzo, G. Uniformly Sized Molecularly Imprinted Polymers (MIPs) for 17 β -Estradiol. *Macromol. Chem. Phys.* 2002, 203, 1532–1538, doi:10.1002/1521-3935(200207)203:10/11<1532::AID-MACP1532>3.0.CO;2-C.
73. Aeinehvand, R.; Zahedi, P.; Kashani-Rahimi, S.; Fallah-Darrehchi, M.; Shamsi, M. Synthesis of Poly(2-Hydroxyethyl Methacrylate)-Based Molecularly Imprinted Polymer Nanoparticles Containing Timolol Maleate: Morphological, Thermal, and Drug Release along with Cell Biocompatibility Studies. *Polym. Adv. Technol.* 2017, 28, 828–841, doi:10.1002/pat.3986.
74. Ramanavičius, A.; Ramanavičienė, A.; Malinauskas, A. Electrochemical Sensors Based on Conducting Polymer—Polypyrrole. *Electrochim. Acta* 2006, 51, 6025–6037, doi:10.1016/j.electacta.2005.11.052.
75. Moreira Gonçalves, L. Electropolymerized Molecularly Imprinted Polymers: Perceptions Based on Recent Literature for Soon-to-Be World-Class Scientists. *Curr. Opin. Electrochem.* 2021, 25, 100640, doi:10.1016/j.coelec.2020.09.007.
76. Figueiredo, L.; Erny, G.L.; Santos, L.; Alves, A. Applications of Molecularly Imprinted Polymers to the Analysis and Removal of Personal Care Products: A Review. *Talanta* 2016, 146, 754–765, doi:10.1016/j.talanta.2015.06.027.
77. Cui, F.; Zhou, Z.; Zhou, H.S. Molecularly Imprinted Polymers and Surface Imprinted Polymers Based Electrochemical Biosensor for Infectious Diseases. *Sensors* 2020, 20, 996, doi:10.3390/s20040996.
78. Schirhagl, R.; Ren, K.; Zare, R.N. Surface-Imprinted Polymers in Microfluidic Devices. *Sci. China Chem.* 2012, 55, 469–483, doi:10.1007/s11426-012-4544-7.
79. Wackerlig, J.; Lieberzeit, P.A. Molecularly Imprinted Polymer Nanoparticles in Chemical Sensing – Synthesis, Characterisation and Application. *Sensors Actuators B Chem.* 2015, 207, 144–157, doi:10.1016/j.snb.2014.09.094.
80. Cheong, W.J.; Yang, S.H.; Ali, F. Molecular Imprinted Polymers for Separation Science: A Review of Reviews. *J. Sep. Sci.* 2013, 36, 609–628, doi:10.1002/jssc.201200784.
81. Poma, A.; Guerreiro, A.; Whitcombe, M.J.; Piletska, E. V.; Turner, A.P.F.; Piletsky, S.A. Solid-Phase Synthesis of Molecularly Imprinted Polymer Nanoparticles with a Reusable Template-"Plastic Antibodies". *Adv. Funct. Mater.* 2013, 23, 2821–2827, doi:10.1002/adfm.201202397.
82. Beyazit, S.; Tse Sum Bui, B.; Haupt, K.; Gonzato, C. Molecularly Imprinted Polymer Nanomaterials and Nanocomposites by Controlled/Living Radical Polymerization. *Prog. Polym. Sci.* 2016, 62, 1–21, doi:10.1016/j.progpolymsci.2016.04.001.
83. Svenson, J.; Nicholls, I.A. On the Thermal and Chemical Stability of Molecularly Imprinted Polymers. *Anal. Chim. Acta* 2001, 435, 19–24, doi:10.1016/S0003-2670(00)01396-9.

84. Bossi, A.; Bonini, F.; Turner, A.P.F.; Piletsky, S.A. Molecularly Imprinted Polymers for the Recognition of Proteins: The State of the Art. *Biosens. Bioelectron.* 2007, 22, 1131–1137, doi:10.1016/j.bios.2006.06.023.
85. Uzun, L.; Turner, A.P.F. Molecularly-Imprinted Polymer Sensors: Realising Their Potential. *Biosens. Bioelectron.* 2016, 76, 131–144, doi:10.1016/j.bios.2015.07.013.
86. Sharma, P.S.; Dabrowski, M.; D'Souza, F.; Kutner, W. Surface Development of Molecularly Imprinted Polymer Films to Enhance Sensing Signals. *TrAC - Trends Anal. Chem.* 2013, 51, 146–157.
87. Gavrilă, A.-M.; Stoica, E.-B.; Iordache, T.-V.; Sârbu, A. Modern and Dedicated Methods for Producing Molecularly Imprinted Polymer Layers in Sensing Applications. *Appl. Sci.* 2022, 12, 3080, doi:10.3390/app12063080.
88. Lowdon, J.W.; Diliën, H.; Singla, P.; Peeters, M.; Cleij, T.J.; van Grinsven, B.; Eersels, K. MIPs for Commercial Application in Low-Cost Sensors and Assays – An Overview of the Current Status Quo. *Sensors Actuators, B Chem.* 2020, 325, 128973, doi:10.1016/j.snb.2020.128973.
89. Bräuer, B.; Unger, C.; Werner, M.; Lieberzeit, P.A. Biomimetic Sensors to Detect Bioanalytes in Real-Life Samples Using Molecularly Imprinted Polymers: A Review. *Sensors* 2021, 21, 5550, doi:10.3390/s21165550.
90. Crapnell, R.; Hudson, A.; Foster, C.; Eersels, K.; Grinsven, B.; Cleij, T.; Banks, C.; Peeters, M. Recent Advances in Electrosynthesized Molecularly Imprinted Polymer Sensing Platforms for Bioanalyte Detection. *Sensors* 2019, 19, 1204, doi:10.3390/s19051204.
91. da Silva, E.T.S.G.; Souto, D.E.P.; Barragan, J.T.C.; de F. Giarola, J.; de Moraes, A.C.M.; Kubota, L.T. Electrochemical Biosensors in Point-of-Care Devices: Recent Advances and Future Trends. *ChemElectroChem* 2017, 4, 778–794, doi:10.1002/celec.201600758.
92. Lopes, F.; Pacheco, J.G.; Rebelo, P.; Delerue-Matos, C. Molecularly Imprinted Electrochemical Sensor Prepared on a Screen Printed Carbon Electrode for Naloxone Detection. *Sensors Actuators, B Chem.* 2017, 243, 745–752, doi:10.1016/j.snb.2016.12.031.
93. Vidal, J.-C.; Garcia-Ruiz, E.; Castillo, J.-R. Recent Advances in Electropolymerized Conducting Polymers in Amperometric Biosensors. *Microchim. Acta* 2003, 143, 93–111, doi:10.1007/s00604-003-0067-4.
94. Canfarotta, F.; Czulak, J.; Guerreiro, A.; Cruz, A.G.; Piletsky, S.; Bergdahl, G.E.; Hedström, M.; Mattiasson, B. A Novel Capacitive Sensor Based on Molecularly Imprinted Nanoparticles as Recognition Elements. *Biosens. Bioelectron.* 2018, 120, 108–114, doi:10.1016/j.bios.2018.07.070.
95. Di Masi, S.; Garcia Cruz, A.; Canfarotta, F.; Cowen, T.; Marote, P.; Malitesta, C.; Piletsky, S.A. Synthesis and Application of Ion-Imprinted Nanoparticles in Electrochemical Sensors for Copper (II) Determination. *ChemNanoMat* 2019, 5, 754–760, doi:10.1002/cnma.201900056.
96. Luo, Q.; Yu, N.; Shi, C.; Wang, X.; Wu, J. Surface Plasmon Resonance Sensor for Antibiotics Detection Based on Photo-Initiated Polymerization Molecularly Imprinted Array. *Talanta* 2016, 161, 797–803, doi:10.1016/j.talanta.2016.09.049.

97. Castro-Grijalba, A.; Montes-García, V.; Cordero-Ferradás, M.J.; Coronado, E.; Pérez-Juste, J.; Pastoriza-Santos, I. SERS-Based Molecularly Imprinted Plasmonic Sensor for Highly Sensitive PAH Detection. *ACS Sensors* 2020, 5, 693–702, doi:10.1021/acssensors.9b01882.
98. Mugo, S.M.; Lu, W. Determination of β -Estradiol by Surface-Enhance Raman Spectroscopy (SERS) Using a Surface Imprinted Methacrylate Polymer on Nanoporous Biogenic Silica. *Anal. Lett.* 2022, 55, 378–387, doi:10.1080/00032719.2021.1932969.
99. Li, S.; Yin, G.; Zhang, Q.; Li, C.; Luo, J.; Xu, Z.; Qin, A. Selective Detection of Fenaminosulf via a Molecularly Imprinted Fluorescence Switch and Silver Nano-Film Amplification. *Biosens. Bioelectron.* 2015, 71, 342–347, doi:10.1016/j.bios.2015.04.066.
100. Cennamo, N.; D’Agostino, G.; Galatus, R.; Bibbò, L.; Pesavento, M.; Zeni, L. Sensors Based on Surface Plasmon Resonance in a Plastic Optical Fiber for the Detection of Trinitrotoluene. *Sensors Actuators B Chem.* 2013, 188, 221–226, doi:10.1016/j.snb.2013.07.005.
101. Pesavento, M.; Zeni, L.; De Maria, L.; Alberti, G.; Cennamo, N. SPR-Optical Fiber-Molecularly Imprinted Polymer Sensor for the Detection of Furfural in Wine. *Biosensors* 2021, 11, 72, doi:10.3390/bios11030072.
102. Fang, L.; Jia, M.; Zhao, H.; Kang, L.; Shi, L.; Zhou, L.; Kong, W. Molecularly Imprinted Polymer-Based Optical Sensors for Pesticides in Foods: Recent Advances and Future Trends. *Trends Food Sci. Technol.* 2021, 116, 387–404, doi:10.1016/j.tifs.2021.07.039.
103. Ahmad, O.S.; Bedwell, T.S.; Esen, C.; Garcia-Cruz, A.; Piletsky, S.A. Molecularly Imprinted Polymers in Electrochemical and Optical Sensors. *Trends Biotechnol.* 2019, 37, 294–309, doi:10.1016/j.tibtech.2018.08.009.
104. Emir Diltemiz, S.; Keçili, R.; Ersöz, A.; Say, R. Molecular Imprinting Technology in Quartz Crystal Microbalance (QCM) Sensors. *Sensors* 2017, 17, 454, doi:10.3390/s17030454.
105. Torad, N.L.; Zhang, S.; Amer, W.A.; Ayad, M.M.; Kim, M.; Kim, J.; Ding, B.; Zhang, X.; Kimura, T.; Yamauchi, Y. Advanced Nanoporous Material-Based QCM Devices: A New Horizon of Interfacial Mass Sensing Technology. *Adv. Mater. Interfaces* 2019, 6, 1900849, doi:10.1002/admi.201900849.
106. Vashist, S.K.; Vashist, P. Recent Advances in Quartz Crystal Microbalance-Based Sensors. *J. Sensors* 2011, 2011, 1–13, doi:10.1155/2011/571405.
107. Tang, J.; Torad, N.L.; Salunkhe, R.R.; Yoon, J.H.; Al Hossain, M.S.; Dou, S.X.; Kim, J.H.; Kimura, T.; Yamauchi, Y. Towards Vaporized Molecular Discrimination: A Quartz Crystal Microbalance (QCM) Sensor System Using Cobalt-Containing Mesoporous Graphitic Carbon. *Chem. - An Asian J.* 2014, 9, 3238–3244, doi:10.1002/asia.201402629.
108. Van Grinsven, B.; Eersels, K.; Peeters, M.; Losada-Pérez, P.; Vandenryt, T.; Cleij, T.J.; Wagner, P. The Heat-Transfer Method: A Versatile Low-Cost, Label-Free, Fast, and User-Friendly Readout Platform for Biosensor Applications. *ACS Appl. Mater. Interfaces* 2014, 6, 13309–13318, doi:10.1021/am503667s.

109. Betlem, K.; Down, M.P.; Foster, C.W.; Akthar, S.; Eersels, K.; van Grinsven, B.; Cleij, T.J.; Banks, C.E.; Peeters, M. Development of a Flexible MIP-Based Biosensor Platform for the Thermal Detection of Neurotransmitters. *MRS Adv.* 2018, 3, 1569–1574, doi:10.1557/adv.2017.634.
110. Eersels, K.; Diliën, H.; Lowdon, J.; Steen Redeker, E.; Rogosic, R.; Heidt, B.; Peeters, M.; Cornelis, P.; Lux, P.; Reutelingsperger, C.; et al. A Novel Biomimetic Tool for Assessing Vitamin K Status Based on Molecularly Imprinted Polymers. *Nutrients* 2018, 10, 751, doi:10.3390/nu10060751.
111. Arreguin-Campos, R.; Eersels, K.; Lowdon, J.W.; Rogosic, R.; Heidt, B.; Caldara, M.; Jiménez-Monroy, K.L.; Diliën, H.; Cleij, T.J.; van Grinsven, B. Biomimetic Sensing of Escherichia Coli at the Solid-Liquid Interface: From Surface-Imprinted Polymer Synthesis toward Real Sample Sensing in Food Safety. *Microchem. J.* 2021, 169, 106554, doi:10.1016/j.microc.2021.106554.
112. van Grinsven, B.; Eersels, K.; Akkermans, O.; Ellermann, S.; Kordek, A.; Peeters, M.; Deschaume, O.; Bartic, C.; Diliën, H.; Steen Redeker, E.; et al. Label-Free Detection of Escherichia Coli Based on Thermal Transport through Surface Imprinted Polymers. *ACS Sensors* 2016, 1, 1140–1147, doi:10.1021/acssensors.6b00435.
113. Lowdon, J.W.; Eersels, K.; Rogosic, R.; Boonen, T.; Heidt, B.; Diliën, H.; van Grinsven, B.; Cleij, T.J. Surface Grafted Molecularly Imprinted Polymeric Receptor Layers for Thermal Detection of the New Psychoactive Substance 2-Methoxphenidine. *Sensors Actuators, A Phys.* 2019, 295, 586–595, doi:10.1016/j.sna.2019.06.029.
114. Cornelis, P.; Vandenryt, T.; Wackers, G.; Kellens, E.; Losada-Pérez, P.; Thoelen, R.; De Ceuninck, W.; Eersels, K.; Drijkoningen, S.; Haenen, K.; et al. Heat Transfer Resistance as a Tool to Quantify Hybridization Efficiency of DNA on a Nanocrystalline Diamond Surface. *Diam. Relat. Mater.* 2014, 48, 32–36, doi:10.1016/j.diamond.2014.06.008.
115. Givanoudi, S.; Cornelis, P.; Rasschaert, G.; Wackers, G.; Iken, H.; Rolka, D.; Yongabi, D.; Robbens, J.; Schöning, M.J.; Heyndrickx, M.; et al. Selective Campylobacter Detection and Quantification in Poultry: A Sensor Tool for Detecting the Cause of a Common Zoonosis at Its Source. *Sensors Actuators, B Chem.* 2021, 332, 129484, doi:10.1016/j.snb.2021.129484.
116. Stilman, W.; Campolim Lenzi, M.; Wackers, G.; Deschaume, O.; Yongabi, D.; Mathijssen, G.; Bartic, C.; Gruber, J.; Wübbenhorst, M.; Heyndrickx, M.; et al. Low Cost, Sensitive Impedance Detection of E. Coli Bacteria in Food-Matrix Samples Using Surface-Imprinted Polymers as Whole-Cell Receptors. *Phys. Status Solidi Appl. Mater. Sci.* 2022, 219, 2100405, doi:10.1002/pssa.202100405.
117. Steen Redeker, E.; Eersels, K.; Akkermans, O.; Royackers, J.; Dyson, S.; Nurekeyeva, K.; Ferrando, B.; Cornelis, P.; Peeters, M.; Wagner, P.; et al. Biomimetic Bacterial Identification Platform Based on Thermal Wave Transport Analysis (TWTA) through Surface-Imprinted Polymers. *ACS Infect. Dis.* 2017, 3, 388–397, doi:10.1021/acsinfectdis.7b00037.
118. McClements, J.; Seumo Tchekwagep, P.M.; Vilela Strapazon, A.L.; Canfarotta, F.; Thomson, A.; Czulak, J.; Johnson, R.E.; Novakovic, K.; Losada-Pérez, P.; Zaman, A.; et al. Immobilization of Molecularly Imprinted Polymer Nanoparticles onto Surfaces Using Different Strategies: Evaluating the Influence of the Functionalized Interface on the Performance of a Thermal Assay for the Detection of the Cardiac

Biomarker Troponin I. *ACS Appl. Mater. Interfaces* 2021, 13, 27868–27879, doi:10.1021/acsami.1c05566.

119. Jamieson, O.; Soares, T.C.C.; de Faria, B.A.; Hudson, A.; Mecozzi, F.; Rowley-Neale, S.J.; Banks, C.E.; Gruber, J.; Novakovic, K.; Peeters, M.; et al. Screen Printed Electrode Based Detection Systems for the Antibiotic Amoxicillin in Aqueous Samples Utilising Molecularly Imprinted Polymers as Synthetic Receptors. *Chemosensors* 2019, 8, 5, doi:10.3390/chemosensors8010005.

120. Crapnell, R.D.; Jesadabundit, W.; García-Miranda Ferrari, A.; Dempsey-Hibbert, N.C.; Peeters, M.; Tridente, A.; Chailapakul, O.; Banks, C.E. Toward the Rapid Diagnosis of Sepsis: Detecting Interleukin-6 in Blood Plasma Using Functionalized Screen-Printed Electrodes with a Thermal Detection Methodology. *Anal. Chem.* 2021, 93, 5931–5938, doi:10.1021/acs.analchem.1c00417.

Preface to Chapter 2

After studying and evaluating the different recognition elements of a biosensor, it is evident that synthetic receptor elements, especially molecularly imprinted polymers (MIPs), can be an interesting alternative to biological sensing elements in biosensor applications. Enzymatic biosensors, for instance, may experience instability and consequently short shelf-life under specific circumstances. This is a drawback from an economical perspective and can lead to them being of limited use in challenging circumstances. MIPs instead, represent a very robust and chemically stable sensing element in biosensor devices, which allows them to operate in a wide range of conditions and environments.

The use of MIP-based sensors as an alternative to enzymatic-biosensors for glucose monitoring is discussed in the following chapter. This clearly represents a crucial application for managing and diagnosing hyperglycaemia and therefore diabetes. The next chapter offers a thorough overview of recent developments in the creation of MIP-based sensors for glucose detection. The limitations of the glucose sensing technologies currently present on the market are studied along with the significance of glucose monitoring in the management of diabetes. Subsequently, the basic principles and application areas of MIPs-based glucose sensors are thoroughly discussed, along with MIP production techniques, integration into sensing platforms, and readout technologies employed. Furthermore, this chapter highlights the challenges and promising approaches taken in the development of MIP-based glucose sensors for healthcare applications. This will define the scientific methodology used to construct and test MIP-based glucose sensors in this thesis.

Chapter 2

Recent Advances in Molecularly Imprinted Polymers for Glucose Monitoring: From Fundamental Research to Commercial Application

Adapted from:

Caldara, M.*; Kulpa, J.; Lowdon, J.W.; Cleij, T.J.; Diliën, H.; Eersels, K.; Grinsven, B.v. Recent Advances in Molecularly Imprinted Polymers for Glucose Monitoring: From Fundamental Research to Commercial Application.

Chemosensors 2023, 11, 32.

<https://doi.org/10.3390/chemosensors11010032>



Abstract

Molecularly imprinted polymers (MIPs) have gained growing interest among researchers worldwide, due to their key features that make these materials interesting candidates for implementation as receptors into sensor applications. In fact, MIP-based glucose sensors could overcome the stability issues associated with the enzymes present in commercial glucose devices. Various reports describe the successful development of glucose MIPs and their coupling to a wide variety of transducers for creating sensors that are able to detect glucose in various matrices. In this review, we have summarized and critically evaluated the different production methods of glucose MIPs and the different transducer technologies used in MIP-based glucose sensors, and analysed these from a commercial point of view. In this way, this review sets out to highlight the most promising approaches in MIP-based sensing in terms of both manufacturing methods and readout technologies employed. In doing so, we aim at delineating potential future approaches and identifying potential obstacles that the MIP-sensing field may encounter in an attempt to penetrate the commercial, analytical market.

Keywords: glucose sensing; molecularly imprinted polymers; artificial receptors; glucose monitoring; non-enzymatic glucose sensors; clinical analysis; health diagnostics

Introduction

Glucose Sensing

Glucose plays a key role in numerous biological processes, such as cellular respiration and glycosylation.[1,2] Once its metabolism is disturbed, it may lead to a variety of diseases, such as hyperinsulinism and diabetes.[3,4] The latter is characterized by a high concentration of glucose in the blood and other physiological fluids (hyperglycaemia). Classical diabetes diagnostic tests, therefore, aim at directly assessing glucose levels in the blood of patients. More specifically, when the sugar concentration is higher than 7 mM after no caloric intake for a minimum of 8h or higher than 11.1 mM two hours after an oral glucose tolerance test (OGTT), the individual is considered to be affected by diabetes.[5] Diabetes is an incurable disease that causes a plethora of symptoms, including increased thirst and hunger, diabetic ketoacidosis, or hyperosmolar coma.[6] However, it does not only cause different discomforts, but is also responsible for severe long-term complications, such as kidney failure, stroke, and coronary heart disease.[6,7] For these reasons, the World Health Organization (WHO) classifies it as one of the top ten causes of death in adults.[8] Unfortunately, this condition has become increasingly more common and predictions estimate that by 2045, the number of sufferers will reach 693 million adults.[9] Due to the potentially life-threatening consequences of hyper- and hypoglycaemia, it is crucial that diabetics monitor their blood glucose levels closely and adjust their diet and insulin therapy accordingly. This has led to the emergence and spread of several low-cost biosensor technologies, such as glucose meters, that enable patients to self-monitor their blood glucose levels. These devices have become indispensable in diabetes management in the current society.[10,11] Before advancements in blood glucose monitoring were introduced, analysis was carried out using urine samples. Most of these tests were based on the technology developed by Benedict in 1908, which relied on the oxidation of glucose in the urine sample by a copper reagent.[12] In 1962, an enzyme membrane electrode system based on glucose oxidase (GOx) was introduced that allowed for the direct electrochemical detection of glucose in whole blood samples.[13] This breakthrough led to the development of the first commercial glucose meter in the 1970s,[14] which gradually evolved over the past few decades into the first continuous glucose monitoring (CGM) system that was introduced in 1999.[15] Over the years, three generations of enzyme-based sensors have been fabricated and commercialized (**Figure 2.1**).[16]

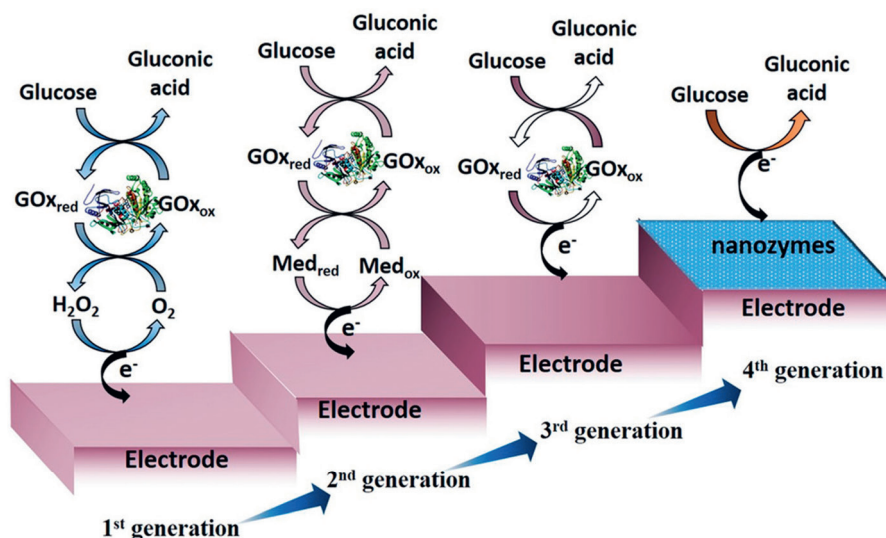


Figure 2.1 Schematic representation of the working principle of different generations of electrochemical glucose sensors. Figure reproduced with permission from ref. [16].

The first-generation glucose sensing system used oxygen as the electron acceptor, but it had a significant limitation due to the influence of dissolved oxygen in the blood samples, which could compromise the accuracy of the measurement.[17] To address this issue, a second generation of glucose sensors was developed, which relied on electron transfer from the enzymes to artificial electron receptors, known as redox dyes.[18] This approach helped minimize the interference from dissolved oxygen and improved the reliability of the measurements. Further advancements led to the development of the third generation of glucose sensors, which took a step further in simplifying the sensing process by utilizing direct electron transfer to the electrode.[19] By eliminating the need for artificial electron receptors, these sensors became even more efficient and provided more reliable results. Continuing the trend of innovation, the market is now transitioning towards the fourth generation of glucose sensors, which is expected to revolutionize glucose sensing technology. These new sensors will no longer rely on enzymes, as depicted in **Figure 2.1**. This development promises to overcome the stability issues commonly associated with enzyme-based sensors and opens up possibilities for significant improvements in terms of cost-effectiveness and selectivity.[21,22] These advancements are expected to benefit not only patients with diabetes who require regular glucose monitoring but also the healthcare industry as a whole by providing more accurate, efficient, and accessible glucose sensing solutions. All medical procedures, including diagnostic tests, can be categorized into the following two major groups: invasive and non-invasive procedures. In glucose monitoring, this often depends on the physiological sample under study.[23] Invasive glucose monitoring implies that the samples in which the glucose levels are measured can only be obtained by puncturing the skin of a patient.[24] For instance, in traditional self-monitoring of blood glucose (SMBG), a drop of blood is drawn from the fingertip of a patient.[25] Many development studies were

performed to optimize this procedure to reduce the pain associated with the measurement, resulting in the use of a blood lancet rather than a traditional needle and syringe.[26] However, this method still causes discomfort and increases the risks of blood-related infections.[27] Therefore, there has been a shift in the research focus towards the development of minimally invasive and non-invasive methods in recent years, although invasive blood glucose monitoring is still the most widely spread commercial approach.[28,29] Non-invasive glucose monitoring typically aims at measuring the glucose concentration in other physiological fluids, such as urine, saliva, sweat, or tears, and relating them to the current blood glucose levels.[30] The increased comfort that these methods offer patients also enables us to increase the number of measurements, opening up the possibility of creating new-generation systems for continuous monitoring.[31] Both the invasive and non-invasive methods can be analysed with different readout technologies, including electrochemical, mass-sensitive, optical, and thermal methods, with electrochemical transducers being the most used.[32] Since the topic has attracted increasing interest, and due to the benefits of non-invasive monitoring, innovative glucose biosensor technologies have been continuously explored. In fact, numerous studies reported in the last few years have focused on the development of novel wearable sensors that would enable patient-oriented, rapid, and convenient tracking of glucose.[33,34,35] Such sensors could be incorporated in, for instance, smartwatches.[36] However, the most important challenge associated with the current-generation blood glucose monitoring techniques is the specificity and stability of such sensors in different physiological matrices.[37] A crucial step to overcome these issues lies in the development of new recognition materials that can offer alternatives to the current enzyme-based sensors. Therefore, this review will focus on reviewing the current advances in molecularly imprinted polymers (MIPs) for glucose detection and critically assessing which approaches are the most compatible with the current trend of evolving toward non-invasive glucose monitoring.

General Background on MIPs

Molecularly imprinted polymers (MIPs) have attracted wide interest over the last few decades, as these materials can mimic the natural antibody–antigen and enzyme–substrate systems, but overcome most of the issues that are commonly encountered when using natural receptors in non-physiological conditions.[38] The general principle behind MIP synthesis is the interaction between a target molecule, a functional monomer, and a cross-linking agent. First, the functional monomer(s) and the target molecules form a complex by interactions between their functional groups,[39] then the cross-linker stabilizes the complex and is responsible for the rigidity of the polymer. After extraction of the template molecule, nanocavities that are complementary to the extracted molecule are formed (**Figure 2.2**).[40] This complementarity is both morphological and structural, ensuring that the target can selectively rebind to the receptor, which is similar to the key-and-lock mechanism that antibodies and enzymes use to detect their target.[41]

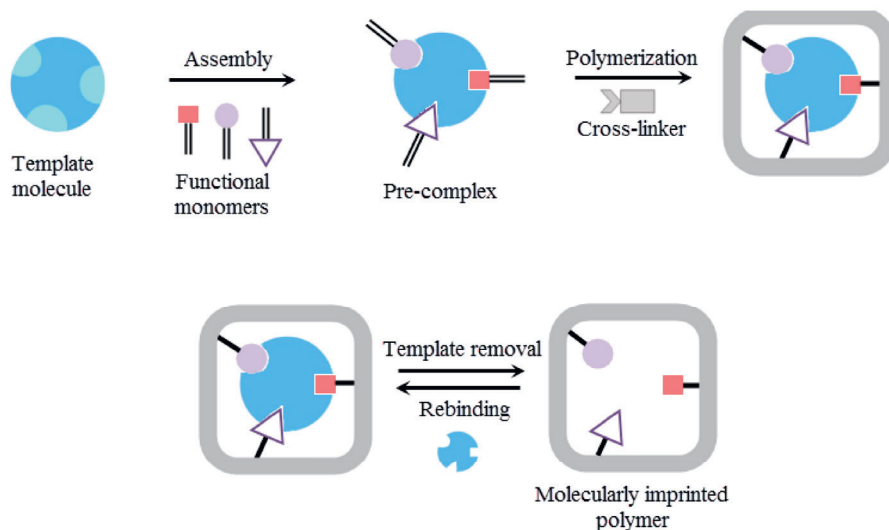


Figure 2.2 Schematic representation of generic synthesis and rebinding of molecularly imprinted polymers. Figure reproduced with permission from ref. [40].

Molecularly imprinted polymers can be synthesized using a wide variety of polymerization approaches, including bulk, precipitation, emulsion, photopolymerization, and electropolymerization.[42] Normally, MIPs do not possess signal output ability, which means that they need to be coupled to an appropriate transducer technology to translate the rebinding event into a readable signal.[43] Different works have demonstrated the successful integration of the polymers with several readout technologies, including, but not limited to, the heat-transfer method (HTM), quartz crystal microbalance (QCM), surface plasmon resonance (SPR), surface-enhanced Raman scattering (SERS), chromatographic techniques and various electrochemical transducers.[44,45,46,47] From a historical perspective, MIPs were reported for the first time in the 1930s.[48,49] However, it was not until the mid-1980s that this technology started to attract wide interest among the scientific community with the works from K. Mosbach and G. Wulff.[50,51,52] Around ten years later, the first works focused on the use of MIPs in sensing technologies started to appear.[52] Since then, with the emergence of computational technologies and novel methods used to integrate imprinted polymers into readout technologies, MIP-based sensors have become increasingly popular within the scientific community.[53,54] Nowadays, MIP-based sensors are engineered in such a way that they can serve in a versatile array of environments, including physiological fluids,[55] foodstuffs, (**Chapter 4**)[56,57] and wastewater.[58]

Advantages of MIP-Based Sensors in Glucose Sensing

Molecularly imprinted polymers (MIPs) are also known as plastic or synthetic antibodies because they represent a synthetic alternative to biological recognition elements typically found in biosensors.[59] Due to their synthetic nature, they have several key advantages over natural receptors, such as enzymes and antibodies, mainly resulting from their high stability and robustness at different pH and temperatures.[60] The enzyme-based sensors have low stability, which inevitably results in the short shelf-life of the final product.[61] As a result, the scientific community is increasingly moving toward

the realization of novel enzyme-free sensors.[62,63] As mentioned above, stability is a key feature of imprinted polymers and consequently of MIP-based sensors; furthermore, their preparation entails a rather short and cost-effective synthesis process.[64] However, despite all the benefits that these materials can provide to the field of biosensors, the commercialization of MIP-sensors has not yet fulfilled its potential.[65] For instance, home test devices for glucose monitoring are still monopolized by glucose oxidase bio meters, which measure the concentration of glucose in fingertip's blood.[66] With all the aforementioned assets that MIP-based technologies could provide, they may bring a new perspective to glucose monitoring. As mentioned earlier, we aim to categorize and evaluate the different MIP-based technologies for glucose detection developed in the last few years and assess their advantages and drawbacks in the framework of moving towards stable, disposable enzyme-free sensors for non-invasive blood glucose monitoring. We will critically assess which approaches are the most promising and which manufacturing and transducer technologies would be ideally suited to bring MIP-based sensors closer to the commercial glucose monitoring market.

Production Methods of MIPs for Glucose Detection

In order to synthesize molecularly imprinted polymers, different reagents are required, including a functional monomer(s), template, cross-linker, and a polymerization initiator.[67,68] Their ratio with respect to one another greatly influences the specific interaction between the polymer and the template, and subsequently the binding capacity and imprinting factor of the resulting MIP.[69,70] Depending on the type of polymerization, initiators and solvents also play a vital role in the whole process.[71] Numerous polymerization techniques used to synthesize molecularly imprinted polymers have been explored in the last few decades, (**Table 2.1**)[72,73] including bulk polymerization, electropolymerization, and photopolymerization.[73,74,75,76] More recently, MIPs have been used in combination with other materials such as gold nanoparticles to boost the sensitivity of the resulting sensor or nylon to open up the possibility of creating wearable glucose sensors.[77,78] Inevitably, a slightly different synthetic pathway needs to be employed for such sensors, often leading to additional steps in the fabrication process.

Reagents for the Production of MIPs

Functional Monomers

The role of the functional monomer is to create a complex with a template molecule before the polymerization.[71] Therefore, the selected monomer needs to be carefully chosen in order to maximize interaction with the template and create receptors with a high rebinding affinity to the target. Monomers that contain free carboxyl groups are of particular interest for creating non-covalent MIPs, as they can act as both hydrogen donors and acceptors and favour hydrogen bonding between the polymer and template.[79] Methacrylic acid (MAA), for example, has been extensively used as a monomer for MIP synthesis, due to its ability to form electrostatic interactions and hydrogen bonds with a plethora of functional groups on different template molecules.[80] Other functional monomers commonly used for the synthesis of MIPs are as follows: acrylamide (AAM), acrylic acid (AA), 4-vinylphenylboronic acid (VPBA), 4-vinylpyridine (4-VP), and pyrrole (PY).[81] Additionally, the growing popularity of MIPs has resulted in the synthesis of novel tailor-made functional monomers, opening up the possibility of producing imprinted materials with higher rebinding capabilities. Different functional monomers have also been successfully employed for the synthesis of glucose-imprinted polymers. The monomer choice is strictly linked to the synthetic approach undertaken to create the MIPs. For instance, a rational-design study in which Gaussian 2009 software was used to simulate the interaction between glucose and three commonly used functional monomers in free-radical polymerization (MAA, AAM, and 4-VP) revealed that MAA provides a stronger interaction with glucose, as well as the lowest energy value during the self-assembly phase.[82] However, another study conducted using the same program provided evidence that the reaction with AAM can occur more spontaneously than with MAA.[83] Different studies have subsequently reported the successful use of both MAA[82,84,85] and AAM,[86,87] as well as its derivative diacetone acrylamide (DAAM) [88]. Other functional monomers employed in polymer synthesis included AA, which provided interactions with the hydroxyl groups of glucose [89], VPBA, which forms a covalent complex with the template,[90,91] vinyl acetate,[92] and 3-amino-4-hydroxybenzoic acid.[93] Electropolymerization of pyrrole to create glucose-imprinted MIPs was demonstrated as an alternative approach in an attempt to automatize the synthesis procedure.[77,94] The obtained MIPs were then coupled with nylon fibres[77] or nitrogen-rich carbon conductive-coated TNO structures, which opens up the possibility to integrate electropolymerized glucose MIPs in wearable applications.[94]

Template

The vast majority of the synthetic approaches mentioned above employed D-glucose as template molecule.[77,88,89,90,94] However, as glucose lacks functional groups that enable strong interactions with these monomers, more recently, a dummy imprinting approach was introduced by the authors of this paper (**Chapter 3**), using glucuronic acid as a template (**Figure 2.3**).[87]

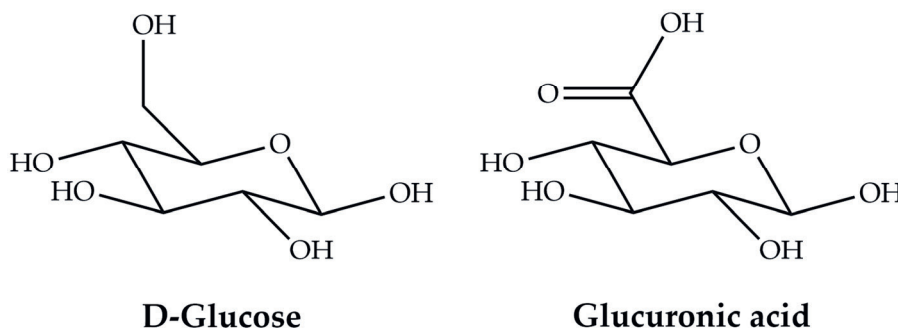


Figure 2.3 Chemical structures of D-glucose and glucuronic acid.

Cross-Linker

The role of the cross-linker is to enable the formation of a rigid polymer network, so its structure will not be changed by the template removal; hence, the binding sites will not be damaged. At the same time, this would allow the formation of a porous structure into which the targets can diffuse when immersing the MIP into the sample under study.[95] If the amount of cross-linking is too low, the polymer will not be mechanically stable, while if the cross-linking degree is too high, it may reduce the binding capacity of the polymer, as the target cannot penetrate into the polymer matrix and there will be fewer recognition sites available for rebinding.[81] The main drawback related to the cross-linker molecules employed for MIP fabrication is that while the rational design is often aimed at selecting functional monomers with appropriate hydrogen donor/acceptor properties, the cross-linker can also interact with the template and contribute to rebinding. This is a process that is hard to control and can lead to non-specific interactions. For the development of MIP-based glucose sensors, different cross-linkers were implemented and among these, the most commonly used is ethylene glycol dimethacrylate (EGDMA).[85,87,88,89] Another reported cross-linker commonly used for the production of glucose MIPs is N,N'-methylenebisacrylamide.[82,86,96]

Polymerization Methods Employed for Glucose-MIP Fabrication

Thermal Polymerization Approaches

One of the most used methods to produce MIPs is the thermally initiated bulk polymerization approach.[97] This straightforward technique consists of adding a template, functional monomer, cross-linker, and initiator in a solvent and allowing the formation of a pre-polymerization complex through self-assembly. The solution is then polymerized and the resulting product is a monolithic bulk polymer that needs to be ground and extracted with solvents. The interesting features of this approach from a commercial point-of-view are the fact that it is relatively straightforward and allows for the

creation of large batches of material cost-effectively. The major drawbacks are related to the tedious grinding and sieving procedure, which is time-consuming, leads to a large loss of product and the generation of a heterogeneous mixture of micro-scaled particles, which increases the batch-to-batch variation and makes it hard to reliably calibrate the resulting sensors.[97,98] The approach has also been employed in the synthesis of MIPs for glucose detection.[85,87] Within this method, different initiators can be employed to trigger the polymerization reaction. As such, molecules such as azobisisobutyronitrile (AIBN) or benzoyl peroxide were used to initiate the polymerization process. Another approach used to produce bulk MIPs included the oxidation of pyrrole by $\text{FeCl}_3 \cdot 6\text{H}_2\text{O}$, which initiated the formation of polypyrrole.[77] Thermally initiated polymerization can also be used to form thin polymer films; this approach allows the formation of MIP films directly onto the substrate. The approach has been used for the production of glucose MIP films on substrates such as Petri dishes[99] or Ni foam.[82,96]

Precipitation and Emulsion Polymerization

To overcome the problems associated with free-radical monolithic bulk polymerization, research on more controllable polymerization methods used to create homogenous particles has intensified over the past decade. Precipitation polymerization is a popular approach in which the reagents are soluble in a solvent that is chosen in such a way that after the polymerization reaction is completed, the resulting polymer is insoluble, and therefore precipitates in the form of small particles.[100] Another popular approach is emulsion polymerization, a technique used to create spherical MIP beads of various dimensions that can be stringently controlled by optimizing the reaction conditions. In this method, surfactant molecules are added to the pre-polymerization mixture, resulting in the formation of spherical beads of surfactant that contain the reagents. The monomers act as oil phases that are shielded from the water phase (the solvent) by the surfactant and undergo cross-linking inside a micro reactor, leading to more homogenous spherical particles with a tuneable shape.[100] Both techniques have been used for the synthesis of MIP particles that were incorporated into sensing devices for glucose detection.[84,92] Although precipitation and emulsion polymerization have been demonstrated on an industrial scale for various other polymer applications, the creation of MIPs for glucose detection on a large scale is not particularly appealing. Emulsion polymerization would require extra purification steps to remove remnant surfactant and although the particles are more homogenous in size, research has shown that the binding affinity of the MIPs is highly heterogenic, as the formation of an emulsion affects the stability of template–monomer interactions during imprinting. Likewise, the very diluted medium in which precipitation polymerization takes place not only results in a low reaction yield, but also leads to an imprinting effect that is mainly based on several low-affinity interactions, leading to MIPs with limited binding affinity and significant batch-to-batch variance.[101]

Electropolymerization

An interesting approach to synthesize molecularly imprinted polymer films that has gained increasing attention from researchers worldwide is electropolymerization. The technique is particularly interesting, as it allows the growth of polymer films in situ onto electrodes by applying electrochemical energy to the system.[74] The advantages over other methods are the high control of the layer thickness and the direct grafting onto the electrode surface,[102,103] resulting in a homogeneous and highly reproducible MIP-functionalized substrate that can be used in electro analysis.[74] This set of

features means that they are serious alternatives to commercial enzyme-based electrodes for glucose sensing, as it would also be relatively straightforward to create large batches of MIP-covered chips in an automated manner. Several papers reported this polymerization technique to obtain electropolymerized MIPs for glucose sensing.[94,104,105,106] In a recent work, a glucose MIP was synthesized on laser-pyrolyzed paper electrodes using 3-amino-4-hydroxybenzoic acid (3,4-AHBA) as a functional monomer.[93] In another published work, a MIP-based screen-printed gold electrode was fabricated by electropolymerizing AAM/N,N'-methylene bis(acrylamide) (NNMBA) in the presence of glucose (**Figure 2.4**). Selectivity analyses of the electropolymerized MIP sensor were carried out using two interfering analytes that coexist in physiological saliva samples, lactose and sucrose.[86]

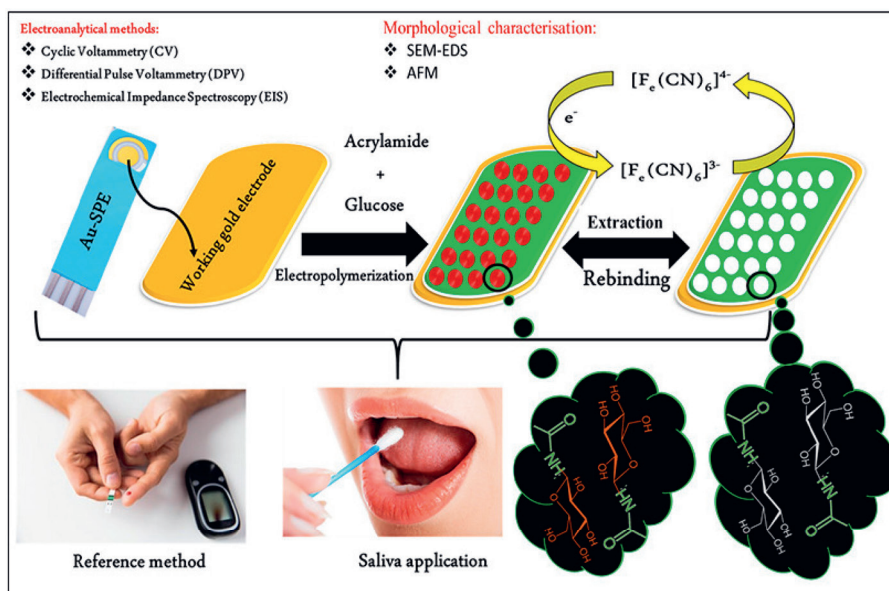


Figure 2.4 Fabrication of a MIP-based Au SPE by electropolymerizing AAM/NNMBA in the presence of glucose and its application in saliva samples. Figure reproduced with permission from ref. [86]. Copyright 2019, Elsevier.

Electropolymerization can also be used to generate gold nanoparticle-decorated MIPs, and the benefits of such a method were reported to be ultra-high sensitivity, cost-effectiveness, and fast fabrication.[78] Another innovation that stems from this production method is the modification of MIPs with carbon dots and chitosan, which yields highly sensitive and selective MIP-based electrochemical sensors.[83,107] The main drawbacks associated with electropolymerization are the possible low degree of cross-linking (which hinders the rigidity of the polymeric structure[108]), the limited choice of electro-active monomers (leading to the troublesome rational design of MIPs for certain specific targets) and the difficult up-scaling of the fabrication process (which inevitably results in a diminished commercial potential for such technologies).[65]

Electrospinning

Electrospinning is a method used to create matrices of micro- to nanoscopic fibres[109] that offer a very high surface-to-volume ratio. This leads to MIPs with relatively high sensitivity in comparison to other approaches.[110] The technique also offers the possibility of creating wearable textiles into which MIPs can easily be integrated for continuous sensing.[111] In 2021 for instance, the use of electrospinning to incorporate glucose MIPs into a nylon-based fibre was reported (**Figure 2.5**). The findings of this study illustrate a two-step production method (MIP synthesis and electrospinning) for the development of MIP-based wearable glucose sensors that can monitor the amount of glucose in sweat as a marker for blood glucose levels.[77] Subsequently, the sensor's selectivity was assessed by exposing the platform to a solution that contained similar molecules (fructose, galactose, and sucrose), in addition to some common constituents of sweat, including urea and L-lactate. The approach is also interesting, as it is possible to mass-produce batches of fibres in a relatively straightforward, fast, and low-cost manner. However, the MIPs still need to be made via a separate polymerization approach. In this case, this occurs via the oxidation of pyrrole and pluronic P123 in bulk.

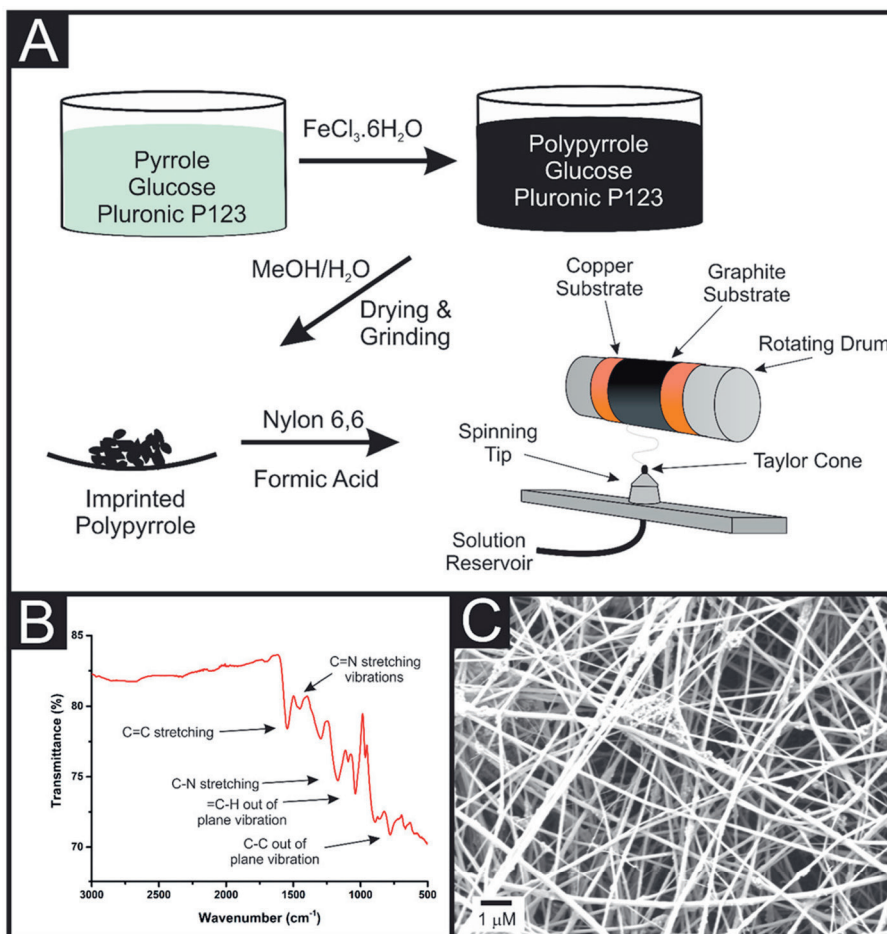


Figure 2.5 (A) Illustration of the production of electrospun MIP sensors. (B) FT-IR analysis of the polypyrrole MIP. (C) Image of electrospun nylon fibres embedded with PPy MIPs for the detection of glucose. Figure reproduced with permission from ref. [77]. Copyright 2021, American Chemical Society.

Photopolymerization

Photopolymerization is a technique that uses the energy of a light source to initiate a polymerization reaction. Although the approach is often similar to thermally induced polymerization techniques, it requires the use of different reagents. Depending on the specific approach applied, photo initiators, photosensitive functional polymers, photo-cross-linkable polymers, and RAFT agents need to be employed in the process.[112]

Similar to thermally induced bulk free-radical polymerization, photo initiated free-radical polymerization is a widely used technique for MIP production. This approach requires a photo initiator

able to initiate the polymerization reaction when exposed to irradiation.[113] The technique has been reported for the synthesis of MIP films/coating for glucose recognition on various substrates, such as QCM electrodes,[114] ITO glass plates,[90] and stainless-steel wires.[91]

Photosensitive functional polymers provide an opportunity to achieve a polymerization reaction without using an initiator reagent by using a photosensitive monomer. This approach has been implemented for the development of a MIP-based glucose electrochemical sensor, by exposing a gold electrode covered with a solution of photosensitive monomers and target to UV irradiation.[108] In two different works, photo-cross-linkable polymers were used to obtain MIP micelles[115] or nanoparticles,[116] which were then electrodeposited onto a bare gold electrode, and finally photo-cross-linked to obtain MIP-functionalized gold electrodes. The specific advantages of each imprinting approach are similar to those in thermally induced methods, allowing the detection of different targets as different polymers can be used, as well as targets that cannot withstand high temperatures. On the other hand, they suffer the same disadvantages that are described above for each polymerization approach and are not compatible with targets that are sensitive to irradiation with high-energy light sources.

Reversible addition–fragmentation chain transfer (RAFT) living polymerization is a photopolymerization approach that allows us to stringently control the polymerization parameters and can be achieved under mild conditions at room temperature in aqueous solutions.[117] RAFT polymerization has been successfully utilized for the synthesis of glucose-imprinted polymer particles, with sizes ranging from 200 to 400 nm. The produced MIPs have proven to be effective in detecting glucose in complex matrices, such as human urine samples.[88]

Novel Synthetic Approaches for Glucose MIPs

The above-mentioned techniques represent the most used techniques for the production of molecularly imprinted polymers. However, in recent years, novel approaches for MIP synthesis have been developed. Between these, the most promising approach is undoubtedly the so-called solid-phase synthesis of nanoMIPs proposed by the group of Prof. Piletsky.[118] This technique has proven its high industrial potential, as it has been utilized in the successful imprinting of a wide variety of targets by using an automated synthesis protocol.[118] The method has also been employed for the fabrication of electroresponsive nanoMIPs for glucose recognition.[119]

Additionally, another approach employed for producing MIP-based glucose sensors involves the production of cross-linked MIP micelles, which were then coupled to glucose oxidase to develop a novel synergistic enzyme MIP detection system.[120]

Table 2.1 Fabrication methods and modifications employed for the production of MIP-based sensing materials for glucose recognition.

Production Method	Approach Modification	Real-Life Sample	LoD	Ref.
Thermal polymerization	MIP particles immobilized onto Al-PVC substrate	Urine	PBS: 19.4 μ M Urine: 44.4 μ M	[87]

Thermal polymerization	MIP-based working electrode	-	43.7 ± 1.6 mV/mmol L ⁻¹	[85]
Thermal polymerization and electrospinning	MIP particles electrospun into nylon 6,6 fibre	Artificial sweat	PBS: 0.10 ± 0.01 mM Artif. sweat: 0.12 ± 0.01 mM	[77]
Thermal polymerization	MIP particles drop-casted onto an Au electrode	-	4.4 mg L ⁻¹	[89]
Thermal polymerization	-	Artificial tear fluid	10 µg mL ⁻¹	[99]
Thermal polymerization	MIP@Ni foam	-	-; 0.45 mM	[82,96]
Precipitation polymerization	GO-MIP sensor	Blood	PBS: 0.02 µm	[84]
Suspension polymerization	MIP-based working electrode	-	53 µM	[92]
Electropolymerization	AuNP-MIP fabricated directly on the gold wire	Blood	PBS and blood: 1.25 nM	[78]
Electropolymerization	MIP-based Au-SPE	Saliva	PBS: 0.59 µg mL ⁻¹ Saliva: 3.32 µM	[86]
Electropolymerization	MIP-based SPCE	Saliva and blood	PBS: 0.19 ± 0.015 µM Saliva and blood: -	[104]
Electropolymerization	MIP/CuCo/SPCE	Artificial and whole blood	PBS: 0.65 ± 0.10 µM Art. blood: 12.02 ± 0.6 mg dL ⁻¹ Whole blood: -	[105]
Electropolymerization	Electrode modified with chitosan and carbon dots	Blood	PBS: 0.09 µM Blood: 0.11 µM	[107]
Electropolymerization	Laser-pyrolyzed paper substrate	-	1.77 mmol dm ⁻³	[93]
Electropolymerization	Electrode modified with chitosan and carbon dots	Blood and rice wine	PBS: 4.6 nM Blood: 6.41 nM Rice wine: -	[83]
Electropolymerization	CS (MIP)-NiO electrode	-	2.0 µM	[106]
Electropolymerization	TNO substrate	-	1.0 µM	[94]
Photopolymerization	MIP layer onto Au QCM electrode	-	0.07 mM	[114]
Photopolymerization	MIP layer onto ITO glass plate	-	-	[90]

Photopolymerization	MIP coating onto stainless-steel wire	Bovine serum, human urine and plant tissues	PBS: 0.7 μ M Real-life samples: -	[91]
Photopolymerization	RAFT polymerized MIPs coating onto GO/GCE substrate	Urine	PBS: 5.88 μ M Urine: -	[88]
Photopolymerization	MIP micelles electrodeposited onto the electrode surface	Simulative serum	Buffer: 0.05 mM Sim. serum: -	[115]
Photopolymerization	Photo-cross-linkable polymer	Simulative serum	Buffer: 0.2 μ g mL ⁻¹ Sim. serum: -	[108]
Photopolymerization	Au@MIP NPs electrodeposited onto the electrode surface	Urine	Buffer: 0.003 nM Urine: -	[116]
Solid-phase synthesis	-	-	0.43 mM	[119]
Cross-linked MIP micelles	Fe ₃ O ₄ @Au-GOx-MIPs catalytic system	-	5.0 μ M	[120]

Readout Technologies Employed for MIP-Based Glucose Detection

In order to convert the binding event between the MIP and target into a readable signal, the imprinted polymer needs to be integrated into a sensor platform, by coupling it to an appropriate readout technology.[121] The choice of the transducer employed for signal conversion is crucial for the development of affordable and reliable biosensors; in fact, many examples of very sensitive MIP-based sensors can be found in the literature, but some of them are coupled with highly specialized and costly lab equipment. These sensor technologies are interesting for high-end detection purposes in analytical labs but are less suited for application in point-of-care diagnosis. The great commercial success of glucometers is due to the fact that they are based on simple conductio- or amperometric transduction principles that can be integrated into handheld applications. Furthermore, they are easily calibrated and lead to a very simple concentration reading that enables end-users to measure their blood glucose levels in a fast, relatively low-cost, and user-friendly manner.[10,122] Since the introduction of the first generation of glucose biosensors, remarkable progress in the development of miniaturized and low-cost glucose sensing technologies, both in terms of substrates (e.g. test strips) and transducers (glucometers), has been made.[123,124] Despite different works reporting novel MIP-based sensors for glucose and many other analytes, the field seems to struggle in the last steps toward the commerciality of such technologies.[65] One of the main explanations for this is the greater interest of the scientific community in fabricating more and more sensitive biosensors, rather than trying to engineer promising technologies to develop more affordable and versatile instruments that offer a commercial benefit to the end-users. In this sense, the most sensitive MIP-based sensors in real-life samples have a limit of detection (LoD) of 1.25 nM in blood,[78] 0.12 mM in artificial sweat,[77] 3.32 μM in saliva,[86] 44.4 μM in urine, (**Chapter 3**)[87] and 55.5 μM in artificial tear fluids.[99] Although the most sensitive MIP-based glucose sensor found in the literature demonstrates a much lower LoD in buffer solutions[116] (0.003 nM) when compared to the above-mentioned works, the fabrication of an ultrasensitive device for glucose detection represents an academic exercise rather than a useful development in health diagnostics. In fact, the concentrations of the sugar in physiological fluids are in the millimolar or micromolar range.

The majority of readout technologies employed for glucose detection using MIPs continued on the tradition of using electrochemical transducer principles to create user-friendly readout technology.[125] The specific techniques that were used include amperometry, voltammetry, potentiometry, and electrochemical impedance spectroscopy. Although electrochemical readouts represent the most validated transducer in the glucose sensing field, in the last few years, different alternative technologies have been successfully coupled to MIP-based platforms for the detection of sugars [126]. Therefore, MIP sensors for glucose that use transducers such as QCM,[114] HTM, (**Chapter 3**)[87] SPR,[127] GC-MS,[91] and fluorescence spectroscopy[99] have started to appear in the last two decades.

MIP-Based Electrochemical Glucose Sensors

Electroanalytical techniques are a collection of different methods that use electrical stimulation to study surface changes upon rebinding of an analyte or the presence of the analyte in solution. As mentioned, the classic glucometers employ amperometry coupled with an enzyme that is able to selectively oxidize glucose; the techniques have also proven their efficacy when coupled to a MIP-based platform.[128,129] In particular, MIP-based amperometric glucose sensors have been fabricated by preparing molecularly imprinted polymer layers onto different types of electrodes.[93,105,106] In a

recently published work, the fabrication of a selective MIP glucose sensor based on the direct oxidation of the molecule on a bimetal catalyst with a MIP was reported (**Figure 2.6**). In this work, the sensor proved to be highly sensitive and demonstrated excellent performance in artificial and whole blood samples using chronoamperometry analysis. Moreover, the selectivity of the MIP-based platform was thoroughly evaluated by the exposure of the sensor to a wide variety of possible interferences (uric acid, acetaminophen, dopamine, ascorbic acid and L-cysteine), other monosaccharides (galactose, mannose, fructose, and xylose) and disaccharides (sucrose, lactose, and maltose).[105]

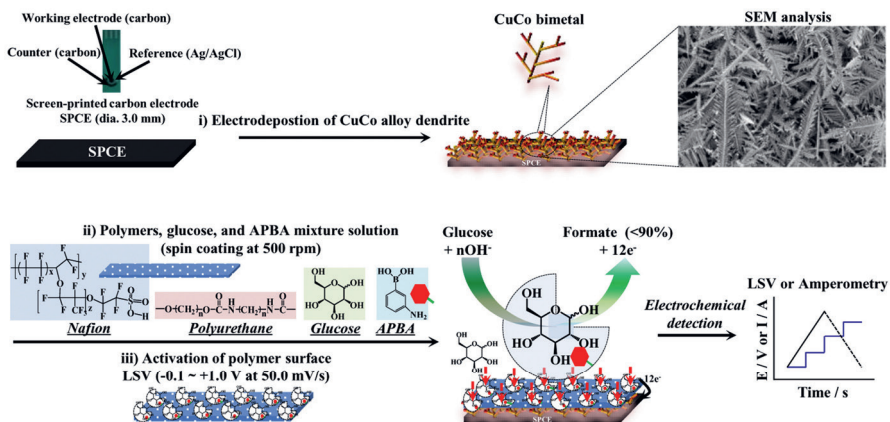


Figure 2.6 Representation of the glucose-imprinted polymer preparation and the two electrochemical readouts employed for the rebinding studies. Figure reproduced with permission from ref. [105]. Copyright 2018, Elsevier.

In MIP-based potentiometric sensors, generally, the MIP is incorporated into a polymeric membrane and then functions as a conventional ionophore of ion-sensitive electrodes.[130] As such, many works about potentiometric MIP sensors have been reported.[130,131] Between these, some research groups have demonstrated the applicability of potentiometric MIP sensors for glucose detection in buffer solutions,[85] as well as in physiological samples, such as saliva and blood.[104] Many MIP-based electrochemical biosensors use voltammetry as an electroanalytical method to detect a specific analyte.[132,133,134] Voltammetric sensors can recognize a target by analysing the current change as a function of the potential applied. Voltammetry can then be subdivided into many different types of techniques, depending on the mode of potential control. As such, techniques such as cyclic voltammetry (CV) [84,90,92,107,115,120], linear sweep voltammetry (LSV),[105] square wave voltammetry, (SWV)[78,88,108] differential pulse voltammetry (DPV)[83,86,94,107,119] and differential pulse stripping voltammetry (DPSV)[116] have been successfully applied in combination with MIP-based technologies for glucose analysis. In these sensors, the MIP acts as a recognition element that is able to selectively bind to the functionalized surface, resulting in a current change when a potential is applied. An unusual approach using a voltammetric MIP sensor can be seen in **Figure 2.7**; in this work, a synergistic enzyme–enzyme mimic (represented by the imprinted polymer) system has been developed and the sensor’s performance was thoroughly evaluated using CV voltammetry. The

fabricated sensor has proven to be highly selective towards D-glucose over three other structural analogues of the sugar (mannose, galactose and D-xylose).

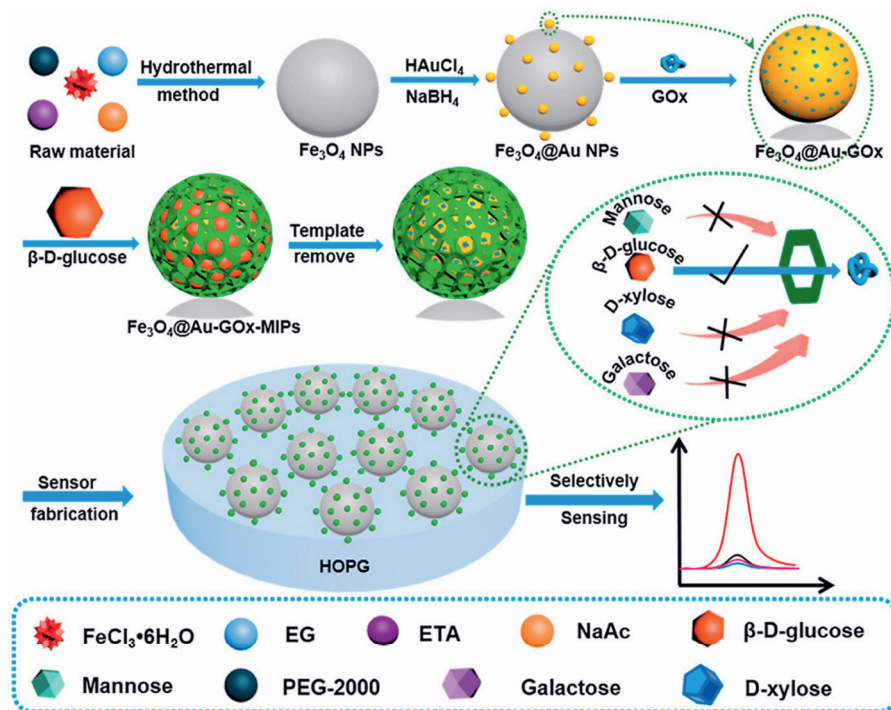


Figure 2.7 Preparation of the Fe₃O₄@Au-GOx-MIPS sensor and representation of the sensing mechanism achieved with CV analysis. Figure reproduced with permission from ref. [120]. Copyright 2022, Elsevier.

Another electrochemical method used in MIP biosensors that has gained attention in the last few years is electrochemical impedance spectroscopy (EIS).[135] Impedimetric MIP biosensors allow the direct detection of a target without using any enzyme labels by measuring changes in charge conductance and capacitance at the sensor surface when the binding event occurs.[135,136] Thus, different impedimetric sensors for non-enzymatic glucose recognition have been developed in the last five years.[82,86,96] Even though several MIP-based electrochemical sensors for glucose detection have demonstrated to be a promising and reliable alternative to enzymatic devices (**Table 2.2**), factors such as their reproducibility in relevant environments and application in different physiological matrices still need to be addressed. In general, electrochemical MIP-based glucose sensors can build on the knowledge obtained in the decades of development in electrochemical enzyme-based glucose sensing. Furthermore, by coupling electrochemical readouts to electrodeposition techniques or electrospinning, there is the potential to use them for continuous monitoring. With this in mind, MIPs function in a different manner than enzymes and no ions are created during binding. Therefore, the effects are usually capacitive and require a reference electrode to distinguish rebinding effects from solvent exchange effects. This makes data interpretation and calibration more difficult. In addition, they require

some instrumentation and can only be combined with electrically conducting chip substrates. Therefore, in contrast to enzyme-based glucose monitoring, where electrochemical approaches have shown to be the most suitable tool, in MIP-based glucose sensing, other non-electrochemical approaches might offer certain benefits from a commercial perspective that allow them to become the most predominantly used technology.

Table 2.2 MIP-based glucose sensors using electrochemical readout technologies.

Readout Technology	Real-Life Sample	LoD	Ref.
Chronoamperometry	-	1.77 mmol dm ⁻³ ; 2.0 μM	[93,106]
Chronoamperometry	Artificial and whole blood	Art. blood: 12.02 ± 0.6 mg dL ⁻¹ Whole blood: -	[105]
Potentiometry	-	43.7 ± 1.6 mV/mmol L ⁻¹	[85]
Potentiometry	Saliva and blood	PBS: 0.19 ± 0.015 μM Saliva and blood: -	[104]
CV	-	0.02 μM;-; 53 μM; 0.09 μM; 5.0 μM	[84,90,92,107,120]
CV	Simulative serum	Buffer: 0.05 mM Sim. serum: -	[115]
SWV	Simulative serum	Buffer: 0.2 μg mL ⁻¹ Sim. serum: -	[108]
SWV	Human urine	PBS: 5.88 μM Urine: -	[88]
SWV	Blood	1.25 nM	[78]
DPV	-	1.0 μM; 0.43 mM	[94,119]
DPV	Blood	PBS: 0.09 μM Blood: 0.11 μM	[107]
DPV	Blood and rice wine	Blood: 6.41 nM Rice wine: -	[83]
DPV	Saliva	PBS: 0.59 μg mL ⁻¹ Saliva: 3.32 μM	[86]
DPSV	Human urine	Buffer: 0.003 nM Urine: -	[116]
EIS	-	-; PBS: 0.59 μg mL ⁻¹ Saliva: 3.32 μM; 0.45 mM	[82,86,96]

Other MIP-Sensing Readout Technologies for Glucose Detection

MIPs are versatile materials that could be integrated into a wide array of non-electrochemical transducers.[52,137] In fact, different works have shown the potential of MIP-based sensors associated with readout technologies that rely on optical, thermal and mass-sensitive methodologies. (**Table 2.3**)[137] The first MIP for glucose recognition was developed more than a decade ago; in this work, molecularly imprinted hydrogels were synthesized and their rebinding capabilities were analysed colorimetrically by using a spectrophotometer.[138] Another colorimetric method (DNS assay) was

successfully employed to evaluate the separation of different sugars from urine samples using imprinted polymers.[139] Although these early applications of colorimetric assays gave a deeper understanding of the binding characteristics of the synthesized polymers, they are not suited for diagnostic applications and, in the case of the latter, were mainly used as separation materials rather than sensing elements [140]. Other optical-based technologies have been effectively employed in combination with imprinted polymers, where the MIP film was directly analysed via different techniques. In two different works, MIP films selective for glucose recognition were prepared onto a gold layer and proof-of-applications in plant tissues or urine were achieved by Raman spectroscopy[141] and surface plasmon resonance (SPR),[127] respectively. Another example of optical readout coupled with MIPs for glucose detection was reported in literature.[99] In this work, a fluorescent MIP film was found to proportionally emit reduced fluorescence with increasing concentrations of glucose in synthetic tear fluids.[99] Optical transducers offer the benefit that they have been used extensively over the past few decades for the highly sensitive detection of numerous compounds in the most advanced analytical applications. For glucose detection, however, they are not suited due to their non-portable and expensive nature. On the other hand, very cheap lateral flow assays, which have also demonstrated great commercial biosensor success, in addition to glucometers (COVID-19 self-tests, pregnancy tests, etc.), have limited application in glucose sensing as they are often qualitative (providing a positive/negative result), while diabetics need to quantify the result. Therefore, the only approach that seems commercially interesting is to work with colorimetric detection principles that allow for quantification by means of a simple handheld spectrophotometer, or even a smartphone camera with an appropriate software package. Recently, a thermal readout principle that is similar to electrochemical approaches but requires less expensive machinery and offers straightforward data interpretation has been demonstrated for glucose detection (**Figure 2.8**). Two studies performed by two different research groups have shown different MIP synthesis approaches and have coupled them to the so-called heat-transfer method (HTM) for the detection of the sugar in artificial,[77] as well as physiological, samples.[87] In one of these works, selectivity analyses were performed by analysing the thermal response of the sensor to three different saccharides (fructose, lactose and sucrose) and demonstrated the sensor's ability to discriminate between these small molecules. (**Chapter 3**)[87] The approach is very simple, as glucose MIPs are immobilized onto a cheap chip substrate, and a temperature gradient is applied over the chip using two thermometers and a heat source. Rebinding of glucose leads to a concentration-dependent change in this gradient. The method is extremely low-cost, requiring little to no equipment and data interpretation is very simple, leading to facile calibration. The main problem with HTM as readout technology resides in the difficult miniaturization of the transducer and the need to equilibrate the signal, which, therefore, limits its application in wearable applications for continuous monitoring.

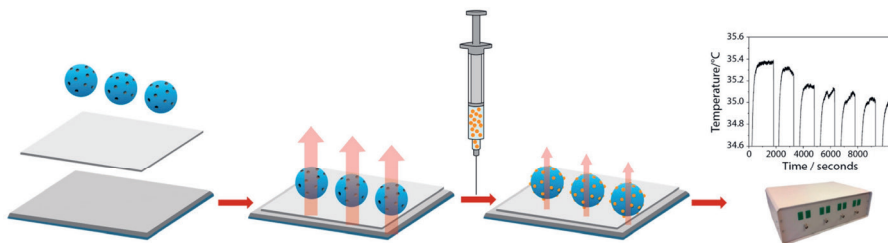


Figure 2.8 Representation of HTM analysis after glucose rebinding to the MIP-based platform. Figure reproduced with permission from ref. [87].

In a work from 2016, a MIP biocompatible probe was developed and coupled with GC-MS for specific glucose monitoring in bovine serum, human urine and plant tissues (aloe leaf).[91] Although the work demonstrates the successful application of the probe in different matrices, the coupling with a technology such as GC-MS highly limits the possibilities of the sensors, due to the costs and the need for trained professionals to operate the instrument. Another non-electrochemical readout technology effectively employed in recent years in the field of MIP-based sensing is quartz crystal microbalance (QCM).[44] Mass-sensitive devices have been used by two different research groups in combination with MIP-coated QCM chips for glucose detection.[89,114] Although linear dose–response curves were obtained with increasing sugar levels, a real-life sample application is needed to accurately evaluate the sensor’s performance in a relevant environment. Moreover, QCMs are hard to miniaturize and mass produce, require gold-coated quartz substrates, which are relatively costly, and it is hard to distinguish specific rebinding from non-specific adsorption and medium change, making this approach a little less attractive from a commercial point of view.

Table 2.3 MIP-based sensors coupled with non-electrochemical readout technologies.

Readout Technology	Real-Life Sample	LoD	Ref.
Raman	Apple	PBS: $1 \mu\text{g mL}^{-1}$ Apple: -	[141]
SPR	Urine	-	[127]
Fluorescence spectroscopy	Artificial tear fluid	$10 \mu\text{g mL}^{-1}$	[99]
HTM	Artificial sweat	PBS: $0.10 \pm 0.01 \text{ mM}$ Artif. sweat: $0.12 \pm 0.01 \text{ mM}$	[77]
HTM	Urine	PBS: $19.4 \mu\text{M}$ Urine: $44.4 \mu\text{M}$	[87]
GC-MS	Bovine serum, human urine and plant tissues	PBS: $0.7 \mu\text{M}$ Real-life samples: -	[91]
QCM	-	4.4 mg L^{-1} ; 0.07 mM	[89,114]

Promising MIP-Based Technologies for Glucose Sensing

The success of enzyme-based home glucose monitoring can be explained by the fact that there was a large market need, as diabetics previously had no means of routinely assessing their blood glucose levels. This has led to a significant improvement in diabetic treatment and, as a result, the life quality of patients. Since their conception, electrochemical enzymatic glucose sensors have evolved tremendously and have dominated the market. Nonetheless, as the need for continuous monitoring devices and cheaper handheld solutions will continue to increase in the coming years, research towards new and improved ways of measuring glucose will also continue. Therefore, some of the MIP-based glucose sensors developed in the last few years could offer a valid alternative, especially in certain subfields that require specific device characteristics. Although MIPs and MIP sensors are still considered by many as a niche research area, mainly because of the absence of MIP sensors on the market, we conclude that some promising studies on MIP glucose sensors are present in the literature and should be further evaluated to reduce the gap with traditional enzymatic sensors (**Table 2.4**).

Table 2.4 Overview of promising MIP technologies for glucose sensing.

Readout Technology	MIPs Production Method	Real-Life Sample	LoD	Ref.
Chronoamperometry	Electropolymerization	Artificial and whole blood	Art. blood: $12.02 \pm 0.6 \text{ mg dL}^{-1}$ Whole blood: -	[105]
Potentiometry	Electropolymerization	Saliva and blood	PBS: $0.19 \pm 0.015 \mu\text{M}$ Saliva and blood: -	[104]
CV	Photopolymerization + electrodeposition	Simulative serum	Buffer: 0.05 mM Sim. serum: -	[115]
SWV	Photopolymerization	Simulative serum	Buffer: $0.2 \mu\text{g mL}^{-1}$ Sim. serum: -	[108]
SWV	Photopolymerization (RAFT)	Human urine	PBS: $5.88 \mu\text{M}$ Urine: -	[88]
SWV	Electropolymerization	Blood	1.25 nM	[78]
DPV	Electropolymerization	Blood	PBS: $0.09 \mu\text{M}$ Blood: $0.11 \mu\text{M}$	[107]
DPV	Electropolymerization	Blood and rice wine	Blood: 6.41 nM Rice wine: -	[83]
DPV	Electropolymerization	Saliva	PBS: $0.59 \mu\text{g mL}^{-1}$ Saliva: $3.32 \mu\text{M}$	[86]
DPV	Solid-phase synthesis	-	0.43 mM	[119]
DPSV	Photopolymerization + electrodeposition	Human urine	Buffer: 0.003 nM Urine: -	[116]
Fluorescence spectroscopy	Thermal polymerization	Artificial tear fluid	$10 \mu\text{g mL}^{-1}$	[99]
HTM	Thermal polymerization + electrospinning	Artificial sweat	PBS: $0.10 \pm 0.01 \text{ mM}$ Artif. sweat: $0.12 \pm 0.01 \text{ mM}$	[77]
HTM	Bulk polymerization	Urine	PBS: $19.4 \mu\text{M}$ Urine: $44.4 \mu\text{M}$	[87]

Chronoamperometry	Electropolymerization	Artificial and whole blood	Art. blood: 12.02 ± 0.6 mg dL ⁻¹ Whole blood: -	[105]
Potentiometry	Electropolymerization	Saliva and blood	PBS: 0.19 ± 0.015 μM Saliva and blood: -	[104]
CV	Photopolymerization + electrodeposition	Simulative serum	Buffer: 0.05 mM Sim. serum: -	[115]
SWV	Photopolymerization	Simulative serum	Buffer: 0.2 μg mL ⁻¹ Sim. serum: -	[108]
SWV	Photopolymerization (RAFT)	Human urine	PBS: 5.88 μM Urine: -	[88]
SWV	Electropolymerization	Blood	1.25 nM	[78]
DPV	Electropolymerization	Blood	PBS: 0.09 μM Blood: 0.11 μM	[107]
DPV	Electropolymerization	Blood and rice wine	Blood: 6.41 nM Rice wine: -	[83]
DPV	Electropolymerization	Saliva	PBS: 0.59 μg mL ⁻¹ Saliva: 3.32 μM	[86]
DPV	Solid-phase synthesis	-	0.43 mM	[119]
DPSV	Photopolymerization + electrodeposition	Human urine	Buffer: 0.003 nM Urine: -	[116]
Fluorescence spectroscopy	Thermal polymerization	Artificial tear fluid	10 μg mL ⁻¹	[99]
HTM	Thermal polymerization + electrospinning	Artificial sweat	PBS: 0.10 ± 0.01 mM Artif. sweat: 0.12 ± 0.01 mM	[77]
HTM	Bulk polymerization	Urine	PBS: 19.4 μM Urine: 44.4 μM	[87]

The different characteristics of the sensor should be taken into account when analysing the valorisation potential of a sensing device. The major bottleneck in terms of commercialization in MIP-based glucose sensing lies in the synthesis approach of the receptors. Mass production is still largely missing with regard to MIPs, although several methods could offer a solution in the future. Bulk polymerization could be an interesting approach if the heterogeneity can be addressed or accounted for through calibration. However, the process of grinding, sieving, and extraction should be optimized and automated. More controlled approaches of photo- and thermal polymerization might overcome the heterogeneity issue in the future. Notwithstanding, at this point the yield of these approaches needs to be approved to make these approaches commercially viable. A potential solution might be to integrate the MIPs directly into a sensing substrate. This can be achieved by directly immobilizing the MIPs onto an electrically conducting surface through electropolymerization or by impregnating MIPs into fibres by, e.g. electrospinning or electrodepositions. Both methods are currently not scalable and additional research has to be conducted, but one can envision that it should be possible to automate the production process and produce large batches of homogenous MIP-covered chips. For now, the synthesis approach that appears to be the most mature in terms of commercialization is the solid-phase approach that can be automated in a reactor. The reaction yield needs to be improved, but significant

progress has been made in this respect in recent years. Although the scalability of the MIP synthesis procedure entails the largest bottleneck concerning their commercialization, transducers undoubtedly play a key role in the development of competitive glucose sensors. Expensive and inaccessible transducers (e.g. GC-MS, Raman spectrometers and SPR systems) are greatly disadvantaged in the development of PoC sensors, which is the main application for glucose sensors. Therefore, affordable and miniaturized readout technologies represent the election choice and between these, electrochemical readout technologies have made astonishing improvements in terms of affordability, miniaturization, and reliability. They profit from the commercial advances made in enzyme-based sensing and are compatible with some of the most promising MIP synthesis approaches, allowing for continuous monitoring approaches. Optical readout techniques, as mentioned before, are typically either very sensitive and used for lab-based sample analysis or extremely low-cost and user-friendly and used for qualitative diagnosis. However, as illustrated in the study mentioned in the table above, it would also be possible to use a handheld optical detector. In this case, a fluorescent spectroscopy approach was tested, which technically could be used for handheld sensing, but the requirement of an excitation source and fluorescent labels/monomers makes the technology more sensitive and also probably more expensive than electrochemical alternatives. A colorimetric alternative could offer a solution to this problem in the future. The HTM approach also has its benefits, mainly laying in the minimum amount of instrumentation required and the straightforward data interpretation, but miniaturization still has to be achieved and researched. Despite the fact that none of the MIP-based glucose sensors are at the stage of commercialization yet due to the bottlenecks discussed above, the performance of these sensors is rapidly increasing. Some of them reach sensitivities that are superior to those of enzyme-based platforms at a much lower cost, not only achieving detection in blood, but also in other matrices such as urine and sweat. As we move towards the non-invasive monitoring of glucose, these bodily fluids offer several advantages. The concentration in these samples is typically lower, but the MIP-based sensors have proven to have linear ranges in relevant concentration regimes, which offers a commercial advantage over the traditional glucometers.

Conclusions

Recent advances in MIP-based sensor technology published in academic studies demonstrate that these devices are rapidly approaching real-life applications. Their long shelf-life, chemical stability, and low cost make them advantageous over enzymes. In addition, these devices have proven to work in challenging environments such as urine and sweat that contain lower concentrations of glucose. This illustrates their potential application in non-invasive and continuous monitoring tools. However, the main bottleneck that must be addressed remains in the synthesis of large batches of homogenous MIPs. This facet of MIP technology has long been neglected, while enzymatic biosensors, as well as immunosensors, have benefited from decades to even centuries of research on the function, synthesis, and immobilization of these natural receptors.

Slowly, MIP technology is trying to close this gap, with scholars devoting attention to MIP synthesis procedures that not only lead to highly performant MIPs from an academic perspective, but also take the potential scalability and possibility for mass production into account. Technologies such as solid-phase synthesis that takes place in automated reactors or fully automated electrospinning or electropolymerization approaches are rapidly evolving in this direction and multiple research groups are investigating ways to improve the more traditional approaches in this respect. As a result, we believe that MIP-based technologies may be a strong alternative to traditional enzymatic devices in the future and, by addressing the aforementioned obstacles to their commercialization, may finally reach the market. In combination with the continuously growing need for personalized medicine and non-invasive sampling, MIP-based glucose sensors could profit from the momentum and academic know-how in the coming decade or two, to achieve the next step towards commercialization, and therefore real-life application.

References Chapter 2

1. Gerich, J.E.; Meyer, C.; Woerle, H.J.; Stumvoll, M. Renal Gluconeogenesis. *Diabetes Care* 2001, 24, 382–391, doi:10.2337/diacare.24.2.382.
2. Andrali, S.S.; Qian, Q.; Özcan, S. Glucose Mediates the Translocation of NeuroD1 by O-Linked Glycosylation. *Journal of Biological Chemistry* 2007, 282, 15589–15596, doi:10.1074/jbc.M701762200.
3. Deshpande, A.D.; Harris-Hayes, M.; Schootman, M. Epidemiology of Diabetes and Diabetes-Related Complications. *Phys. Ther.* 2008, 88, 1254–1264, doi:10.2522/ptj.20080020.
4. Arnoux, J.-B.; de Lonlay, P.; Ribeiro, M.-J.; Hussain, K.; Blankenstein, O.; Mohnike, K.; Valayannopoulos, V.; Robert, J.-J.; Rahier, J.; Sempoux, C.; et al. Congenital Hyperinsulinism. *Early Hum. Dev.* 2010, 86, 287–294, doi:10.1016/j.earlhumdev.2010.05.003.
5. Egan, A.M.; Dinneen, S.F. What Is Diabetes? *Medicine* 2019, 47, 1–4, doi:10.1016/j.mpmed.2018.10.002.
6. Tao, Z.; Shi, A.; Zhao, J. Epidemiological Perspectives of Diabetes. *Cell Biochem. Biophys.* 2015, 73, 181–185, doi:10.1007/s12013-015-0598-4.
7. Gregg, E.W.; Sattar, N.; Ali, M.K. The Changing Face of Diabetes Complications. *Lancet Diabetes Endocrinol.* 2016, 4, 537–547, doi:10.1016/S2213-8587(16)30010-9.
8. Saeedi, P.; Petersohn, I.; Salpea, P.; Malanda, B.; Karuranga, S.; Unwin, N.; Colagiuri, S.; Guariguata, L.; Motala, A.A.; Ogurtsova, K.; et al. Global and Regional Diabetes Prevalence Estimates for 2019 and Projections for 2030 and 2045: Results from the International Diabetes Federation Diabetes Atlas, 9th Edition. *Diabetes Res. Clin. Pract.* 2019, 157, 107843, doi:10.1016/j.diabres.2019.107843.
9. Cole, J.B.; Florez, J.C. Genetics of Diabetes Mellitus and Diabetes Complications. *Nat. Rev. Nephrol.* 2020, 16, 377–390, doi:10.1038/s41581-020-0278-5.
10. Zhu, H.; Li, L.; Zhou, W.; Shao, Z.; Chen, X. Advances in Non-Enzymatic Glucose Sensors Based on Metal Oxides. *J. Mater. Chem. B* 2016, 4, 7333–7349, doi:10.1039/C6TB02037B.
11. Hina, A.; Saadeh, W. Noninvasive Blood Glucose Monitoring Systems Using Near-Infrared Technology—A Review. *Sensors* 2022, 22, 4855, doi:10.3390/s22134855.
12. Hirsch, I. Introduction: History of Glucose Monitoring. *ADA Clinical Compendia* 2018, 2018, 1–1, doi:10.2337/db20181-1.
13. Clark, L.C.; Lyons, C. Electrode Systems for Continuous Monitoring in Cardiovascular Surgery. *Annals of the New York Academy of sciences* 2006, 102, 29–45, doi:10.1111/j.1749-6632.1962.tb13623.x.
14. Clarke, S.F.; Foster, J.R. A History of Blood Glucose Meters and Their Role in Self-Monitoring of Diabetes Mellitus. *Br. J. Biomed. Science* 2012, 69, 83–93, doi:10.1080/09674845.2012.12002443.

15. Olczuk, D.; Priefer, R. A History of Continuous Glucose Monitors (CGMs) in Self-Monitoring of Diabetes Mellitus. *Diabetes & Metabolic Syndrome: Clinical Research & Reviews* 2018, 12, 181–187, doi:10.1016/j.dsx.2017.09.005.
16. Adeel, M.; Asif, K.; Rahman, Md.M.; Daniele, S.; Canzonieri, V.; Rizzolio, F. Glucose Detection Devices and Methods Based on Metal–Organic Frameworks and Related Materials. *Adv. Funct. Mater.* 2021, 31, 2106023, doi:10.1002/adfm.202106023.
17. Okuda-Shimazaki, J.; Yoshida, H.; Sode, K. FAD Dependent Glucose Dehydrogenases – Discovery and Engineering of Representative Glucose Sensing Enzymes. *Bioelectrochemistry* 2020, 132, 107414, doi:10.1016/j.bioelechem.2019.107414.
18. Ferri, S.; Kojima, K.; Sode, K. Review of Glucose Oxidases and Glucose Dehydrogenases: A Bird’s Eye View of Glucose Sensing Enzymes. *J. Diabetes Science Technol* 2011, 5, 1068–1076, doi:10.1177/193229681100500507.
19. Park, S.; Boo, H.; Chung, T.D. Electrochemical Non-Enzymatic Glucose Sensors. *Anal. Chim. Acta* 2006, 556, 46–57, doi:10.1016/j.aca.2005.05.080.
20. Adeniyi, O.; Nwahara, N.; Mwanza, D.; Nyokong, T.; Mashazi, P. High-Performance Non-Enzymatic Glucose Sensing on Nanocomposite Electrocatalysts of Nickel Phthalocyanine Nanorods and Nitrogen Doped-Reduced Graphene Oxide Nanosheets. *Appl. Surf. Sci.* 2023, 609, 155234, doi:10.1016/j.apsusc.2022.155234.
21. Naikoo, G.A.; Awan, T.; Salim, H.; Arshad, F.; Hassan, I.U.; Pedram, M.Z.; Ahmed, W.; Faruck, H.L.; Aljabali, A.A.A.; Mishra, V.; et al. Fourth-generation Glucose Sensors Composed of Copper Nanostructures for Diabetes Management: A Critical Review. *Bioeng. Transl. Med.* 2022, 7, doi:10.1002/btm2.10248.
22. Petrulėvičienė, M.; Juodkazytė, J.; Savickaja, I.; Karpicz, R.; Morkvenaite-Vilkonciene, I.; Ramanavicius, A. BiVO₄-Based Coatings for Non-Enzymatic Photoelectrochemical Glucose Determination. *Journal of Electroanalytical Chemistry* 2022, 918, 116446, doi:10.1016/j.jelechem.2022.116446.
23. Vashist, S.K. Non-Invasive Glucose Monitoring Technology in Diabetes Management: A Review. *Anal. Chim. Acta* 2012, 750, 16–27, doi:10.1016/j.aca.2012.03.043.
24. Wilkins, E.; Atanasov, P. Glucose Monitoring: State of the Art and Future Possibilities. *Med. Eng. Phys.* 1996, 18, 273–288, doi:10.1016/1350-4533(95)00046-1.
25. al Hayek, A.A.; Robert, A.A.; al Dawish, M.A. Differences of FreeStyle Libre Flash Glucose Monitoring System and Finger Pricks on Clinical Characteristics and Glucose Monitoring Satisfactions in Type 1 Diabetes Using Insulin Pump. *Clin Med Insights Endocrinol. Diabetes* 2019, 12, 117955141986110, doi:10.1177/1179551419861102.
26. Heinemann, L. Finger Pricking and Pain: A Never Ending Story. *J. Diabetes Science Technol* 2008, 2, 919–921, doi:10.1177/193229680800200526.

27. Jain, P.; Joshi, A.M.; Mohanty, S.P. IGLU: An Intelligent Device for Accurate Noninvasive Blood Glucose-Level Monitoring in Smart Healthcare. *IEEE Consumer Electronics Magazine* 2020, 9, 35–42, doi:10.1109/MCE.2019.2940855.
28. Lee, H.; Hong, Y.J.; Baik, S.; Hyeon, T.; Kim, D. Enzyme-Based Glucose Sensor: From Invasive to Wearable Device. *Adv. Healthcare Mater.* 2018, 7, 1701150, doi:10.1002/adhm.201701150.
29. Tang, L.; Chang, S.J.; Chen, C.-J.; Liu, J.-T. Non-Invasive Blood Glucose Monitoring Technology: A Review. *Sensors* 2020, 20, 6925, doi:10.3390/s20236925.
30. Ferrante do Amaral, C.E.; Wolf, B. Current Development in Non-Invasive Glucose Monitoring. *Med. Eng. Phys.* 2008, 30, 541–549, doi:10.1016/J.MEDENGGPHY.2007.06.003.
31. Delbeck, S.; Vahlsing, T.; Leonhardt, S.; Steiner, G.; Heise, H.M. Non-Invasive Monitoring of Blood Glucose Using Optical Methods for Skin Spectroscopy—Opportunities and Recent Advances. *Anal. Bioanal. Chem.* 2019, 411, 63–77, doi:10.1007/s00216-018-1395-x.
32. Villena Gonzales, W.; Mobashsher, A.; Abbosh, A. The Progress of Glucose Monitoring—A Review of Invasive to Minimally and Non-Invasive Techniques, Devices and Sensors. *Sensors* 2019, 19, 800, doi:10.3390/s19040800.
33. Salim, A.; Lim, S. Recent Advances in Noninvasive Flexible and Wearable Wireless Biosensors. *Biosens. Bioelectron.* 2019, 141, 111422, doi:10.1016/j.bios.2019.111422.
34. Jin, X.; Liu, C.; Xu, T.; Su, L.; Zhang, X. Artificial Intelligence Biosensors: Challenges and Prospects. *Biosens. Bioelectron.* 2020, 165, 112412, doi:10.1016/j.bios.2020.112412.
35. Johnston, L.; Wang, G.; Hu, K.; Qian, C.; Liu, G. Advances in Biosensors for Continuous Glucose Monitoring Towards Wearables. *Front. Bioeng. Biotechnol.* 2021, 9, doi:10.3389/fbioe.2021.733810.
36. Zhao, J.; Lin, Y.; Wu, J.; Nyein, H.Y.Y.; Bariya, M.; Tai, L.-C.; Chao, M.; Ji, W.; Zhang, G.; Fan, Z.; et al. A Fully Integrated and Self-Powered Smartwatch for Continuous Sweat Glucose Monitoring. *ACS Sens.* 2019, 4, 1925–1933, doi:10.1021/acssensors.9b00891.
37. Bolla, A.S.; Priefer, R. Blood Glucose Monitoring- an Overview of Current and Future Non-Invasive Devices. *Diabetes & Metabolic Syndrome: Clinical Research & Reviews* 2020, 14, 739–751, doi:10.1016/j.dsx.2020.05.016.
38. Parisi, O.I.; Francomano, F.; Dattilo, M.; Patitucci, F.; Prete, S.; Amone, F.; Puoci, F. The Evolution of Molecular Recognition: From Antibodies to Molecularly Imprinted Polymers (MIPs) as Artificial Counterpart. *J. Funct. Biomater.* 2022, 13, 12, doi:10.3390/jfb13010012.
39. Spivak, D. Optimization, Evaluation, and Characterization of Molecularly Imprinted Polymers. *Adv. Drug Deliv. Rev.* 2005, 57, 1779–1794, doi:10.1016/j.addr.2005.07.012.
40. Saylan, Y.; Akgönüllü, S.; Yavuz, H.; Ünal, S.; Denizli, A. Molecularly Imprinted Polymer Based Sensors for Medical Applications. *Sensors* 2019, 19, 1279, doi:10.3390/s19061279.

41. Yan, H.; Row, K. Characteristic and Synthetic Approach of Molecularly Imprinted Polymer. *Int. J. Mol. Sci.* 2006, 7, 155–178, doi:10.3390/i7050155.
42. Wackerlig, J.; Lieberzeit, P.A. Molecularly Imprinted Polymer Nanoparticles in Chemical Sensing – Synthesis, Characterisation and Application. *Sens. Actuators B Chem.* 2015, 207, 144–157, doi:10.1016/j.snb.2014.09.094.
43. Liu, G.; Huang, X.; Li, L.; Xu, X.; Zhang, Y.; Lv, J.; Xu, D. Recent Advances and Perspectives of Molecularly Imprinted Polymer-Based Fluorescent Sensors in Food and Environment Analysis. *Nanomaterials* 2019, 9, 1030, doi:10.3390/nano9071030.
44. Emir Diltemiz, S.; Keçili, R.; Ersöz, A.; Say, R. Molecular Imprinting Technology in Quartz Crystal Microbalance (QCM) Sensors. *Sensors* 2017, 17, 454, doi:10.3390/s17030454.
45. Nawaz, T.; Ahmad, M.; Yu, J.; Wang, S.; Wei, T. A Recyclable Tetracycline Imprinted Polymeric SPR Sensor: In Synergy with Itaconic Acid and Methacrylic Acid. *New Journal of Chemistry* 2021, 45, 3102–3111, doi:10.1039/D0NJ05364C.
46. Malitesta, C.; Mazzotta, E.; Picca, R.A.; Poma, A.; Chianella, I.; Piletsky, S.A. MIP Sensors – the Electrochemical Approach. *Anal. Bioanal. Chem.* 2012, 402, 1827–1846, doi:10.1007/s00216-011-5405-5.
47. Bers, K.; Eersels, K.; van Grinsven, B.; Daemen, M.; Bogie, J.F.J.; Hendriks, J.J.A.; Bouwmans, E.E.; Püttmann, C.; Stein, C.; Barth, S.; et al. Heat-Transfer Resistance Measurement Method (HTM)-Based Cell Detection at Trace Levels Using a Progressive Enrichment Approach with Highly Selective Cell-Binding Surface Imprints. *Langmuir* 2014, 30, 3631–3639, doi:10.1021/la5001232.
48. Polyakov, M.; Stadnik, P.; Paryckij, M.; Malkin, I.; Duchina, F. On the Structure of Silica. *Zhurnal Fizieskoj Khimii* 1933, 454–456.
49. Polyakov, M. v; Kuleshina, L.; Neimark, I. On the Dependence of Silica Gel Adsorption Properties on the Character of Its Porosity. *Zhurnal Fizieskoj Khimii* 1937, 10, 100–112.
50. Wulff, G.; Poll, H.-G.; Minárik, M. Enzyme-Analogue Built Polymers. XIX. Racemic Resolution on Polymers Containing Chiral Cavities. *J. Liq. Chromatogr.* 1986, 9, 385–405, doi:10.1080/01483918608076643.
51. Andersson, L.; Sellergren, B.; Mosbach, K. Imprinting of Amino Acid Derivatives in Macroporous Polymers. *Tetrahedron Lett.* 1984, 25, 5211–5214, doi:10.1016/S0040-4039(01)81566-5.
52. BelBruno, J.J. Molecularly Imprinted Polymers. *Chem. Rev.* 2019, 119, 94–119, doi:10.1021/acs.chemrev.8b00171.
53. Zhang, H. Molecularly Imprinted Nanoparticles for Biomedical Applications. *Advanced Materials* 2020, 32, 1806328, doi:10.1002/adma.201806328.
54. Crapnell, R.; Hudson, A.; Foster, C.; Eersels, K.; Grinsven, B.; Cleij, T.; Banks, C.; Peeters, M. Recent Advances in Electrosynthesized Molecularly Imprinted Polymer Sensing Platforms for Bioanalyte Detection. *Sensors* 2019, 19, 1204, doi:10.3390/s19051204.

55. Lowdon, J.W.; Eersels, K.; Arreguin-Campos, R.; Caldara, M.; Heidt, B.; Rogosic, R.; Jimenez-Monroy, K.L.; Cleij, T.J.; Diliën, H.; van Grinsven, B. A Molecularly Imprinted Polymer-Based Dye Displacement Assay for the Rapid Visual Detection of Amphetamine in Urine. *Molecules* 2020, 25, 5222, doi:10.3390/molecules25225222.
56. Caldara, M.; Lowdon, J.W.; Royakkers, J.; Peeters, M.; Cleij, T.J.; Diliën, H.; Eersels, K.; van Grinsven, B. A Molecularly Imprinted Polymer-Based Thermal Sensor for the Selective Detection of Melamine in Milk Samples. *Foods* 2022, 11, 2906, doi:10.3390/foods11182906.
57. Arreguin-Campos, R.; Frigoli, M.; Caldara, M.; Crapnell, R.D.; Ferrari, A.G.-M.; Banks, C.E.; Cleij, T.J.; Diliën, H.; Eersels, K.; van Grinsven, B. Functionalized Screen-Printed Electrodes for the Thermal Detection of Escherichia Coli in Dairy Products. *Food Chem.* 2023, 404, 134653, doi:10.1016/j.foodchem.2022.134653.
58. Fernando, P.U.A.I.; Glasscott, M.W.; Pokrzywinski, K.; Fernando, B.M.; Kosgei, G.K.; Moores, L.C. Analytical Methods Incorporating Molecularly Imprinted Polymers (MIPs) for the Quantification of Microcystins: A Mini-Review. *Crit. Rev. Anal. Chem.* 2022, 52, 1244–1258, doi:10.1080/10408347.2020.1868284.
59. Haupt, K.; Mosbach, K. Plastic Antibodies: Developments and Applications. *Trends Biotechnol.* 1998, 16, 468–475, doi:10.1016/S0167-7799(98)01222-0.
60. Majdinasab, M.; Daneshi, M.; Louis Marty, J. Recent Developments in Non-Enzymatic (Bio)Sensors for Detection of Pesticide Residues: Focusing on Antibody, Aptamer and Molecularly Imprinted Polymer. *Talanta* 2021, 232, 122397, doi:10.1016/j.talanta.2021.122397.
61. Dong, Q.; Ryu, H.; Lei, Y. Metal Oxide Based Non-Enzymatic Electrochemical Sensors for Glucose Detection. *Electrochim. Acta* 2021, 370, 137744, doi:10.1016/j.electacta.2021.137744.
62. Adeel, M.; Rahman, Md.M.; Caligiuri, I.; Canzonieri, V.; Rizzolio, F.; Daniele, S. Recent Advances of Electrochemical and Optical Enzyme-Free Glucose Sensors Operating at Physiological Conditions. *Biosens. Bioelectron.* 2020, 165, 112331, doi:10.1016/j.bios.2020.112331.
63. Chen, X.; Wu, G.; Cai, Z.; Oyama, M.; Chen, X. Advances in Enzyme-Free Electrochemical Sensors for Hydrogen Peroxide, Glucose, and Uric Acid. *Microchimica Acta* 2014, 181, 689–705, doi:10.1007/s00604-013-1098-0.
64. Bedwell, T.S.; Whitcombe, M.J. Analytical Applications of MIPs in Diagnostic Assays: Future Perspectives. *Anal. Bioanal. Chem.* 2016, 408, 1735–1751, doi:10.1007/s00216-015-9137-9.
65. Lowdon, J.W.; Diliën, H.; Singla, P.; Peeters, M.; Cleij, T.J.; van Grinsven, B.; Eersels, K. MIPs for Commercial Application in Low-Cost Sensors and Assays – An Overview of the Current Status Quo. *Sens. Actuators B Chem* 2020, 325, 128973, doi:10.1016/j.snb.2020.128973.
66. Boselli, L.; Pomili, T.; Donati, P.; Pompa, P.P. Nanosensors for Visual Detection of Glucose in Biofluids: Are We Ready for Instrument-Free Home-Testing? *Materials* 2021, 14, 1978, doi:10.3390/ma14081978.

67. Refaat, D.; Aggour, M.G.; Farghali, A.A.; Mahajan, R.; Wiklander, J.G.; Nicholls, I.A.; Piletsky, S.A. Strategies for Molecular Imprinting and the Evolution of MIP Nanoparticles as Plastic Antibodies—Synthesis and Applications. *Int. J. Mol. Sci.* 2019, 20, 6304, doi:10.3390/ijms20246304.
68. He, S.; Zhang, L.; Bai, S.; Yang, H.; Cui, Z.; Zhang, X.; Li, Y. Advances of Molecularly Imprinted Polymers (MIP) and the Application in Drug Delivery. *Eur. Polym. J.* 2021, 143, 110179, doi:10.1016/j.eurpolymj.2020.110179.
69. Yilmaz, E.; Mosbach, K.; Haupt, K. Influence of Functional and Cross-Linking Monomers and the Amount of Template on the Performance of Molecularly Imprinted Polymers in Binding Assays. *Analytical Communications* 1999, 36, 167–170, doi:10.1039/a901339c.
70. Lowdon, J.W.; Ishikura, H.; Kvernenes, M.K.; Caldara, M.; Cleij, T.J.; van Grinsven, B.; Eersels, K.; Diliën, H. Identifying Potential Machine Learning Algorithms for the Simulation of Binding Affinities to Molecularly Imprinted Polymers. *Computation* 2021, 9, 103, doi:10.3390/computation9100103.
71. Dong, W.; Yan, M.; Zhang, M.; Liu, Z.; Li, Y. A Computational and Experimental Investigation of the Interaction between the Template Molecule and the Functional Monomer Used in the Molecularly Imprinted Polymer. *Anal. Chim. Acta* 2005, 542, 186–192, doi:10.1016/j.aca.2005.03.032.
72. Boysen, R.I.; Schwarz, L.J.; Nicolau, D. v.; Hearn, M.T.W. Molecularly Imprinted Polymer Membranes and Thin Films for the Separation and Sensing of Biomacromolecules. *J. Sep. Sci.* 2017, 40, 314–335, doi:10.1002/jssc.201600849.
73. Pichon, V.; Delaunay, N.; Combès, A. Sample Preparation Using Molecularly Imprinted Polymers. *Anal. Chem* 2020, 92, 16–33, doi:10.1021/acs.analchem.9b04816.
74. Moreira Gonçalves, L. Electropolymerized Molecularly Imprinted Polymers: Perceptions Based on Recent Literature for Soon-to-Be World-Class Scientists. *Curr. Opin. Electrochem.* 2021, 25, 100640, doi:10.1016/j.coelec.2020.09.007.
75. Paruli, E.I.; Soppera, O.; Haupt, K.; Gonzato, C. Photopolymerization and Photostructuring of Molecularly Imprinted Polymers. *ACS Appl. Polym. Mater.* 2021, 3, 4769–4790, doi:10.1021/acsapm.1c00661.
76. Ramanavicius, S.; Samukaite-Bubniene, U.; Ratautaite, V.; Bechelany, M.; Ramanavicius, A. Electrochemical Molecularly Imprinted Polymer Based Sensors for Pharmaceutical and Biomedical Applications (Review). *J. Pharm. Biomed. Anal.* 2022, 215, 114739, doi:10.1016/j.jpba.2022.114739.
77. Crapnell, R.D.; Street, R.J.; Ferreira-Silva, V.; Down, M.P.; Peeters, M.; Banks, C.E. Electrospun Nylon Fibers with Integrated Polypyrrole Molecularly Imprinted Polymers for the Detection of Glucose. *Anal. Chem* 2021, 93, 13235–13241, doi:10.1021/acs.analchem.1c02472.
78. Sehit, E.; Drzazgowska, J.; Buchenau, D.; Yesildag, C.; Lensen, M.; Altintas, Z. Ultrasensitive Nonenzymatic Electrochemical Glucose Sensor Based on Gold Nanoparticles and Molecularly Imprinted Polymers. *Biosens. Bioelectron.* 2020, 165, 112432, doi:10.1016/j.bios.2020.112432.

79. Kadhem, A.J.; Gentile, G.J.; Fidalgo de Cortalezzi, M.M. Molecularly Imprinted Polymers (MIPs) in Sensors for Environmental and Biomedical Applications: A Review. *Molecules* 2021, 26, 6233, doi:10.3390/molecules26206233.
80. Algieri, C.; Drioli, E.; Guzzo, L.; Donato, L. Bio-Mimetic Sensors Based on Molecularly Imprinted Membranes. *Sensors* 2014, 14, 13863–13912, doi:10.3390/s140813863.
81. Chen, L.; Wang, X.; Lu, W.; Wu, X.; Li, J. Molecular Imprinting: Perspectives and Applications. *Chem. Soc. Rev.* 2016, 45, 2137–2211, doi:10.1039/C6CS00061D.
82. Li, X.; Niu, X.H.; Wu, H.Y.; Meng, S.C.; Zhang, W.C.; Pan, J.M.; Qiu, F.X. Impedimetric Enzyme-Free Detection of Glucose via a Computation-Designed Molecularly Imprinted Electrochemical Sensor Fabricated on Porous Ni Foam. *Electroanalysis* 2017, 29, 1243–1251, doi:10.1002/elan.201600721.
83. Wu, H.; Zheng, W.; Jiang, Y.; Xu, J.; Qiu, F. Construction of a Selective Non-Enzymatic Electrochemical Sensor Based on Hollow Nickel Nanospheres/Carbon Dots–Chitosan and Molecularly Imprinted Polymer Film for the Detection of Glucose. *New Journal of Chemistry* 2021, 45, 21676–21683, doi:10.1039/D1NJ03864H.
84. Alexander, S.; Baraneedharan, P.; Balasubrahmanyam, S.; Ramaprabhu, S. Highly Sensitive and Selective Non Enzymatic Electrochemical Glucose Sensors Based on Graphene Oxide-Molecular Imprinted Polymer. *Materials Science and Engineering: C* 2017, 78, 124–129, doi:10.1016/j.msec.2017.04.045.
85. Widayani; Yanti; Wungu, T.D.K.; Suprijadi Preliminary Study of Molecularly Imprinted Polymer-Based Potentiometric Sensor for Glucose. *Procedia Eng.* 2017, 170, 84–87, doi:10.1016/j.proeng.2017.03.016.
86. Diouf, A.; Bouchikhi, B.; el Bari, N. A Nonenzymatic Electrochemical Glucose Sensor Based on Molecularly Imprinted Polymer and Its Application in Measuring Saliva Glucose. *Materials Science and Engineering: C* 2019, 98, 1196–1209, doi:10.1016/j.msec.2019.01.001.
87. Caldara, M.; Lowdon, J.W.; Rogosic, R.; Arreguin-Campos, R.; Jimenez-Monroy, K.L.; Heidt, B.; Tschulik, K.; Cleij, T.J.; Diliën, H.; Eersels, K.; et al. Thermal Detection of Glucose in Urine Using a Molecularly Imprinted Polymer as a Recognition Element. *ACS Sens.* 2021, 6, 4515–4525, doi:10.1021/acssensors.1c02223.
88. Zhu, Q.; Li, X.; Xiao, Y.; Xiong, Y.; Wang, S.; Xu, C.; Zhang, J.; Wu, X. Synthesis of Molecularly Imprinted Polymer via Visible Light Activated RAFT Polymerization in Aqueous Media at Room Temperature for Highly Selective Electrochemical Assay of Glucose. *Macromol. Chem. Phys.* 2017, 218, 1700141, doi:10.1002/macp.201700141.
89. Mirmohseni, A.; Pourata, R.; Shojaei, M. Application of Molecularly Imprinted Polymer for Determination of Glucose by Quartz Crystal Nanobalance Technique. *IEEE Sens. J.* 2014, 14, 2807–2812, doi:10.1109/JSEN.2014.2316819.

90. Yoshimi, Y.; Narimatsu, A.; Nakayama, K.; Sekine, S.; Hattori, K.; Sakai, K. Development of an Enzyme-Free Glucose Sensor Using the Gate Effect of a Molecularly Imprinted Polymer. *Journal of Artificial Organs* 2009, 12, 264–270, doi:10.1007/s10047-009-0473-4.
91. Chen, G.; Qiu, J.; Fang, X.; Xu, J.; Cai, S.; Chen, Q.; Liu, Y.; Zhu, F.; Ouyang, G. Boronate Affinity-Molecularly Imprinted Biocompatible Probe: An Alternative for Specific Glucose Monitoring. *Chem. Asian J.* 2016, 11, 2240–2245, doi:10.1002/asia.201600797.
92. Farid, M.M.; Goudini, L.; Piri, F.; Zamani, A.; Saadati, F. Molecular Imprinting Method for Fabricating Novel Glucose Sensor: Polyvinyl Acetate Electrode Reinforced by MnO₂/CuO Loaded on Graphene Oxide Nanoparticles. *Food Chem.* 2016, 194, 61–67, doi:10.1016/j.foodchem.2015.07.128.
93. Bossard, B.; Grothe, R.A.; Martins, A.B.; Lobato, A.; Tasić, N.; Paixão, T.R.L.C.; Gonçalves, L.M. Nanographene Laser-Pyrolyzed Paper Electrodes for the Impedimetric Detection of d-Glucose via a Molecularly Imprinted Polymer. *Monatshfte für Chemie - Chemical Monthly* 2022, 1, 3, doi:10.1007/s00706-022-02997-7.
94. Karaman, C.; Karaman, O.; Atar, N.; Yola, M.L. A Molecularly Imprinted Electrochemical Biosensor Based on Hierarchical Ti₂Nb₁₀O₂₉ (TNO) for Glucose Detection. *Microchimica Acta* 2022, 189, 24, doi:10.1007/s00604-021-05128-x.
95. Muhammad, T.; Nur, Z.; Piletska, E. v.; Yimit, O.; Piletsky, S.A. Rational Design of Molecularly Imprinted Polymer: The Choice of Cross-Linker. *Analyst* 2012, 137, 2623, doi:10.1039/c2an35228a.
96. Wu, H.; Tian, Q.; Zheng, W.; Jiang, Y.; Xu, J.; Li, X.; Zhang, W.; Qiu, F. Non-Enzymatic Glucose Sensor Based on Molecularly Imprinted Polymer: A Theoretical, Strategy Fabrication and Application. *Journal of Solid State Electrochemistry* 2019, 23, 1379–1388, doi:10.1007/s10008-019-04237-1.
97. Pérez-Moral, N.; Mayes, A.G. Comparative Study of Imprinted Polymer Particles Prepared by Different Polymerisation Methods. *Anal. Chim. Acta* 2004, 504, 15–21, doi:10.1016/S0003-2670(03)00533-6.
98. Tamayo, F.G.; Casillas, J.L.; Martin-Esteban, A. Evaluation of New Selective Molecularly Imprinted Polymers Prepared by Precipitation Polymerisation for the Extraction of Phenylurea Herbicides. *J. Chromatogr. A* 2005, 1069, 173–181, doi:10.1016/j.chroma.2005.02.029.
99. Manju, S.; Hari, P.R.; Sreenivasan, K. Fluorescent Molecularly Imprinted Polymer Film Binds Glucose with a Concomitant Changes in Fluorescence. *Biosens. Bioelectron.* 2010, 26, 894–897, doi:10.1016/j.bios.2010.07.025.
100. Kamaruzaman, S.; Nasir, N.M.; Mohd Faudzi, S.M.; Yahaya, N.; Mohamad Hanapi, N.S.; Wan Ibrahim, W.N. Solid-Phase Extraction of Active Compounds from Natural Products by Molecularly Imprinted Polymers: Synthesis and Extraction Parameters. *Polymers (Basel)* 2021, 13, 3780, doi:10.3390/polym13213780.
101. Herrera-Chacón, A.; Cetó, X.; del Valle, M. Molecularly Imprinted Polymers - towards Electrochemical Sensors and Electronic Tongues. *Anal. Bioanal. Chem.* 2021, 413, 6117–6140, doi:10.1007/s00216-021-03313-8.

102. Buenucesco, C.E.; Tiu, B.D.B.; Lee, L.P.; Sabido, P.M.G.; Nuesca, G.M.; Caldon, E.B.; del Mundo, F.R.; Advincula, R.C. Electropolymerized-Molecularly Imprinted Polymers (E-MIPS) as Sensing Elements for the Detection of Dengue Infection. *Anal. Bioanal. Chem.* 2022, 414, 1347–1357, doi:10.1007/s00216-021-03757-y.
103. Pernites, R.; Ponnappati, R.; Felipe, M.J.; Advincula, R. Electropolymerization Molecularly Imprinted Polymer (E-MIP) SPR Sensing of Drug Molecules: Pre-Polymerization Complexed Terthiophene and Carbazole Electroactive Monomers. *Biosens Bioelectron* 2011, 26, 2766–2771, doi:10.1016/j.bios.2010.10.027.
104. Kim, D.-M.; Moon, J.-M.; Lee, W.-C.; Yoon, J.-H.; Choi, C.S.; Shim, Y.-B. A Potentiometric Non-Enzymatic Glucose Sensor Using a Molecularly Imprinted Layer Bonded on a Conducting Polymer. *Biosens. Bioelectron.* 2017, 91, 276–283, doi:10.1016/j.bios.2016.12.046.
105. Cho, S.J.; Noh, H.-B.; Won, M.-S.; Cho, C.-H.; Kim, K.B.; Shim, Y.-B. A Selective Glucose Sensor Based on Direct Oxidation on a Bimetal Catalyst with a Molecular Imprinted Polymer. *Biosens. Bioelectron.* 2018, 99, 471–478, doi:10.1016/j.bios.2017.08.022.
106. Li, H.X.; Yao, W.; Wu, Q.; Xia, W.S. Glucose Molecularly Imprinted Electrochemical Sensor Based on Chitosan and Nickel Oxide Electrode. *Adv. Mat. Res.* 2014, 1052, 215–219, doi:10.4028/www.scientific.net/AMR.1052.215.
107. Zheng, W.; Wu, H.; Jiang, Y.; Xu, J.; Li, X.; Zhang, W.; Qiu, F. A Molecularly-Imprinted-Electrochemical-Sensor Modified with Nano-Carbon-Dots with High Sensitivity and Selectivity for Rapid Determination of Glucose. *Anal. Biochem* 2018, 555, 42–49, doi:10.1016/j.ab.2018.06.004.
108. Fang, C.; Yi, C.; Wang, Y.; Cao, Y.; Liu, X. Electrochemical Sensor Based on Molecular Imprinting by Photo-Sensitive Polymers. *Biosens. Bioelectron.* 2009, 24, 3164–3169, doi:10.1016/j.bios.2009.03.030.
109. Ding, J.; Zhang, J.; Li, J.; Li, D.; Xiao, C.; Xiao, H.; Yang, H.; Zhuang, X.; Chen, X. Electrospun Polymer Biomaterials. *Prog. Polym. Sci.* 2019, 90, 1–34, doi:10.1016/j.progpolymsci.2019.01.002.
110. Ramakrishna, S.; Fujihara, K.; Teo, W.-E.; Yong, T.; Ma, Z.; Ramaseshan, R. Electrospun Nanofibers: Solving Global Issues. *Materials Today* 2006, 9, 40–50, doi:10.1016/S1369-7021(06)71389-X.
111. Wang, X.; Kim, Y.-G.; Drew, C.; Ku, B.-C.; Kumar, J.; Samuelson, L.A. Electrostatic Assembly of Conjugated Polymer Thin Layers on Electrospun Nanofibrous Membranes for Biosensors. *Nano Lett.* 2004, 4, 331–334, doi:10.1021/nl034885z.
112. Fuchs, Y.; Soppera, O.; Haupt, K. Photopolymerization and Photostructuring of Molecularly Imprinted Polymers for Sensor Applications—A Review. *Anal. Chim. Acta* 2012, 717, 7–20, doi:10.1016/j.aca.2011.12.026.
113. Decker, C. Photoinitiated Crosslinking Polymerisation. *Prog. Polym. Sci.* 1996, 21, 593–650, doi:10.1016/0079-6700(95)00027-5.
114. Ersöz, A.; Denizli, A.; Özcan, A.; Say, R. Molecularly Imprinted Ligand-Exchange Recognition Assay of Glucose by Quartz Crystal Microbalance. *Biosens. Bioelectron.* 2005, 20, 2197–2202, doi:10.1016/j.bios.2004.07.030.

115. Yang, Y.; Yi, C.; Luo, J.; Liu, R.; Liu, J.; Jiang, J.; Liu, X. Glucose Sensors Based on Electrodeposition of Molecularly Imprinted Polymeric Micelles: A Novel Strategy for MIP Sensors. *Biosens. Bioelectron.* 2011, 26, 2607–2612, doi:10.1016/j.bios.2010.11.015.
116. Zhao, W.; Zhang, R.; Xu, S.; Cai, J.; Zhu, X.; Zhu, Y.; Wei, W.; Liu, X.; Luo, J. Molecularly Imprinted Polymeric Nanoparticles Decorated with Au NPs for Highly Sensitive and Selective Glucose Detection. *Biosens. Bioelectron.* 2018, 100, 497–503, doi:10.1016/j.bios.2017.09.020.
117. Pan, G.; Zhang, Y.; Guo, X.; Li, C.; Zhang, H. An Efficient Approach to Obtaining Water-Compatible and Stimuli-Responsive Molecularly Imprinted Polymers by the Facile Surface-Grafting of Functional Polymer Brushes via RAFT Polymerization. *Biosens. Bioelectron.* 2010, 26, 976–982, doi:10.1016/j.bios.2010.08.040.
118. Poma, A.; Guerreiro, A.; Whitcombe, M.J.; Piletska, E. v.; Turner, A.P.F.; Piletsky, S.A. Solid-Phase Synthesis of Molecularly Imprinted Polymer Nanoparticles with a Reusable Template—“Plastic Antibodies.” *Adv. Funct. Mater.* 2013, 23, 2821–2827, doi:10.1002/adfm.201202397.
119. Garcia-Cruz, A.; Ahmad, O.S.; Alanazi, K.; Piletska, E.; Piletsky, S.A. Generic Sensor Platform Based on Electro-Responsive Molecularly Imprinted Polymer Nanoparticles (e-NanoMIPs). *Microsyst. Nanoeng.* 2020, 6, 83, doi:10.1038/s41378-020-00193-3.
120. Cheng, Y.; Chen, T.; Fu, D.; Liu, M.; Cheng, Z.; Hua, Y.; Liu, J. The Construction of Molecularly Imprinted Electrochemical Biosensor for Selective Glucose Sensing Based on the Synergistic Enzyme-Enzyme Mimic Catalytic System. *Talanta* 2022, 242, 123279, doi:10.1016/j.talanta.2022.123279.
121. Piletsky, S.A.; Turner, N.W.; Laitenberger, P. Molecularly Imprinted Polymers in Clinical Diagnostics—Future Potential and Existing Problems. *Med. Eng. Phys.* 2006, 28, 971–977, doi:10.1016/j.medengphy.2006.05.004.
122. Zhang, Y.; Li, N.; Xiang, Y.; Wang, D.; Zhang, P.; Wang, Y.; Lu, S.; Xu, R.; Zhao, J. A Flexible Non-Enzymatic Glucose Sensor Based on Copper Nanoparticles Anchored on Laser-Induced Graphene. *Carbon* 2020, 156, 506–513, doi:10.1016/j.carbon.2019.10.006.
123. Wang, J. Glucose Biosensors: 40 Years of Advances and Challenges. *Electroanalysis* 2001, 13, 983–988, doi:https://doi.org/10.1002/1521-4109(200108)13:12<983::AID-ELAN983>3.0.CO;2-%23.
124. Chen, C.; Xie, Q.; Yang, D.; Xiao, H.; Fu, Y.; Tan, Y.; Yao, S. Recent Advances in Electrochemical Glucose Biosensors: A Review. *RSC Adv.* 2013, 3, 4473, doi:10.1039/c2ra22351a.
125. Hönes, J.; Müller, P.; Surridge, N. The Technology Behind Glucose Meters: Test Strips. *Diabetes Technol. Ther.* 2008, 10, S-10-S-26, doi:10.1089/dia.2008.0005.
126. Pickup, J.C.; Hussain, F.; Evans, N.D.; Rolinski, O.J.; Birch, D.J.S. Fluorescence-Based Glucose Sensors. *Biosens. Bioelectron.* 2005, 20, 2555–2565, doi:10.1016/j.bios.2004.10.002.
127. Banerji, S.; Peng, W.; Kim, Y.-C.; Booksh, K.S. Molecularly Imprinted Polymerization-Based Surface Plasmon Resonance Sensing for Glucose Detection in Human Urine. In *Proceedings of the Smart Medical and Biomedical Sensor Technology IV*; Cullum, B.M., Carter, J.C., Eds.; SPIE, October 18 2006; Vol. 6380, p. 6380.

128. Wang, L.; Li, Y. A Sensitive Amperometric Sensor Based on CuO and Molecularly Imprinted Polymer Composite for Determination of Danazol in Human Urine. *Int J Electrochem. Sci.* 2022, 17, doi:10.20964/2022.11.72.
129. Weng, C.; Yeh, W.; Ho, K.; Lee, G. A Microfluidic System Utilizing Molecularly Imprinted Polymer Films for Amperometric Detection of Morphine. *Sens. Actuators B Chem* 2007, 121, 576–582, doi:10.1016/j.snb.2006.04.111.
130. Wang, J.; Liang, R.; Qin, W. Molecularly Imprinted Polymer-Based Potentiometric Sensors. *TrAC Trends in Analytical Chemistry* 2020, 130, 115980, doi:10.1016/j.trac.2020.115980.
131. Liu, K.; Song, Y.; Song, D.; Liang, R. Plasticizer-Free Polymer Membrane Potentiometric Sensors Based on Molecularly Imprinted Polymers for Determination of Neutral Phenols. *Anal. Chim. Acta* 2020, 1121, 50–56, doi:10.1016/j.aca.2020.04.074.
132. Elfadil, D.; Lamaoui, A.; della Pelle, F.; Amine, A.; Compagnone, D. Molecularly Imprinted Polymers Combined with Electrochemical Sensors for Food Contaminants Analysis. *Molecules* 2021, 26, 4607, doi:10.3390/molecules26154607.
133. Lu, D.; Zhu, D.Z.; Gan, H.; Yao, Z.; Luo, J.; Yu, S.; Kurup, P. An Ultra-Sensitive Molecularly Imprinted Polymer (MIP) and Gold Nanostars (AuNS) Modified Voltammetric Sensor for Facile Detection of Perfluorooctane Sulfonate (PFOS) in Drinking Water. *Sens. Actuators B Chem* 2022, 352, 131055, doi:10.1016/j.snb.2021.131055.
134. Seguro, I.; Rebelo, P.; Pacheco, J.G.; Delerue-Matos, C. Electropolymerized, Molecularly Imprinted Polymer on a Screen-Printed Electrode—A Simple, Fast, and Disposable Voltammetric Sensor for Trazodone. *Sensors* 2022, 22, 2819, doi:10.3390/s22072819.
135. Bahadir, E.B.; Sezginürk, M.K. A Review on Impedimetric Biosensors. *Artif Cells Nanomed. Biotechnol.* 2016, 44, 248–262, doi:10.3109/21691401.2014.942456.
136. Kim, M.; Iezzi, R.; Shim, B.S.; Martin, D.C. Impedimetric Biosensors for Detecting Vascular Endothelial Growth Factor (VEGF) Based on Poly(3,4-Ethylene Dioxathiophene) (PEDOT)/Gold Nanoparticle (Au NP) Composites. *Front. Chem.* 2019, 7, 234, doi:10.3389/fchem.2019.00234.
137. Haupt, K.; Mosbach, K. Molecularly Imprinted Polymers and Their Use in Biomimetic Sensors. *Chem. Rev.* 2000, 100, 2495–2504, doi:10.1021/cr990099w.
138. Parmpi, P.; Kofinas, P. Biomimetic Glucose Recognition Using Molecularly Imprinted Polymer Hydrogels. *Biomaterials* 2004, 25, 1969–1973, doi:10.1016/j.biomaterials.2003.08.025.
139. Okutucu, B.; Önal, S. Molecularly Imprinted Polymers for Separation of Various Sugars from Human Urine. *Talanta* 2011, 87, 74–79, doi:10.1016/j.talanta.2011.09.043.
140. Cheong, W.J.; Yang, S.H.; Ali, F. Molecular Imprinted Polymers for Separation Science: A Review of Reviews. *Journal of separation science* 2013, 36, 609–628, doi:10.1002/jssc.201200784.

141. Muhammad, P.; Liu, J.; Xing, R.; Wen, Y.; Wang, Y.; Liu, Z. Fast Probing of Glucose and Fructose in Plant Tissues via Plasmonic Affinity Sandwich Assay with Molecularly-Imprinted Extraction Microprobes. *Anal. Chim. Acta* 2017, 995, 34–42, doi:10.1016/j.aca.2017.09.044.

Preface to Chapter 3

Chapter 2 discussed and highlighted possible approaches and obstacles that MIP-based sensors may face in their effort to become a viable alternative to traditional glucose detection devices. Their long shelf-life, high resistance, and low cost production make them advantageous over enzymatic sensors. In addition, MIP-based devices have proven to work in challenging environments and matrices, thus illustrating their potential application as non-invasive and continuous monitoring tools. Given its working principle and successful integration with imprinted polymers reported in literature, the so-called "Heat-Transfer Method (HTM)" can be categorized as one of the promising readout technologies for the detection of glucose using MIP-based sensors.

As a result, in **Chapter 3**, a research study on the fabrication and evaluation of a MIP-based biosensor targeting glucose using HTM is presented. In this work, the thermal transducer was used in combination with glucose MIPs to create a sensor for the detection of this critical biomarker in clinically relevant samples and concentrations. To this end, MIP particles were synthesized using a bulk polymerization and a dummy imprinting approach. The prepared MIP particles were then micro-contact deposited onto an aluminium-polyvinyl chloride (Al-PVC) substrate to generate a thermally conductive receptor layer, which was then evaluated via HTM method. Sensitivity and selectivity of the developed platform were studied via HTM analysis by exposing the platform to glucose and other saccharides in buffer solutions. Finally, a real-world sample analysis in human urine samples spiked with glucose demonstrated promising linearity and sensitivity, making the developed low-cost platform very interesting for commercial applications and follow-up studies.

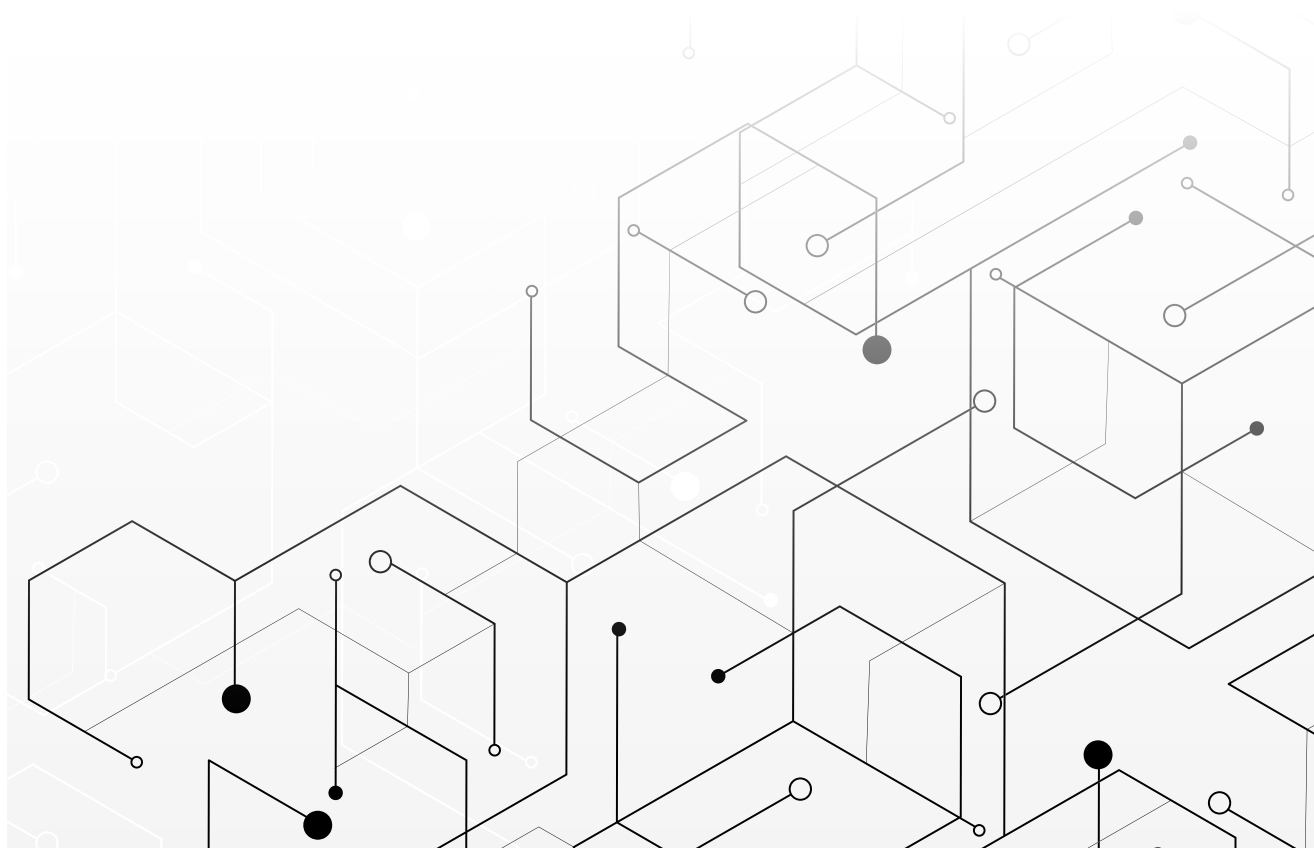
Chapter 3

Thermal Detection of Glucose in Urine Using a Molecularly Imprinted Polymer as a Recognition Element

Adapted from:

Caldara, M.*, Lowdon, J. W., Rogosic, R., Arreguin-Campos, R., Jimenez-Monroy, K. L., Heidt, B., Tschulik, K., Cleij, T. J., Diliën, H., Eersels, K., & van Grinsven, B. Thermal Detection of Glucose in Urine Using a Molecularly Imprinted Polymer as a Recognition Element.

ACS Sensors 2021, 6(12), 4515–4525.
<https://doi.org/10.1021/acssensors.1c02223>



Abstract

Glucose bio-sensing technologies have received increasing attention in the last few decades, primarily due to the fundamental role that glucose metabolism plays in diseases (e.g. diabetes). Molecularly imprinted polymers (MIPs) could offer an alternative means of analysis to a field that is traditionally dominated by enzyme-based devices, posing superior chemical stability, cost-effectiveness, and ease of fabrication. Their integration into sensing devices as recognition elements has been extensively studied with different readout methods such as quartz-crystal microbalance or impedance spectroscopy. In this work, a dummy imprinting approach is introduced, describing the synthesis and optimization of a MIP toward the sensing of glucose. Integration of this polymer into a thermally conductive receptor layer was achieved by micro-contact deposition. In essence, the MIP particles are pressed into a polyvinyl chloride adhesive layer using a polydimethylsiloxane stamp. The prepared layer is then evaluated with the so-called heat-transfer method, allowing the determination of the specificity and the sensitivity of the receptor layer. Furthermore, the selectivity was assessed by analysing the thermal response after infusion with increasing concentrations of different saccharide analogues in phosphate-buffered saline (PBS). The obtained results show a linear range of the sensor of 0.019–0.330 mM for the detection of glucose in PBS. Finally, a potential application of the sensor was demonstrated by exposing the receptor layer to increasing concentrations of glucose in human urine samples, demonstrating a linear range of 0.044–0.330 mM. The results obtained in this paper highlight the applicability of the sensor both in terms of non-invasive glucose monitoring and for the analysis of food samples.

Keywords: molecularly imprinted polymers; glucose sensing; heat-transfer method; non-invasive glucose monitoring; non-enzymatic glucose sensor.

Introduction

Glucose is the most abundant monosaccharide in nature and the most used aldohexose in living organisms.[1] It is essential in major catabolic cycles, including oxidative phosphorylation and glycolysis for the creation of glycogens, proteins, and lipids.[2] The monitoring of glucose in these systems is therefore of great importance as the molecule is a vital cog in the molecular machinery of many processes. Sensors that can deliver a fast, reliable, and cost-effective determination of glucose have therefore gained increasing attention in the past decades. Glucose sensors cover a wide range of possible applications, ranging from diabetes monitoring and food analysis, through to environmental monitoring and medical diagnostics.[3–5] Certainly, the most crucial application of glucose sensors is in the diagnosis and monitoring of diabetes mellitus, also known as diabetes. Diabetes is an incurable metabolic disease, characterized by high levels of blood glucose. The initial symptoms often include frequent urination, increased thirst, and blurry vision, and if not treated it could cause many disconcerting and life-threatening medical complications.[6,7] The number of people with diabetes is increasing tremendously, and the World Health Organization (WHO) estimates 693 million diabetics worldwide by 2045.[8] In the United States alone, an increase of 54% from 2015 to 2030 is estimated. This will cause an increase in the total annual cost associated with diabetes by 53% from \$407.6 billion in 2016 to more than \$622 billion by 2030.[9] Therefore, it is of utmost importance to have a simple, fast, and robust sensing device to detect glucose both for the diagnosis and monitoring of diabetes to amortize these costs. Currently, commercial devices are mostly enzymatic-based electrochemical sensors in which the enzyme consists of glucose dehydrogenase or glucose oxidase;[10–13] in some devices, these enzymes are coupled with other agents, such as chromogenic agents to obtain colorimetric test strips.[14,15] The main limitation of these sensors lies in the low stability derived from the quaternary structure of the folded enzyme.[16] Therefore, a lot of attention has been given toward the development of non-enzymatic electrochemical sensors that do not suffer the same drawback.[17] Several enzyme-free glucose sensors have been developed in the past decades, with most of them being amperometric and colorimetric sensors.[18–21] Even though these non-enzymatic sensors overcame the stability issue, they presented new issues to resolve. The biggest challenges of which concern the mechanism of glucose oxidation on bare platinum surfaces, being innately unselective, leading to the possibility of interacting with multiple saccharides and consequently affecting the quantitative nature of the electrochemical sensors.[16] Thus, despite significant developments in the evolution of electrochemical sensors, fully non-invasive, fast, and cheap glucose-monitoring approaches are still required.

One such emerging technology that offers promise to overcome the above-mentioned issues is the use of molecularly imprinted polymers (MIPs) in sensory arrays.[22,23] MIPs are synthetic polymer-based smart materials that contain nanocavities capable of selectively binding a molecular target. They are analogous to the natural antibody–antigen system,[24–26] though they do not suffer from the same instability in harsh environments. MIPs have received an increasing amount of attention from the scientific community[27–32] with their advantages over antibodies and enzymes extending past simple stability and encompassing factors such as simple preparation, low cost, higher physical robustness, resistance to extreme temperature and pressure, and resistance to acids, bases, and organic solvents.[33] These benefits increase the list of possible matrices with which analysis can be conducted, whereas with traditional affinity reagents, this would be unfeasible. With this said, another aspect that must be considered is the readout technology that the receptor layer is coupled with. Traditionally electrochemical readout platforms have been associated with the sensing of glucose.

However, these methods exploit the electrochemical reaction that occurs when glucose interacts with specific enzymes and antibodies. This electrochemical reaction is absent in a MIP-based sensory platform. Therefore it is a logical step to pair the synthetic receptor with a more compatible readout technology, such as the so-called “heat transfer method” (HTM). The HTM is a thermal sensing readout platform developed over the course of last 10 years.[34] The method has received increasing attention in the last few years and has recently been applied in the detection of bacteria and small molecules via the use of surface-imprinted polymers[35,36] and MIPs.[37–39] In essence, the method is capable of measuring the thermal resistance across a liquid–solid phase boundary, with MIPs being the receptor layer deposited between the two. The system employed makes use of a 3D printed polyether ether ketone (PEEK) flow cell in close contact with a copper block and the receptor layer (**light grey material, Figure 3.1**) As a target analyte is introduced in the liquid phase, it binds to the deposited MIPs, changing its thermodynamic properties, leading to a change in the thermal conduction path between the liquid phase and the solid phase (**Figure 3.1**). This difference is measured by monitoring the temperature of the liquid phase by means of a thermocouple, while the solid phase is continuously heated to 37 °C and is monitored by a complimentary thermocouple. The overall change in the recorded temperature in the liquid phase is observed as increasing concentrations of the analyte are introduced to the receptor layer, thus building a relationship between the increasing thermal resistance of the receptor layer and the concentration of the target present (**Equation 3.1**).

$$R_{th} = \frac{T_1 - T_2}{P} \quad (3.1)$$

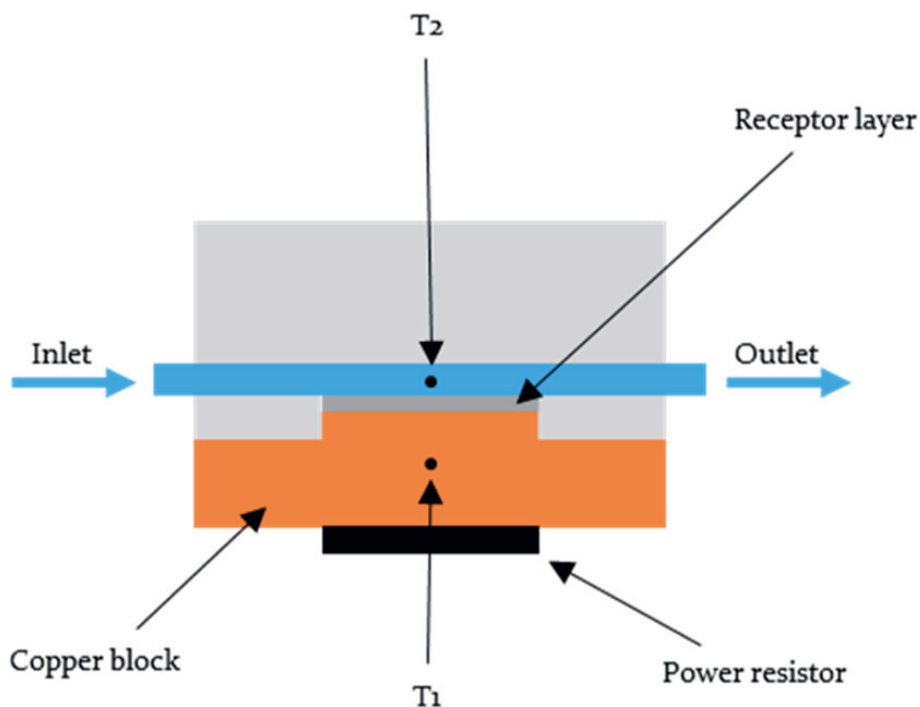


Figure 3.1 Schematic illustration of the setup used during HTM analysis. The light-grey structure embedding the receptor layer and in close contact with the copper block represents a 3D printed polyether ether ketone (PEEK) flow cell.

The chapter describes how a MIP-based sensor coupled with the HTM can be utilized in the sensing of glucose and how its application can be extended to physiological samples, such as urine. With this said, a consideration must be made when synthesizing a MIP capable of binding glucose. The absence of a functional group in the glucose molecule that is able to form a strong interaction with a monomer such as acrylamide (AAM) makes the direct imprinting of glucose a tricky task; therefore, a dummy imprinting approach is favoured. Glucuronic acid (GA) was selected as the dummy template and acrylamide as a functional monomer. This approach allows the formation of a strong interaction between the $-\text{COOH}$ of GA and the functional monomer (**Figure 3.2**) and would therefore allow stronger interactions than those possible between glucose and AAM. Liquid chromatography–mass spectrometry (LC–MS) was used to demonstrate the binding capabilities of the dummy imprinted polymer to glucose. Furthermore, by varying the ratios of the template–monomer–cross-linker, it was possible to identify the best composition in terms of the imprinting efficiency by comparing the MIP with its corresponding non-imprinted polymer (NIP). Once the best composition was obtained, the MIP particles were immobilized on a polyvinyl chloride (PVC) layer and deposited on an aluminium substrate to obtain a thermally conductive receptor layer that could be extensively analysed with the HTM. The analysis demonstrated the efficiency and reproducibility of the MIP-based platform for the detection of glucose. The selectivity of the receptor layer was then determined by analysing the response of the sensor to different carbohydrates and comparing the obtained dose–response curves with those obtained for glucose.

Furthermore, the response of the receptor layer to urine samples containing known concentrations of glucose was evaluated. The resulting limit-of-detection (LoD) and linear range for glucose were compared with the physiological concentrations of the molecule in urine. In this way the applicability of the sensor in glucose monitoring both for medical diagnostics and food analysis was evaluated.

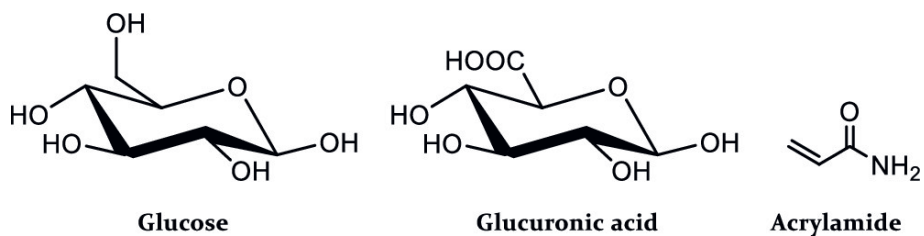


Figure 3.2 Chemical structures of glucose, glucuronic acid, and AAM.

Materials and Methods

Chemicals and Reagents

Prior to the polymerization, stabilizers were removed from the functional and crosslinking monomers by passing the reagents over a column packed with aluminium oxide. Acrylamide ($\geq 99\%$), ethylene glycol dimethacrylate (98%), 2,2'-azobis(2-methylpropionitrile) (98%), tetrahydrofuran ($\geq 99.9\%$), dimethyl sulfoxide ($\geq 99.9\%$), acetic acid ($\geq 99\%$), d-fructose ($\geq 99\%$), d-lactose monohydrate ($\geq 99.5\%$), and sucrose ($\geq 99.5\%$) were supplied by Sigma-Aldrich. d-Glucuronic acid (98%) and methanol ($\geq 99\%$) were supplied by Fisher Scientific. d-Glucose ($\geq 98\%$) was purchased from TCI Chemicals. All solutions were prepared with deionized water with a resistivity of $18.1 \text{ M}\Omega \text{ cm}^{-1}$ or with phosphate-buffered saline (PBS) solutions. Polydimethylsiloxane (PDMS) stamps were made with a Sylgard 184 elastomer kit obtained from Mavom N.V. (Schelle, Belgium). Aluminium chips were supplied by Brico NV (Korbeek-Lo, Belgium) and cut to the desired dimensions ($1 \times 1 \text{ cm}$). Medi-Test Glucose test strips for the rapid detection of glucose in urine were purchased from VWR International.

Synthesis of Dummy MIPs

Dummy MIPs were synthesized accordingly to a previously described procedure.[40,41] To this end, functional monomer (AAM, 2 mmol, 142 mg), template (d-glucuronic acid, 0.25 mmol, 48.5 mg), cross-linker (EGDMA, 3 mmol, 566 μL), and thermal initiator (AIBN, 0.25 mmol, 40 mg) were dissolved in 3 mL of dimethyl sulfoxide (DMSO). The mixture was then purged with N_2 to remove any oxygen from the mixture before the initiation of polymerization. The polymerization was carried out at $65 \text{ }^\circ\text{C}$ for 10 h to allow the polymerization to be fully completed. The obtained monolithic bulk MIP was then mechanically ground, before washing with methanol to remove any unreacted components. Once extracted, the MIP particles were placed in a vial and dried in an oven overnight at $65 \text{ }^\circ\text{C}$. The dried particles were then milled four times using a Fritsch Planetary Micro Mill Pulverisette7 premium line (300 rpm, 5 min, 10 mm balls). After milling, the particles were sieved at a 1.0 mm amplitude using a Fritsch Analysette 3 until a sufficient amount of the polymer was in the collection plate to achieve micro particles with sizes smaller than $100 \mu\text{m}$. Finally, the template molecule (GA) was removed from the MIP by continuous Soxhlet extraction with a 1:6 mixture of acetic acid and methanol for 16 h, followed by another Soxhlet extraction with pure methanol for 16 h, and particles were then dried overnight at $65 \text{ }^\circ\text{C}$. A reference NIP was prepared in parallel following the same procedure.

Thermal Gravimetric Analysis and Fourier-Transform Infrared Analysis

The removal of the template from the MIP was determined through thermal gravimetric analysis (TGA) using a TA Instruments TGA 550 Auto Advanced. Measurements were performed under a nitrogen atmosphere at a heating rate of $10 \text{ }^\circ\text{C}/\text{min}$. For each measurement, 2.5–4 mg of the polymer sample was used. The amount of polymers used for each measurement was between 2.5 and 4 mg. Further confirmation of template removal was conducted with an IR-Affinity-1S Fourier transform infrared (FTIR) spectrometer (Shimadzu Corp., Kyoto, Japan) coupled to an attenuated total reflectance (ATR) crystal, comparing the spectra of extracted, non-extracted, and GA samples. The instrument was set up to run 32 scans per measurement with a spectral resolution of 4 cm^{-1} . The IR spectra were recorded between 4000 and 400 cm^{-1} . The ATR crystal was cleaned with ethanol 70% v/v and acetone before starting the measurement for each new sample. A background spectrum was taken before measuring every new sample to account for environmental changes.

Batch Rebinding Experiments

Rebinding experiments were conducted as follows: 20 mg of MIP/NIP particles was incubated with 5 mL solutions of glucose in deionized water with concentrations ranging from 0.055 to 0.55 mM. The samples were then placed on a rocking table at 125 rpm for 90 min, before removing them and allowing the particles to settle. The resulting settled suspensions were filtered, and the filtrate was collected. The remaining free concentration of the target (C_f) in solution was then determined by LC–MS analysis. To enable these values to be calculated, a calibration graph for glucose was first generated by analysing the peak areas of the chromatogram at 198.09 m/z $[M + NH_4]^+$ for each of the concentrations.

LC-MS Analysis

The LC–MS system is composed of the following parts: a NEXERA ultra high performance liquid chromatography system, equipped with a Shimadzu LC-30AD solvent delivery unit, a Shimadzu CT-20AC column oven (max. column length 300 mm), an SPD-M30A photodiode array detector, and a single quadrupole mass spectrometer (LCMS 2020). The MS used a dual ionization source consisting of both electron spray ionization (ESI) and atmospheric pressure chemical ionization. The short column used was a Waters XSelect CSH C18 3 mm \times 30 mm with a particle size of 3.5 μm operating at 30 °C. Solvent gradient 5% acetonitrile in water followed by a gradient to 95% acetonitrile in water and flushing of the column at 95% water. Both solvents were modified with 0.1% ammonium acetate. The obtained data was analysed using a MestReNova Software version 12.0.0.

Deposition of Dummy MIP Particles by Micro-contact Stamping

Aluminium plates were polished and cut to obtain the desired dimensions (1 cm \times 1 cm with a thickness of 0.5 cm). To immobilize MIP particles, a PVC adhesive layer (0.4 wt% PVC dissolved in tetrahydrofuran) was deposited on the aluminium chip by spin coating (2000 rpm for 60 s with an acceleration of 1000 rpm s^{-1}). To stamp the particles on the PVC layer, a PDMS substrate, covered with a monolayer of MIP particles, was used. The PVC layer was heated for 2 h at a temperature above its glass transition temperature (100 °C), allowing the beads to sink into the polymer layer. The samples were cooled down prior to thermal measurements, and any unbound particles were washed off with distilled water. In this way, planar sensor electrodes were created in a very straightforward and low-cost manner. This is necessary because although reusing MIPs is possible, it would require regenerating the binding sites in the nanocavities by rigorous washing. This is not desirable so the design needs to be as low cost as possible to enable their use as disposable electrodes.

Sensing Setup

The thermal detection platform is described thoroughly in previous work.[42–44] Functionalized chips were pressed mechanically with their backside onto a copper block serving as a heat provider. The temperature of the copper underneath the sample, T_1 , was monitored by a K-type thermocouple (TC Direct). This information was fed into a temperature control unit that stringently controlled T_1 by modifying the voltage over the power resistor (Farnell, Utrecht, The Netherlands) that heats the copper, using a software-based (Labview, National Instruments, Austin, TX, United States) proportional-integral-derivative (PID) controller ($P = 10$, $I = 8$, $D = 0$). The functionalized side of the chip faced a polyether ether ketone (PEEK) flow cell, which was sealed with an O-ring to avoid leakage, defining a contact area of 28 mm² and an inner volume of 110 μL . The flow cell is connected to a tubing system,

allowing the exchange of liquids in a controlled and automated fashion by means of a syringe pump. Every injection of the tested analytes was performed using a flowrate of 0.250 mL/min for 5 min. The temperature of the liquid inside the flow cell, T_2 , was measured by a second thermocouple placed 1 mm above the chip. For each rebinding measurement, the signal was stabilized in PBS that was used as a background solvent for the measurements. The concentration of the target or analogue inside the flow was gradually increased (0.055–0.33 mM). The signal was allowed to stabilize for 20 min between subsequent additions. Data was analysed by monitoring the decrease in T_2 after each addition (heat-transfer method or HTM) while maintaining T_1 at a constant 37.00 °C. This process was repeated for each of the following compounds using the above-mentioned concentrations: glucose, fructose, sucrose, and lactose, alongside the reference NIP.

Sensing Setup

Human urine samples were collected from a healthy individual and tested with a commercially available glucose-urine test. The absence of glucose in the collected samples was confirmed using Medi-Test Glucose urine test strips. Afterward, the urine samples were spiked with increasing concentrations of glucose (0.055–0.33 mM), and the obtained dilution series was then used for HTM analysis using the same sensing setup previously reported for both the analysis of the MIP/NIP.

Results and Discussion

Template Removal Confirmation

One of the critical steps in the preparation of MIPs is the template removal.[45] If any template molecules remain in the MIP network, less cavities will be available for the rebinding and therefore the rebinding capacity of the polymer will be inevitably affected. To ensure complete template removal from the synthesized MIP, TGA and FTIR analysis of non-extracted MIPs, extracted MIPs, and NIPs were performed. In the FTIR spectrum (**Figure 3.3**), the distinctive peak of GA (black line) at 3300–3500 cm^{-1} (OH stretch) and the bands between 1050 and 950 cm^{-1} attributed to a combination of CO stretching and OH bending can be clearly observed. These are considered as the characteristic peaks of carbohydrates.[46,47] It can be clearly noticed that these peaks are not present in the NIP and extracted MIP spectra (green and blue lines) but instead present in the non-extracted MIP (red line).

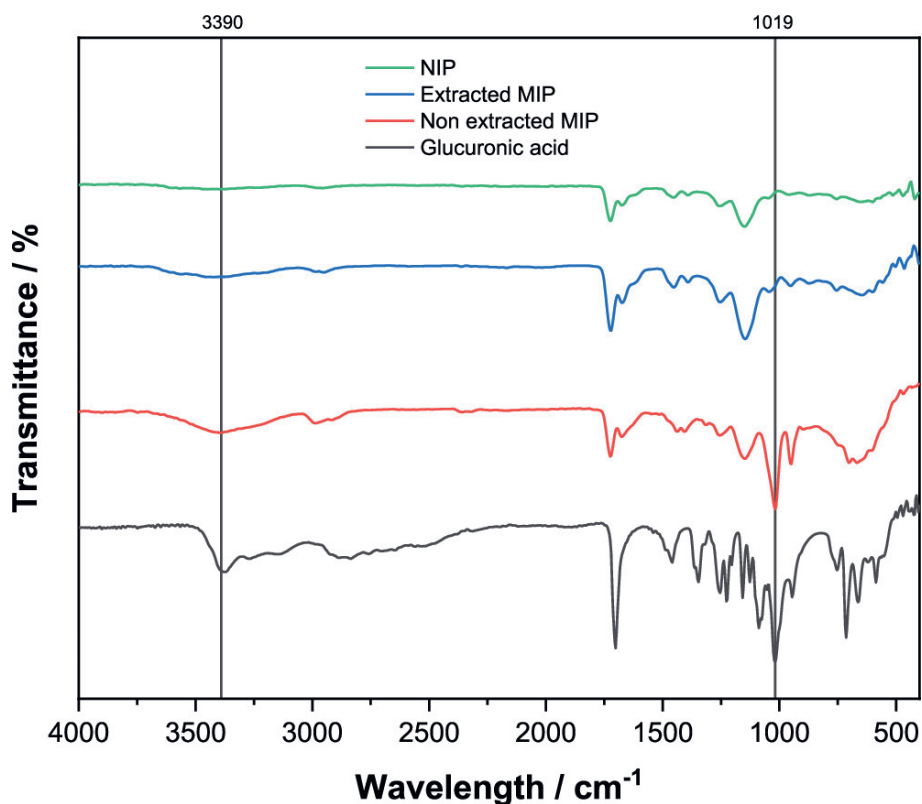


Figure 3.3 FT-IR analysis of the NIP, extracted MIP, non-extracted MIP, and GA.

To further confirm the successful extraction of the template from the MIP, TGA analysis was performed (**Figure 3.4**). The TGA results show almost identical behaviour of the extracted MIP and NIP, where the degradation starts to take place at around 280 $^{\circ}\text{C}$. On the other hand, a significant weight loss can be noticed in the non-extracted MIP starting from 110 $^{\circ}\text{C}$, indicating the presence of GA in the polymer before extraction.

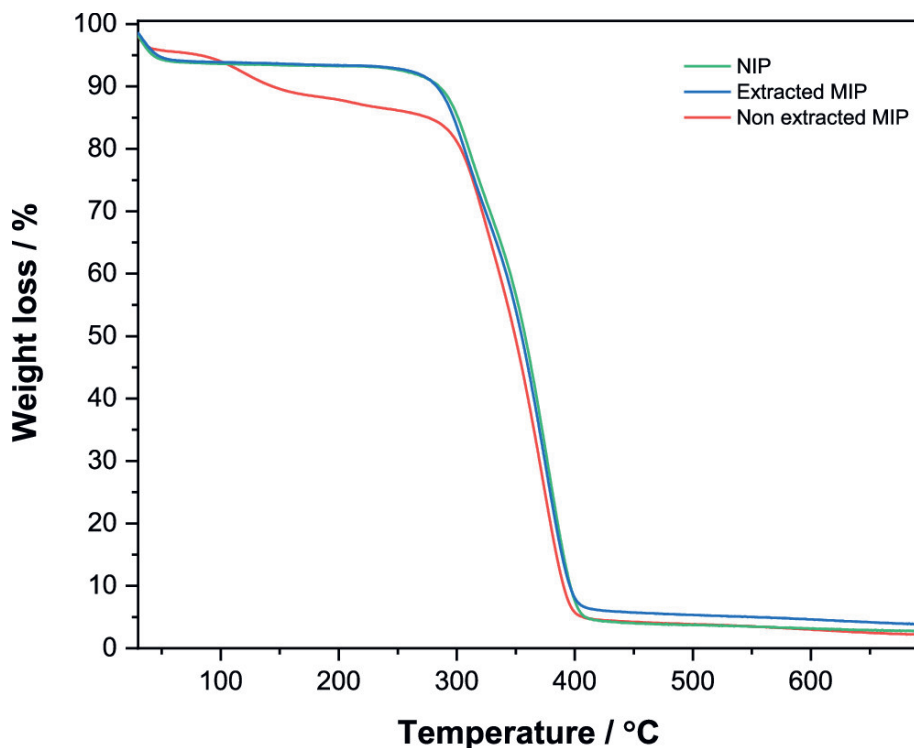


Figure 3.4 TGA analysis of the NIP, extracted MIP, and non-extracted MIP.

Considering the FTIR and TGA results, it can be said with confidence that there is no significant presence of GA in the polymer after continuous Soxhlet extraction.

Glucose Binding Analysis via LC-MS

In order to identify the best composition for the binding of glucose, four different ratios of the template/monomer/cross-linker were synthesized and tested (**Table 3.1**). The compositions tested were based on the common ratios of the components found in the literature using AAM as a functional monomer, EGDMA as a cross-linker, and DMSO as a protogenic solvent.

Table 3.1 Synthesized MIP/NIP Compositions

MIP/NIP	GA (mg)	AAM (eq.)	EGDMA (eq.)	AIBN (mg)	Solvent	T (°C)
MIP1	48.5	6	12	40	DMSO	65
NIP1		6	12	40	DMSO	65
MIP2	48.5	8	12	40	DMSO	65
NIP2		8	12	40	DMSO	65

MIP3	48.5	6	16	40	DMSO	65
NIP3		6	16	40	DMSO	65
MIP4	48.5	8	16	40	DMSO	65
NIP4		8	16	40	DMSO	65

For each composition, a corresponding binding isotherm was generated by analysing the free concentration of glucose found in solution, C_f (mM) from the batch rebinding experiments. These values were then used to extrapolate the corresponding substrate bound (S_b) ($\mu\text{mol g}^{-1}$) values, which indicate the number of moles of glucose bound per gram of the polymer at each data point, [48] thus enabling the obtained S_b to be plotted against C_f . The data were fit with Origin, version 2019b (OriginLabs Corporation, Northampton, MA, USA) using an allometric ($y = ax^b$) fit. All MIPs (black squares) were plotted alongside their corresponding NIP (red squares) (**Figure 3.5**). Of the compositions analysed, MIP/NIP-03 presented the lowest overall maximum binding capacities of $9.26 \mu\text{mol g}^{-1}$ for the MIP and $2.37 \mu\text{mol g}^{-1}$ for the NIP (**Figure 3.5c**), thus demonstrating that with the higher concentration of the cross-linker and a lower amount of the functional monomer, the amount of cavities generated within the material was less when compared to the other compositions. MIP-01 (**Figure 3.5a**) and MIP-02 (**Figure 3.5b**) demonstrated similar binding capacities of 15.29 and $15.59 \mu\text{mol g}^{-1}$, respectively. Though the values for these MIPs are similar, the values for their corresponding NIPs are not similar, with NIP-01 showing a maximum binding capacity of $12.41 \mu\text{mol g}^{-1}$ and NIP-02 a maximum binding capacity of $4.28 \mu\text{mol g}^{-1}$. It can therefore be stipulated that the higher amount of the functional monomer in MIP-02 generates binding sites with higher affinity than the non-specific interactions observed in its corresponding MIP. The lower concentration of the functional monomer (MIP-01) demonstrates a less specific nature as MIP-01 demonstrates a similar maximum binding capacity to that of its NIP.

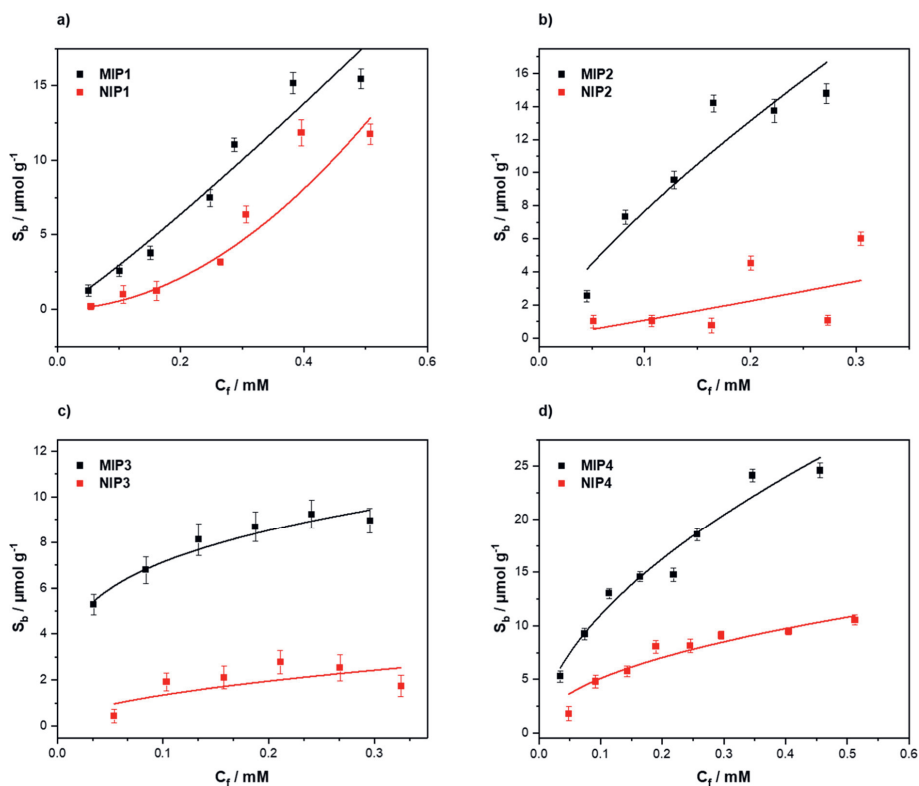


Figure 3.5 Rebinding analysis with LC-MS of (a) MIP/NIP1, (b) MIP/NIP2, (c) MIP/NIP3, and (d) MIP/NIP4.

This therefore indicates that a certain threshold of the functional monomer is required to generate more specific molecular recognition. The reverse of this trend can be witnessed within MIP-03 and MIP-04, though the cross-linker concentrations within these MIPs are higher than those with MIP-01 and MIP-02, thus indicating that the amount of the cross-linker present also affects the amount of specific binding observed between the MIP/NIP. MIP-04 has the highest of all the observed maximum binding capacities with a value of $25.39 \mu\text{mol g}^{-1}$ and a corresponding NIP value of $10.88 \mu\text{mol g}^{-1}$ (**Figure 3.5d**). To complement these values and to place a metric upon the amount of specific binding per MIP/NIP, the imprint factor (IF) was calculated for each formulation. The IF value is defined as the amount of S_b at a defined C_f for the MIP devised by the S_b value of the NIP at the same C_f value. The C_f value for this calculate tends toward the lower ends as these values tend to be unaffected by the saturation effects when higher concentrations of the analyte are present. With this in mind, $C_f = 0.2 \text{ mM}$ was selected to calculate the IF values for each of the MIPs. These values were calculated directly from the fitted binding isotherms and are reported in **Table 3.2**. Of the compositions analysed, it is unsurprising that MIP/NIP-01 has the lowest specific binding toward glucose with an IF value of 2.12. The difference between the binding observed with the MIP/NIP is too similar, with this visually apparent lack of difference being reinforced by the calculated metric. It is however surprising that MIP/NIP-04 has a lower associated IF value when comparing the visually inspected graph. MIP-02 and MIP-03 were calculated to have similar

IF values, with MIP-02 demonstrating to be the more specific of the two with an IF value of 5.18 when compared to an MIP-03 value of 4.15. Again, these values are clearly a direct result of the amount of the cross-linker and monomer used in the synthesis of the MIP/NIP. MIP-02 has a higher concentration of the monomer compared to the cross-linker, enabling a higher degree of specific binding due to the higher degree of interactions possible between the monomer and template. The same trend can be seen between the MIP-01 and MIP-04, with MIP-04 having the higher amount of a functional monomer and subsequently slightly higher IF values in comparison. Overall, when considering both the maximum binding capacity and the associated IF values of each MIP, it is clear that the MIP that should be used in further experimentation is MIP-02. MIP-02 has a respectable maximum binding capacity while also retaining a higher IF when compared to the other compositions.

Table 3.2 Synthesized MIP/NIP Compositions

MIP/NIP	R ²	S _b /μmol g ⁻¹ (at C _f = 0.2 mM)	IF (at C _f = 0.2 mM)
1	0.9457	MIP: 6.54	2.12
	0.9058	NIP: 3.08	
2	0.8783	MIP: 13.05	5.18
	0.3874	NIP: 2.52	
3	0.9503	MIP: 8.6	4.15
	0.4508	NIP: 2.07	
4	0.9602	MIP: 16.09	2.29
	0.906	NIP: 7.03	

Rebinding Analysis via the HTM

After depositing the MIP/NIPs on aluminium chips that were spin coated with a thin layer of PVC (**Figure 3.6**), the functionalized surfaces were subjected to HTM analysis.

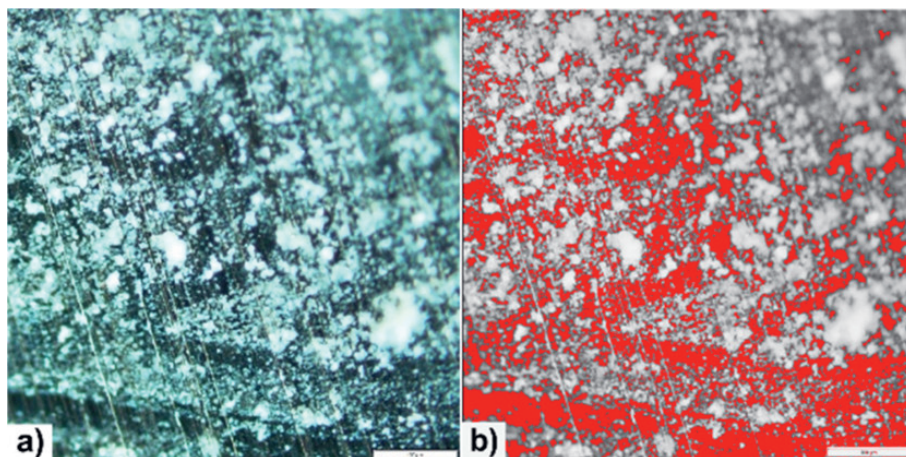


Figure 3.6 (a) Microscopy analysis of aluminium chips with deposited MIP particles. **(b)** Highlighted background in red showing a substrate without particles. Image was taken at 20× magnification.

In doing so, each of the functionalized surfaces was exposed to increasing concentrations of glucose (0.00–0.33 mM) over a defined time frame (**Figure 3.7**). The measurements were conducted in PBS (pH = 7.4) with a stabilization temperature of 37 °C so as to imitate the physiological conditions and to ensure that the conducted measurements were relatable to the potential real-world samples.

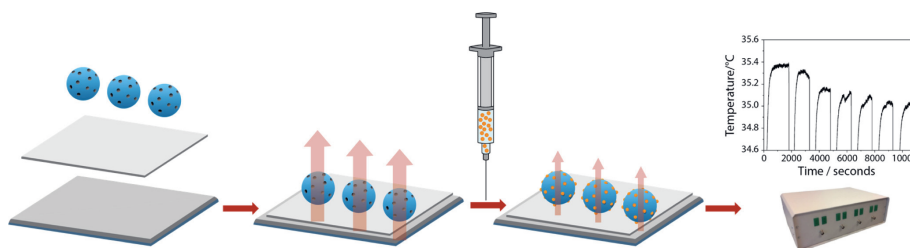


Figure 3.7 Schematic representation of the deposition of the MIP particles and rebinding analysis with the HTM.

The analysis of both MIPs and NIPs was conducted in the exact same manner to enable the direct comparison of substrates functionalized with both kinds of receptors. During the analysis, it can be clearly seen that the temperature inside the flow cell decreases when a higher concentration of glucose is introduced in the flow cell with the MIP particles (**Figure 3.8a**, black line). This behaviour is characteristic of an analyte that is binding to the MIP, as binding events at the surface of the receptor

typically lead to an increased thermal resistance at the solid–liquid interface, which impedes the flow of heat to the solution inside the flow cell. In comparison, the same behaviour is not observed during the analysis of the NIP (**Figure 3.8a**, red line), though there is a negligible decrease inside the flow cell when a high concentration of glucose is present. This decrease, however, is primarily due to the non-specific binding interactions that the glucose can have with any surface functionalities present in the NIP. The change in the temperature inside the flow cell can also be represented as a change in thermal resistance at the liquid-phase interface. The time-resolved thermal resistance data (R_{th}) of the MIP (black line) show that the decrease in temperature observed in **Figure 3.8a** can indeed be attributed to an increase in thermal resistance caused by glucose binding to the MIP particles (**Figure 3.8b**). When R_{th} is calculated for the NIP (red line), it is clear that the NIP does not behave in the same manner as the MIP and the thermal resistance of the receptor does not change much over the entire tested concentration range. These results are comparable with the ones presented in previous works where other biomolecules (vitamin k and other small molecules such as histamine, nicotine, and serotonin) were analysed with the same thermal readout setup. [42,49]

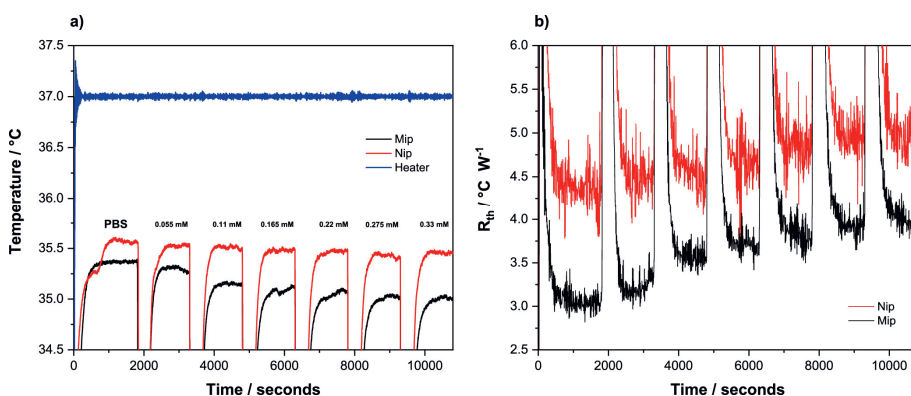


Figure 3.8 (a) Temperature profile and **(b)** R_{th} variations of the MIP/NIP after infusions with varying concentrations of glucose (0.00–0.33 mM) in PBS.

The time-resolved temperature profiles for the MIP and NIP were used to construct dose–response curves, plotting the effect size as a function of the change in temperature against the concentration of glucose introduced into the flow cell (**Figure 3.9**).

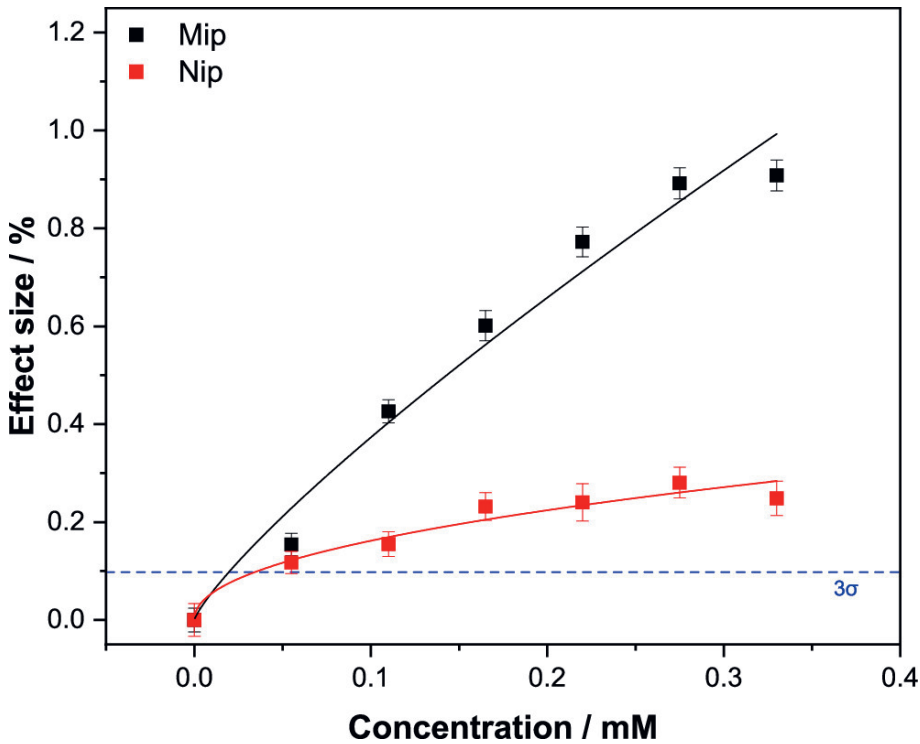


Figure 3.9 Dose–response curve obtained by HTM analysis of the MIP/NIP after infusions of different concentrations of glucose, the blue dashed line reveals the LoD (3σ method) at $\pm 19.4 \mu\text{M}$. Error bars and mean values are calculated using the noise of the signal and are the average of multiple measurements.

The effect size (%) was obtained by dividing the decrease in temperature at each concentration by the average baseline temperature obtained after stabilization in PBS (**Equation 3.2**).

$$\text{Effect size (\%)} = \frac{\Delta T}{T_{\text{PBS}}} \times 100 \quad (3.2)$$

The data was fit with Origin, version 2019b (OriginLabs Corporation, Northampton, MA, USA) using an allometric ($y = ax^b$) fit for both the MIP (black curve, $R^2 = 0.9593$) and NIP (red curve, $R^2 = 0.89887$).

The LoD was calculated from the dose–response curve of the MIP (blue dashed line) using the 3σ method, corresponding to three times the maximum y-axis noise on the signal throughout the measurement. The reason for taking the error on the measurement signal (intra-sample variability) rather than the standard error on the average of three measurements (inter-sample variability) is that the former is bigger than the latter. While this shows the sensitivity limitations of the low-cost readout technology, it also demonstrates that the electrode production process is highly reproducible and leads to a high degree of repeatability in the resulting sensor platform. This y-value was then plotted and its intercept with the black curve was the calculated LoD for the sensor being $19.4 \mu\text{M}$. The calculated

intercept for the LoD (19.4 μM) is greater than the curve plotted for the NIP data, demonstrating that the sensor is capable of detecting concentrations of glucose that bind specifically. Therefore, this adds a degree of reliability to the sensor as it is able to differentiate between non-specifically bound and specifically bound glucose. The sensor demonstrates the saturation effects toward the higher concentrations (above 0.25 mM) and seems to plateau as the concentration tends toward 0.33 mM. The reference NIP is shown to saturate at much lower concentrations (0.2 mM) and has an observably lower effect size in comparison to the MIP.

Selectivity Analysis of the Receptor Layer

To demonstrate the selectivity of the optimized MIP toward glucose, further HTM analysis was conducted. The same experimental parameters and procedures as per the glucose rebinding analysis with the HTM readout were used for the analysis of the analogues. The tested competitive analytes were selected based on the chemical structure and function in the body, therefore a monosaccharide (fructose) and two disaccharides (sucrose and lactose) were tested, and the binding response was analysed. To this end, fructose was analysed due to its similarity with glucose, though it is important to notice that despite having the same chemical formula ($\text{C}_6\text{H}_{12}\text{O}_6$), they differ structurally. To further determine the selectivity of the sensor, sucrose and lactose were analysed. Both molecules are composed of two monosaccharide units, one of them being glucose and the second one being fructose and galactose, respectively. In order to observe a direct comparison between glucose and the other tested analytes, the same concentration ranges previously analysed (0.055–0.33 mM) were applied, and the thermal response was then transformed directly into an effect size (%) as previously described (**Equation 3.2**).

The effect sizes were then plotted against the concentration for each analyte, and the different dose–response curves for MIPs (**Figure 3.10a**) and NIPs (**Figure 3.10b**) were obtained. Overall, none of the tested analytes demonstrated a higher binding affinity than glucose toward the MIP (**Figure 3.10a**). This difference was apparent from a C_f of 0.05 mM, where there is a clear differential between glucose and the other molecules. The difference in effect size is then seen to increase as the concentration of the analyte in solution does, demonstrating a higher selectivity toward glucose at higher concentrations. This said, when analysing samples at the lower C_f range, the analogues still have the potential to interfere with the sensor as they interact with the sensor in the LoD range. For medical diagnostics, this is not a problem as the physiological concentrations encountered are typically higher but it might limit the use of the sensor in industrial applications such as monitoring fermentation processes in large bioreactors. When analysing the NIP data, the analogues demonstrate a similar affinity to that of glucose. Of the compounds tested, lactose is the most similar to glucose with the signal being barely differentiable. This highlights the non-specific interactions between the NIP and the other analogues, though as with glucose an IF value can be calculated for each of the compounds (**Table 3.3**).

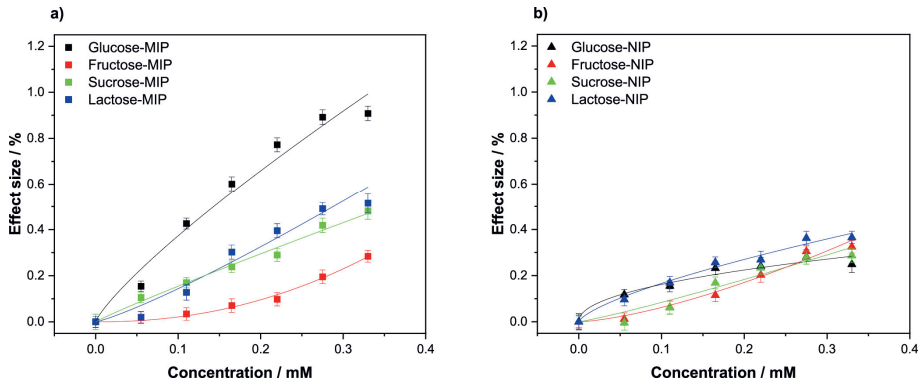


Figure 3.10 (a) HTM analysis of compounds (glucose, fructose, sucrose, and lactose) introduced inside the flow cell and infused at increasing concentrations in PBS (0.00–0.33 mM) and their corresponding dose–response curves for (a) MIPs and (b) NIPs. Error bars and mean values are calculated using the noise of the signal and are the average of multiple measurements.

Table 3.3 IF Values of the tested analytes at $C_f = 0.2$ mM

Analyte	IF ($C_f = 0.2$ mM)
Glucose	2.95
Sucrose	1.60
Lactose	1.22
Fructose	0.56

It should be noted that the disaccharides containing one glucose unit in their structure (sucrose and lactose) have a higher affinity for the MIP when comparing the IF of these with the one of fructose. Since the nanocavities present in the polymer are specifically made to fit a GA (and therefore glucose) unit, the response shown for sucrose and lactose is attributed to the presence of the glucose unit.

Application of the MIP Sensor for the Determination of Glucose Levels in Human Urine Samples

The applicability of the sensor for medical diagnostics was illustrated in by investigating the sensor’s ability to determine the glucose levels in urine samples. The same experimental parameters and procedures as per the analysis conducted in PBS were used for the analysis of glucose levels in human urine samples. To this end, urine samples were collected from a healthy volunteer and analysed with a commercial enzyme-based colorimetric glucose detection kit in order to confirm the absence of glucose in the collected urine samples (**Figure 3.11**).



Figure 3.11 Test strips for detection of glucose in urine show no presence of glucose in the collected urine samples.

In order to show a direct comparison between the thermal response obtained in PBS and the one obtained in urine samples, the urine samples were spiked with the same concentration of glucose (0.055–0.33 mM) previously analysed. Dose-response curves for both the MIP and NIP were obtained by plotting the effect size as a function of the change in temperature against the concentration of glucose in urine introduced in the flow cell (**Figure 3.12**). The effect of size (%) was calculated in the same manner using the previously reported equation (**Equation 3.2**). The data was fit with Origin, version 2019b (OriginLabs Corporation, Northampton, MA, USA) using an allometric ($y = ax^b$) fit for both the MIP (black curve, $R^2 = 0.9753$) and NIP (red curve, $R^2 = 0.5756$). The LoD was calculated using the same method as the one obtained from the curve in PBS (3σ method) and was found to be 44.4 μM .

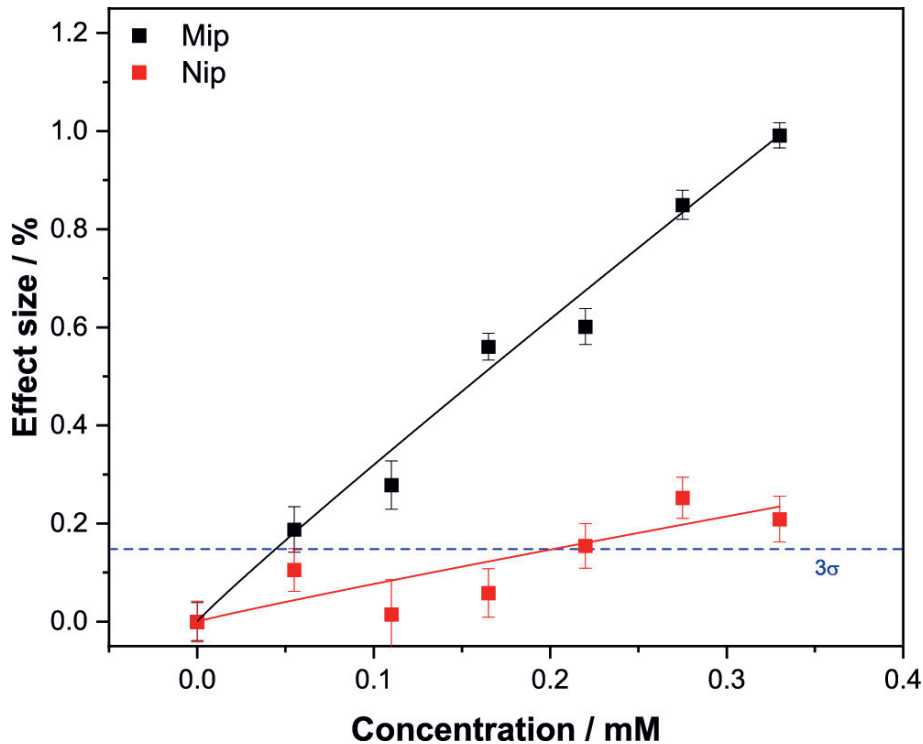


Figure 3.12 Dose–response curve obtained by HTM analysis of the MIP/NIP after infusions of different concentrations of glucose in spiked human urine samples, the blue dashed line reveals the LoD (3σ method) at $\pm 44.4 \mu\text{M}$. Error bars and mean values are calculated using the noise of the signal and are the average of multiple measurements.

Similar to the experiments performed in PBS, the calculated intercept for the LoD in urine samples is greater than the curve plotted for the NIP data, demonstrating that the sensor is capable of detecting glucose in a quantitative and specific manner in human urine samples as well as in PBS. When comparing the dose response curves obtained with the HTM analysis using PBS or urine as a medium, the sensor demonstrates a very similar behaviour. It can be clearly noticed that in both the dose–response curves (**Figures 3.9 and 3.12**), an observably lower effect size is observed for the reference NIP when compared with the MIP. Even though the calculated LoD is higher in urine than in PBS samples, 44.4 and 19.4 μM , respectively, the sensitivity of the sensor in urine is higher than the one calculated for many commercial enzyme–based sensors and therefore demonstrates the applicability of the sensor in the monitoring and quantification of glucose in diabetic patients.

Selectivity Analysis of the Receptor Layer in Human Urine Samples

The selectivity of the developed platform in human urine samples was demonstrated with further HTM analysis. This was achieved by analysing the thermal response after injection of the same compounds

(fructose, sucrose and lactose) and concentrations used for the selectivity studies in buffer solutions. The recorded thermal response was then transformed into an effect size (%) as previously described (Equation 3.2) and plotted against the injected concentration of the analyte in urine samples (Figure 3.13).

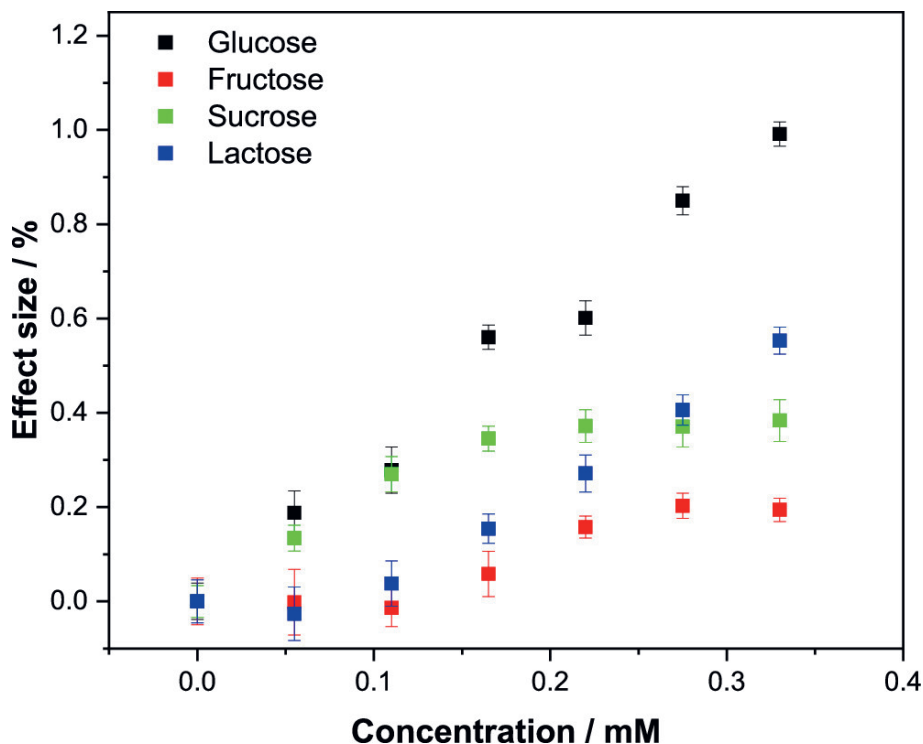


Figure 3.13 HTM analysis of compounds introduced inside the flow cell and infused at increasing concentrations (0.00–0.033 mM) in human urine samples and their corresponding dose–response curves for MIPs. Error bars and mean values are calculated using the noise of the signal and are the average of multiple measurements.

Overall, none of the tested alternative analytes show a higher binding affinity towards the MIPs than Glucose. This difference was apparent from the first injection (0.05 mM), in addition the difference in effect size is seen to increase as the concentration of the analyte introduced does. This demonstrates a higher selectivity toward glucose at higher concentrations. It can be noticed that the disaccharides containing a glucose unit (sucrose and lactose) show a higher rebinding effect than fructose, attributed to the fact that the navocavities present in the MIP are made to fit a GA (and therefore a glucose) unit. Since the effect sizes obtained in PBS are comparable with the ones obtained in human urine samples for each of the tested compounds, it is demonstrated that selectivity and specificity of the sensor are not highly affected by the matrix in which the analytes are present.

Conclusions

In this work, a straightforward approach for the synthesis of MIPs for glucose using a dummy imprinting technique was presented. The imprinted polymer was prepared using GA as the dummy template to obtain receptors that could bind glucose. By preparing MIPs with different molar ratios of GA/AAM/EGDMA, an optimized MIP recipe was obtained to ensure the specific interaction between the target and the receptor. Template removal from these synthesized MIPs was studied using FTIR and TGA, providing a strong proof that the template molecule is indeed removed and functions optimally. Rebinding experiments analysed with LC-MS proceeded to be used to construct binding isotherms for each of the compositions. These isotherms were analysed in terms of maximum binding capacity and IF values, where MIP-02 was determined to have the best composition for binding glucose ($IF = 5.18$, $S_b \text{ max} = 15.59 \mu\text{mol g}^{-1}$). The optimized MIP was then scrutinized further by thermal analysis with the HTM. The analysis of the MIP samples was performed in phosphate buffer solutions, where a LoD of $19.4 \mu\text{M}$ and a linear range of $19.4\text{--}330 \mu\text{M}$ was achieved. The sensor therefore operates in a concentration regime that is two orders of magnitude higher than physiological concentrations encountered in blood. However, for other applications such as the detection of glucose in sweat, urine, food products, or industrial applications, the higher apparent sensitivity renders it beneficial over traditional, commercial enzymatic glucose sensors. The same analysis was then conducted for different analogues of glucose (sucrose, lactose, and fructose), determining that the sensor had greater affinity toward glucose than any of the molecules tested. Finally, the MIP particles demonstrated their efficiency in detecting glucose in physiological fluids. To this end, human urine samples were collected and analysed with the HTM. The sensor exhibited an LOD of $44.4 \mu\text{M}$ and a linear range of $44.4\text{--}330 \mu\text{M}$, demonstrating the applicability of the sensor in both establishing urine glucose concentrations. The combination of a low-cost detection platform with a straightforward, easily scalable production process, leading to a disposable glucose sensor that is competitive to state-of-the-art sensor platforms, makes these findings very interesting in terms of commercial applications. Hence it is worthwhile to conduct follow-up research to further optimize the sensor and integrate it into a handheld or wearable device. The results demonstrate that the sensor might offer a non-invasive, low-cost alternative to traditional enzyme-based and/or electrochemical methods in terms of medical diagnostics. In addition, the sensitivity of the sensor also makes it interesting to study other potential applications such as its use in food analysis or the monitoring of industrial fermentation processes.

References Chapter 3

1. Vaulont, S.; Vasseur-Cognet, M.; Kahn, A. Glucose Regulation of Gene Transcription. *J. Biol. Chem.* 2000, 275, 31555– 31558, doi:10.1074/jbc.r000016200
2. du Plessis, S.; Agarwal, A.; Mohanty, G.; van der Linde, M. Oxidative Phosphorylation versus Glycolysis: What Fuel Do Spermatozoa Use?. *Asian J. Androl.* 2015, 17, 230, doi:10.4103/1008-682X.135123
3. Klonoff, D. C. Continuous Glucose Monitoring: Roadmap for 21st century diabetes therapy. *Diabetes Care* 2005, 28, 1231– 1239, doi:10.2337/diacare.28.5.1231
4. Lin, Y.; Yu, P.; Hao, J.; Wang, Y.; Ohsaka, T.; Mao, L. Continuous and Simultaneous Electrochemical Measurements of Glucose, Lactate, and Ascorbate in Rat Brain Following Brain Ischemia. *Anal. Chem.* 2014, 86, 3895– 3901, doi:10.1021/ac4042087
5. Kropff, J.; Bruttomesso, D.; Doll, W.; Farret, A.; Galasso, S.; Luijf, Y. M.; Mader, J. K.; Place, J.; Boscarì, F.; Pieber, T. R.; Renard, E.; DeVries, J. H. Accuracy of two continuous glucose monitoring systems: a head-to-head comparison under clinical research centre and daily life conditions. *Diabetes, Obes. Metab.* 2015, 17, 343, doi:10.1111/dom.12378
6. Coster, S.; Gulliford, M.; Seed, P.; Powrie, J.; Swaminathan, R. Monitoring Blood Glucose Control in Diabetes Mellitus: A Systematic Review. *Health Technol. Assess.* 2000, 4, 1– 93, doi:10.3310/hta4120
7. American Diabetes Association Diagnosis and Classification of Diabetes Mellitus. *Diabetes Care* 2014, 37 Suppl 1, S81– 90, doi:10.2337/DC14-S081
8. Cho, N. H.; Shaw, J. E.; Karuranga, S.; Huang, Y.; da Rocha Fernandes, J. D.; Ohlrogge, A. W.; Malanda, B. IDF Diabetes Atlas: Global Estimates of Diabetes Prevalence for 2017 and Projections for 2045. *Diabetes Res. Clin. Pract.* 2018, 138, 271– 281, doi:10.1016/j.diabres.2018.02.023
9. Rowley, W. R.; Bezold, C.; Arikan, Y.; Byrne, E.; Krohe, S. Diabetes 2030: Insights from Yesterday, Today, and Future Trends. *Popul. Health Manag.* 2017, 20, 6– 12, doi:10.1089/pop.2015.0181
10. Chen, A.; Chatterjee, S. Nanomaterials Based Electrochemical Sensors for Biomedical Applications. *Chem. Soc. Rev.* 2013, 42, 5425, doi: 10.1039/c3cs35518g
11. Nichols, S. P.; Koh, A.; Storm, W. L.; Shin, J. H.; Schoenfisch, M. H. Biocompatible Materials for Continuous Glucose Monitoring Devices. *Chem. Rev.* 2013, 113, 2528– 2549, doi:10.1021/cr300387j
12. Shokrehodaie, M.; Quinones, S. Review of Non-Invasive Glucose Sensing Techniques: Optical, Electrical and Breath Acetone. *Sensors* 2020, 20, 1251, doi:10.3390/s20051251
13. Malitesta, C.; Palmisano, F.; Torsi, L.; Zambonin, P. G. Glucose Fast-Response Amperometric Sensor Based on Glucose Oxidase Immobilized in an Electropolymerized Poly(o-Phenylenediamine) Film. *Anal. Chem.* 1990, 62, 2735– 2740, doi:10.1021/ac00223A016
14. Luo, X.; Xia, J.; Jiang, X.; Yang, M.; Liu, S. Cellulose-Based Strips Designed Based on a Sensitive Enzyme Colorimetric Assay for the Low Concentration of Glucose Detection. *Anal. Chem.* 2019, 91, 15461– 15468, doi:10.1021/acs.analchem.9B03180

15. Cha, R.; Wang, D.; He, Z.; Ni, Y. Development of Cellulose Paper Testing Strips for Quick Measurement of Glucose Using Chromogen Agent. *Carbohydr. Polym.* 2012, 88, 1414– 1419, doi:10.1016/j.carbpol.2012.02.028
16. Park, S.; Boo, H.; Chung, T. D. Electrochemical Non-Enzymatic Glucose Sensors. *Anal. Chim. Acta* 2006, 556, 46– 57, doi:10.1016/j.aca.2005.05.080
17. Sehit, E.; Altintas, Z. Significance of Nanomaterials in Electrochemical Glucose Sensors: An Updated Review (2016–2020). *Biosens. Bioelectron.* 2020, 159, 112165, doi:10.1016/j.bios.2020.112165
18. Gao, H.; Xiao, F.; Ching, C. B.; Duan, H. One-Step Electrochemical Synthesis of PtNi Nanoparticle-Graphene Nanocomposites for Nonenzymatic Amperometric Glucose Detection. *ACS Appl. Mater. Interfaces* 2011, 3, 3049– 3057, doi:10.1021/AM200563F
19. Park, S.; Chung, T. D.; Kim, H. C. Nonenzymatic Glucose Detection Using Mesoporous Platinum. *Anal. Chem.* 2003, 75, 3046– 3049, doi:10.1021/ac0263465
20. Zhang, L.; Li, H.; Ni, Y.; Li, J.; Liao, K.; Zhao, G. Porous Cuprous Oxide Microcubes for Non-Enzymatic Amperometric Hydrogen Peroxide and Glucose Sensing. *Electrochem. Commun.* 2009, 11, 812– 815, doi:10.1016/j.elecom.2009.01.041
21. Emir, G.; Dilgin, Y.; Ramanaviciene, A.; Ramanavicius, A. Amperometric Nonenzymatic Glucose Biosensor Based on Graphite Rod Electrode Modified by Ni-Nanoparticle/Polypyrrole Composite. *Microchem. J.* 2021, 161, 105751, doi:10.1016/j.microc.2020.105751
22. Ratautaite, V.; Samukaite-Bubniene, U.; Plausinaitis, D.; Boguzaitė, R.; Balciunas, D.; Ramanaviciene, A.; Neunert, G.; Ramanavicius, A. Molecular Imprinting Technology for Determination of Uric Acid. *Int. J. Mol. Sci.* 2021, 22, 5032, doi:10.3390/ijms22095032
23. Viter, R.; Kunene, K.; Genys, P.; Jevdokimovs, D.; Erts, D.; Sutka, A.; Bisetty, K.; Viksna, A.; Ramanaviciene, A.; Ramanavicius, A. Photoelectrochemical Bisphenol S Sensor Based on ZnO-Nanoroads Modified by Molecularly Imprinted Polypyrrole. *Macromol. Chem. Phys.* 2020, 221, 1900232, doi:10.1002/macp.201900232
24. Belbruno, J. J. Molecularly Imprinted Polymers. *Chemical Reviews* 2019, 119, 94– 119, doi:10.1021/acs.chemrev.8b00171
25. Ye, L.; Haupt, K. Molecularly Imprinted Polymers as Antibody and Receptor Mimics for Assays, Sensors and Drug Discovery. *Anal. Bioanal. Chem.* 2004, 378, 1887– 1897, doi:10.1007/s00216-003-2450-8
26. Lavignac, N.; Allender, C. J.; Brain, K. R. Current Status of Molecularly Imprinted Polymers as Alternatives to Antibodies in Sorbent Assays. *Anal. Chim. Acta* 2004, 510, 139– 145, doi:10.1016/j.aca.2003.12.066
27. Zhang, H. *Molecularly Imprinted Nanoparticles for Biomedical Applications. Advanced Materials; Wiley-VCH Verlag, 2020 January Vol. 32.*

28. Wackerlig, J.; Lieberzeit, P. A. Molecularly imprinted polymer nanoparticles in chemical sensing - Synthesis, characterisation and application. *Sens. Actuators, B* 2015, 207, 144– 157, doi:10.1016/j.snb.2014.09.094
29. Schirhagl, R.; Qian, J.; Dickert, F. L. Immunosensing with Artificial Antibodies in Organic Solvents or Complex Matrices. *Sens. Actuators, B* 2012, 173, 585– 590, doi:10.1016/j.snb.2012.07.036
30. Piletsky, S. A.; Alcock, S.; Turner, A. P. F. Molecular Imprinting: At the Edge of the Third Millennium. *Trends Biotechnol.* 2001, 19, 9– 12, doi:10.1016/s0167-7799(00)01523-7
31. Ramanavicius, S.; Jagminas, A.; Ramanavicius, A. Advances in Molecularly Imprinted Polymers Based Affinity Sensors (Review). *Polymers* 2021, 13, 974, doi:10.3390/polym13060974
32. Ramanavicius, S.; Ramanavicius, A. Conducting Polymers in the Design of Biosensors and Biofuel Cells. *Polymers* 2021, 13, 49, doi:10.3390/polym13010049
33. Liu, G.; Huang, X.; Li, L.; Xu, X.; Zhang, Y.; Lv, J.; Xu, D. Recent Advances and Perspectives of Molecularly Imprinted Polymer-Based Fluorescent Sensors in Food and Environment Analysis. *Nanomaterials* 2019, 9, 1030, doi:10.3390/nano9071030
34. van Grinsven, B.; Eersels, K.; Peeters, M.; Losada-Pérez, P.; Vandenryt, T.; Cleij, T. J.; Wagner, P. The Heat-Transfer Method: A Versatile Low-Cost, Label-Free, Fast, and User-Friendly Readout Platform for Biosensor Applications. *ACS Appl. Mater. Interfaces* 2014, 6, 13309– 13318, doi:10.1021/am503667s
35. Steen Redeker, E.; Eersels, K.; Akkermans, O.; Royakkers, J.; Dyson, S.; Nurekeyeva, K.; Ferrando, B.; Cornelis, P.; Peeters, M.; Wagner, P.; Diliën, H.; van Grinsven, B.; Cleij, T. J. Biomimetic Bacterial Identification Platform Based on Thermal Wave Transport Analysis (TWTA) through Surface-Imprinted Polymers. *ACS Infect. Dis.* 2017, 3, 388– 397, doi:10.1021/acsinfectdis.7b00037
36. Arreguin-Campos, R.; Eersels, K.; Lowdon, J. W.; Rogosic, R.; Heidt, B.; Caldara, M.; Jiménez-Monroy, K. L.; Diliën, H.; Cleij, T. J.; van Grinsven, B. Biomimetic Sensing of Escherichia Coli at the Solid-Liquid Interface: From Surface-Imprinted Polymer Synthesis toward Real Sample Sensing in Food Safety. *Microchem. J.* 2021, 169, 106554, doi:10.1016/j.microc.2021.106554
37. Crapnell, R. D.; Street, R. J.; Ferreira-Silva, V.; Down, M. P.; Peeters, M.; Banks, C. E. Electrospun Nylon Fibers with Integrated Polypyrrole Molecularly Imprinted Polymers for the Detection of Glucose. *Anal. Chem.* 2021, 93, 13235– 13241, doi:10.1021/acs.analchem.1c02472
38. Crapnell, R. D.; Canfarotta, F.; Czulak, J.; Johnson, R.; Betlem, K.; Mecozzi, F.; Down, M. P.; Eersels, K.; van Grinsven, B.; Cleij, T. J.; Law, R.; Banks, C. E.; Peeters, M. Thermal Detection of Cardiac Biomarkers Heart-Fatty Acid Binding Protein and ST2 Using a Molecularly Imprinted Nanoparticle-Based Multiplex Sensor Platform. *ACS Sens.* 2019, 4, 2838– 2845, doi:10.1021/acssensors.9b01666
39. Peeters, M. M.; van Grinsven, B.; Foster, C.; Cleij, T.; Banks, C. Introducing Thermal Wave Transport Analysis (TWTA): A Thermal Technique for Dopamine Detection by Screen-Printed Electrodes Functionalized with Molecularly Imprinted Polymer (MIP) Particles. *Molecules* 2016, 21, 552, doi:10.3390/molecules21050552

40. Lowdon, J. W.; Eersels, K.; Arreguin-Campos, R.; Caldara, M.; Heidt, B.; Rogosic, R.; Jimenez-Monroy, K. L.; Cleij, T. J.; Diliën, H.; van Grinsven, B. A Molecularly Imprinted Polymer-Based Dye Displacement Assay for the Rapid Visual Detection of Amphetamine in Urine. *Molecules* 2020, 25, 5222, doi:10.3390/molecules25225222
41. Lowdon, J. W.; Diliën, H.; van Grinsven, B.; Eersels, K.; Cleij, T. Colorimetric Sensing of Amoxicillin Facilitated by Molecularly Imprinted Polymers. *Polymers* 2021, 13, 2221, doi:10.3390/polym13132221
42. Eersels, K.; Diliën, H.; Lowdon, J.; Steen Redeker, E.; Rogosic, R.; Heidt, B.; Peeters, M.; Cornelis, P.; Lux, P.; Reutelingsperger, C.; Schurgers, L.; Cleij, T.; van Grinsven, B. A Novel Biomimetic Tool for Assessing Vitamin K Status Based on Molecularly Imprinted Polymers. *Nutrients* 2018, 10, 751, doi:10.3390/nu10060751
43. Lowdon, J. W.; Eersels, K.; Rogosic, R.; Boonen, T.; Heidt, B.; Diliën, H.; van Grinsven, B.; Cleij, T. J. Surface Grafted Molecularly Imprinted Polymeric Receptor Layers for Thermal Detection of the New Psychoactive Substance 2-Methoxyphenidine. *Sens. Actuators, A* 2019, 295, 586– 595, doi:10.1016/j.sna.2019.06.029
44. Rogosic, R.; Lowdon, J. W.; Heidt, B.; Diliën, H.; Eersels, K.; Van Grinsven, B.; Cleij, T. J. Studying the Effect of Adhesive Layer Composition on MIP-Based Thermal Biosensing. *Phys. Status Solidi A* 2019, 216, 1800941, doi:10.1002/pssa.201800941
45. Lorenzo, R.; Carro, A.; Alvarez-Lorenzo, C.; Concheiro, A. To Remove or Not to Remove? The Challenge of Extracting the Template to Make the Cavities Available in Molecularly Imprinted Polymers (MIPs). *Int. J. Mol. Sci.* 2011, 12, 4327– 4347, doi:10.3390/ijms12074327
46. Kacuráková, M.; Mathlouthi, M. FTIR and Laser-Raman Spectra of Oligosaccharides in Water: Characterization of the Glycosidic Bond. *Carbohydr. Res.* 1996, 284, 145– 157, doi:10.1016/0008-6215(95)00412-2
47. Wolkers, W. F.; Oliver, A. E.; Tablin, F.; Crowe, J. H. A Fourier-Transform Infrared Spectroscopy Study of Sugar Glasses. *Carbohydr. Res.* 2004, 339, 1077– 1085, doi:10.1016/j.carres.2004.01.016
48. Thoelen, R.; Vansweevelt, R.; Duchateau, J.; Horemans, F.; D'Haen, J.; Lutsen, L.; Vanderzande, D.; Ameloot, M.; vandeVen, M.; Cleij, T. J.; Wagner, P. A MIP-Based Impedimetric Sensor for the Detection of Low-MW Molecules. *Biosens. Bioelectron.* 2008, 23, 913– 918, doi:10.1016/j.bios.2007.08.020
49. Peeters, M.; Csipai, P.; Geerets, B.; Weustenraed, A.; van Grinsven, B.; Thoelen, R.; Gruber, J.; de Ceuninck, W.; Cleij, T. J.; Troost, F. J.; Wagner, P. Heat-Transfer-Based Detection of l-Nicotine, Histamine, and Serotonin Using Molecularly Imprinted Polymers as Biomimetic Receptors. *Anal. Bioanal. Chem.* 2013, 405, 6453– 6460, doi:10.1007/s00216-013-7024-9

Preface to Chapter 4

In the last decades, MIPs have attracted increasing attention, firstly as sorbent materials in separation science, and more recently as synthetic receptor elements in biosensor devices. Several MIP-based sensors have been developed and coupled with a wide array of transducers for the detection of important biomarkers in the healthcare sector. The research focus of MIP-based sensing platforms is now shifting towards the development of sensors able to recognize the target in complex matrices (patient samples, food products...) and to improve the MIP synthesis process towards mass-production. In **Chapter 3**, the use of low-cost bulk MIP particles for the thermal detection of glucose was illustrated. The research concluded with the detection of glucose in a challenging matrix, such as human urine samples using HTM as transducer technology. The findings therefore demonstrate the potential of such a MIP-based platform for non-invasive diabetes monitoring.

In the following chapter, the versatility of MIP-based HTM platforms is evaluated by developing a similar sensor application in food safety. We will develop MIPs for the detection melamine, an harmful molecule sometimes found in milk and milk products. In this study, a MIP-based thermal biosensor will be fabricated using a similar, low-cost fabrication process to the one described in the previous chapter. Selectivity and sensitivity of the platform towards melamine will be initially evaluated in CaCl_2 solutions (to mimic dairy products) with the HTM method. Furthermore, by analysing and recording the thermal response of the sensor in untreated melamine-spiked milk samples, we will try to demonstrate a proof-of-application. The ability to reliably identify melamine-contaminated milk samples, which is a crucial issue in food safety analysis, would further illustrate the sensor's wide application range.

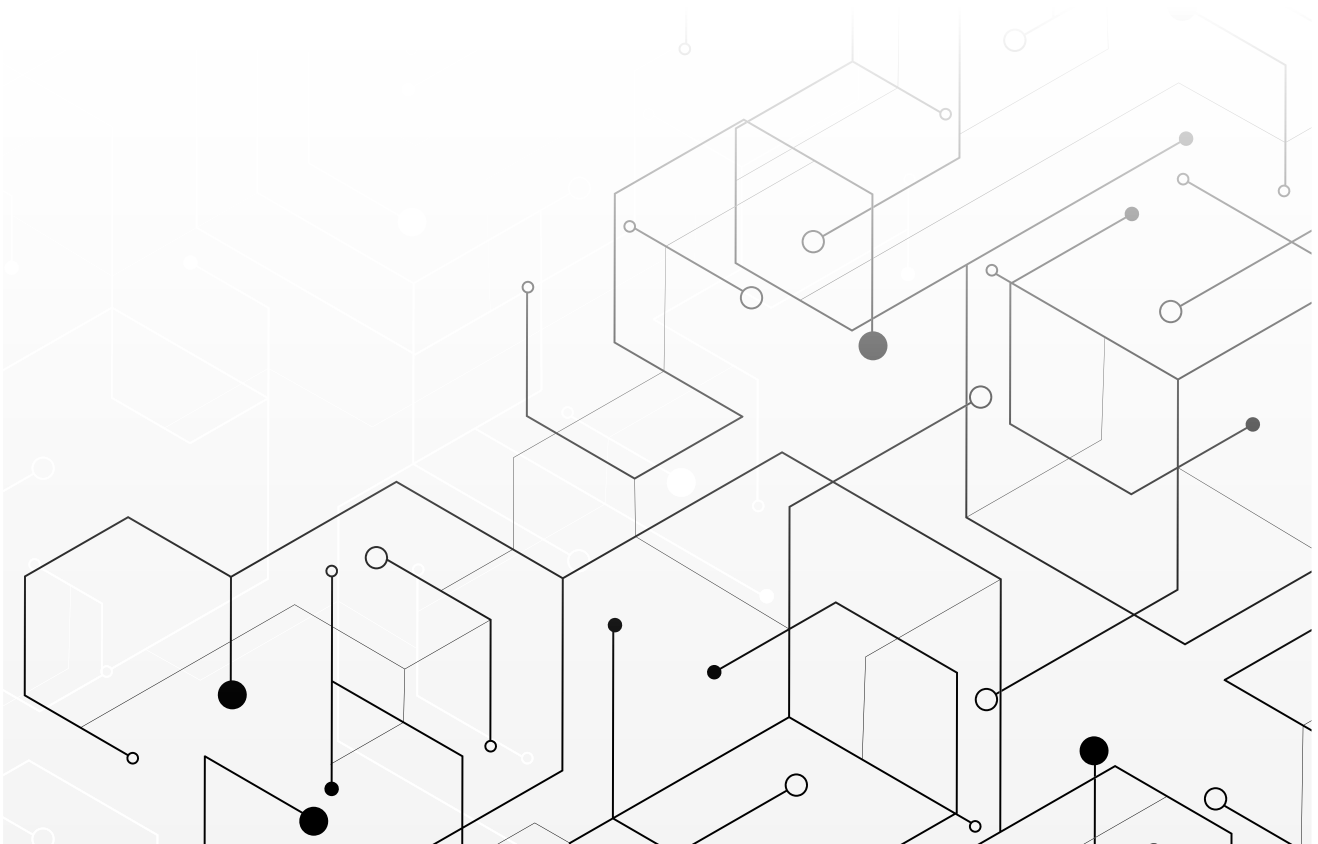
Chapter 4

A Molecularly Imprinted Polymer-Based Thermal Sensor for the Selective Detection of Melamine in Milk Samples

Adapted from:

Caldara, M.*; Lowdon, J.W.; Royackers, J.; Peeters, M.; Cleij, T.J.; Diliën, H.; Eersels, K.; van Grinsven, B. A Molecularly Imprinted Polymer-Based Thermal Sensor for the Selective Detection of Melamine in Milk Samples.

Foods 2022, 11(18), 2906.
<https://doi.org/10.3390/foods11182906>



Abstract

In recent years, melamine-sensing technologies have increasingly gained attention, mainly due to the misuse of the molecule as an adulterant in milk and other foods. Molecularly imprinted polymers (MIPs) are ideal candidates for the recognition of melamine in real-life samples. The prepared MIP particles were incorporated into a thermally conductive layer via micro-contact deposition and its response towards melamine was analysed using the heat-transfer method (HTM). The sensor displayed an excellent selectivity when analysing the thermal response to other chemicals commonly found in foods, and its applicability in food safety was demonstrated after evaluation in untreated milk samples, demonstrating a limit of detection of 6.02 μM . As the EU/US melamine legal limit in milk of 2.5 mg/kg falls within the linear range of the sensor, it can offer an innovative solution for routine screening of milk samples in order to detect adulteration with melamine. The results shown in this work thus demonstrate the great potential of a low-cost thermal platform for the detection of food adulteration in complex matrices.

Keywords: melamine; molecularly imprinted polymers (MIPs); milk; heat-transfer method (HTM); food adulteration testing; low-cost melamine detection

Introduction

Melamine ($C_3H_6N_6$) is a heterocyclic organic compound that is widely used in combination with formaldehyde and other agents to produce synthetic resins. Melamine resins are hard and highly durable materials, which find their application in the manufacture of many products, such as kitchenware and laminates.[1] Furthermore, because of its high nitrogen content (66% by mass), low price, and the fact that protein levels in milk are indirectly assessed via the total nitrogen content, it has been added intentionally into milk in order to mimic protein-rich milk products.[2,3] The oral ingestion of high concentrations of melamine can cause serious health issues, including bladder cancer,[4] renal failure,[5] or even fatality in humans and animals.[6,7] For this reason, the maximum residual levels allowed in milk and milk products are set at 2.5 mg/kg by The Codex Alimentarius Committee (CAC).[8] Sensors that allow for routine screening of dairy products in a low-cost manner could enable end-users and industrial stakeholders at various points in the dairy production value chain so as to identify melamine adulteration rapidly and significantly decrease its adverse effects on the general healthcare system.[9] In the last few years, several well-established techniques have been developed for the quantification of melamine levels in milk products. However, most of these essays are based on expensive lab-based technologies such as high-performance liquid chromatography (HPLC),[10] liquid chromatography–tandem mass spectrometry (LC–MS/MS)[11,12], and surface-enhanced Raman scattering spectroscopy (SERS)[13,14]. Although current laboratory tests are very sensitive and can accurately determine the melamine levels in the samples, the analysis is typically slow and costly. Moreover, such complex matrices often require pre-treatment of the food sample to accurately perform these analyses.[15,16] As a result, standard practice is to only take samples at regulatory intervals and to screen them for melamine adulteration, leaving several cases unnoticed. Low-cost alternatives that allow for routine screening of products are thus highly desirable. Although low-cost melamine sensors are already present in the market, they usually do not offer quantifiable information in terms of the legal limit and they require reagents or labels. Moreover, these commercial sensors are based on enzymes, colloidal gold, or antibodies, with the main disadvantage for these being their limited stability, thus leading to relatively short shelf-life and the need for storing the sensor at determined temperatures and conditions. Biosensors could offer a low-cost alternative and in recent years, biosensors based on so-called molecularly imprinted polymers (MIPs) have specifically gained attention.[17–20] MIPs are synthetic receptors capable of selectively binding to a target through a “lock and key” mechanism and, as such, are considered synthetic substitutes of natural antibodies.[21] MIPs have been extensively studied in the last decades, and their high application potential in food safety and clinical diagnostics[22–25] is primarily due to the advantages over their natural counterparts in terms of chemical and environmental stability, straightforward preparation, and cost-effectiveness [26,27]. These features make MIPs ideal candidates for the recognition of different molecules and biomarkers in complex matrices.[28–30] To develop viable sensors, MIPs need to be combined with a readout technology that is capable of converting binding events at the receptor surface into a quantifiable signal, while operating in complex media. The heat-transfer method (HTM)[31] can detect temperature changes across a solid–liquid interface, allowing for various targets, ranging from small molecules to bacteria, and, more recently, viral antigens for COVID-19 diagnosis.[32–36] In short, when the target solution is introduced into the flow cell, MIP particles bind to the analyte, resulting in a thermal change at the interface. This change is then detected as a change in temperature in the medium above a sensor chip, registered by a thermocouple placed inside the flow cell (TC-2), while another thermocouple (TC-1), coupled to a PID-based temperature control system, stringently steers the input temperature underneath the sample (**Figure 4.1**). By actively steering the temperature input and

monitoring the temperature output, the sensor is able to monitor the difference in thermal resistance across the solid–liquid interface.

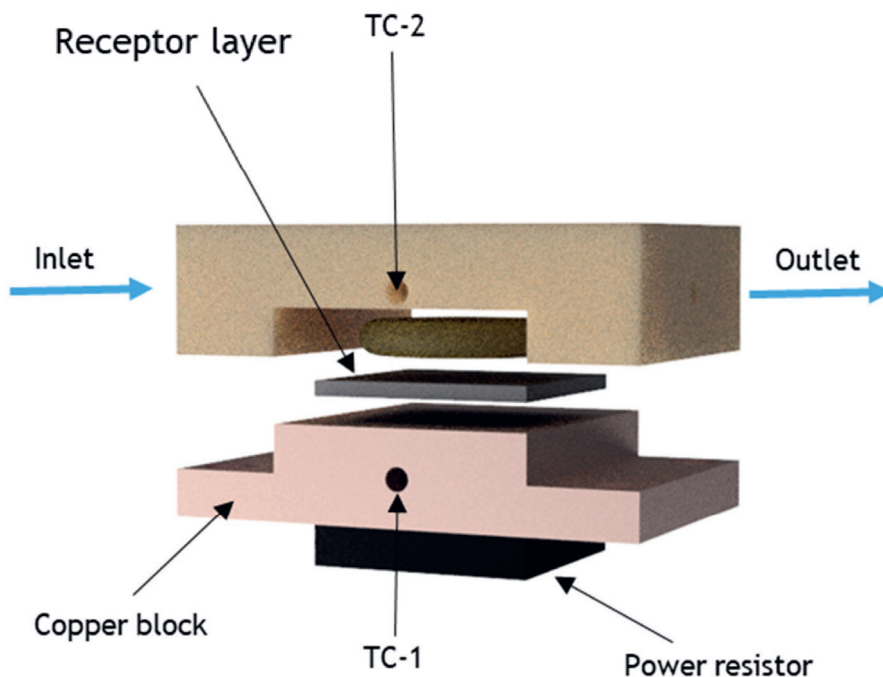


Figure 4.1 Graphical representation of the HTM analysis setup.

The study in this chapter aims to prove that an HTM-coupled, MIP-based melamine receptor can form the basis for routine analysis and a low-cost adulteration sensor in untreated food samples. Therefore, in this work, MIPs were synthesized and optimized for the detection of melamine by varying the recipe composition. The rebinding performance of each of the resulting MIPs was analysed using UV–VIS spectroscopy. The analysis of the rebinding capabilities and the imprinting efficiency of the different recipe compositions permitted the selection of the best MIP ratio, which was then used throughout the chapter for all of the HTM measurements. The optimized MIP particles were then integrated into a sensing chip via micro-contact deposition on a polyvinyl chloride-covered aluminium HTM substrate. The resulting sensor illustrated the specificity and reproducibility of the MIP-platform for the detection of melamine in CaCl_2 when compared with the corresponding NIP. The selectivity of the layer was established by comparing the thermal response of the receptor layer to the target and molecules that are commonly found in milk samples (cyanuric acid and lactose) or other contaminants found in different foods and beverages (bisphenol A). To demonstrate the application of the sensor in food safety analysis, it was exposed to known concentrations of melamine in untreated milk samples, and the thermal response was recorded and evaluated. The resulting linear range and LoD were compared with the legal limit in EU and USA, proving the applicability of the MIP-based platform for the monitoring and detection of melamine levels in food samples.

Materials and Methods

Chemicals and Reagents

Melamine (99%), D-lactose monohydrate ($\geq 99.5\%$), bisphenol A ($\geq 99\%$), polyvinyl chloride (MQ200), acetic acid (99.8%), calcium chloride ($\geq 97\%$), methacrylic acid (99.5%), tetrahydrofuran (99.5%), dimethyl sulfoxide (99.7%), and 2,2'-azobis(2-methylpropionitrile) (98%) were purchased from Sigma-Aldrich Chemie B.V. (Zwijndrecht, the Netherlands). Ethylene glycol dimethacrylate (98%) and methanol ($\geq 99.9\%$) were obtained from TCI Chemicals. Cyanuric acid (99%) and ethanol (96%) were purchased from Fisher Scientific (Landsmeer, the Netherlands). Prior to polymerization, functional and cross-linking monomers were passed over an aluminium-oxide-packed column to remove stabilizers. All stock solutions were prepared with Milli-Q water of $18.2 \text{ M}\Omega \text{ cm}^{-1}$. Polydimethylsiloxane (PDMS) stamps were made using the Sylgard 184 elastomer kit supplied by Mavom N.V. (Schelle, Belgium). Aluminium chips were obtained from Brico N.V. (Korbeek-Lo, Belgium) and cut to 1 cm^2 surfaces. The melamine rapid test kit was purchased from Ballya Bio-Med Co., Ltd. (Guangzhou, China).

Synthesis of Molecularly Imprinted Polymers

The ratios and procedures employed for the synthesized MIPs were based on previous literature regarding the monolithic polymerization of molecularly imprinted polymers for other targets.[37,38] The best rebinding efficiency in this study was obtained with a 1:14:28 ratio of template/monomer/cross-linker. In short, MEL template (0.25 mmol, 31.5 mg), MAA functional monomer (3.5 mmol, 297 μL), EGDMA cross-linker (7 mmol, 1.32 mL), and AIBN initiator (0.24 mmol, 40 mg) were dissolved in dimethyl sulfoxide (DMSO; 5 mL). The reaction mixture was bubbled with N_2 for 20 min to remove the oxygen before polymerization. Next, the mixture was heated to $65 \text{ }^\circ\text{C}$ for 8 h. The resulting bulk MIP were then ground into finer particles and washed with methanol to remove unreacted reagents. The MIP solids were then collected by filtration and dried in an oven for 12 h at $65 \text{ }^\circ\text{C}$. The dried particles were milled three times using a Fritsch Planetary Micro Mill Pulverisette7 premium line (300 rpm, 3 min, and 10 mm balls), after which the powder was collected and stored. Finally, melamine was extracted from the MIP via Soxhlet extraction (1:10 mixture of DI water to ethanol) for 16 h, and subsequently methanol for another 16 h. The extraction cycles were repeated until no template molecule was detected via UV-VIS spectroscopy. The extracted particles were then dried at $65 \text{ }^\circ\text{C}$ for 12 h. A reference NIP was prepared in parallel following the same procedure, but in the absence of the analyte.

Fourier-Transform Infrared Spectroscopy

Complete template extraction was confirmed through comparative IR spectroscopic analysis of the extracted MIP and non-extracted MIP and NIP samples, using an IR Spirit Fourier transform infrared (FT-IR) spectrometer (Shimadzu Corp., Kyoto, Japan) set at 64 scans and 8 cm^{-1} spectral resolution per measurement, with a spectral range of 4000 to 400 cm^{-1} .

Batch Rebinding Experiments

Optical batch rebinding experiments were recorded with a Shimadzu UV-1900i spectrophotometer. To establish the binding affinity of the MIP/NIP, 20 mg of MIP/NIP particles were incubated with 5 mL solutions of melamine in Milli-Q water, with a concentration range from 0.02 to 0.5 mM. The samples were then shaken at 130 rpm for 90 min. The suspensions were then left to settle, after which the

filtrate was collected and analysed using a UV–Vis spectrophotometer. The remaining unbound concentration of melamine (C_f) in solution was then determined by UV–Vis spectroscopy, using a calibration curve for melamine that was generated prior at λ_{max} (235 nm).

Preparation and Characterization of MIP-Based Receptor Layer

The MIP-based receptor layer was prepared according to previous literature (**Chapter 3**), with slight modifications.[39] First, a polyvinyl chloride (PVC) adhesive layer was deposited on the aluminium chip by spin coating (1000 rpm for 60 s with an acceleration of 1000 rpm s^{-1}) a 2.0 wt% PVC solution in tetrahydrofuran. Next, a PDMS substrate (1 cm^2), covered with a monolayer of MIP particles, was used to stamp the particles into the PVC layer. The PVC layer was heated to above the glass transition temperature (100°C), allowing the particles to settle into the polymer layer. After cooling, the unbound particles were washed away with DI water before thermal measurements. The developed platform was characterized by analysing the sensor's surface prior to and after deposition of the MIP particles onto the Al-PVC substrate. To this end, the samples were punched into 12 mm disks and after gold coating, the samples were imaged using a Jeol JSM-IT200 InTouchScope scanning electron microscope (JEOL, Peabody, MA, USA) at $V = 10 \text{ keV}$. For analysis of the chemical composition of the Al-PVC layer and of the deposited MIP particles, the samples were then studied under an energy dispersive X-ray analyser (EDX) coupled to the Jeol JSM-IT200 microscope (see **Figure 4.2**).

Characterization of MIP-based receptor layer

In order to characterize and demonstrate the successful deposition of the MIP particles onto the Al-PVC substrate, SEM and EDX analysis of the receptor layer prior and after deposition were performed (**Figure 4.2**). When comparing the SEM images of the Al-PVC layer before and after deposition it is evident the large amount of imprinted micro particles deposited onto the substrate (**Figure 4.2C**), while in **Figure 4.2A** a smooth layer onto the aluminium substrate can be observed. An examination of the chemical properties of the Al-PVC layer via EDX analysis (**Figure 4.2B**) shows the presence of Al, C, O, and Cl confirming the formation of the PVC layer onto the Al substrate. Instead, when analysing the deposited MIP particle (**Figure 4.2D**) it can be clearly noticed the prevalence of the elements C and O. This result can be expected considering the chemical structures of monomer and cross-linker used to produce the imprinted polymer.

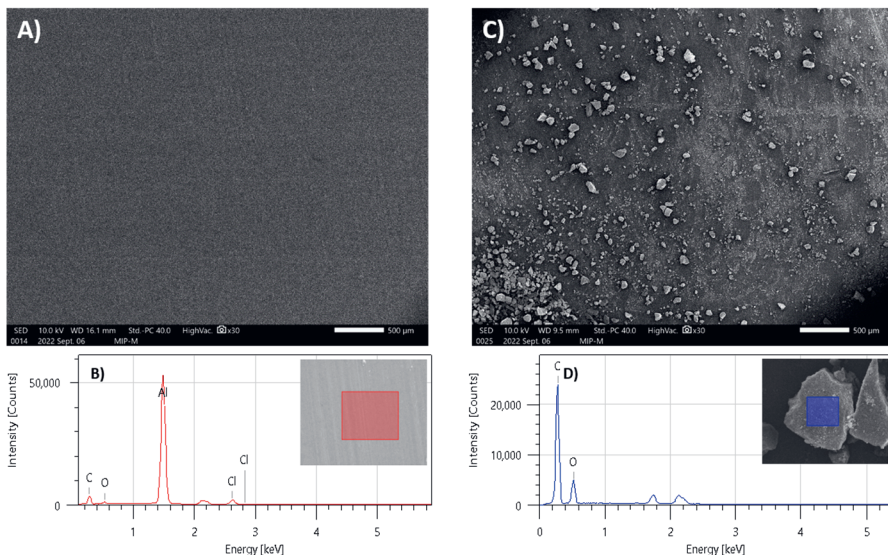


Figure 4.2 SEM images of **A)** Al-PVC layer and **C)** MIP-based receptor layer. EDX analysis of **B)** Al-PVC layer and **D)** deposited MIP particle.

Heat-Transfer Sensing Setup

The thermal detection platform has been described in detail in previous work.[40] In short, the MIP-coated aluminium substrates were attached to a copper heat sink. The temperature of the heat sink, T_1 , was stringently controlled using a K-type thermocouple (TC Direct, Nederweert, the Netherlands), a power resistor (Farnell, Utrecht, the Netherlands), and a software-based proportional-integral-derivative (PID) controller ($P = 10$, $I = 8$, $D = 0$) in Labview (National Instruments, Austin, TX, USA). The MIP layer was exposed to the samples under analysis by means of an injection moulded polycarbonate (PC) flow cell ($A = 28 \text{ mm}^2$, $V = 110 \text{ }\mu\text{L}$). Samples were injected into the flow cell by means of a syringe pump at a flowrate of 0.250 mL/min for 5 min. To monitor the thermal resistance at the solid–liquid interface (the MIP-functionalized surface), a second thermocouple monitored the temperature inside the flow cell, T_2 , at a constant input temperature of $37.00 \text{ }^\circ\text{C}$. To mimic milk, CaCl_2 solutions (1.6 mM) were used as buffer solutions to stabilize the signal. Gradually, the melamine or analogue concentration in buffer (or milk for the real sample analysis) was increased within the regulatory relevant concentration regime ($15\text{--}90 \text{ }\mu\text{M}$). The signal was allowed to stabilize for 20 min between each addition. The specificity was assessed by comparing the MIP response to that of the NIP reference, while the selectivity was examined using cyanuric acid, bisphenol A, and lactose as the analogue molecules.

Thermal Detection of Melamine in Milk Samples

The absence of melamine in the analysed milk samples was confirmed using a commercial melamine rapid test kit (Ballya Bio-Med Co., Ltd., Guangzhou, China). Afterwards, the untreated milk samples were spiked with increasing melamine concentrations, and the obtained solutions were employed for thermal analysis using the HTM setup.

Results and Discussion

Batch Rebinding via UV-Vis

Four MIP compositions were synthesized and their capacity to specifically bind melamine in aqueous samples was assessed (**Table 4.1**). All of the compositions were prepared with methacrylic acid (MAA) as a functional monomer in order to create hydrogen bonds with the melamine molecule. Ethylene glycol dimethacrylate (EGDMA) and 2,2'-azobis(2-methylpropionitrile) (AIBN) were used as the cross-linker molecule and thermal initiator, respectively.

Table 4.1 Synthesized MIP/NIP compositions.

MIP/NIP	Melamine (mg)	MAA (eq.)	EGDMA (eq.)	AIBN (mg)	DMSO (mL)	R ²	Max S _b (μmol g ⁻¹)	IF (at C _f = 0.1 mM)
MIP1	31.5	14	28	40	5	0.988	30.00	2.22
NIP1	-	14	28	40	5	0.898	19.66	-
MIP2	31.5	3	20	40	5	0.980	19.12	0.96
MIP2	-	3	20	40	5	0.953	22.44	-
MIP3	31.5	6	20	40	5	0.985	27.11	0.82
MIP3	-	6	20	40	5	0.987	25.55	-
MIP4	31.5	12	40	40	5	0.946	22.53	0.56
MIP4	-	12	40	40	5	0.983	25.94	-

After synthesis, the MIPs were washed and the template was extracted by means of Soxhlet extraction, with template removal being confirmed by FT-IR analysis (**Figure 4.3**).

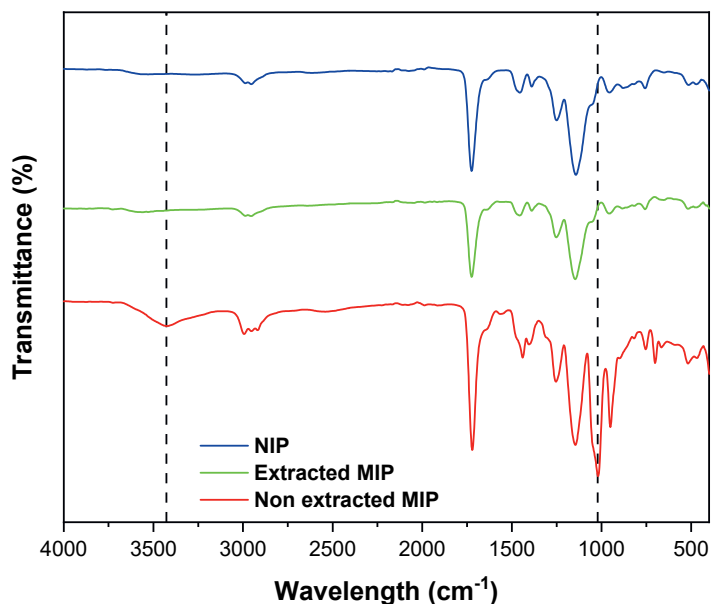


Figure 4.3 FT-IR analysis of the NIP, extracted MIP and non-extracted MIP.

For each composition, a dose–response curve was constructed by calculating the free concentration of melamine found in the solution (C_f) (mM) after the rebinding experiment, and to obtain the corresponding substrate bound (S_b) ($\mu\text{mol g}^{-1}$) values, which indicate the amount of target bound (in micromoles) per grams of MIP at each data point. Finally, the obtained C_f and S_b values were plotted and dose–response curves for all of the synthesized MIP/NIP compositions were obtained. The data were fitted (allometrically; $y = ax^b$) with Origin 2021b (OriginLabs Corporation, Northampton, MA, USA). In **Figure 4.4**, each of the synthesized MIP compositions (black squares) are plotted together with the corresponding NIP (red squares).

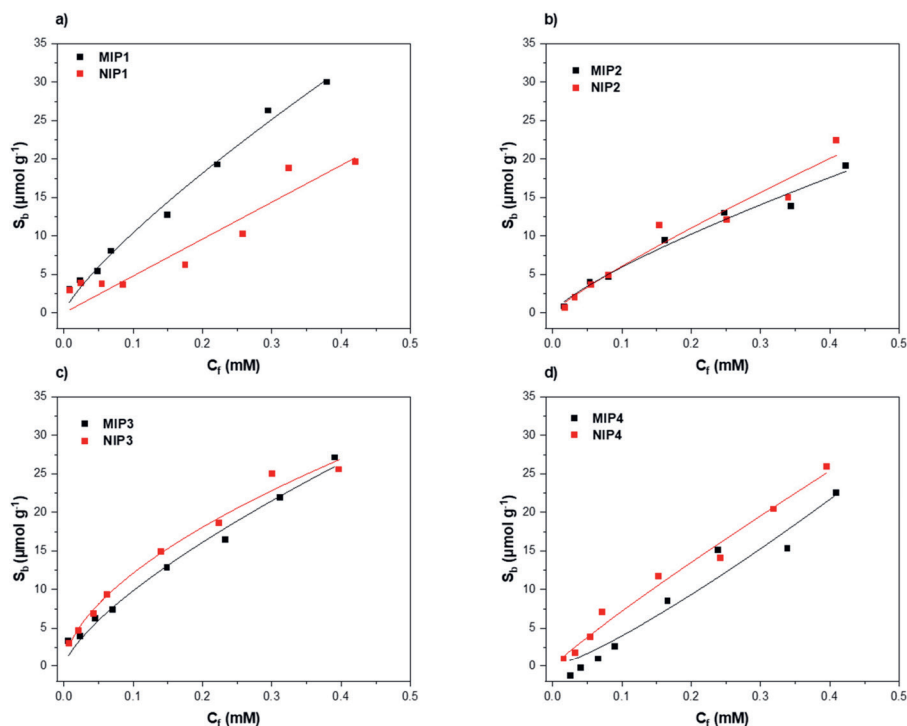


Figure 4.4 Rebinding analysis with UV–VIS spectroscopy of (a) MIP/NIP1, (b) MIP/NIP2, (c) MIP/NIP3, and (d) MIP/NIP4.

Of the examined formulations, MIP-2 displayed the lowest overall maximum binding capacity with a maximum S_b of $19.12 \mu\text{mol g}^{-1}$, and in contrast, MIP-1 had the highest maximum binding capacity (max $S_b = 30.00 \mu\text{mol g}^{-1}$), thus demonstrating that higher concentrations of functional monomer (MAA) and cross-linker (EGDMA) are needed to generate a higher number of nanocavities in the polymer. When comparing MIP-2 and MIP-3, it should be noted that with a higher concentration of monomer (MIP-3), a higher binding capacity was obtained. However, it was surprising that MIP-4 exhibited a slightly lower binding capacity than MIP-3 (22.53 and $27.11 \mu\text{mol g}^{-1}$). MIP-4 was prepared with the same monomer:cross-linker ratio as MIP-3, but with doubled equivalents with respect to the template, thus showing that doubling the concentration of monomer and cross-linker but maintaining a constant monomer:cross-linker ratio led to a similar maximum binding capacity. In order to comprehensively scrutinize the specific binding per MIP/NIP and to compare the performance of MIPs made with different recipes, the imprinting factor (IF) was calculated for each composition. The IF value is defined as the S_b value at a defined C_f for MIP divided by the S_b value of the corresponding NIP at the same C_f , and is a measure of the specificity of the developed MIP system. To obtain a more accurate comparison between the different formulations, C_f values at 0.1 mM were selected to calculate the IF values for each MIP/NIP (**Table 4.1**). When analysing the IF of the four compositions, it was clear that MIP-1 demonstrated the best specificity with an IF of 2.22. When analysing the other MIP compositions (MIP-2, MIP-3, and MIP-4), these showed a slightly lower maximum binding capacity, as per the one

calculated for MIP-1, which could mainly be attributed to a higher degree of non-specific binding, demonstrated by the high S_b values of the corresponding NIPs. This resulted in IF values ranging from 0.56–0.96, thus showing that most of the improvement in the binding capacity could be attributed to an increase in non-specific binding sites, which was also confirmed by the fact that the corresponding NIPs had an even higher S_b value than the corresponding MIPs. Therefore, when considering both the maximum binding capacity and the IF values for each of the formulations, it was clear that the MIP that should be used for the remainder of the experiments was MIP-1

Rebinding Analysis Using HTM

After preparation of the receptor layer via micro-contact deposition, the thermal response of the functionalized aluminium surfaces to melamine was examined using the HTM method. The receptor layer was therefore exposed to different concentrations of melamine (0–90 μM) in 1.6 mM CaCl_2 solutions over a defined time period (**Figure 4.5**). To enable direct comparison between MIPs and NIPs, the analysis was run in parallel. A distinct decrease in temperature within the flow cell was observed when a higher concentration of melamine was introduced across the MIP-based receptor layer (black line). This trend was traced back to the interactions between the MIP particles and the analyte. More specifically, MIP contained recognition sites that were complementary to the melamine molecule in the shape, size, and distribution of the functional groups, thus allowing the analyte to perfectly fit in the nanocavities present in the polymeric network. When the binding event occurred, the MIP cavities at the surface of the receptor layer were gradually filled, changing the thermodynamic properties of the interfacial layer, which translated into an increase in the interfacial thermal resistance, registered as a diminished heat flow through the sample into the solution inside the flow cell (**Figure 4.5a**, black line). In comparison, the same effect could be observed when analysing the thermal response of the NIP (**Figure 4.5a**, red line), but the decrease in temperature in the flow cell in response to higher concentrations of melamine was much lower. This trend was mainly attributed to non-specific interactions between melamine and functional groups on the NIP surface. The temperature profiles over time were used to construct dose–response curves for both MIP and NIP by plotting the different concentrations of melamine injected against the effect size as a function of the temperature change. The effect size was calculated using the same equation (**Equation 4.1**) reported in previous work (**Chapter 3**).

$$\text{Effect size (\%)} = \frac{\Delta T}{T_{\text{CaCl}_2}} \times 100 \quad (4.1)$$

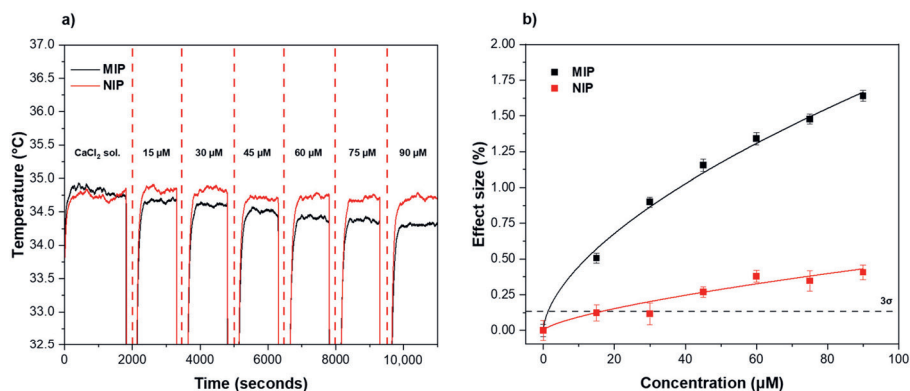


Figure 4.5 (a) Temperature profiles and (b) dose–response curves (from HTM analysis) of the MIP/NIP-based receptor layer after injections with increasing concentrations of melamine (0–90 μM) in CaCl_2 . The LoD (3σ method) of $\pm 1.45 \mu\text{M}$ is indicated by the black dashed line. Triplicate measurements were used to calculate the error bars and mean values.

In short, the value was obtained by dividing the temperature decrease after each injection by the average baseline temperature obtained after stabilization in CaCl_2 . An allometric ($y = ax^b$) fit was used for both the MIP (black curve, $R^2 = 0.9891$) and NIP (red curve, $R^2 = 0.8638$) using Origin, version 2021b (OriginLab Corporation, Northampton, MA, USA). From the dose–response graph, the LoD of the MIP (black dashed line) was calculated using the 3σ method, corresponding to the concentration at which the effect size became greater than three times the maximum noise on the temperature signal (y-axis) of the measurement. The LoD was obtained by calculating the 3σ -value and drawing a horizontal line on the curve at this y-value. The intercept of the 3σ line with the linear part of the MIP curve showed a LoD for the sensor equal to $1.45 \mu\text{M}$. The capability of the sensor to bind melamine in a specific manner was demonstrated by analysing the intercept for the LoD for the MIP with the corresponding intercept for the NIP curve, the latter resulting in a significantly higher LoD value. Moreover, the sensor demonstrated a strong linear trend with little saturation effect when exposed to concentrations ranging from 0 to $90 \mu\text{M}$. The reference NIP, instead, showed saturation at low concentrations and had a clearly lower effect size when compared with the MIP.

Selectivity Analysis of the Receptor Layer

To determine the selectivity, the functionalized receptor layer was exposed to different analogue molecules, commonly found in contaminated milk and other foodstuffs (e.g. cyanuric acid, bisphenol A, and lactose) and the sensor's response was recorded via HTM thermal analysis (**Figure 4.6**). The same concentration ranges (0– $90 \mu\text{M}$) were employed and the temperature profiles were converted into an effect size (%) using **Equation 4.1**. As observed, the affinity of MIP towards melamine was much greater than for the structural analogues (**Figure 4.6a**), already demonstrating a clear difference from the first analyte injection ($15 \mu\text{M}$). The effect size increased with increasing the analyte concentrations, demonstrating a much higher specificity of the sensor toward melamine at higher concentrations. **Figure 4.6b** shows the difference in effect size between melamine and the other tested compounds at

90 μM , demonstrating that the thermal readout was also able to selectively recognize melamine over structural analogues at higher concentrations.

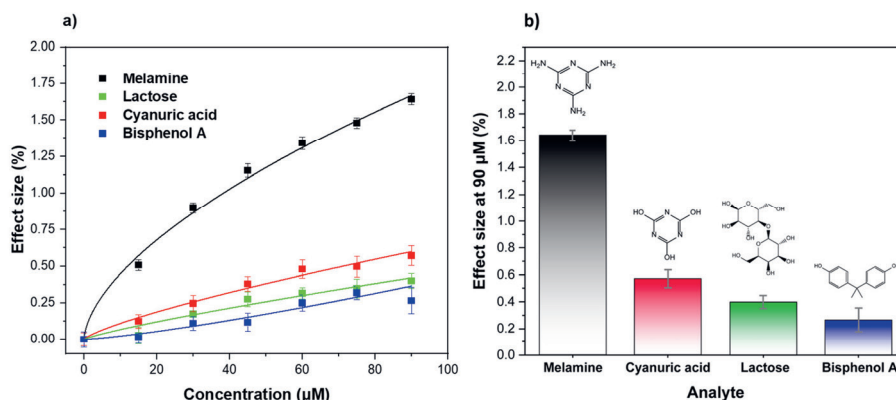


Figure 4.6 (a) Dose–response curves obtained via HTM analysis of different molecules (melamine, cyanuric acid, lactose, and bisphenol A) and (b) comparison of the calculated effect sizes at 90 μM . Triplicate measurements were used to calculate the error bars and mean values.

In order to provide a more comprehensive investigation of the selectivity of the sensor platform, the selectivity factor was calculated (Table 4.2) for all of the analogues under study. In short, the values were calculated by dividing the effect size values obtained after exposure of the sensor to the target molecule, using the values recorded after infusion with the same concentrations of the tested analogues. The selectivity factor was calculated at a concentration of 2.5 mg/kg. This concentration represents the legal limit of melamine in milk samples, and thus provides a key indication of the selectivity of the sensor in a real-world sample analysis. It can be seen that MIP revealed an effect size 3.62 times greater than the one recorded for its most similar structural analogue—cyanuric acid. The selectivity factor is even bigger for the other analogue molecules, which demonstrates that the structural difference between the analogue and target plays a key role during the recognition/binding event and that the presence of these molecules in food samples (e.g. milk) would not affect the reliability of the HTM-based sensor.

Table 4.2 Selectivity factors of the developed thermal platform.

Substance	Selectivity Factor
Cyanuric acid	3.62
Bisphenol A	12.14
Lactose	5.76

Real-Life Sample Analysis: Detection of Melamine in Milk Samples

To establish the applicability of the sensor as a tool for identifying illegal melamine food adulteration, the thermal variations of the receptor layer were recorded and analysed while being exposed to

increasing concentrations of melamine in untreated, semi-skimmed milk samples (**Figure 4.7**). The same experimental setup and parameters as per the rebinding analysis in CaCl_2 were used for the investigation of melamine levels in milk. The absence of melamine in the non-spiked milk samples was confirmed with a commercially available colloidal gold immunochromatography assay for rapid melamine detection. To accurately compare the thermal measurement recorded in CaCl_2 solution with the one obtained in milk samples, the milk samples were spiked to reach the same melamine concentration range (15–90 μM) as for the CaCl_2 solution. Both the temperature profiles and the extrapolated dose–response curves for MIP and NIP showed a similar trend to the one obtained in the buffer solutions (**Figure 4.5** and **Figure 4.7**). The LoD was 6.02 μM . The data obtained in milk samples display a comparable trend with the experiments performed in CaCl_2 both in terms of rebinding efficiency and sensitivity, demonstrating that the sensor platform retained a high specificity in more complex real-life samples, such as untreated semi-skimmed milk. When comparing the LoDs in the different matrices, it was unsurprising that the sensor was less sensitive when employed directly in milk samples as a result of the complexity of the matrix employed.

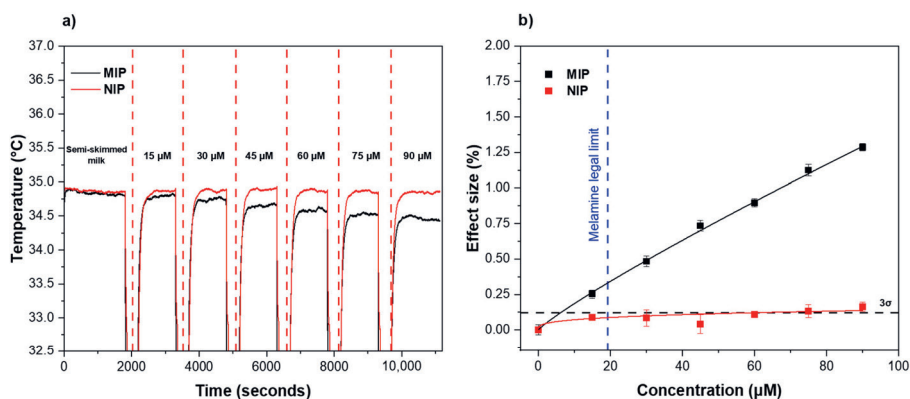


Figure 4.7 (a) Temperature profile and **(b)** dose–response curve obtained by an HTM analysis of the MIP/NIP-based receptor layer after infusions of different concentrations of melamine in spiked semi-skimmed milk samples. The black dashed line shows the LoD (3σ method) at $\pm 6.02 \mu\text{M}$. The blue dashed line indicates the legal limit of melamine in milk set by EU/US regulators. Triplicate measurements were used to calculate the error bars and mean values.

As can be seen in **Table 4.3**, our sensor demonstrated a higher LoD when compared with other potentially interesting new sensor platforms reported in the literature in recent years. However, the LoD in milk samples was still three times lower than the established legal limit of melamine in milk (blue dashed line) and therefore demonstrated the sensor’s potential as a novel low-cost tool to routinely screen milk samples without any pre-treatment needed.

Table 4.3. Comparison of recently developed sensors for melamine detection in food samples.

Readout Technology	Limit of Detection	Real Sample Analysis	Sample Pre-treatment	Ref.
Differential pulse voltammetry (DPV)	8.21×10^{-12} M	Liquid milk	Pre-treatment needed	[41]
Colorimetric assay (UV-VIS)	0.099 μ M	Raw milk	Pre-treatment needed	[42]
Surface-enhanced Raman spectroscopy (SERS)	0.012 mmol L ⁻¹	Whole milk	Pre-treatment needed	[43]
Quartz crystal microbalance (QCM)	2.3 ng mL ⁻¹	Liquid milk	Pre-treatment needed	[44]
Surface-enhanced Raman spectroscopy (SERS)	0.1 ppm	Milk powder	Pre-treatment needed	[14]
Liquid Chromatography-Tandem Mass Spectrometry (LC-MS/MS)	0.02–0.05 mg/kg	Egg powder, soy protein	Pre-treatment needed	[11]
Heat-Transfer Method (HTM)	6.02 μ M (759.24 ng mL ⁻¹)	Whole milk	No pre-treatment needed	This work

Conclusions

This study demonstrates the preparation of molecularly imprinted polymers for the detection of melamine in both artificial and real-life milk samples using thermal analysis. Out of all formulations, MIP-1 evidently performed the best in terms of both specificity and rebinding capacity ($IF = 2.22$ and $S_b = 30 \mu\text{mol g}^{-1}$). Using the HTM method, the sensitivity of the MIP-based sensing platform in CaCl_2 solutions was evaluated, showing a linear range of $1.45\text{--}90 \mu\text{M}$ and a LoD of $1.45 \mu\text{M}$ in the thermal data. Furthermore, the sensor proved to be highly selective towards melamine in comparison with structural analogues, milk components, and other contaminants found in beverages, demonstrating the efficiency of this platform in analysing untreated, real-life samples. In fact, the obtained results in milk showed a linear range of $6.02\text{--}90 \mu\text{M}$ and a LoD of $6.02 \mu\text{M}$, demonstrating the potential of the sensor in food analysis. The combination of an easily scalable production process with a cost-effective readout technology make these results very appealing for commercial applications, and will stimulate further development towards its integration into handheld devices.

References Chapter 4

1. Zheng, G.; Boor, B.E.; Schreder, E.; Salamova, A. Exposure to Melamine and Its Derivatives in Childcare Facilities. *Chemosphere* 2020, 244, 125505, doi:10.1016/j.chemosphere.2019.125505.
2. Ingelfinger, J.R. Melamine and the Global Implications of Food Contamination. *New England Journal of Medicine* 2008, 359, 2745–2748, doi:10.1056/NEJMp0808410.
3. Anirudhan, T.S.; Christa, J.; Deepa, J.R. Extraction of Melamine from Milk Using a Magnetic Molecularly Imprinted Polymer. *Food Chem.* 2017, 227, 85–92, doi:10.1016/j.foodchem.2016.12.090.
4. Liu, J. dong; Liu, J. jun; Yuan, J. hui; Tao, G. hua; Wu, D. sheng; Yang, X. fei; Yang, L. qing; Huang, H. yan; Zhou, L.; Xu, X. yun; et al. Proteome of Melamine Urinary Bladder Stones and Implication for Stone Formation. *Toxicol. Lett.* 2012, 212, 307–314, doi:10.1016/j.toxlet.2012.05.017.
5. Tyan, Y.-C.; Yang, M.-H.; Jong, S.-B.; Wang, C.-K.; Shiea, J. Melamine Contamination. *Anal. Bioanal. Chem.* 2009, 395, 729–735, doi:10.1007/s00216-009-3009-0.
6. Ding, N.; Yan, N.; Ren, C.; Chen, X. Colorimetric Determination of Melamine in Dairy Products by Fe₃O₄ Magnetic Nanoparticles–H₂O₂–ABTS Detection System. *Anal. Chem.* 2010, 82, 5897–5899, doi:10.1021/ac100597s.
7. Brown, C.A.; Jeong, K.-S.; Poppenga, R.H.; Puschner, B.; Miller, D.M.; Ellis, A.E.; Kang, K.-I.; Sum, S.; Cistola, A.M.; Brown, S.A. Outbreaks of Renal Failure Associated with Melamine and Cyanuric Acid in Dogs and Cats in 2004 and 2007. *Journal of Veterinary Diagnostic Investigation* 2007, 19, 525–531, doi:10.1177/104063870701900510.
8. WHO International Experts Limit Melamine Levels in Food Available online: <https://www.who.int/news/item/11-1-2010-international-experts-limit-melamine-levels-in-food> (accessed on 1 June 2022).
9. Li, Q.; Song, P.; Wen, J. Melamine and Food Safety: A 10-Year Review. *Curr. Opin. Food Sci.* 2019, 30, 79–84, doi:10.1016/j.cofs.2019.05.008.
10. Filazi, A.; Sireli, U.T.; Ekici, H.; Can, H.Y.; Karagoz, A. Determination of Melamine in Milk and Dairy Products by High Performance Liquid Chromatography. *J. Dairy Sci.* 2012, 95, 602–608, doi:10.3168/jds.2011-4926.
11. Rodriguez Mondal, A.M.; Desmarchelier, A.; Konings, E.; Acheson-Shalom, R.; Delatour, T. Liquid Chromatography-Tandem Mass Spectrometry (LC-MS/MS) Method Extension to Quantify Simultaneously Melamine and Cyanuric Acid in Egg Powder and Soy Protein in Addition to Milk Products. *J. Agric. Food Chem.* 2010, 58, 11574–11579, doi:10.1021/jf102900k
12. Deng, X. jun; Guo, D. hua; Zhao, S. zhen; Han, L.; Sheng, Y. gang; Yi, X. hai; Zhou, Y.; Peng, T. A Novel Mixed-Mode Solid Phase Extraction for Simultaneous Determination of Melamine and Cyanuric Acid in Food by Hydrophilic Interaction Chromatography Coupled to Tandem Mass Chromatography. *Journal of Chromatography B* 2010, 878, 2839–2844, doi:10.1016/j.jchromb.2010.08.038.

13. Nilghaz, A.; Mousavi, S.M.; Amiri, A.; Tian, J.; Cao, R.; Wang, X. Surface-Enhanced Raman Spectroscopy Substrates for Food Safety and Quality Analysis. *J. Agric. Food Chem* 2022, 70, 2022, doi:10.1021/acs.jafc.2c00089.
14. Nie, B.; Luo, Y.; Shi, J.; Gao, L.; Duan, G. Bowl-like Pore Array Made of Hollow Au/Ag Alloy Nanoparticles for SERS Detection of Melamine in Solid Milk Powder. *Sens. Actuators B Chem* 2019, 301, 127087, doi:10.1016/j.snb.2019.127087.
15. Ritota, M.; Manzi, P. Melamine Detection in Milk and Dairy Products: Traditional Analytical Methods and Recent Developments. *Food Anal. Methods* 2018, 11, 128–147, doi:10.1007/s12161-017-0984-1.
16. Tang, J.; Ying, Y.; Pan, X.D.; Jiang, W.; Wu, P.G. Elements Analysis of Infant Milk Formula by ICP-OES: A Comparison of Pretreatment Methods. *Accreditation and Quality Assurance* 2014, 19, 99–103, doi:10.1007/s00769-014-1039-6.
17. Saylan, Y.; Yilmaz, F.; Özgür, E.; Derazshamshir, A.; Yavuz, H.; Denizli, A. Molecular Imprinting of Macromolecules for Sensor Applications. *Sensors* 2017, 17, 898, doi:10.3390/s17040898.
18. Haghdoost, S.; Arshad, U.; Mujahid, A.; Schranzhofer, L.; Lieberzeit, P.A. Development of a MIP-Based QCM Sensor for Selective Detection of Penicillins in Aqueous Media. *Chemosensors* 2021, 9, 362, doi:10.3390/chemosensors9120362.
19. Ramanavicius, S.; Samukaite-Bubniene, U.; Ratautaite, V.; Bechelany, M.; Ramanavicius, A. Electrochemical Molecularly Imprinted Polymer Based Sensors for Pharmaceutical and Biomedical Applications (Review). *J. Pharm. Biomed. Anal.* 2022, 215, 114739, doi:10.1016/j.jpba.2022.114739.
20. Akgönüllü, S.; Özgür, E.; Denizli, A. Recent Advances in Quartz Crystal Microbalance Biosensors Based on the Molecular Imprinting Technique for Disease-Related Biomarkers. *Chemosensors* 2022, Vol. 10, Page 106 2022, 10, 106, doi:10.3390/chemosensors10030106.
21. Haupt, K.; Mosbach, K. Molecularly Imprinted Polymers and Their Use in Biomimetic Sensors. 2000, 100, 2495-2504 doi:10.1021/cr990099w.
22. Fang, L.; Jia, M.; Zhao, H.; Kang, L.; Shi, L.; Zhou, L.; Kong, W. Molecularly Imprinted Polymer-Based Optical Sensors for Pesticides in Foods: Recent Advances and Future Trends. *Trends Food Sci Technol* 2021, 116, 387–404, doi:10.1016/j.tifs.2021.07.039.
23. Piletsky, S.A.; Turner, N.W.; Laitenberger, P. Molecularly Imprinted Polymers in Clinical Diagnostics—Future Potential and Existing Problems. *Med. Eng. Phys.* 2006, 28, 971–977, doi:10.1016/j.medengphy.2006.05.004.
24. Ramström, O.; Skudar, K.; Haines, J.; Patel, P.; Brü, O. Food Analyses Using Molecularly Imprinted Polymers. *J. Agric. Food Chem.* 2001, 49, 2105-2114, doi:10.1021/jf001444h.
25. Chen, C.; Luo, J.; Li, C.; Ma, M.; Yu, W.; Shen, J.; Wang, Z. Molecularly Imprinted Polymer as an Antibody Substitution in Pseudo-Immunoassays for Chemical Contaminants in Food and Environmental Samples. *J. Agric. Food Chem.* 2018, 66, 11, 2561-2571, doi:10.1021/acs.jafc.7b05577.

26. Fu, Y.; Pessagno, F.; Manesiotes, P.; Borrull, F.; Fontanals, N.; Maria Marcé, R. Preparation and Evaluation of Molecularly Imprinted Polymers as Selective SPE Sorbents for the Determination of Cathinones in River Water. *Microchemical Journal* 2022, 175, 107100, doi:10.1016/j.microc.2021.107100.
27. Lowdon, J.W.; Ishikura, H.; Kvernenes, M.K.; Caldara, M.; Cleij, T.J.; van Grinsven, B.; Eersels, K.; Diliën, H. Identifying Potential Machine Learning Algorithms for the Simulation of Binding Affinities to Molecularly Imprinted Polymers. *Computation* 2021, 9, 103, doi:10.3390/computation9100103.
28. Pirzada, M.; Sehit, E.; Altintas, Z. Cancer Biomarker Detection in Human Serum Samples Using Nanoparticle Decorated Epitope-Mediated Hybrid MIP. *Biosens. Bioelectron.* 2020, 166, 112464, doi:10.1016/j.bios.2020.112464.
29. Akgönüllü, S.; Armutcu, C.; Denizli, A. Molecularly Imprinted Polymer Film Based Plasmonic Sensors for Detection of Ochratoxin A in Dried Fig. *Polymer Bulletin* 2022, 79, 4049–4067, doi:10.1007/s00289-021-03699-6.
30. Rico-Yuste, A.; Abouhany, R.; Urraca, J.L.; Descalzo, A.B.; Orellana, G.; Moreno-Bondi, M.C. Eu(III)-Templated Molecularly Imprinted Polymer Used as a Luminescent Sensor for the Determination of Tenuazonic Acid Mycotoxin in Food Samples. *Sens. Actuators B Chem* 2021, 329, 129256, doi:10.1016/j.snb.2020.129256.
31. van Grinsven, B.; vanden Bon, N.; Strauven, H.; Grieten, L.; Murib, M.; Jiménez Monroy, K.L.; Janssens, S.D.; Haenen, K.; Schöning, M.J.; Vermeeren, V.; et al. Heat-Transfer Resistance at Solid–Liquid Interfaces: A Tool for the Detection of Single-Nucleotide Polymorphisms in DNA. *ACS Nano* 2012, 6, 2712–2721, doi:10.1021/nn300147e.
32. Eersels, K.; Diliën, H.; Lowdon, J.; Steen Redeker, E.; Rogosic, R.; Heidt, B.; Peeters, M.; Cornelis, P.; Lux, P.; Reutelingsperger, C.; et al. A Novel Biomimetic Tool for Assessing Vitamin K Status Based on Molecularly Imprinted Polymers. *Nutrients* 2018, 10, 751, doi:10.3390/nu10060751.
33. Arreguin-Campos, R.; Eersels, K.; Lowdon, J.W.; Rogosic, R.; Heidt, B.; Caldara, M.; Jiménez-Monroy, K.L.; Diliën, H.; Cleij, T.J.; van Grinsven, B. Biomimetic Sensing of Escherichia Coli at the Solid-Liquid Interface: From Surface-Imprinted Polymer Synthesis toward Real Sample Sensing in Food Safety. *Microchemical Journal* 2021, 169, 106554, doi:10.1016/j.microc.2021.106554.
34. McClements, J.; Bar, L.; Singla, P.; Canfarotta, F.; Thomson, A.; Czulak, J.; Johnson, R.E.; Crapnell, R.D.; Banks, C.E.; Payne, B.; et al. Molecularly Imprinted Polymer Nanoparticles Enable Rapid, Reliable, and Robust Point-of-Care Thermal Detection of SARS-CoV-2. *ACS Sens.* 2022, 7, 1122–1131, doi:10.1021/acssensors.2c00100.
35. Arreguin-Campos, R.; Eersels, K.; Rogosic, R.; Cleij, T.J.; Diliën, H.; van Grinsven, B. Imprinted Polydimethylsiloxane-Graphene Oxide Composite Receptor for the Biomimetic Thermal Sensing of Escherichia Coli. *ACS Sens.* 2022, 7, 1467–1475, doi:10.1021/acssensors.2c00215.
36. Givanoudi, S.; Cornelis, P.; Rasschaert, G.; Wackers, G.; Iken, H.; Rolka, D.; Yongabi, D.; Robbens, J.; Schöning, M.J.; Heyndrickx, M.; et al. Selective Campylobacter Detection and Quantification in Poultry:

A Sensor Tool for Detecting the Cause of a Common Zoonosis at Its Source. *Sens. Actuators B Chem* 2021, 332, 129484, doi:10.1016/j.snb.2021.129484.

37. Zhu, L.; Xu, G.; Wei, F.; Yang, J.; Hu, Q. Determination of Melamine in Powdered Milk by Molecularly Imprinted Stir Bar Sorptive Extraction Coupled with HPLC. *J. Colloid Interface Sci.* 2015, 454, 8–13, doi:10.1016/j.jcis.2015.05.008.

38. Lowdon, J.W.; Eersels, K.; Arreguin-Campos, R.; Caldara, M.; Heidt, B.; Rogosic, R.; Jimenez-Monroy, K.L.; Cleij, T.J.; Diliën, H.; van Grinsven, B. A Molecularly Imprinted Polymer-Based Dye Displacement Assay for the Rapid Visual Detection of Amphetamine in Urine. *Molecules* 2020, 25, doi:10.3390/molecules25225222.

39. Caldara, M.; Lowdon, J.W.; Rogosic, R.; Arreguin-Campos, R.; Jimenez-Monroy, K.L.; Heidt, B.; Tschulik, K.; Cleij, T.J.; Diliën, H.; Eersels, K.; et al. Thermal Detection of Glucose in Urine Using a Molecularly Imprinted Polymer as a Recognition Element. *ACS Sens.* 2021, 6, 4515–4525, doi:10.1021/acssensors.1c02223.

40. Rogosic, R.; Lowdon, J.W.; Heidt, B.; Diliën, H.; Eersels, K.; van Grinsven, B.; Cleij, T.J. Studying the Effect of Adhesive Layer Composition on MIP-Based Thermal Biosensing. *Physica Status Solidi (A) Applications and Materials Science* 2019, 216, doi:10.1002/pssa.201800941.

41. An, J.; Li, L.; Ding, Y.; Hu, W.; Duan, D.; Lu, H.; Ye, D.; Zhu, X.; Chen, H. A Novel Molecularly Imprinted Electrochemical Sensor Based on Prussian Blue Analogue Generated by Iron Metal Organic Frameworks for Highly Sensitive Detection of Melamine. *Electrochim Acta* 2019, 326, 134946, doi:10.1016/j.electacta.2019.134946.

42. Liu, X.; Wang, J.; Wang, Y.; Huang, C.; Wang, Z.; Liu, L. In Situ Functionalization of Silver Nanoparticles by Gallic Acid as a Colorimetric Sensor for Simple Sensitive Determination of Melamine in Milk. *ACS Omega* 2021, 6, 23630–23635, doi.org/10.1021/acsomega.1c03927.

43. Hu, Y.; Feng, S.; Gao, F.; Li-Chan, E.C.Y.; Grant, E.; Lu, X. Detection of Melamine in Milk Using Molecularly Imprinted Polymers–Surface Enhanced Raman Spectroscopy. *Food Chem.* 2015, 176, 123–129, doi:10.1016/j.foodchem.2014.12.051.

44. Ceylan Cömert, Ş.; Özgür, E.; Uzun, L.; Odabaşı, M. The Creation of Selective Imprinted Cavities on Quartz Crystal Microbalance Electrode for the Detection of Melamine in Milk Sample. *Food Chem.* 2022, 372, 131254, doi:10.1016/j.foodchem.2021.131254.

Preface to Chapter 5

As previously discussed, a biosensor consists of a sensing platform in contact with a transducer able to transform the obtained signal. One of the key steps involved in the fabrication of biosensors is the immobilization/deposition of the sensing element onto a suitable substrate. In the previous chapters, two MIP-based platforms were fabricated by depositing bulk MIP-particles onto a thermally conductive substrate (Al-PVC layer) using a micro-contact stamping approach. Though the developed biosensor platforms demonstrated good selectivity and sensitivity to the respective targets, the deposition process employed consists of multiple steps and necessitates the use of various chemicals and machinery, which is obviously undesirable as it may result in batch-to-batch variations and increased production costs.

Therefore, the following chapter presents a literature review on various deposition techniques for the integration of MIPs in sensor applications. The chapter compares the benefits and disadvantages of various MIP deposition techniques, including mechanical, electrochemical, chemical, and vacuum deposition methods. The chapter emphasizes the significance of the deposition technique when evaluating the performance of MIP-based sensors and provides valuable insights into commercially viable methods for developing MIP-based sensing devices that may one day reach the commercial market. The goal of the literature study is to identify a deposition method that allows for systematic mass production of MIP-covered sensor chips that could bring the developed sensor platforms closer to a market-ready application in the future.

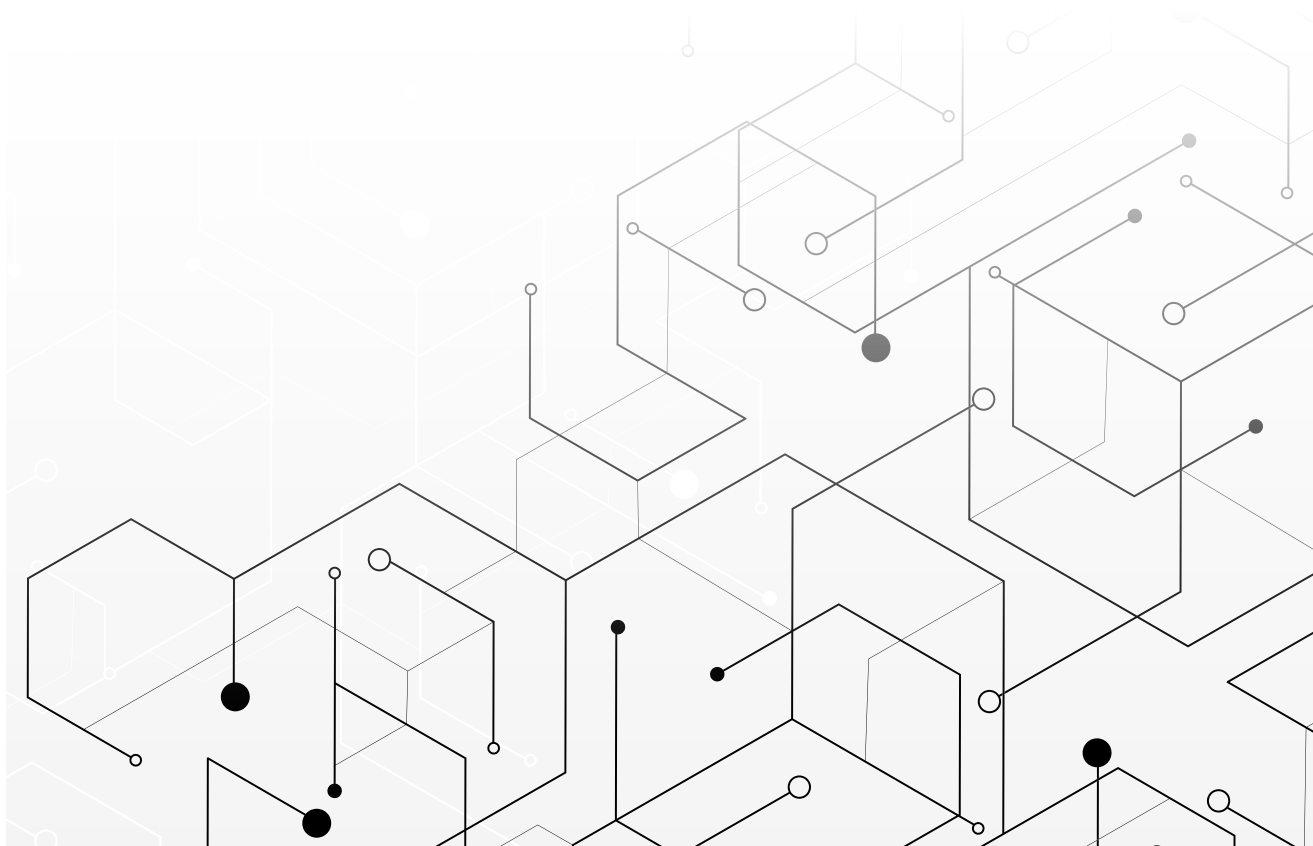
Chapter 5

Deposition Methods for the Integration of Molecularly Imprinted Polymers (MIPs) in Sensor Applications

Adapted from:

Caldara, M.; van Wissen, G.; Cleij, T.J.; Diliën, H.; van Grinsven, B.; Eersels, K.; Lowdon, J.W.* Deposition Methods for the Integration of Molecularly Imprinted Polymers (MIPs) in Sensor Applications.

Advanced Sensor Research 2023, 2200059.
<https://doi.org/10.1002/adsr.202200059>



Abstract

Offering high specificity and selectivity, molecularly imprinted polymers (MIPs) are synthetic polymeric affinity reagents that have become increasingly popular over the last couple of decades. Due to their long-term chemical and physical stability and low production cost, they have become an increasingly popular choice of receptor in the realm of sense. MIPs have therefore been associated with the detection of small molecules, proteins, cells, and pathogens, proving a highly robust and useful tool in the production of next-gen sensing platforms. This said, the development of these sensors pivots on one simple fact. These receptors have to be deposited onto a substrate for their desired application. The deposition of MIPs during sensor fabrication is therefore of great importance, with the field utilizing an array of mechanical and chemical deposition methods to achieve this. To this end, this review, sets aim at coalescing these different deposition approaches, classifying them, and outlining their utility when it comes to receptor design and integration. In this way it offers a knowledge base on current deposition methods and potential future approaches.

Introduction

The concept of molecular imprinting was introduced as early as the 1930s, while first records of molecularly imprinted polymers (MIPs) date back to the 1980s with pioneering work by Mosbach, Sellergren, and Wulff, synthesizing MIPs based on noncovalent and covalent interactions, respectively.[1-4] MIPs are generally defined as highly cross-linked synthetic polymeric structures that are able to selectively bind target analytes, thus mimicking the natural antibody–antigen mechanism.[5] The presence of highly specific nanocavities within the polymeric matrix compliment the morphology and chemical functionality of the desired target species, facilitate this “lock and key” interaction associated with biological receptors. Critical constituent components (e.g. functional monomer, functional cross-linker, porogenic solvent, and initiator) are used to achieve this, forming a complex interwoven structure of ionic interactions, hydrogen bonding, and Van Der Waals interactions between the template species and these components prior to polymerization.[6] Once initiated under thermal or photochemical conditions these components form a rigid polymeric structure encapsulating the target species, capturing its likeness and generating said nanocavities. After polymerization, the target is extracted by mechanical means or by washing with appropriate solvents under Soxhlet conditions, yielding a vacant polymeric material ready for use (**Figure 5.1**).[5] Early research focused on the development of these receptors towards small molecules, though as the field has expanded so has the list of potential targets with proteins, bacteria, fungi, and viruses being key species of interest.[7-9] In turn, this catalysed the development and utilization of new polymerization methods that could facilitate the synthesis of MIPs toward more complex analytes.[10-12]

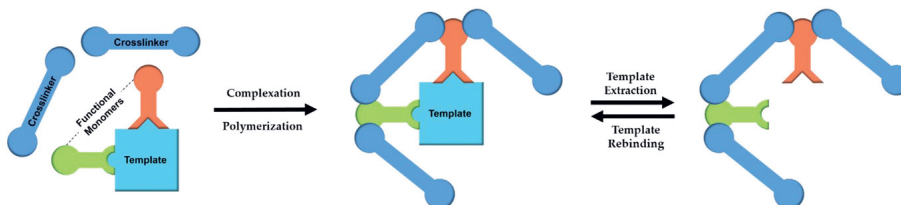


Figure 5.1 A general schematic of the classical preparation of MIPs, demonstrating the “lock & key” mechanism that is associated.

These synthetic approaches can be divided into three main categories, polymerization in solution, solid phase synthesis, and electropolymerization.[12-15] Methods such as bulk, precipitation, and suspension polymerization fall under solution-based synthesis.[16-18] The primary drawback of these methods lies in poor homogeneity in particle shapes and sizes, which is reflected in the less optimal reproducible performance of the receptors.[19] This said, these methods offer the advantage of straightforward synthesis and therefore remain a staple for the synthesis of MIPs for small molecules.[16,17,20] In an attempt to mitigate these negative aspects, a surface grafting approach utilizes solution based synthesis by facilitating receptor layer formation directly onto a substrate by means of covalent bonding.[21]

Alternatively, solid phase synthesis utilizes the immobilization of the template species onto a solid support, while removable MIP particles are formed at the supports. This eliminates the need for the harsh extraction methodologies.[12,22,23] After polymerization, low-affinity receptor particles are removed by washing the solid support with cold water, and the higher affinity MIPs with hot water.

Thus yielding MIPs with a higher degree of homogeneity in terms of template affinity, but also in relation to shape and size.[12] As the template is bound to a solid support, a whole host of templates are possible (e.g. molecules, peptides, and proteins) with the main drawback of the approach being associated with the low yields of the collected high affinity MIPs.

In contrast to these categories of polymerization, electropolymerization enables the polymerization of a conjugated monomer directly onto a substrate and yields a polymeric film instead of particle.[11] Though this draws parallels with a surface grafting, the deposited layer is non covalently bound to the surface and relies upon adsorption to the surface instead.[24] The substrate functions as the working electrode and the polymer film is deposited directly by anodic oxidation.[25] One of the major advantages is that this enables precise control over the formed polymer film thickness by carefully choosing the reaction conditions, increasing the reproducibility of the imprinting process.[26,27]

Overall, the various approaches allow the production to be tailored towards a desired template species, with the resulting receptors having excellent physical properties (resistance to harsh temperatures and pH) that can be applied in a variety of scenarios (sample pre-treatment, chromatography, targeted drug delivery, purification, and sensing.[5,28-35] Of these applications, coupling MIPs with sensing technologies has become ever more popular over the last decade, with a large proportion of MIP based research being focused at the development of MIP based sensing platforms.[29,36] Integration of MIPs into sensing platforms is achieved by coupling the receptor with a transducer element that can translate a binding event at the surface of the MIP into a tangible signal. The technologies that are currently associated with MIPs can be divided into electrochemical, optical, mass-sensitive and thermal devices (Figure 5.2).[37-39]

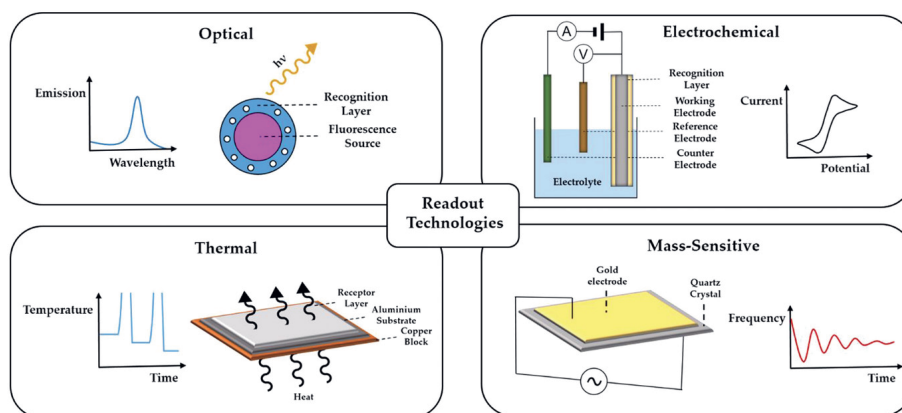


Figure 5.2 A depiction of the various readout technologies that are currently associated with molecularly imprinted polymers including: optical, electrochemical, thermal, and mass-sensitive methodologies.

Electrochemical sensing can employ a variety of electroanalytical techniques such as voltammetric, amperometric, or impedimetric measurements, which can be categorized by whether the response is generated by the analyte binding to the receptor or by the analyte itself.[36] Amperometry is an example of the former, wherein the setup consists of two electrodes being separated by a MIP-

membrane. Upon analyte binding, the polymer undergoes conformational changes, affecting counter ion diffusion, resulting in a measurable change of the membrane electro conductivity.[40] An example of the latter are voltammetric measurements, where an electrochemically active analyte is either oxidized or reduced on a MIP-modified electrode.[41] The modification of the electrode with MIPs allows for selective adsorption of the analyte and prevents interfering species from reaching the electrode. Furthermore, selectivity can be further increased by employing a suitable potential range allowing for a more precise determination of the analyte due to its oxidation or reduction at a characteristic potential.[42]

Optical sensing, on the other hand, relies on the measurement of changes in optical properties, like fluorescence or surface plasmon resonance (SPR) upon binding of the analyte and the following transduction into an electronic signal.[37] The most commonly employed optical property for sensing is fluorescence because of its high sensitivity resulting in low limits of detections (LODs).[43] Prominent examples are core-shell materials consisting of a fluorescent quantum or carbon dot core and a MIP-shell as the recognition element, in which fluorescence quenching is observed upon analyte binding.[44, 45] Even lower LODs can be achieved by using SPR as the measured optical property.[46] Similarly to fluorescence sensors, SPR sensors are often core-shell materials, with the core usually consisting of metallic nanoparticles like gold NP that are sensitive toward changes in refractive index upon rebinding.[47]

Another extremely sensitive readout approach is the detection of surface mass loading in, e.g. quartz crystal microbalances (QCM). This technique makes use of the reverse piezoelectric effect of quartz crystals, wherein a mechanical wave is brought to resonance by administering an AC-electric field. Mass loading on the surface of the crystals will lead to a change in its resonance frequency which is monitored over time.[48] The advantage of using QCM technique is the ability to detect a large amount of different analytes with little consideration of other physical properties, which is shown by piezoelectric sensors designed toward molecules, proteins and bacteria.[49-51] In spite of this, the mass sensitivity is limited when low molecular weight targets want to be detected.

Calorimetric methods utilizing MIPs also exist. For example, the straightforward, versatile thermal based detection method, known as the "heat-transfer-method" (HTM), has proved its efficiency in the sensing of small molecules, proteins and bacteria.[7,20,39] Herein, MIP particles or imprinted polymeric layers are deposited onto a solid substrate, which is in contact with a liquid phase. The solid phase is heated to a constant temperature by a heat source and simultaneously, the temperature of the liquid phase is monitored. The heat flow travels through the MIP coated recognition layer and upon analyte rebinding a change of thermal resistance can be observed by a change in the liquid's phase temperature.[39]

Though all these technologies incorporate and utilize MIPs in completely different ways, they all require these synthetic receptors to be deposited onto a transducer to function. This is a crucial step in the sensor fabrication, and is often overlooked or neglected. To date, there is not one defined method of coupling a MIP with a specific transducer, with researchers currently using a range of different techniques to do so. This review therefore wishes to chronicle and differentiate the formats in which MIPs can be deposited. Thus, highlighting each approach and potential modifications that can be conducted to integrate synthetic receptors for specific readout technologies.

Mechanical MIP deposition

The integration of MIPs into sensing platforms can be achieved through several approaches. The actual choice of a specific approach over another must be carefully considered as it affects the readout technology used and thus the potential applications of the sensor.[52,53] Several mechanical deposition methods have been used in recent years to produce MIP-based sensor platforms capable of targeting a wide variety of targets, from small molecules and proteins to viruses and bacteria.[54] In these methods, the sensor production process requires little or no chemical functionalization, making these methods very attractive in terms of marketability, which is considered a major challenge for MIP-based sensors.[55] In this chapter, we will focus on approaches achieved via physical deposition methods, such as micro-contact stamping, drop casting of MIP particles or of the pre-polymerization mixture, and the incorporation of MIPs into electrodes.

Micro-contact Stamping

Most commonly, micro-contact stamping finds its home in the world of soft lithography where it is used to shape polymeric surfaces by introducing a mould.[56] The value of this process has therefore been realized by the MIP field, with its primary application in the imprinting of macromolecular targets.[57-60] In this approach, two solid substrates are prepared and then placed on top of each other in a “sandwich” conformation; one of the substrates presents the template immobilized on a stamp and the other one represents the solid support, usually functionalized with a viscous oligomer layer. While the two substrates are in contact, the crosslinking process is completed and the stamp with the immobilized template is removed leaving cavities in the formed polymeric layer that resemble the target in shape and functionality[61] (**Figure 5.3**).

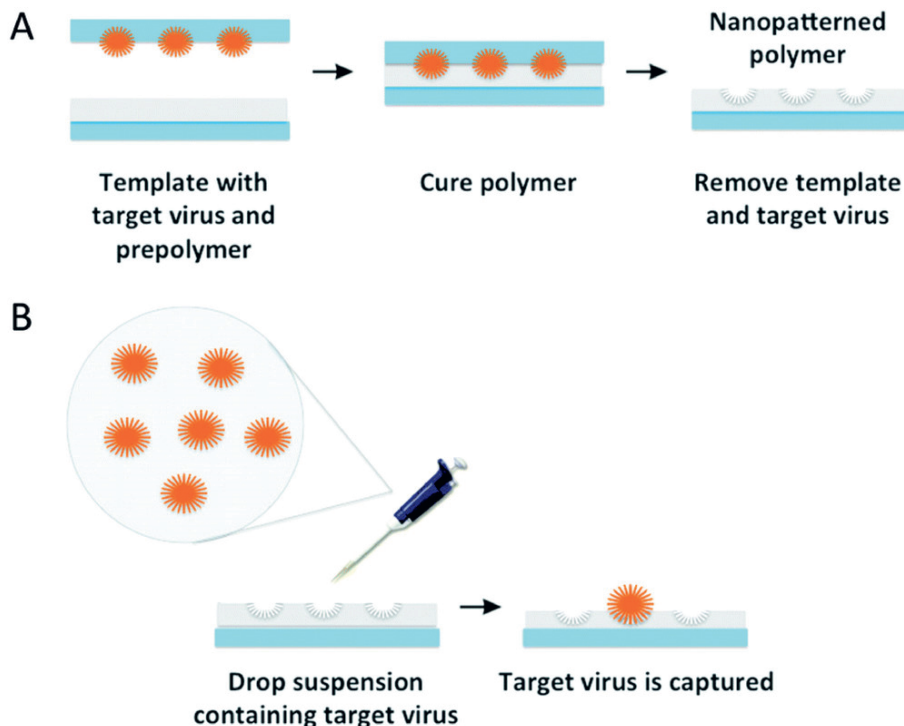


Figure 5.3 Schematic representation of micro-contact stamping deposition for virus imprinting. Reproduced with permission.[61] Copyright 2015, Royal Society of Chemistry (CC-BY).

The micro-contact stamping method allows the preparation of imprinted polymer layers that have proven their efficiency for the detection of several macromolecular targets, such as bacteria,[7,62-71] viruses,[61,72,73] fungi,[74] and proteins.[75] Another benefit of this approach is the variety of readouts that could be employed using surfaces prepared with this technique, in fact these imprinted layers have been used with electrochemical,[7,69,73] thermal,[7,65,68,71] Raman,[66,67] and QCM[70,72,75] readout technologies. It should also be noted that by slightly varying the chemical composition of the substrate and stamp employed for the imprinting (**Table 5.1**), the sensitivity and selectivity of the sensor could be strongly affected,[7,76] thus leaving a great margin for improvement of such imprinted layers.

Table 5.1 Summary of research articles that utilize micro-contact stamping for deposition or imprinting.

Target	Readout Technology	Approach modification	Imprinting technique / MIP deposition	Ref.
<i>Mycob. smegmatis;</i> <i>Cyanobact.</i>	AFM	PDMS substrate, glass stamp	Imprinting	[62,63]
<i>Escherichia Coli</i>	AFM and PF-QNM	Poly(styrene-co-DVB) substrate, glass functionalized with TMVS stamp	Imprinting	[64]
<i>E. Coli;</i> <i>C. Coli</i> and <i>C. jejuni;</i> <i>Saccharomyc.</i>	HTM, EIS, QCM	Polyurethane substrate, PDMS stamp	Imprinting	[65,68-71,74]
<i>E. coli</i> and <i>B. cereus</i>	Confocal Raman microscopy and PLS-DA	Heavy Duty Ink substrate, glass functionalized with APTES and DSS stamp	Imprinting	[66]
<i>Escherichia coli</i>	Confocal Raman microscopy and PLS-DA	Poly(styrene-co-DVB) substrate, glass functionalized with APTES and DSS stamp	Imprinting	[67]
<i>Escherichia coli</i>	HTM	Polyurethane-urea substrate, PDMS stamp	Imprinting	[7]
<i>Influenza A (HK68) virus</i> and <i>Newcastle disease virus (NDV)</i>	Fluorescence microscopy	PDMS substrate, PDMS stamp	Imprinting	[61]
<i>Influenza A virus</i>	QCM	Poly(AMM-co-MAA-co-MMA-co-VP) substrate, glass stamp	Imprinting	[72]
<i>Tobacco mosaic virus (TMV)</i>	EIS	Poly(VP-co-MAA) substrate, glass stamp	Imprinting	[73]
Lysozyme	QCM	Poly(MMA-co-TRIM) substrate, CaCO ₃ nanoparticles layer stamp	Imprinting	[75]
Glucose; Histamine; L-nicotine and serotonin; melamine	HTM	Al-PVC substrate, PDMS stamp	Deposition	[20,77-79]

Histamine	EIS	Al-MDMO-PPV substrate, PDMS stamp	Deposition	[80]
Histamine	EIS	Al-PVC substrate, PDMS stamp	Deposition	[81]
Serotonin	EIS	Al-PPV substrate, PDMS stamp	Deposition	[82]
Histamine	EIS	IDEE-polyurethane film substrate, no stamp	Deposition	[83]

A variant to this approach has also been used for the deposition of MIP micro particles on a solid support. In this method, polymer particles are immobilized on a stamp and then this is applied to an adhesive layer, resulting in the formation of a MIP layer. The stamp used to immobilize the particles is usually PDMS, and as for the adhesive layer different polymers, such as PVC or conjugated polymers (e.g. PPV), have been used successfully. The formed receptor layer is then used as sensing element for different types of transducers, such as HTM (**Chapters 3 and 4**) [20,77-79] or EIS[80-83] allowing the detection of several markers. The major drawback of micro-contact stamping lies in the irreproducible nature of the formed layers, primarily stemming from how the analyte species is stamped into the polymeric layer. To date there has been no in-depth study that verifies how the template/MIP is distributed onto the polymer layer during the stamping/curing, making the exact replication of functionalized substrates near an impossibility. This critical factor must be addressed if the technology is to be mass-produced, otherwise each stamp will afford a different surface coverage and particle/imprint distributions therefore lending itself to heterogeneous and irreproducible receptors.

Some progress has been made towards providing a solution to this conundrum, with concepts such as producing a “master stamp” showing great promise. This concept is exemplified in the literature for the imprinting of yeast.[84] To this end, PDMS is poured over a yeast imprinted surface that was synthesized prior and left to cure for two days, thus enabling a stamp to be generated that captures the likeness of the imprint sites but in silicone instead. After the curing process, the PDMS stamp is removed, and can be subsequently used for the production of further functionalized surfaces. The main idea is that the “master stamp” can be used to produce imprinted layers with the exact same distribution of receptors sites and surface coverage as the original layer, and therefore increases the reproducibility and standardization of the layers formed. A research group has taken this concept one step further by combining this process with continuous roll-to-roll imprinting enabling the mass manufacture of imprints for blood cancer cells.[85] Though promising, these modified versions of micro-contact imprinting still have their limitations. As the “master stamp” is used more, the resolution and definition of the stamp reduces meaning that the quality of the imprints also declines. This is not an issue in the short term but for mass production this becomes problematic, as more master stamps have to be produced and the process begins to draw parallels with the original micro-contact imprint methodology.

Drop Casting

A simple and rapid technique for immobilizing micro- and nanoparticles on different substrates is the so-called “drop casting”. This deposition method, as the name suggest, relies on the formation of a

layer on a solid flat surface by adding a drop of suspended particles and leaving it to “stand & dry” in order to evaporate the remaining solvent. In the case of MIP particles, this technique is mostly used to immobilize the particles onto different types of electrodes. Different works have reported the drop casting of suspended MIP particles on sensing platforms without addition of supplementary components.[86-90] However, lack of control over particle distribution and limited adhesion at the surface leads to significant limitations in terms of reproducibility. In order to enhance this process, the technique can be modified by mixing the suspended imprinted particles with other components used as binders, (e.g. PVC or chitosan) therefore overcoming the adhesion issues.[91-96] Alternatively, an adhesive thin film can be applied prior to the drop casting procedure encapsulating the particles (e.g. polypyrrole [97] and agarose [98,99]), though the encapsulation may decrease the sensitivity of the receptor.

Recently, a novel optical-chemical sensor has been developed demonstrating the flexibility of drop-casting.[100]

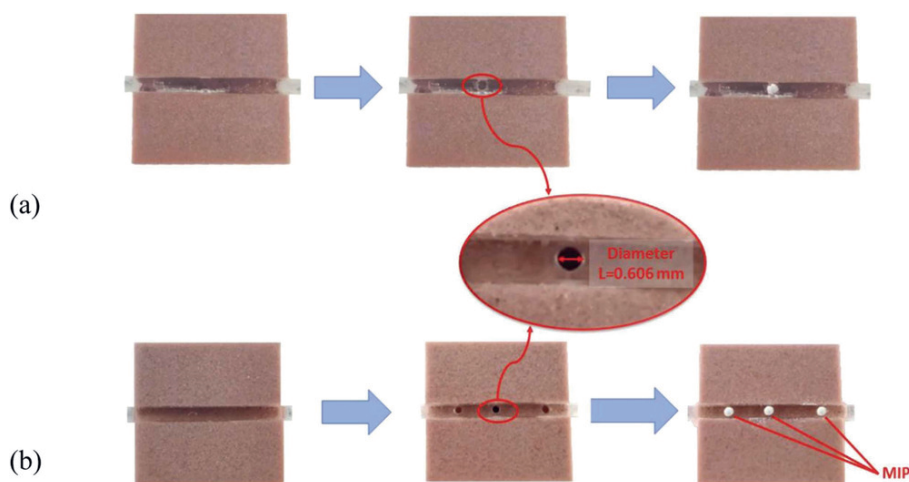


Figure 5.4 Construction of the MIP-based platform. Configuration with a) one or b) three micro-holes, with permission.[100] Copyright 2022, Elsevier.

In this work, a 1 mm plastic optical fibre was used as a solid substrate; two different configurations with one or three microholes were obtained by drilling into the exposed core of the fibre. Afterward, the MIP prepolymerization mixture was drop cast in the holes and a thermal polymerization was carried out to obtain MIP micro particles (**Figure 5.4**). The obtained platform showed remarkable selectivity and sensitivity by SPR analysis.[100] As the method facilitates the incorporation of presynthesized receptor particles, drop-casting can be applied across a large range of potential targets and readout technologies (**Table 5.2**).

Table 5.2 A summary of research articles where drop casting is utilized as the deposition method of choice.

Target	Readout Technology	Substrate	Binder	Ref.
Creatinine; Troponin I	HTM	Screen printed electrode	None	[88,89]
Bisphenol A	SERS	Spherical polystyrene close-packed array	PS beads	[90]
Sertraline	DPV	Screen printed electrode	PVC	[96]
Caffeine	EIS and Chronopotentiom.	Screen printed electrode	PVC and o-NPOE	[95]
Diquat; Nalbuphine	Potentiom.	Screen printed electrode	PVC and DOP	[92,94]
Albumin	QCM	Screen printed electrode	None	[87]
Amoxicillin	HTM	Screen printed electrode	Polypyrrole	[97]
Parathion	LSV	Glassy carbon electrode	Chitosan	[93]
2,4-dichlorophenoxy acetic acid	DPV	Screen printed electrode	Agarose	[98]
Alfuzosin and solifenacin	Potentiom.	Carbon paste electrode	PVC and NPOE	[91]
Amoxicillin	DPV	Glassy carbon electrode	None	[86]
Cocaine	Potentiom.	Ion selective electrode	PVC and NPOE	[101]
2,4,6-trinitrotoluene (TNT) and 2,4-dinitrophenol (DNP)	DPV	Graphite epoxy composite (GEC) electrode	Sol-gel immobilization	[102]
Bovine serum albumin	EIS	Glassy carbon electrode	Agarose	[99]
Furfural	SPR	Plastic optical fibre	None	[100]

Dip Coating

The dip coating technique is a simple and low-cost method to obtain thin-film coatings on a substrate. The process can be divided into three main stages: dipping, withdrawal, and evaporation (**Figure 5.5**). Since MIP particles synthesized by bulk polymerization are usually in the micro meter size range and thus tend to precipitate when suspended, their deposition via the classical technique is difficult to achieve. Therefore, to achieve the deposition of MIP micro particles via dip coating the particles need to be mixed with another adhesive component; in previous work, this was achieved by combining the

micro particles with an agarose solution, followed by crosslinking treatment.[103] In recent years, the technique has been employed to functionalize thermocouples with nanoMIPs as synthetic receptors. The functionalized substrates were used as thermal sensors for the detection of various targets, such as small molecules [104] and proteins.[88,105]

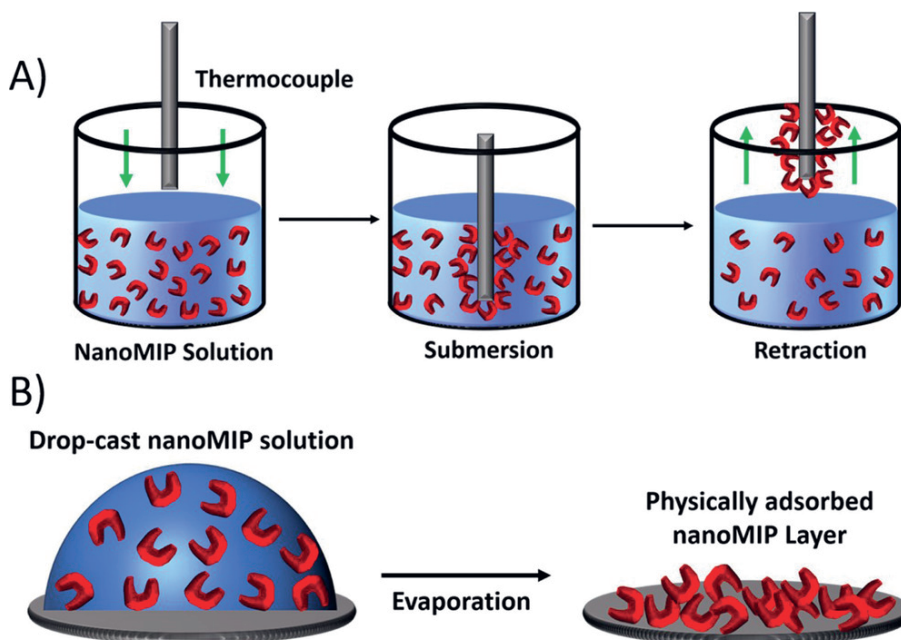


Figure 5.5 A) Different stages of the dip coating process compared with B) drop-casting deposition technique Reproduced with permission.[88] Copyright 2021, American Chemical Society (CC-BY).

Direct Electrode Incorporation/Screen Printing

As electrochemical readout technologies become ever more popular, so has the appeal of integrating MIPs directly into electrodes that compliment these platforms. Multiple approaches have been attempted ranging from electropolymerization to in-situ polymerization, though more simplistic mechanical approaches have shown great promise.[36] One of these approaches utilizes bulk polymerized MIP particles and incorporates them directly onto an electrode's surface by use of carbon paste. [106] The MIP particles are directly mixed with the paste, enabling the distribution of the receptors across the entire electrode. Applications of this approach facilitate the detection of a wide range of potential analytes including, but not limited to, small organic molecules [107-122] and ions.[123-125] Additional materials can be added to the paste, boosting the conductivity of the composite and enhancing the sensitivity of the system, with common additives including carbon

nanotubes [108,110,111,124,125] or platinum nanoparticles.[113] In recent years, this concept has been taken even further with advancements in the field of screen printing. Rather than applying the MIP loaded graphene paste to a pre-existing electrode, instead the MIP particles are combined with graphene ink and screen printed directly as electrodes.[121,122] Thus, material waste is greatly reduced, electrode homogeneity is increased, and the substrate that the electrode is printed onto can be engineered towards more environmental friendly materials.[126] Furthermore, this has opened up the possibility of developing facile flexible electrochemical sensors that can be tailored toward a specific application in terms of substrate material, receptor, and print design.

The drawbacks of this freedom are diminished binding capacities and reduced linear ranges when exposed to a desired target analyte. As the MIP particles are combined with either a paste or ink, the surface of the receptor becomes saturated with graphene preventing a target analyte interacting with the specific binding sites. As a result the essential blocking of the receptor reduces the aforementioned linear range and selectivity of the sensor, though the sensitivity remains somewhat constant as graphene is excellent at absorbing species.

Electrochemical MIP deposition

Electrochemical deposition methods are categorized by their use of electric currents as either a way of applying force to repel/attract ions or to deposit ionic material onto an electrode. Thus, electropolymerization and electrospinning are the two main methods for the deposition of MIPs that embody this principle. As such, mass is added across a substrate in the form of fibres that contain MIPs or by thin film formation respectively.[127]

Electropolymerization

Electropolymerization is a deposition method in which a conductive polymeric coating/film is formed across a conductive substrate/electrode when an electroactive monomer is subjected to potentials that cause its oxidation and reduction.[25] More commonly, this approach is associated with the direct formation of imprinted layers at a substrate's surface, allowing imprinting during the deposition process by simply introducing a template species to the polymerization mixture.[128] This straightforward alteration has spawned an entire sector in the field of MIPs, proving popular for the imprinting of small molecules and larger (bacteria and proteins) species.[129, 130] This process is easily achieved using voltammetric,[131] galvanostatic,[132] and potentiostatic conditions,[133] though voltammetric electropolymerization has proven to be the far more popular approach. In essence, a monomer is oxidized and reduced by sweeping across a set range of potentials, via cyclic voltammetry, stimulating polymerization. The thickness of the resulting polymeric layer is tuned by altering the sweep/scan rate, thus affecting the rate at which the polymer forms on a substrate. A three-electrode setup is the standard for this deposition approach, consisting of a working electrode (where the coating is deposited), a counter electrode and a reference electrode (**Figure 5.6**).[134]

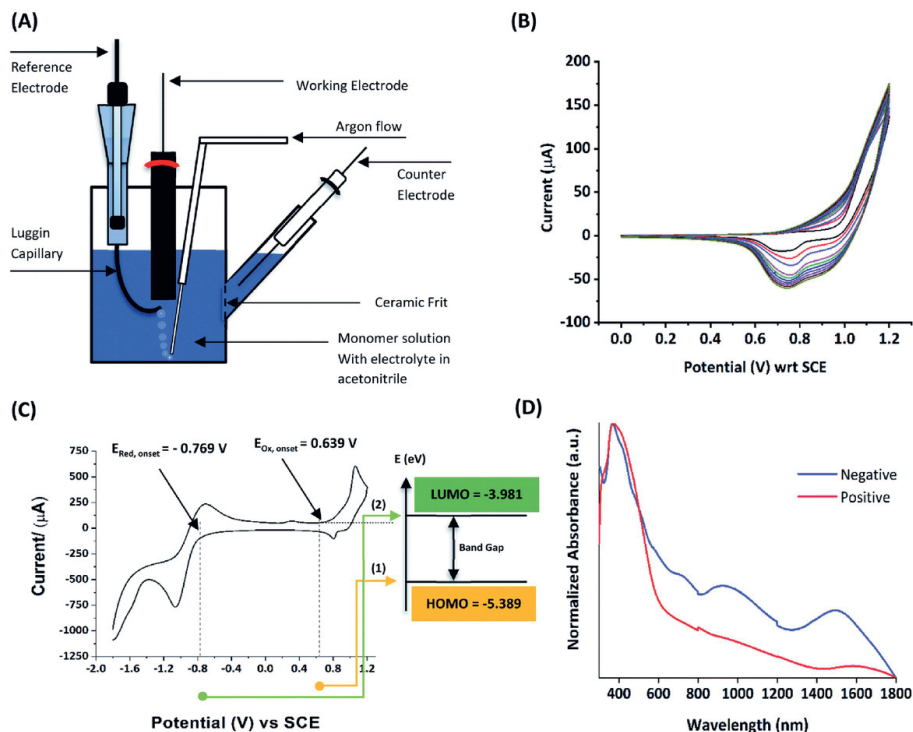


Figure 5.6 A) An electropolymerization setup, showing the critical components necessary, followed by B) a typical cyclic voltammograms (CV) that is collected during the electropolymerization process. Reproduced with permission.[135] Copyright 2022, Royal Society of Chemistry (CC-BY).

The range of the potential sweep is monomer-dependent, with the redox potential differing depending on the compound selected.[136] The most common compounds to undergo electropolymerization are pyrrole,[137] aniline,[138] and dopamine,[139] with these compounds being amongst the easiest to polymerize. For example, it has been reported that polypyrrole layers imprinted with clofibric acid can be successfully prepared by means of cyclic voltammetry.[140] The layers are deposited onto gold coated wafers (working electrode) by cycling the applied potential between -0.2 and 0.8 V across an aqueous solution containing clofibric acid, KNO_3 and PBS. After the synthesis, the layers were washed with 70% ethanol and a solution of potassium chloride/hydrochloric acid to remove unreacted monomer and the template compound. The resulting layer's physical characteristics were then studied, determining the response towards clofibric acid, the selectivity, the hydrophobicity by contact angle, and the layer thickness. AFM imaging revealed that the deposited material had a circular structure $<1 \mu\text{m}$ (diameter) on the surface, with a surface roughness of between 6 and 8 nm. Overall, this piece of research highlights the facile nature of the approach, with its applications being far spread and applied to many different molecules across the field (Table 5.3).

Table 5.3 Examples of research articles utilizing electrodeposition and their associated approach modifications.

Template	Readout technology	Approach modification	Ref.
SARS-CoV-2	Electrochemical impedance	Monomer: N-hydroxymethylacrylamide Cross-linker: N,N'-methylenebisacrylamide Electrolyte: PBS Solvent: H ₂ O Applied potential: -1.4 V to -0.2 V Cycles: 25 Scan rate: 50–100 mV s ⁻¹	[141]
Ascorbic acid	DPV	Monomer: Pyrrole Electrolyte: LiClO ₄ Solvent: H ₂ O Applied potential: -0.5 V to 0.8 V Cycles: 10 Scan rate: 50 mV s ⁻¹	[142]
NS1	QCM	Monomer: terthiophene Electrolyte: PBS Solvent: ACN Applied potential: 0 V to 1.1 V Cycles: 10 Scan rate: 50 mV s ⁻¹	[143]
Tryptamine	CV	Monomer: Pyrrole Electrolyte: HCl Solvent: H ₂ O Applied potential: -0.6 V to 1.0 V Cycles: 10 Scan rate: 100 mV s ⁻¹	[144]
Furosemide	CV	Monomer: o-phenylenediamine Electrolyte: acetate buffer Applied potential: 0 V to 1.0 V	[145]

		Cycles: 20 Scan rate: 100 mV s ⁻¹	
Dopamine	Electrochemical impedance	Monomer: Pyrrole Electrolyte: LiClO ₄ Applied potential: -0.8 V to 1.0 V Cycles: 5 Scan rate: 100 mV s ⁻¹	[146]
Further examples:			[147-153]

The main drawback of electropolymerization lies in the fact that electroactive monomers have to be utilized for layer formation/deposition. This means that there are a limited number of viable options that have been used to demonstrate MIPs can be deposited in this fashion. The limited library proves problematic when selecting a monomer that has optimum interactions with the template species, meaning it is hard to specifically tailor an electropolymerized layer towards a desired analyte. This said, custom monomers are slowly emerging that have greater structural diversity and offer more in terms of tailored specific interaction and stem from the field of traditional conjugated polymers.[154] Another downside is the substrate that the material is being electropolymerized onto has to be conductive, and even this is a challenge as metal such as copper and aluminium can be easily oxidized during the electrodeposition meaning that commonly gold, platinum, and carbon are the materials of choice.

Electrospinning

Electrospinning is a method of producing fibres (micro–nanoscale) by means of applying an electric force to a charged polymer thread that is generated in a melt or solution and drawing them out into the desired dimensions.[155] Due to its unconventional electrical approach, this deposition technique is therefore discussed in a subsection of the electrochemical MIP deposition. In essence, a polymer solution is pumped through a charged needle. As the solution passes through, the liquid's surface becomes charged and the electrostatic repulsion begins to overcome the surface tension of the solution. As the solution leaves the needle, it is ejected towards a collection plate/drum that rotates and draws the solution near. As the solution flies toward the collector, the solvent evaporates and the remaining polymer is drawn out forming fibres (**Figure 5.7**).[156]

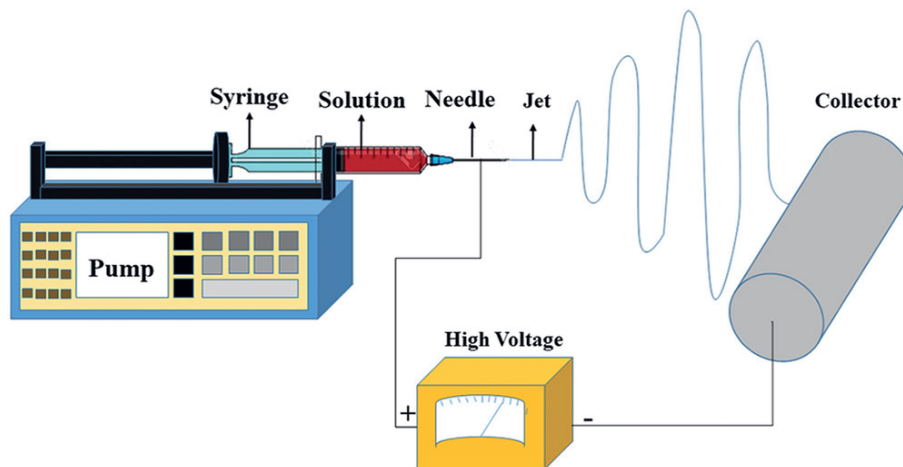


Figure 5.7 Electrospinning schematic of imprinted nylon 6 nanofibers for the extraction of bisphenol A from waste water. Reproduced with permission.[157] Copyright 2018, John Wiley and sons.

Depending on the physical characteristics of the polymer solution, the electric field applied, drum rotation, and injection speed, it is possible to tailor the process towards a desired fibre size and morphology.[158] As the method is solution based, prior to spinning, MIPs can be dispersed into the liquid phase, yielding electro-spun fibres with MIPs distributed throughout the produced fibres. Mild spinning conditions also favour the use of this approach, as the MIP particles are not exposed to high temperatures or other damaging conditions.[159] This principle was also demonstrated by encapsulating benzyl paraben imprinted polymers in styrene, before studying the extraction capabilities of the prepared fibres by analysing spiked sea, tap, and bottled water samples.[160] The prepared MIP particles were implemented into the polymer fibres by mixing MIP particles into a polystyrene (10% w/v) solution in DMF, before electrospinning fibres using a 30 KV applied voltage across a 15 cm distance at 1.0 mL h^{-1} , yielding nanofibers.

This methodology has been widely adopted by the MIP community with many variations of this process possible, utilizing different applied voltages, plate distances, flow rates, and matrix polymer compositions. An overview of literature referring to these modifications can be found in **Table 5.4**, outlining what parameters have been changed to achieve the incorporation/deposition of the MIP particles inside the fibers generated.

Table 5.4 A summary of articles where MIPs are implemented into electrospun fibres and the associated experimental modifications used to achieve this.

Template	Readout technology	Approach modification	Ref.
----------	--------------------	-----------------------	------

Theophylline /17β-estradiol	Microscopy and radioligand binding analysis	PET (10% w/v) matrix polymer in DCM 0.8–0.9 mm inner diameter needle 20 kV applied voltage 20 cm distance between plates Flow rate not specified	[161]
4-aminopyridine	Indirect detection by studying cell growth	5% (w/v) pLDLLA in DCM, before adding MIP particles 17 kV applied voltage 17.5 cm distance between plates 0.6 mL h ⁻¹ spin rate	[162]
Ascorbic acid	DPV	PVP/CA matrix polymer in acetone/DCM 1:110 kV applied voltage 20 cm distance between plates 1 mL h ⁻¹ flow rate	[163]
Propranolol	HPLC-MS/MS	PET (10% w/v) in DCM with MIP particles 0.8–0.9 mm inner diameter needle 20 kV applied voltage 20 cm distance between plates Flow rate not specified	[164]
Rhodamine B	HPLC	PET matrix polymer in DCM 0.8 mm inner diameter needle 18 kV applied voltage 15 cm distance between plates Flow rate not specified	[165]
Dexamethasone	Optical analysis (UV–visible spectroscopy)	PCL matrix polymer in CHCl ₃ /DMF 19.5 kV applied voltage 14.5 cm distance between plates 0.45 mL h ⁻¹ flow rate	[166]
2,4-dichlorophenoxyacetic acid	Fluorescence	-	[167]
2,4-dinitrotoluene	HPLC	10–12 kV applied voltage	[168]

		0.1 mm min ⁻¹ flow rate	
Naringin	HPLC	Syringe was fixed vertically 18 kV applied voltage Cross linking conducted at 30 °C	[169]
Naringin	HPLC	Incorporation of TEOS into the spun fibres Crosslinking conducted at 30 °C Template removal with hydrofluoric acid	[170]
2,4-dichlorophenoxyacetic acid	HPLC	0.8 mm diameter metal tip 20 cm distance between plates Driving voltage of 30 kV Aluminium foil electrode	[171]
Further examples:			[172-174]

Alternatively, the molecular imprinting process can occur during the electrospinning and subsequent deposition of the material.[175] In contrast to the previous iteration, this approach enables the entirety of the electro-spun surface to act as a receptor rather than relying on particles distributed throughout the bulk of the material. Introducing a template species into the pre-spun polymeric solution allows for the formation of imprints within the fibres after spinning.[176] The downside of “in-situ spinning” being that the deposited layer is not highly cross-linked, which is normally definitive of MIPs as this instils rigidity and receptor stability. This said, strong ionic interactions stabilized by a template species have the potential to mimic this highly cross-linked characteristic and fibres spun have mimetic capabilities, or post crosslinking of the polymer are a possibility.[177] This approach was highlighted with the formation of nanofiber films for the sensitive detection of 2,4,6-tribromophenol (TDP) by spin coating a solution containing TDP alongside the monomer β -cyclodextrin (β -CD) and poly-vinylbutyral (PVB) as electrospinning matrix.[178] The mixture was placed in a 10 mL syringe fitted with a metallic needle of 0.4 mm inner diameter, and was fitted horizontally opposing a stainless steel electrode that was directly connected to a high-voltage power supply. Between the tip and collector was applied 18 kV, with the distance between the two being 10 cm, and the flow rate of the solution 0.5 mL h⁻¹. The TDP doped polymer fibres were directly electrospun onto a polished glassy carbon electrode (GCE), and postcuring of the polymeric fibres was achieved by immersing in hexamethylene diisocyanate (HMDI) at room temperature for 24 h (**Figure 5.8**). The resulting layer showed great sensitivity towards the TDP, having a linear range between 0.9–10 × 10⁻⁹ M and a calculated LoD of 0.629 × 10⁻⁹ M when analysed with a quartz crystal microbalance (QCM). Further examples can be found in **Table 5.4**, highlighting the versatility of the approach.

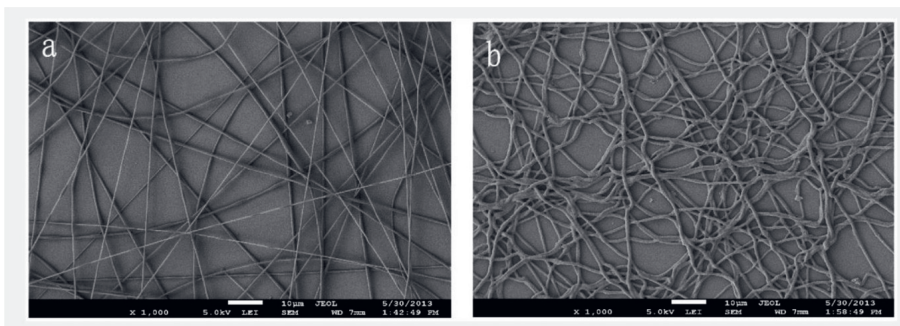


Figure 5.8 SEM morphology of nanofibers a) before cross-linked; and b) after cross-linking. Reproduced with permissions.[178] Copyright 2016, MDPI (CC-BY). The primary downside to this technique is that the embedded MIP particles are not homogeneously spread throughout the spun fibre, leading to sensor reliability issues. Furthermore, depending on the size of the particles that are captured in the fibre, surface area can be lost due to high levels of encapsulation and particles being buried. Thus leads to the further limitation of there being a maximum amount of MIP particles that can be mixed with the spun polymer matrix, with excessive amount resulting in poor fibre production and reduced mechanical properties. Therefore, it is probably because of these drawbacks that the technique has not yet been widely implemented in MIP-based detection platforms.

Chemical deposition

One of the major challenges associated with the development of sensing platforms is the reproducibility of the method employed to fabricate such sensors. In many MIP-based sensing technologies, the preferred approach to prepare the imprinted polymer is bulk polymerization, due to its ease and scalability of polymer synthesis. Although bulk polymerization represents a rapid and simple preparation method, the integration of bulk MIP particles into sensing devices could lead to sensors with poor repeatability and high batch-to-batch variance.[179] In addition, it has been shown by different sources that MIP films lead to better performances when compared with bulk MIPs-based platforms that hold the same chemical composition.[97,180] The ways in which this can be utilized for MIP deposition are through the generation of thin films or the direct grafting of a receptor.

Thin Films

Thin films, also described as “in-situ polymerization” or self-assembly polymerization,[181] are achieved by adding (usually by drop casting technique) the prepolymerization mixture on the surface of a substrate and subsequently polymerized (**Figure 5.9**). The focus is the formation of MIP films across different substrates via UV light or thermal initiation, leading to the direct formation/deposition of a receptor. In recent years, the development of MIP thin films has gained increasing attention, stemming primarily from their easy incorporation into many readout technologies.[182] Since the polymer film can be designed with several monomers and/or cross-linker molecules, the variation of one of mixture components can have a huge impact not only on the sensitivity of the sensor but also on the transducer used to convert a given signal. For this reason, these films have found application with several readout

technologies such as: HTM,[76,97,183] EIS,[76] CV,[184,185] DPV,[186-189] QCM,[70,190-192] GC-MS,[193,194] SPR,[195,196] APGC-MS/MS,[197] UHPLC-PDA,[198] UV-Vis.[199]

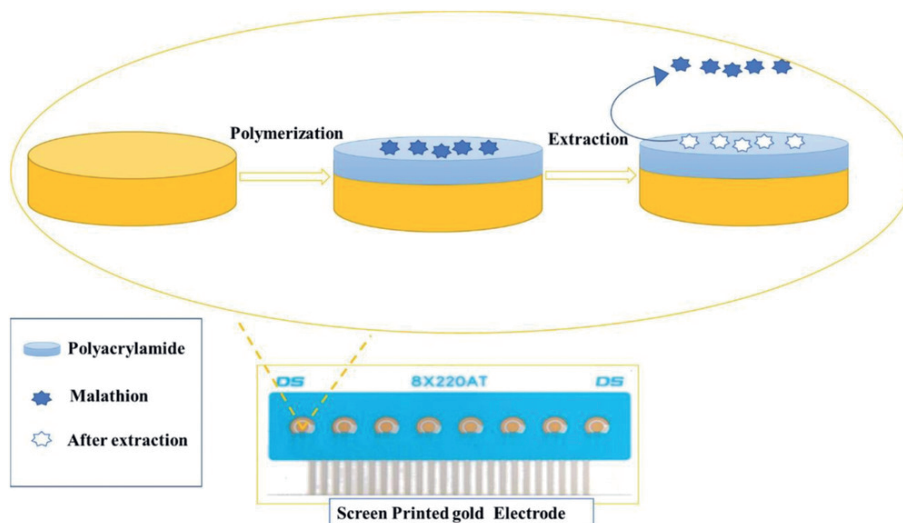


Figure 5.9 Fabrication scheme of MIP films for malathion detection on screen printed gold electrode. Reproduced with permissions.[188] Copyright 2020, Elsevier.

Surface Grafting

Similarly to thin films, surfacing grafting allows MIPs to be generated at a functionalized interface in-situ. This concept is similar to that of electropolymerization, though is defined by the deposited/formed layer being covalently bound to the substrates surface whereas electropolymerized layers rely on adsorption instead.[200] This is made possible by the prior functionalization of the substrate, where reactive chemical functionalities (e.g. hydroxyl, thiol, amine etc.) are introduced across the surface by simple chemical modification.[201] Linker molecules are proceeded to be coupled to the functionalized surface, offering “anchor” points for the growing of the polymeric layer. Typically, these anchors tend to be monomers or photo/thermal initiators that are easily incorporated into the deposited layer during the grafting process, thus offering a covalent linkage directly into the bulk of the deposited material.[202] This approach was highlighted in another published work, where is present covalent binding between 4,4'-azobis(4-cyanopentanoic acid) (ACPA) and (3-aminopropyl)-triethoxysilane (APS) functionalized silica particles.[203] Subsequently, a methacrylic acid (MAA) and ethylene glycol dimethacrylate (EGDMA) based MIP for the detection of D-phenylalanine/anilide was grafted by exposing the functionalized silica particles to these components in toluene while under constant irradiation from a UV light source. Alternatively, it was recently shown how tetraethyl orthosilicate (TEOS) can be bound to hydroxylated steel sheets (10 × 20 mm) enabling the grafting of a MMA/EGDMA based molecularly imprinted polymer for the detection of enrofloxacin.[204] These approaches have been adopted by many researchers in the field, with examples listed in **Table 5.5**.

Table 5.5 Examples where MIPs have been directly surface grafted onto substrates.

Template	Readout technology	Approach modification	Reference
2-methoxyphenidine	Thermal	Substrate: Aluminium (10 × 10 × 5 mm) Surface modification: Hydroxylation Linker: Allyltrimethoxysilane	[205]
Heparin	Electrochemical	Substrate: graphite Surface modification: chloromethylation Diethylthiocarbamate bound	[206]
Uric acid	Electrochemical	Substrate: graphite electrode Surface modification: sol-gel	[207]
Theophylline	Electrochemical	Substrate : carbon nanotubes Surface modification: Hydroxylation Linker: 3-chloropropyl trimethoxysilane	[208]
L-phenylalanine	Electrochemical	Substrate: silica Surface modification: hydroxylation Linker : APS 4,4'-azobis(4-cyano pentanoic acid) bound	[209]
Glucose	Potentiometric	Substrate: Gold nanoparticles deposited on a screen printed carbon electrode Surface modification: Benzoic acid functionalized poly(terthiophene) Linker: amide bond formation	[210]
Further examples:			[211-214]

Due to the relative ease of synthesis, control over layer growth, and general tunability of the deposition method, the direct surface grafting of MIPs is a highly attractive proposition.[215] The method also leans into scalability, with the potential of functionalizing a large surface and cutting them into smaller sensor size pieces with this notion theoretically generating sensors with higher homogeneity. Adversely, this functionalization has to be conducted in a controlled reproducible manner that could prove labour intensive and hard to replicate.

Vacuum deposition methods

Vacuum deposition is characterized as a group of processes that deposit materials species-by-species (e.g. atom-by-atom or molecule-by-molecule) onto a solid surface (or substrate) by operating at pressures below that of the atmosphere (e.g. in vacuum). Material that requires depositing is vaporized and introduced to a substrate, enabling direct layer formation across the surface. As these processes occur in the absence of gaseous species that would normally interfere with molecular or atomic deposition, it is possible to form highly controlled thin films onto the substrate. This class of deposition can be broken down into multiple subclasses including thermal evaporation, sputtering, cathodic arc vaporization, laser ablation, and chemical vapour deposition (CVD).[216-219] Though these different branches of vacuum deposition exist, only CVD has been reported for use in the deposition of MIPs.

Chemical Vapour Deposition

Traditionally CVD is a deposition method by which a vacuum draws volatile precursor compounds across a substrate (typically a wafer), where they can then react and deposit at the surface.[220] The resulting layers are highly robust and most importantly tenable, leading to this process being adopted mainly by the microfabrication industry for the production of semi-conductors.[221] Common materials that are currently deposited this way include silicon, carbon, metals (e.g. titanium, tungsten), and fluorocarbons, though polymer composites are becoming increasingly popular.[222] Different CVD operating conditions are selected based on the material being deposited, with variations regarding the working pressure, vapour characteristics, and substrate heating being just a few parameters that are altered when making this consideration.[223] Currently the most common variation associated with MIPs is initiated chemical vapour deposition (iCVD), which is a method that is traditionally related to the deposition of dense conformal coatings onto solid substrates.[224] In essence, this method uses free-radical polymerization to synthesize thin films across a substrate, where the vaporized constituent components of the polymer (monomer, cross-linker, and initiator) are introduced inside a vacuum chamber containing template-functionalized substrates. The polymerization process is activated thermally by means of a heated filament, radicalizing the differing components and enabling them to react at the surface of the substrate. A cooling stage helps facilitate this step, being placed directly under the functionalized substrate, with an exhaust in close proximity to remove any unreacted material.[225]

This approach has been exemplified by functionalizing anodic aluminium oxide membranes with immunoglobulin (IgG) before using iCVD for the fabrication of imprinted layers (Figure 10).[226] This research demonstrates how a complex biological target can be imprinted effectively by utilizing iCVD, producing highly selective receptors when exposed to other biological markers such as lysozyme and bovine serum albumin. Though highly effective, this approach has some major drawbacks, including the amount of parameters that must be optimized to achieve the synthetic receptor deposition alongside the associated high cost. CVD requires highly specialized equipment, meaning the initial start-up price for production is high and therefore making it less attractive than other more cost-effective approaches.

On the other hand, this approach could prove extremely scalable and has the potential of producing very reproducible layers. The method however requires more study in terms of MIP-based sensor fabrication as there is only one study reported to date.

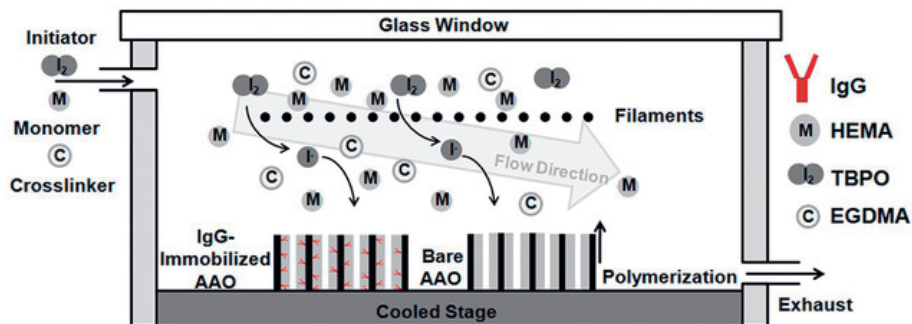


Figure 5.10 The graphical concept of using iCVD for the direct synthesis of MIPs onto functionalized substrates. Reproduced with permissions.[219] Copyright 2013, American Chemical Society.

Conclusion and future outlook

As with the synthesis of imprinted polymers, there are many deposition approaches available for the integration of the resulting synthetic receptors into sensory platforms. The methods highlighted above, are currently the most widely accepted, with the versatility and the limiting factors of each approach discussed.

This said, there is still a vast amount of differing approaches that have not yet been investigated that could prove of high value. A large number of these methods remain in the field of vacuum deposition with thermal evaporation, sputtering, cathodic arc vaporization, and laser ablation remaining untouched and even CVD sparingly utilized in comparison to other approaches. The defining factor for deposition revolves around the idea that either an imprinted layer is formed in situ during sensor fabrication, or if the receptor has been synthesized prior and is being deposited as part of a bulk material. This is reflected in the target analytes each method is associated with, with in situ methods being more favourable for macromolecular targets such as bacteria, cells, and proteins. Whereas receptor particle deposition is more frequently associated with small molecules.

In terms of future prospects for the receptor deposition field, the most valuable advancements will be the ones that enable the scaling, increased reproducibility, and eventual commercialization of synthetic receptors. Of the approaches mentioned currently, electrodeposition and surface grafting offer the highest theoretical scalability, though each has its associated challenges that must be overcome. To date, there are no studies conducted on scaling these technologies with the vast majority of current research aimed at developing sensor toward novel analytes rather than focusing on this issue. This is not to say that researchers are not investigating potential applications of their sensors, but instead use applications to justify analyte selection rather than progressing the field towards more consistent and reliable sensor construction. It can therefore be imagined that the deposition of receptors will become a more crucial factor in the future, with this being a vital stepping-stone for the advancement of the MIP field in general and MIP based sensor technology in particular.

References Chapter 5

1. Polyakov, M. V; Kuleshina, L.; Neimark, I. On the Dependence of Silica Gel Adsorption Properties on the Character of Its Porosity. *Zhurnal Fizieskoj Khimii* 1937, 10, 100–112.
2. Mudd, S. A Hypothetical Mechanism of Antibody Formation. *J. Immunol.* 1932, 23, 423–427.
3. Andersson, L.; Sellergren, B.; Mosbach, K. Imprinting of Amino Acid Derivatives in Macroporous Polymers. *Tetrahedron Lett.* 1984, 25, 5211–5214, doi:10.1016/s0040-4039(01)81566-5.
4. Wulff, G.; Oberkobusch, D.; Minárik, M. Enzyme-Analogue Built Polymers, 18 Chiral Cavities in Polymer Layers Coated on Wide-Pore Silica. *React. Polym. Ion Exch. Sorbents* 1985, 3, 261–275, doi:10.1016/0167-6989(85)90017-0.
5. BelBruno, J.J. Molecularly Imprinted Polymers. *Chem. Rev.* 2019, 119, 94–119, doi:10.1021/acs.chemrev.8b00171.
6. Mahony, J.O.; Nolan, K.; Smyth, M.R.; Mizaikoff, B. Molecularly Imprinted Polymers—Potential and Challenges in Analytical Chemistry. *Anal. Chim. Acta* 2005, 534, 31–39, doi:10.1016/j.aca.2004.07.043.
7. Arreguin-Campos, R.; Eersels, K.; Lowdon, J.W.; Rogosic, R.; Heidt, B.; Caldara, M.; Jiménez-Monroy, K.L.; Diliën, H.; Cleij, T.J.; van Grinsven, B. Biomimetic Sensing of Escherichia Coli at the Solid-Liquid Interface: From Surface-Imprinted Polymer Synthesis toward Real Sample Sensing in Food Safety. *Microchem. J.* 2021, 169, 106554, doi:10.1016/j.microc.2021.106554.
8. Ansari, S.; Masoum, S. Molecularly Imprinted Polymers for Capturing and Sensing Proteins: Current Progress and Future Implications. *TrAC Trends Anal. Chem.* 2019, 114, 29–47, doi:10.1016/j.trac.2019.02.008.
9. Dabrowski, M.; Sharma, P.S.; Iskierko, Z.; Noworyta, K.; Cieplak, M.; Lisowski, W.; Oborska, S.; Kuhn, A.; Kutner, W. Early Diagnosis of Fungal Infections Using Piezomicrogravimetric and Electric Chemosensors Based on Polymers Molecularly Imprinted with D-Arabitol. *Biosens. Bioelectron.* 2016, 79, 627–635, doi:10.1016/j.bios.2015.12.088.
10. Mayes, A.G.; Mosbach, K. Molecularly Imprinted Polymer Beads: Suspension Polymerization Using a Liquid Perfluorocarbon as the Dispersing Phase. *Anal. Chem.* 1996, 68, 3769–3774, doi:10.1021/ac960363a.
11. Panasyuk, T.L.; Mirsky, V.M.; Piletsky, S.A.; Wolfbeis, O.S. Electropolymerized Molecularly Imprinted Polymers as Receptor Layers in Capacitive Chemical Sensors. *Anal. Chem.* 1999, 71, 4609–4613, doi:10.1021/ac9903196.
12. Medina Rangel, P.X.; Laclef, S.; Xu, J.; Panagiotopoulou, M.; Kovensky, J.; Tse Sum Bui, B.; Haupt, K. Solid-Phase Synthesis of Molecularly Imprinted Polymer Nanolabels: Affinity Tools for Cellular Bioimaging of Glycans. *Sci. Rep.* 2019, 9, 3923, doi:10.1038/s41598-019-40348-5.
13. Cormack, P.A.; Elorza, A.Z. Molecularly Imprinted Polymers: Synthesis and Characterisation. *J. Chromatogr. B* 2004, 804, 173–182, doi:10.1016/j.jchromb.2004.02.013.

14. Li, X.; He, Y.; Zhao, F.; Zhang, W.; Ye, Z. Molecularly Imprinted Polymer-Based Sensors for Atrazine Detection by Electropolymerization of o-Phenylenediamine. *RSC Adv.* 2015, 5, 56534–56540, doi:10.1039/c5ra09556e.
15. Poma, A.; Guerreiro, A.; Whitcombe, M.J.; Piletska, E. V.; Turner, A.P.F.; Piletsky, S.A. Solid-Phase Synthesis of Molecularly Imprinted Polymer Nanoparticles with a Reusable Template—“Plastic Antibodies.” *Adv. Funct. Mater.* 2013, 23, 2821–2827, doi:10.1002/adfm.201202397.
16. Lowdon, J.W.; Diliën, H.; van Grinsven, B.; Eersels, K.; Cleij, T.J. Colorimetric Sensing of Amoxicillin Facilitated by Molecularly Imprinted Polymers. *Polymers (Basel)*. 2021, 13, doi:10.3390/polym13132221.
17. Lu, Y.; Zhu, Y.; Zhang, Y.; Wang, K. Synthesizing Vitamin E Molecularly Imprinted Polymers via Precipitation Polymerization. *J. Chem. Eng. Data* 2019, 64, 1045–1050, doi:10.1021/acs.jced.8b00944.
18. Liu, X.; Wu, F.; Au, C.; Tao, Q.; Pi, M.; Zhang, W. Synthesis of Molecularly Imprinted Polymer by Suspension Polymerization for Selective Extraction of p -Hydroxybenzoic Acid from Water. *J. Appl. Polym. Sci.* 2019, 136, 46984, doi:10.1002/app.46984.
19. Yan, H.; Row, K. Characteristic and Synthetic Approach of Molecularly Imprinted Polymer. *Int. J. Mol. Sci.* 2006, 7, 155–178, doi:10.3390/i7050155.
20. Caldara, M.; Lowdon, J.W.; Rogosic, R.; Arreguin-Campos, R.; Jimenez-Monroy, K.L.; Heidt, B.; Tschulik, K.; Cleij, T.J.; Diliën, H.; Eersels, K.; et al. Thermal Detection of Glucose in Urine Using a Molecularly Imprinted Polymer as a Recognition Element. *ACS Sensors* 2021, 6, 4515–4525, doi:10.1021/acssensors.1c02223.
21. Bedwell, T.S.; Whitcombe, M.J. Analytical Applications of MIPs in Diagnostic Assays:Future Perspectives. *Anal. Bioanal. Chem.* 2016, 408, 1735–1751, doi:10.1007/s00216-015-9137-9.
22. Canfarotta, F.; Poma, A.; Guerreiro, A.; Piletsky, S. Solid-Phase Synthesis of Molecularly Imprinted Nanoparticles. *Nat. Protoc.* 2016, 11, 443–455, doi:10.1038/nprot.2016.030.
23. Medina Rangel, P.X.; Laclef, S.; Xu, J.; Panagiotopoulou, M.; Kovensky, J.; Tse Sum Bui, B.; Haupt, K. Solid-Phase Synthesis of Molecularly Imprinted Polymer Nanolabels: Affinity Tools for Cellular Bioimaging of Glycans. *Sci. Rep.* 2019, 9, 3923, doi:10.1038/s41598-019-40348-5.
24. He, S.; Zhang, L.; Bai, S.; Yang, H.; Cui, Z.; Zhang, X.; Li, Y. Advances of Molecularly Imprinted Polymers (MIP) and the Application in Drug Delivery. *Eur. Polym. J.* 2021, 143, 110179, doi:10.1016/j.eurpolymj.2020.110179.
25. Hand, R.A.; Piletska, E.; Bassindale, T.; Morgan, G.; Turner, N. Application of Molecularly Imprinted Polymers in the Anti-Doping Field: Sample Purification and Compound Analysis. *Analyst* 2020, 145, 4716–4736, doi:10.1039/D0AN00682C.
26. Pichon, V.; Chapuis-Hugon, F. Role of Molecularly Imprinted Polymers for Selective Determination of Environmental Pollutants—A Review. *Anal. Chim. Acta* 2008, 622, 48–61, doi:10.1016/j.aca.2008.05.057.

27. Arreguin-Campos, R.; Jiménez-Monroy, K.L.; Diliën, H.; Cleij, T.J.; van Grinsven, B.; Eersels, K. Imprinted Polymers as Synthetic Receptors in Sensors for Food Safety. *Biosensors* 2021, 11, 46, doi:10.3390/bios11020046.
28. Suryanarayanan, V.; Wu, C.-T.; Ho, K.-C. Molecularly Imprinted Electrochemical Sensors. *Electroanalysis* 2010, 22, 1795–1811, doi:10.1002/elan.200900616.
29. Ahmad, O.S.; Bedwell, T.S.; Esen, C.; Garcia-Cruz, A.; Piletsky, S.A. Molecularly Imprinted Polymers in Electrochemical and Optical Sensors. *Trends Biotechnol.* 2019, 37, 294–309, doi:10.1016/j.tibtech.2018.08.009.
30. Ávila, M.; Zougagh, M.; Ríos, Á.; Escarpa, A. Molecularly Imprinted Polymers for Selective Piezoelectric Sensing of Small Molecules. *TrAC Trends Anal. Chem.* 2008, 27, 54–65, doi:10.1016/j.trac.2007.10.009.
31. Geerets, B.; Peeters, M.; Grinsven, B.; Bers, K.; de Ceuninck, W.; Wagner, P. Optimizing the Thermal Read-Out Technique for MIP-Based Biomimetic Sensors: Towards Nanomolar Detection Limits. *Sensors* 2013, 13, 9148–9159, doi:10.3390/s130709148.
32. Latif, U.; Ping, L.; Dickert, F. Conductometric Sensor for PAH Detection with Molecularly Imprinted Polymer as Recognition Layer. *Sensors* 2018, 18, 767, doi:10.3390/s18030767.
33. Piletsky, S.S.; Garcia Cruz, A.; Piletska, E.; Piletsky, S.A.; Aboagye, E.O.; Spivey, A.C. Iodo Silanes as Superior Substrates for the Solid Phase Synthesis of Molecularly Imprinted Polymer Nanoparticles. *Polymers (Basel)*. 2022, 14, 1595, doi:10.3390/polym14081595.
34. Tadd, E.; Zeno, A.; Zubris, M.; Dan, N.; Tannenbaum, R. Adsorption and Polymer Film Formation on Metal Nanoclusters. *Macromolecules* 2003, 36, 6497–6502, doi:10.1021/ma034207z.
35. Crapnell, R.; Hudson, A.; Foster, C.; Eersels, K.; Grinsven, B.; Cleij, T.; Banks, C.; Peeters, M. Recent Advances in Electrosynthesized Molecularly Imprinted Polymer Sensing Platforms for Bioanalyte Detection. *Sensors* 2019, 19, 1204, doi:10.3390/s19051204.
36. Mathieu-Scheers, E.; Bouden, S.; Grillot, C.; Nicolle, J.; Warmont, F.; Bertagna, V.; Cagnon, B.; Vautrin-UI, C. Trace Anthracene Electrochemical Detection Based on Electropolymerized-Molecularly Imprinted Polypyrrole Modified Glassy Carbon Electrode. *J. Electroanal. Chem.* 2019, 848, 113253, doi:10.1016/j.jelechem.2019.113253.
37. Stöckle, B.; Ng, D.Y.W.; Meier, C.; Paust, T.; Bischoff, F.; Diemant, T.; Behm, R.J.; Gottschalk, K.-E.; Ziener, U.; Weil, T. Precise Control of Polydopamine Film Formation by Electropolymerization. *Macromol. Symp.* 2014, 346, 73–81, doi:10.1002/masy.201400130.
38. Piletsky, S.A.; Alcock, S.; Turner, A.P.. Molecular Imprinting: At the Edge of the Third Millennium. *Trends Biotechnol.* 2001, 19, 9–12, doi:10.1016/s0167-7799(00)01523-7.
39. Ramanavicius, S.; Jagminas, A.; Ramanavicius, A. Advances in Molecularly Imprinted Polymers Based Affinity Sensors (Review). *Polymers (Basel)*. 2021, 13, 974, doi:10.3390/polym13060974.

40. Zheng, M.-M.; Gong, R.; Zhao, X.; Feng, Y.-Q. Selective Sample Pretreatment by Molecularly Imprinted Polymer Monolith for the Analysis of Fluoroquinolones from Milk Samples. *J. Chromatogr. A* 2010, 1217, 2075–2081, doi:10.1016/j.chroma.2010.02.011.
41. Alizadeh, T.; Azizi, S. Graphene/Graphite Paste Electrode Incorporated with Molecularly Imprinted Polymer Nanoparticles as a Novel Sensor for Differential Pulse Voltammetry Determination of Fluoxetine. *Biosens. Bioelectron.* 2016, 81, 198–206, doi:10.1016/j.bios.2016.02.052.
42. Sadeghi, S.; Motaharian, A. Voltammetric Sensor Based on Carbon Paste Electrode Modified with Molecular Imprinted Polymer for Determination of Sulfadiazine in Milk and Human Serum. *Mater. Sci. Eng. C* 2013, 33, 4884–4891, doi:10.1016/j.msec.2013.08.001.
43. Yang, W.; Ma, Y.; Sun, H.; Huang, C.; Shen, X. Molecularly Imprinted Polymers Based Optical Fiber Sensors: A Review. *TrAC Trends Anal. Chem.* 2022, 152, 116608, doi:10.1016/j.trac.2022.116608.
44. Yu, J.; Wang, X.; Kang, Q.; Li, J.; Shen, D.; Chen, L. One-Pot Synthesis of a Quantum Dot-Based Molecular Imprinting Nanosensor for Highly Selective and Sensitive Fluorescence Detection of 4-Nitrophenol in Environmental Waters. *Environ. Sci. Nano* 2017, 4, 493–502, doi:10.1039/c6en00395h.
45. Yola, M.L.; Atar, N. Development of Molecular Imprinted Sensor Including Graphitic Carbon Nitride/N-Doped Carbon Dots Composite for Novel Recognition of Epinephrine. *Compos. Part B Eng.* 2019, 175, 107113, doi:10.1016/j.compositesb.2019.107113.
46. Sener, G.; Uzun, L.; Say, R.; Denizli, A. Use of Molecular Imprinted Nanoparticles as Biorecognition Element on Surface Plasmon Resonance Sensor. *Sensors Actuators B Chem.* 2011, 160, 791–799, doi:10.1016/j.snb.2011.08.064.
47. Akgönüllü, S.; Yavuz, H.; Denizli, A. SPR Nanosensor Based on Molecularly Imprinted Polymer Film with Gold Nanoparticles for Sensitive Detection of Aflatoxin B1. *Talanta* 2020, 219, 121219, doi:10.1016/j.talanta.2020.121219.
48. Karaseva, N.A.; Pluhar, B.; Beliaeva, E.A.; Ermolaeva, T.N.; Mizaikoff, B. Synthesis and Application of Molecularly Imprinted Polymers for Trypsin Piezoelectric Sensors. *Sensors Actuators B Chem.* 2019, 280, 272–279, doi:10.1016/j.snb.2018.10.022.
49. Hussain, M.; Kotova, K.; Lieberzeit, P. Molecularly Imprinted Polymer Nanoparticles for Formaldehyde Sensing with QCM. *Sensors* 2016, 16, 1011, doi:10.3390/s16071011.
50. Phan, N.; Sussitz, H.; Lieberzeit, P. Polymerization Parameters Influencing the QCM Response Characteristics of BSA MIP. *Biosensors* 2014, 4, 161–171, doi:10.3390/bios4020161.
51. Spieker, E.; Lieberzeit, P.A. Molecular Imprinting Studies for Developing QCM-Sensors for *Bacillus Cereus*. *Procedia Eng.* 2016, 168, 561–564, doi:10.1016/j.proeng.2016.11.525.
52. Blanco-López, M.C.; Gutiérrez-Fernández, S.; Lobo-Castañón, M.J.; Miranda-Ordieres, A.J.; Tuñón-Blanco, P. Electrochemical Sensing with Electrodes Modified with Molecularly Imprinted Polymer Films. *Anal. Bioanal. Chem.* 2004, 378, 1922–1928, doi:10.1007/s00216-003-2330-2.

53. Piletsky, S.A.; Turner, N.W.; Laitenberger, P. Molecularly Imprinted Polymers in Clinical Diagnostics—Future Potential and Existing Problems. *Med. Eng. Phys.* 2006, 28, 971–977, doi:10.1016/j.medengphy.2006.05.004.
54. Sellergren, B.; Allender, C. Molecularly Imprinted Polymers: A Bridge to Advanced Drug Delivery. *Adv. Drug Deliv. Rev.* 2005, 57, 1733–1741, doi:10.1016/j.addr.2005.07.010.
55. Lowdon, J.W.; Diliën, H.; Singla, P.; Peeters, M.; Cleij, T.J.; van Grinsven, B.; Eersels, K. MIPs for Commercial Application in Low-Cost Sensors and Assays – An Overview of the Current Status Quo. *Sensors Actuators B Chem.* 2020, 325, 128973, doi:10.1016/j.snb.2020.128973.
56. Xia, Y.; Whitesides, G.M. Soft Lithography. *Angew. Chemie Int. Ed.* 1998, 37, 550–575, doi:10.1002/(SICI)1521-3773(19980316)37:5<550::AID-ANIE550>3.0.CO;2-G.
57. Cui, F.; Zhou, Z.; Zhou, H.S. Molecularly Imprinted Polymers and Surface Imprinted Polymers Based Electrochemical Biosensor for Infectious Diseases. *Sensors* 2020, 20, 996, doi:10.3390/s20040996.
58. Aherne, A.; Alexander, C.; Payne, M.J.; Perez, N.; Vulfson, E.N. Bacteria-Mediated Lithography of Polymer Surfaces. *J. Am. Chem. Soc.* 1996, 118, 8771–8772, doi:10.1021/ja960123c.
59. Alexander, C.; Vulfson, E.N. Spatially Functionalized Polymer Surfaces Produced via Cell-Mediated Lithography. *Adv. Mater.* 1997, 9, 751–755, doi:10.1002/adma.19970090916.
60. Ren, K.; Zare, R.N. Chemical Recognition in Cell-Imprinted Polymers. *ACS Nano* 2012, 6, 4314–4318, doi:10.1021/nn300901z.
61. Karthik, A.; Margulis, K.; Ren, K.; Zare, R.N.; Leung, L.W. Rapid and Selective Detection of Viruses Using Virus-Imprinted Polymer Films. *Nanoscale* 2015, 7, 18998–19003, doi:10.1039/c5nr06114h.
62. Ren, K.; Banaei, N.; Zare, R.N. Sorting Inactivated Cells Using Cell-Imprinted Polymer Thin Films. *ACS Nano* 2013, 7, 6031–6036, doi:10.1021/nn401768s.
63. Schirhagl, R.; Hall, E.W.; Fuereder, I.; Zare, R.N. Separation of Bacteria with Imprinted Polymeric Films. *Analyst* 2012, 137, 1495, doi:10.1039/c2an15927a.
64. Werner, M.; Glück, M.S.; Bräuer, B.; Bismarck, A.; Lieberzeit, P.A. Investigations on Sub-Structures within Cavities of Surface Imprinted Polymers Using AFM and PF-QNM. *Soft Matter* 2022, 18, 2245–2251, doi:10.1039/D2SM00137C.
65. Cornelis, P.; Givanoudi, S.; Yongabi, D.; Iken, H.; Duwé, S.; Deschaume, O.; Robbens, J.; Dedecker, P.; Bartic, C.; Wübbenhorst, M.; et al. Sensitive and Specific Detection of E. Coli Using Biomimetic Receptors in Combination with a Modified Heat-Transfer Method. *Biosens. Bioelectron.* 2019, 136, 97–105, doi:10.1016/j.bios.2019.04.026.
66. Bräuer, B.; Werner, M.; Baurecht, D.; Lieberzeit, P.A. Raman and Scanning Probe Microscopy for Differentiating Surface Imprints of E. Coli and B. Cereus. *J. Mater. Chem. B* 2022, 10, 6758–6767, doi:10.1039/D2TB00283C.

67. Bräuer, B.; Thier, F.; Bittermann, M.; Baurecht, D.; Lieberzeit, P.A. Raman Studies on Surface-Imprinted Polymers to Distinguish the Polymer Surface, Imprints, and Different Bacteria. *ACS Appl. Bio Mater.* 2022, 5, 160–171, doi:10.1021/acsabm.1c01020.
68. Givanoudi, S.; Cornelis, P.; Rasschaert, G.; Wackers, G.; Iken, H.; Rolka, D.; Yongabi, D.; Robbens, J.; Schöning, M.J.; Heyndrickx, M.; et al. Selective *Campylobacter* Detection and Quantification in Poultry: A Sensor Tool for Detecting the Cause of a Common Zoonosis at Its Source. *Sensors Actuators B Chem.* 2021, 332, 129484, doi:10.1016/j.snb.2021.129484.
69. Stilman, W.; Campolim Lenzi, M.; Wackers, G.; Deschaume, O.; Yongabi, D.; Mathijssen, G.; Bartic, C.; Gruber, J.; Wübbenhorst, M.; Heyndrickx, M.; et al. Low Cost, Sensitive Impedance Detection of *E. Coli* Bacteria in Food-Matrix Samples Using Surface-Imprinted Polymers as Whole-Cell Receptors. *Phys. status solidi* 2021, 2100405, doi:10.1002/pssa.202100405.
70. Latif, U.; Qian, J.; Can, S.; Dickert, F. Biomimetic Receptors for Bioanalyte Detection by Quartz Crystal Microbalances — From Molecules to Cells. *Sensors* 2014, 14, 23419–23438, doi:10.3390/s141223419.
71. van Grinsven, B.; Eersels, K.; Akkermans, O.; Ellermann, S.; Kordek, A.; Peeters, M.; Deschaume, O.; Bartic, C.; Diliën, H.; Steen Redeker, E.; et al. Label-Free Detection of *Escherichia Coli* Based on Thermal Transport through Surface Imprinted Polymers. *ACS Sensors* 2016, 1, 1140–1147, doi:10.1021/acssensors.6b00435.
72. Wangchareansak, T.; Thitithanyanont, A.; Chuakheaw, D.; Gleeson, M.P.; Lieberzeit, P.A.; Sangma, C. Influenza A Virus Molecularly Imprinted Polymers and Their Application in Virus Sub-Type Classification. *J. Mater. Chem. B* 2013, 1, 2190, doi:10.1039/c3tb00027c.
73. Birnbaumer, G.M.; Lieberzeit, P.A.; Richter, L.; Schirhagl, R.; Milnera, M.; Dickert, F.L.; Bailey, A.; Ertl, P. Detection of Viruses with Molecularly Imprinted Polymers Integrated on a Microfluidic Biochip Using Contact-Less Dielectric Microsensors. *Lab Chip* 2009, 9, 3549, doi:10.1039/b914738a.
74. Stilman, W.; Yongabi, D.; Bakhshi Sichani, S.; Thesseling, F.; Deschaume, O.; Putzeys, T.; Pinto, T.C.; Verstreppe, K.; Bartic, C.; Wübbenhorst, M.; et al. Detection of Yeast Strains by Combining Surface-Imprinted Polymers with Impedance-Based Readout. *Sensors Actuators B Chem.* 2021, 340, 129917, doi:10.1016/j.snb.2021.129917.
75. Zhou, D.; Guo, T.; Yang, Y.; Zhang, Z. Surface Imprinted Macroporous Film for High Performance Protein Recognition in Combination with Quartz Crystal Microbalance. *Sensors Actuators, B Chem.* 2011, 153, 96–102, doi:10.1016/j.snb.2010.10.012.
76. Arreguin-Campos, R.; Eersels, K.; Rogosic, R.; Cleij, T.J.; Diliën, H.; van Grinsven, B. Imprinted Polydimethylsiloxane-Graphene Oxide Composite Receptor for the Biomimetic Thermal Sensing of *Escherichia Coli*. *ACS Sensors* 2022, 7, 1467–1475, doi:10.1021/acssensors.2c00215.
77. Peeters, M.; Csipai, P.; Geerets, B.; Weustenraed, A.; Van Grinsven, B.; Thoelen, R.; Gruber, J.; De Ceuninck, W.; Cleij, T.J.; Troost, F.J.; et al. Heat-Transfer-Based Detection of l-Nicotine, Histamine, and Serotonin Using Molecularly Imprinted Polymers as Biomimetic Receptors. *Anal. Bioanal. Chem.* 2013, 405, 6453–6460, doi:10.1007/s00216-013-7024-9.

78. Vandenryt, T.; Van Grinsven, B.; Eersels, K.; Cornelis, P.; Kholwadia, S.; Cleij, T.J.; Thoelen, R.; De Ceuninck, W.; Peeters, M.; Wagner, P. Single-Shot Detection of Neurotransmitters in Whole-Blood Samples by Means of the Heat-Transfer Method in Combination with Synthetic Receptors. *Sensors (Switzerland)* 2017, 17, doi:10.3390/s17122701.
79. Caldara, M.; Lowdon, J.W.; Royakkers, J.; Peeters, M.; Cleij, T.J.; Diliën, H.; Eersels, K.; van Grinsven, B. A Molecularly Imprinted Polymer-Based Thermal Sensor for the Selective Detection of Melamine in Milk Samples. *Foods* 2022, 11, 2906, doi:10.3390/foods11182906.
80. Bongaers, E.; Alenus, J.; Horemans, F.; Weustenraed, A.; Lutsen, L.; Vanderzande, D.; Cleij, T.J.; Troost, F.J.; Brummer, R.-J.; Wagner, P. A MIP-Based Biomimetic Sensor for the Impedimetric Detection of Histamine in Different PH Environments. *Phys. status solidi* 2010, 207, 837–843, doi:10.1002/pssa.200983307.
81. Horemans, F.; Alenus, J.; Bongaers, E.; Weustenraed, A.; Thoelen, R.; Duchateau, J.; Lutsen, L.; Vanderzande, D.; Wagner, P.; Cleij, T.J. MIP-Based Sensor Platforms for the Detection of Histamine in the Nano- and Micromolar Range in Aqueous Media. *Sensors Actuators B Chem.* 2010, 148, 392–398, doi:10.1016/j.snb.2010.05.003.
82. Peeters, M.; Troost, F.J.; van Grinsven, B.; Horemans, F.; Alenus, J.; Murib, M.S.; Keszthelyi, D.; Ethirajan, A.; Thoelen, R.; Cleij, T.J.; et al. MIP-Based Biomimetic Sensor for the Electronic Detection of Serotonin in Human Blood Plasma. *Sensors Actuators B Chem.* 2012, 171–172, 602–610, doi:10.1016/j.snb.2012.05.040.
83. Venkatesh, S.; Yeung, C.-C.; Li, T.; Lau, S.C.; Sun, Q.-J.; Li, L.-Y.; Li, J.H.; Lam, M.H.W.; Roy, V.A.L. Portable Molecularly Imprinted Polymer-Based Platform for Detection of Histamine in Aqueous Solutions. *J. Hazard. Mater.* 2021, 410, 124609, doi:10.1016/j.jhazmat.2020.124609.
84. Seidler, K.; Polreichová, M.; Lieberzeit, P.; Dickert, F. Biomimetic Yeast Cell Typing—Application of QCMs. *Sensors* 2009, 9, 8146–8157, doi:10.3390/s91008146.
85. Das, A.A.K.; Medlock, J.; Liang, H.; Nees, D.; Allsup, D.J.; Madden, L.A.; Paunov, V.N. Bioimprint Aided Cell Recognition and Depletion of Human Leukemic HL60 Cells from Peripheral Blood. *J. Mater. Chem. B* 2019, 7, 3497–3504, doi:10.1039/C9TB00679F.
86. Güney, S.; Arslan, T.; Yanık, S.; Güney, O. An Electrochemical Sensing Platform Based on Graphene Oxide and Molecularly Imprinted Polymer Modified Electrode for Selective Detection of Amoxicillin. *Electroanalysis* 2021, 33, 46–56, doi:10.1002/elan.202060129.
87. Ma, X.-T.; He, X.-W.; Li, W.-Y.; Zhang, Y.-K. Epitope Molecularly Imprinted Polymer Coated Quartz Crystal Microbalance Sensor for the Determination of Human Serum Albumin. *Sensors Actuators B Chem.* 2017, 246, 879–886, doi:10.1016/j.snb.2017.02.137.
88. McClements, J.; Seumo Tchekwagep, P.M.; Vilela Strapazon, A.L.; Canfarotta, F.; Thomson, A.; Czulak, J.; Johnson, R.E.; Novakovic, K.; Losada-Pérez, P.; Zaman, A.; et al. Immobilization of Molecularly Imprinted Polymer Nanoparticles onto Surfaces Using Different Strategies: Evaluating the Influence of the Functionalized Interface on the Performance of a Thermal Assay for the Detection of the Cardiac

Biomarker Troponin I. *ACS Appl. Mater. Interfaces* 2021, 13, 27868–27879, doi:10.1021/acsami.1c05566.

89. Williams, R.J.; Crapnell, R.D.; Dempsey, N.C.; Peeters, M.; Banks, C.E. Nano-Molecularly Imprinted Polymers for Serum Creatinine Sensing Using the Heat Transfer Method. *Talanta Open* 2022, 5, 100087, doi:10.1016/j.talo.2022.100087.

90. Nguyen, M.T.T.; Giap, H. V.; Nguyen, S.N.; Nguyen, H.L.; Vu, A.H.T.; Nguyen, H.N.; Nguyen, D.T. Molecularly Imprinted Polymer-Coated Gold Nanorods Decorated on Spherical Polystyrene Periodic Array for Surface-Enhanced Raman Detection of Bisphenol A. *Thin Solid Films* 2022, 759, 139465, doi:10.1016/j.tsf.2022.139465.

91. Wadie, M.; Marzouk, H.M.; Rezk, M.R.; Abdel-Moety, E.M.; Tantawy, M.A. A Sensing Platform of Molecular Imprinted Polymer-Based Polyaniline/Carbon Paste Electrodes for Simultaneous Potentiometric Determination of Alfuzosin and Solifenacin in Binary Co-Formulation and Spiked Plasma. *Anal. Chim. Acta* 2022, 1200, 339599, doi:10.1016/j.aca.2022.339599.

92. Hassan, S.S.M.; Kamel, A.H.; Fathy, M.A. A Novel Screen-Printed Potentiometric Electrode with Carbon Nanotubes/Polyaniline Transducer and Molecularly Imprinted Polymer for the Determination of Nalbuphine in Pharmaceuticals and Biological Fluids. *Anal. Chim. Acta* 2022, 1227, 340239, doi:10.1016/j.aca.2022.340239.

93. Yang, Q.; Sun, Q.; Zhou, T.; Shi, G.; Jin, L. Determination of Parathion in Vegetables by Electrochemical Sensor Based on Molecularly Imprinted Polyethyleneimine/Silica Gel Films. *J. Agric. Food Chem.* 2009, 57, 6558–6563, doi:10.1021/jf901286e.

94. Kamel, A.H.; Amr, A.E.-G.E.; Abdalla, N.S.; El-Naggar, M.; Al-Omar, M.A.; Almhizia, A.A. Modified Screen-Printed Potentiometric Sensors Based on Man-Tailored Biomimetics for Diquat Herbicide Determination. *Int. J. Environ. Res. Public Health* 2020, 17, 1138, doi:10.3390/ijerph17041138.

95. Abd-Rabboh, H.S.M.; E. Amr, A.E.-G.; Almhizia, A.A.; Naglah, A.M.; H. Kamel, A. New Potentiometric Screen-Printed Platforms Modified with Reduced Graphene Oxide and Based on Man-Made Imprinted Receptors for Caffeine Assessment. *Polymers (Basel)*. 2022, 14, 1942, doi:10.3390/polym14101942.

96. Khosrokhavar, R.; Motaharian, A.; Milani Hosseini, M.R.; Mohammadsadegh, S. Screen-Printed Carbon Electrode (SPCE) Modified by Molecularly Imprinted Polymer (MIP) Nanoparticles and Graphene Nanosheets for Determination of Sertraline Antidepressant Drug. *Microchem. J.* 2020, 159, 105348, doi:10.1016/j.microc.2020.105348.

97. Jamieson, O.; Soares, T.C.C.; de Faria, B.A.; Hudson, A.; Mecozzi, F.; Rowley-Neale, S.J.; Banks, C.E.; Gruber, J.; Novakovic, K.; Peeters, M.; et al. Screen Printed Electrode Based Detection Systems for the Antibiotic Amoxicillin in Aqueous Samples Utilising Molecularly Imprinted Polymers as Synthetic Receptors. *Chemosensors* 2019, 8, 5, doi:10.3390/chemosensors8010005.

98. Kröger, S.; Turner, A.P.F.; Mosbach, K.; Haupt, K. Imprinted Polymer-Based Sensor System for Herbicides Using Differential-Pulse Voltammetry on Screen-Printed Electrodes. *Anal. Chem.* 1999, 71, 3698–3702, doi:10.1021/ac9811827.

99. Yang, C.; Ji, X.-F.; Cao, W.-Q.; Wang, J.; Zhang, Q.; Zhong, T.-L.; Wang, Y. Molecularly Imprinted Polymer Based Sensor Directly Responsive to Attomole Bovine Serum Albumin. *Talanta* 2019, 196, 402–407, doi:10.1016/j.talanta.2018.12.097.
100. Cennamo, N.; Arcadio, F.; Zeni, L.; Alberti, G.; Pesavento, M. Optical-Chemical Sensors Based on Plasmonic Phenomena Modulated via Micro-Holes in Plastic Optical Fibers Filled by Molecularly Imprinted Polymers. *Sensors Actuators B Chem.* 2022, 372, 132672, doi:10.1016/j.snb.2022.132672.
101. Smolinska-Kempisty, K.; Ahmad, O.S.; Guerreiro, A.; Karim, K.; Piletska, E.; Piletsky, S. New Potentiometric Sensor Based on Molecularly Imprinted Nanoparticles for Cocaine Detection. *Biosens. Bioelectron.* 2017, 96, 49–54, doi:10.1016/j.bios.2017.04.034.
102. Herrera-Chacon, A.; Gonzalez-Calabuig, A.; del Valle, M. Dummy Molecularly Imprinted Polymers Using DNP as a Template Molecule for Explosive Sensing and Nitroaromatic Compound Discrimination. *Chemosensors* 2021, 9, 255, doi:10.3390/chemosensors9090255.
103. Kriz, D.; Mosbach, K. Competitive Amperometric Morphine Sensor Based on an Agarose Immobilised Molecularly Imprinted Polymer. *Anal. Chim. Acta* 1995, 300, 71–75, doi:10.1016/0003-2670(94)00368-V.
104. Canfarotta, F.; Czulak, J.; Betlem, K.; Sachdeva, A.; Eersels, K.; Van Grinsven, B.; Cleij, T.J.; Peeters, M. A Novel Thermal Detection Method Based on Molecularly Imprinted Nanoparticles as Recognition Elements †. *Nanoscale* 2018, 10, 2081, doi:10.1039/c7nr07785h.
105. Crapnell, R.D.; Canfarotta, F.; Czulak, J.; Johnson, R.; Betlem, K.; Mecozzi, F.; Down, M.P.; Eersels, K.; Van Grinsven, B.; Cleij, T.J.; et al. Thermal Detection of Cardiac Biomarkers Heart-Fatty Acid Binding Protein and ST2 Using a Molecularly Imprinted Nanoparticle-Based Multiplex Sensor Platform. *ACS Sensors* 2019, 4, 2838–2845, doi:10.1021/acssensors.9b01666
106. Mostafiz, B.; Bigdeli, S.A.; Banan, K.; Afsharara, H.; Hatamabadi, D.; Mousavi, P.; Hussain, C.M.; Keçili, R.; Ghorbani-Bidkorbeh, F. Molecularly Imprinted Polymer-Carbon Paste Electrode (MIP-CPE)-Based Sensors for the Sensitive Detection of Organic and Inorganic Environmental Pollutants: A Review. *Trends Environ. Anal. Chem.* 2021, 32, e00144, doi:10.1016/j.teac.2021.e00144.
107. Gholivand, M.B.; Torkashvand, M.; Malekzadeh, G. Fabrication of an Electrochemical Sensor Based on Computationally Designed Molecularly Imprinted Polymers for Determination of Cyanazine in Food Samples. *Anal. Chim. Acta* 2012, 713, 36–44, doi:10.1016/j.aca.2011.11.001.
108. Wong, A.; Foguel, M.V.; Khan, S.; Oliveira, F.M. de; Tarley, C.R.T.; Sotomayor, M.D.P.T. Development of an electrochemical sensor modified with MWCNT-COOH and MIP for detection of diuron. *Electrochim. Acta* 2015, 182, 122–130, doi:10.1016/j.electacta.2015.09.054.
109. Alizadeh, T.; Zare, M.; Ganjali, M.R.; Norouzi, P.; Tavana, B. A New Molecularly Imprinted Polymer (MIP)-Based Electrochemical Sensor for Monitoring 2,4,6-Trinitrotoluene (TNT) in Natural Waters and Soil Samples. *Biosens. Bioelectron.* 2010, 25, 1166–1172, doi:10.1016/j.bios.2009.10.003.
110. Monireh Khadem; Faridbod, F.; Norouzi, P.; Foroushani, A.R.; Ganjali, M.R.; Yarahmadi, R.; Shahtaheri, S.J. Voltammetric Determination of Carbofuran Pesticide in Biological and Environmental

Samples Using a Molecularly Imprinted Polymer Sensor, a Multivariate Optimization. *J. Anal. Chem.* 2020, 75, 669–678, doi:10.1134/s1061934820050068.

111. Ghorbani, A.; Ganjali, M.R.; Ojani, R.; Raouf, J. Detection of Chloridazon in Aqueous Matrices Using a Nano-Sized Chloridazon-Imprinted Polymer-Based Voltammetric Sensor. *Int. J. Electrochem. Sci.* 2020, 15, 2913–2922, doi:10.20964/2020.04.17.

112. Hu, L.; Zhou, T.; Feng, J.; Jin, H.; Tao, Y.; Luo, D.; Mei, S.; Lee, Y.-I. A Rapid and Sensitive Molecularly Imprinted Electrochemiluminescence Sensor for Azithromycin Determination in Biological Samples. *J. Electroanal. Chem.* 2018, 813, 1–8, doi:10.1016/j.jelechem.2018.02.010.

113. Nontawong, N.; Amatatongchai, M.; Jarujamrus, P.; Nacapricha, D.; Lieberzeit, P.A. Novel Dual-Sensor for Creatinine and 8-Hydroxy-2'-Deoxyguanosine Using Carbon-Paste Electrode Modified with Molecularly Imprinted Polymers and Multiple-Pulse Amperometry. *Sensors Actuators B Chem.* 2021, 334, 129636, doi:10.1016/j.snb.2021.129636.

114. Sheydaei, O.; Khajehsharifi, H.; Rajabi, H.R. Rapid and Selective Diagnose of Sarcosine in Urine Samples as Prostate Cancer Biomarker by Mesoporous Imprinted Polymeric Nanobeads Modified Electrode. *Sensors Actuators B Chem.* 2020, 309, 127559, doi:10.1016/j.snb.2019.127559.

115. Gholivand, M.B.; Karimian, N.; Malekzadeh, G. Computational Design and Synthesis of a High Selective Molecularly Imprinted Polymer for Voltammetric Sensing of Propazine in Food Samples. *Talanta* 2012, 89, 513–520, doi:10.1016/j.talanta.2012.01.001.

116. Toro, M.J.U.; Marestoni, L.D.; Sotomayor, M.D.P.T. A New Biomimetic Sensor Based on Molecularly Imprinted Polymers for Highly Sensitive and Selective Determination of Hexazinone Herbicide. *Sensors Actuators B Chem.* 2015, 208, 299–306, doi:10.1016/j.snb.2014.11.036.

117. Motaharian, A.; Motaharian, F.; Abnous, K.; Hosseini, M.R.M.; Hassanzadeh-Khayyat, M. Molecularly Imprinted Polymer Nanoparticles-Based Electrochemical Sensor for Determination of Diazinon Pesticide in Well Water and Apple Fruit Samples. *Anal. Bioanal. Chem.* 2016, 408, 6769–6779, doi:10.1007/s00216-016-9802-7.

118. Li, Y.; Liu, J.; Zhang, Y.; Gu, M.; Wang, D.; Dang, Y.; Ye, B.-C.; Li, Y. A Robust Electrochemical Sensing Platform Using Carbon Paste Electrode Modified with Molecularly Imprinted Microsphere and Its Application on Methyl Parathion Detection. *Biosens. Bioelectron.* 2018, 106, 71–77, doi:10.1016/j.bios.2018.01.057.

119. Arvand, M.; Fallahi, P. Voltammetric Determination of Rivastigmine in Pharmaceutical and Biological Samples Using Molecularly Imprinted Polymer Modified Carbon Paste Electrode. *Sensors Actuators B Chem.* 2013, 188, 797–805, doi:10.1016/j.snb.2013.07.092.

120. Goud, K.Y.; M, S.; Reddy, K.K.; Gobi, K.V. Development of Highly Selective Electrochemical Impedance Sensor for Detection of Sub-Micromolar Concentrations of 5-Chloro-2,4-Dinitrotoluene. *J. Chem. Sci.* 2016, 128, 763–770, doi:10.1007/s12039-016-1078-0.

121. Peeters, M.; van Grinsven, B.; Foster, C.; Cleij, T.; Banks, C. Introducing Thermal Wave Transport Analysis (TWTA): A Thermal Technique for Dopamine Detection by Screen-Printed Electrodes

Functionalized with Molecularly Imprinted Polymer (MIP) Particles. *Molecules* 2016, 21, 552, doi:10.3390/molecules21050552.

122. Betlem, K.; Mahmood, I.; Seixas, R.D.; Sadiki, I.; Raimbault, R.L.D.; Foster, C.W.; Crapnell, R.D.; Tedesco, S.; Banks, C.E.; Gruber, J.; et al. Evaluating the Temperature Dependence of Heat-Transfer Based Detection: A Case Study with Caffeine and Molecularly Imprinted Polymers as Synthetic Receptors. *Chem. Eng. J.* 2019, 359, 505–517, doi:10.1016/j.cej.2018.11.114.

123. Ghanei-Motlagh, M.; Taher, M.A. Magnetic Silver(I) Ion-Imprinted Polymeric Nanoparticles on a Carbon Paste Electrode for Voltammetric Determination of Silver(I). *Microchim. Acta* 2017, 184, 1691–1699, doi:10.1007/s00604-017-2157-8.

124. Alizadeh, T.; Ganjali, M.R.; Akhoundian, M.; Norouzi, P. Voltammetric Determination of Ultratrace Levels of Cerium(III) Using a Carbon Paste Electrode Modified with Nano-Sized Cerium-Imprinted Polymer and Multiwalled Carbon Nanotubes. *Microchim. Acta* 2016, 183, 1123–1130, doi:10.1007/s00604-015-1702-6.

125. Alizadeh, T.; Mirzaee, S.; Rafiei, F. All-Solid-State Cr(III)-Selective Potentiometric Sensor Based on Cr(III)-Imprinted Polymer Nanomaterial/MWCNTs/Carbon Nanocomposite Electrode. *Int. J. Environ. Anal. Chem.* 2017, 97, 1283–1297, doi:10.1080/03067319.2017.1408804.

126. Elfadil, D.; Lamaoui, A.; Della Pelle, F.; Amine, A.; Compagnone, D. Molecularly Imprinted Polymers Combined with Electrochemical Sensors for Food Contaminants Analysis. *Molecules* 2021, 26, 4607, doi:10.3390/molecules26154607.

127. Li, C.; Iqbal, M.; Lin, J.; Luo, X.; Jiang, B.; Malgras, V.; Wu, K.C.-W.; Kim, J.; Yamauchi, Y. Electrochemical Deposition: An Advanced Approach for Templated Synthesis of Nanoporous Metal Architectures. *Acc. Chem. Res.* 2018, 51, 1764–1773, doi:10.1021/acs.accounts.8b00119.

128. Moreira Gonçalves, L. Electropolymerized Molecularly Imprinted Polymers: Perceptions Based on Recent Literature for Soon-to-Be World-Class Scientists. *Curr. Opin. Electrochem.* 2021, 25, 100640, doi:10.1016/j.coelec.2020.09.007.

129. Ozcelikay, G.; Kurbanoglu, S.; Zhang, X.; Kosak Soz, C.; Wollenberger, U.; Ozkan, S.A.; Yarman, A.; Scheller, F.W. Electrochemical MIP Sensor for Butyrylcholinesterase. *Polymers (Basel)*. 2019, 11, 1970, doi:10.3390/polym11121970.

130. Peng, L.; Yarman, A.; Jetzschmann, K.J.; Jeoung, J.H.; Schad, D.; Dobbek, H.; Wollenberger, U.; Scheller, F.W. Molecularly Imprinted Electropolymer for a Hexameric Heme Protein with Direct Electron Transfer and Peroxide Electrocatalysis. *Sensors (Switzerland)* 2016, 16, 272, doi:10.3390/s16030272.

131. Losito, I.; Palmisano, F.; Zambonin, P.G. O -Phenylenediamine Electropolymerization by Cyclic Voltammetry Combined with Electrospray Ionization-Ion Trap Mass Spectrometry. *Anal. Chem.* 2003, 75, 4988–4995, doi:10.1021/ac0342424.

132. Uang, Y.M.; Chou, T.C. Criteria for Designing a Polypyrrole Glucose Biosensor by Galvanostatic Electropolymerization. *Electroanalysis* 2002, 14, 1564–1570.

133. Komaba, S.; Seyama, M.; Momma, T.; Osaka, T. Potentiometric Biosensor for Urea Based on Electropolymerized Electroinactive Polypyrrole. *Electrochim. Acta* 1997, 42, 383–388, doi:10.1016/s0013-4686(96)00226-5.
134. de Leon, A.; Advincula, R.C. Conducting Polymers with Superhydrophobic Effects as Anticorrosion Coating. In *Intelligent Coatings for Corrosion Control*; Elsevier, 2015; pp. 409–430 ISBN 9780124115347.
135. Rajapakse, R.M.G.; Watkins, D.L.; Ranathunge, T.A.; Malikaramage, A.U.; Gunarathna, H.M.N.P.; Sandakelum, L.; Wylie, S.; Abewardana, P.G.P.R.; Egodawele, M.G.S.A.M.E.W.D.D.K.; Herath, W.H.M.R.N.K.; et al. Implementing the Donor–Acceptor Approach in Electronically Conducting Copolymers via Electropolymerization. *RSC Adv.* 2022, 12, 12089–12115, doi:10.1039/D2RA01176J.
136. Sotzing, G.A.; Reddinger, J.L.; Reynolds, J.R.; Steel, P.J. Redox Active Electrochromic Polymers from Low Oxidation Monomers Containing 3,4-Ethylenedioxythiophene (EDOT). *Synth. Met.* 1997, 84, 199–201, doi:10.1016/s0379-6779(97)80712-6.
137. Zhou, M.; Heinze, J. Electropolymerization of Pyrrole and Electrochemical Study of Polypyrrole: 1. Evidence for Structural Diversity of Polypyrrole. *Electrochim. Acta* 1999, 44, 1733–1748, doi:10.1016/S0013-4686(98)00293-X.
138. Yang, H.; Bard, A.J. The Application of Fast Scan Cyclic Voltammetry. Mechanistic Study of the Initial Stage of Electropolymerization of Aniline in Aqueous Solutions. *J. Electroanal. Chem.* 1992, 339, 423–449, doi:10.1016/0022-0728(92)80466-H.
139. Roushani, M.; Zalpour, N. Selective Detection of Asulam with In-Situ Dopamine Electropolymerization Based Electrochemical MIP Sensor. *React. Funct. Polym.* 2021, 169, 105069, doi:10.1016/j.reactfunctpolym.2021.105069.
140. Schweiger, B.; Kim, J.; Kim, Y.; Ulbricht, M. Electropolymerized Molecularly Imprinted Polypyrrole Film for Sensing of Clofibrilic Acid. *Sensors* 2015, 15, 4870–4889, doi:10.3390/s150304870.
141. EL Sharif, H.F.; Dennison, S.R.; Tully, M.; Crossley, S.; Mwangi, W.; Bailey, D.; Graham, S.P.; Reddy, S.M. Evaluation of Electropolymerized Molecularly Imprinted Polymers (E-MIPs) on Disposable Electrodes for Detection of SARS-CoV-2 in Saliva. *Anal. Chim. Acta* 2022, 1206, 339777, doi:10.1016/j.aca.2022.339777.
142. Zhang, Z.; Li, Y.; Xu, J.; Wen, Y. Electropolymerized Molecularly Imprinted Polypyrrole Decorated with Black Phosphorene Quantum Dots onto Poly(3,4-Ethylenedioxythiophene) Nanorods and Its Voltammetric Sensing of Vitamin C. *J. Electroanal. Chem.* 2018, 814, 153–160, doi:10.1016/j.jelechem.2018.02.059.
143. Buensuceso, C.E.; Tiu, B.D.B.; Lee, L.P.; Sabido, P.M.G.; Nuesca, G.M.; Caldon, E.B.; del Mundo, F.R.; Advincula, R.C. Electropolymerized-Molecularly Imprinted Polymers (E-MIPs) as Sensing Elements for the Detection of Dengue Infection. *Anal. Bioanal. Chem.* 2022, 414, 1347–1357, doi:10.1007/s00216-021-03757-y.
144. Xing, X.; Liu, S.; Yu, J.; Lian, W.; Huang, J. Electrochemical Sensor Based on Molecularly Imprinted Film at Polypyrrole-Sulfonated Graphene/Hyaluronic Acid-Multiwalled Carbon Nanotubes Modified

Electrode for Determination of Tryptamine. *Biosens. Bioelectron.* 2012, 31, 277–283, doi:10.1016/j.bios.2011.10.032.

145. Kor, K.; Zarei, K. Development and Characterization of an Electrochemical Sensor for Furosemide Detection Based on Electropolymerized Molecularly Imprinted Polymer. *Talanta* 2016, 146, 181–187, doi:10.1016/j.talanta.2015.08.042.

146. Kan, X.; Zhou, H.; Li, C.; Zhu, A.; Xing, Z.; Zhao, Z. Imprinted Electrochemical Sensor for Dopamine Recognition and Determination Based on a Carbon Nanotube/Polypyrrole Film. *Electrochim. Acta* 2012, 63, 69–75, doi:10.1016/j.electacta.2011.12.086.

147. Liu, Y.; Song, Q.J.; Wang, L. Development and Characterization of an Amperometric Sensor for Triclosan Detection Based on Electropolymerized Molecularly Imprinted Polymer. *Microchem. J.* 2009, 91, 222–226, doi:10.1016/j.microc.2008.11.007.

148. Mazzotta, E.; Malitesta, C.; Díaz-Álvarez, M.; Martín-Esteban, A. Electrosynthesis of Molecularly Imprinted Polypyrrole for the Antibiotic Levofloxacin. *Thin Solid Films* 2012, 520, 1938–1943, doi:10.1016/j.tsf.2011.09.039.

149. Couto, R.A.S.; Mounsssef, B.; Carvalho, F.; Rodrigues, C.M.P.; Braga, A.A.C.; Aldous, L.; Gonçalves, L.M.; Quinaz, M.B. Methyrene Screening with Electropolymerized Molecularly Imprinted Polymer on Screen-Printed Electrodes. *Sensors Actuators, B Chem.* 2020, 316, 128133, doi:10.1016/j.snb.2020.128133.

150. El-Sharif, H.F.; Turner, N.W.; Reddy, S.M.; Sullivan, M. V. Application of Thymine-Based Nucleobase-Modified Acrylamide as a Functional Co-Monomer in Electropolymerised Thin-Film Molecularly Imprinted Polymer (MIP) for Selective Protein (Haemoglobin) Binding. *Talanta* 2022, 240, 123158, doi:10.1016/j.talanta.2021.123158.

151. Bai, X.; Zhang, B.; Liu, M.; Hu, X.; Fang, G.; Wang, S. Molecularly Imprinted Electrochemical Sensor Based on Polypyrrole/Dopamine@graphene Incorporated with Surface Molecularly Imprinted Polymers Thin Film for Recognition of Olaquinox. *Bioelectrochemistry* 2020, 132, 107398, doi:10.1016/j.bioelechem.2019.107398.

152. Dykstra, G.; Reynolds, B.; Smith, R.; Zhou, K.; Liu, Y. Electropolymerized Molecularly Imprinted Polymer Synthesis Guided by an Integrated Data-Driven Framework for Cortisol Detection. *ACS Appl. Mater. Interfaces* 2022, 14, 25972–25983, doi:10.1021/acsami.2c02474.

153. Couto, R.A.S.; Costa, S.S.; Mounsssef, B.; Pacheco, J.G.; Fernandes, E.; Carvalho, F.; Rodrigues, C.M.P.; Delerue-Matos, C.; Braga, A.A.C.; Moreira Gonçalves, L.; et al. Electrochemical Sensing of Ecstasy with Electropolymerized Molecularly Imprinted Poly(o-Phenylenediamine) Polymer on the Surface of Disposable Screen-Printed Carbon Electrodes. *Sensors Actuators, B Chem.* 2019, 290, 378–386, doi:10.1016/j.snb.2019.03.138.

154. Anantha-Iyengar, G.; Shanmugasundaram, K.; Nallal, M.; Lee, K.P.; Whitcombe, M.J.; Lakshmi, D.; Sai-Anand, G. Functionalized Conjugated Polymers for Sensing and Molecular Imprinting Applications. *Prog. Polym. Sci.* 2019, 88, 1–129, doi:10.1016/j.progpolymsci.2018.08.001.

155. Teo, W.E.; Ramakrishna, S. A Review on Electrospinning Design and Nanofibre Assemblies. *Nanotechnology* 2006, 17, R89, doi:10.1088/0957-4484/17/14/R01.
156. Bhardwaj, N.; Kundu, S.C. Electrospinning: A Fascinating Fiber Fabrication Technique. *Biotechnol. Adv.* 2010, 28, 325–347.
157. Ardekani, R.; Borhani, S.; Rezaei, B. Simple Preparation and Characterization of Molecularly Imprinted Nylon 6 Nanofibers for the Extraction of Bisphenol A from Wastewater. *J. Appl. Polym. Sci.* 2019, 136, 47112, doi:10.1002/app.47112.
158. Subbiah, T.; Bhat, G.S.; Tock, R.W.; Parameswaran, S.; Ramkumar, S.S. Electrospinning of Nanofibers. *J. Appl. Polym. Sci.* 2005, 96, 557–569, doi:10.1002/app.21481.
159. Patel, K.D.; Kim, H.W.; Knowles, J.C.; Poma, A. Molecularly Imprinted Polymers and Electrospinning: Manufacturing Convergence for Next-Level Applications. *Adv. Funct. Mater.* 2020, 30, 2001955, doi: 10.1002/adfm.202001955.
160. Demirkurt, M.; Olcer, Y.A.; Demir, M.M.; Eroglu, A.E. Electrospun Polystyrene Fibers Knitted around Imprinted Acrylate Microspheres as Sorbent for Paraben Derivatives. *Anal. Chim. Acta* 2018, 1014, 1–9, doi:10.1016/j.aca.2018.02.016.
161. Chronakis, I.S.; Jakob, A.; Hagström, B.; Ye, L. Encapsulation and Selective Recognition of Molecularly Imprinted Theophylline and 17 β -Estradiol Nanoparticles within Electrospun Polymer Nanofibers. *Langmuir* 2006, 22, 8960–8965, doi:10.1021/la0613880.
162. Fallah-Darrehchi, M.; Zahedi, P.; Safarian, S.; Ghaffari-Bohlouli, P.; Aeinehvand, R. Conductive Conduit Based on Electrospun Poly (L-Lactide-Co-D, L-Lactide) Nanofibers Containing 4-Aminopyridine-Loaded Molecularly Imprinted Poly (Methacrylic Acid) Nanoparticles Used for Peripheral Nerve Regeneration. *Int. J. Biol. Macromol.* 2021, 190, 499–507, doi:10.1016/j.ijbiomac.2021.09.009.
163. Zhai, Y.; Wang, D.; Liu, H.; Zeng, Y.; Yin, Z.; Li, L. Electrochemical Molecular Imprinted Sensors Based on Electrospun Nanofiber and Determination of Ascorbic Acid. *Anal. Sci.* 2015, 31, 793–798, doi:10.2116/analsci.31.793.
164. Yoshimatsu, K.; Ye, L.; Lindberg, J.; Chronakis, I.S. Selective Molecular Adsorption Using Electrospun Nanofiber Affinity Membranes. *Biosens. Bioelectron.* 2008, 23, 1208–1215, doi:10.1016/j.bios.2007.12.002.
165. Liu, W.J.; Zeng, F.X.; Jiang, H.; Zhang, X.S.; Li, W.W. Composite Fe₂O₃ and ZrO₂/Al₂O₃ Photocatalyst: Preparation, Characterization, and Studies on the Photocatalytic Activity and Chemical Stability. *Chem. Eng. J.* 2012, 180, 9–18, doi:10.1016/j.cej.2011.10.085.
166. Zahedi, P.; Fallah-Darrehchi, M.; Nadoushan, S.A.; Aeinehvand, R.; Bagheri, L.; Najafi, M. Morphological, Thermal and Drug Release Studies of Poly (Methacrylic Acid)-Based Molecularly Imprinted Polymer Nanoparticles Immobilized in Electrospun Poly (ϵ -Caprolactone) Nanofibers as Dexamethasone Delivery System. *Korean J. Chem. Eng.* 2017, 34, 2110–2118, doi:10.1007/s11814-017-0078-1.

167. Limaee, N.Y.; Rouhani, S.; Olya, M.E.; Najafi, F. Selective 2,4-Dichlorophenoxyacetic Acid Optosensor Employing a Polyethersulfone Nanofiber-Coated Fluorescent Molecularly Imprinted Polymer. *Polymer (Guildf)*. 2019, 177, 73–83, doi:10.1016/j.polymer.2019.05.067.
168. Xue, X.; Lu, R.; Li, Y.; Wang, Q.; Li, J.; Wang, L. Molecularly Imprinted Electrospun Nanofibers for Adsorption of 2,4-Dinitrotoluene in Water. *Analyst* 2018, 143, 3466–3471, doi:10.1039/c8an00734a.
169. Ma, X.; Chen, Z.; Chen, X.; Chen, R.; Zheng, X. Preparation of Imprinted PVB/ β -CD Nanofiber by Electrospinning Technique and Its Selective Binding Abilities for Naringin. *Chinese J. Chem.* 2011, 29, 1753–1758, doi:10.1002/cjoc.201180312.
170. Ma, X.; Liu, J.; Zhang, Z.; Wang, L.; Chen, Z.; Xiang, S. The Cooperative Utilization of Imprinting, Electro-Spinning and a Pore-Forming Agent to Synthesize β -Cyclodextrin Polymers with Enhanced Recognition of Naringin. *RSC Adv.* 2013, 3, 25396–25402, doi:10.1039/c3ra43062f.
171. Chronakis, I.S.; Milosevic, B.; Frenot, A.; Ye, L. Generation of Molecular Recognition Sites in Electrospun Polymer Nanofibers via Molecular Imprinting. *Macromolecules* 2006, 39, 357–361, doi:10.1021/ma052091w.
172. Mohammadi, V.; Saraji, M.; Jafari, M.T. Direct Molecular Imprinting Technique to Synthesize Coated Electrospun Nanofibers for Selective Solid-Phase Microextraction of Chlorpyrifos. *Microchim. Acta* 2019, 186, 1–9, doi:10.1007/s00604-019-3641-0.
173. Zhang, L.; Guo, Y.; Chi, W. hao; Shi, H. guang; Ren, H. qi; Guo, T. ying Electrospun Nanofibers Containing P-Nitrophenol Imprinted Nanoparticles for the Hydrolysis of Paraoxon. *Chinese J. Polym. Sci. (English Ed.)* 2014, 32, 1469–1478, doi:10.1007/s10118-014-1530-x.
174. Cui, Y.; Meng, M.; Sun, D.; Liu, Y.; Pan, J.; Dai, X.; Yan, Y. Facile Synthesis of Imprinted Submicroparticles Blend Polyvinylidene Fluoride Membranes at Ambient Temperature for Selective Adsorption of Methyl P-Hydroxybenzoate. *Korean J. Chem. Eng.* 2017, 34, 600–608, doi:10.1007/s11814-016-0365-2.
175. Ruggieri, F.; D'Archivio, A.A.; Di Camillo, D.; Lozzi, L.; Maggi, M.A.; Mercorio, R.; Santucci, S. Development of Molecularly Imprinted Polymeric Nanofibers by Electrospinning and Applications to Pesticide Adsorption. *J. Sep. Sci.* 2015, 38, 1402–1410, doi:10.1002/jssc.201500033.
176. Zaidi, S.A. Recent Developments in Molecularly Imprinted Polymer Nanofibers and Their Applications. *Anal. Methods* 2015, 7, 7406–7415, doi:10.1039/c5ay01609f.
177. Ghorani, B.; Tucker, N.; Yoshikawa, M. Approaches for the Assembly of Molecularly Imprinted Electrospun Nanofibre Membranes and Consequent Use in Selected Target Recognition. *Food Res. Int.* 2015, 78, 448–464, doi:10.1016/j.foodres.2015.11.014
178. Huang, L.; Li, M.; Wu, D.; Ma, X.; Wu, Z.; Xiang, S.; Chen, S. Molecularly Imprinted Nanofiber Film for Sensitive Sensing 2,4,6-Tribromophenol. *Polymers (Basel)*. 2016, 8, 222, doi:10.3390/polym8060222.
179. Uzun, L.; Turner, A.P.F. Molecularly-Imprinted Polymer Sensors: Realising Their Potential. *Biosens. Bioelectron.* 2016, 76, 131–144, doi:10.1016/j.bios.2015.07.013.

180. Schneider, F.; Piletsky, S.; Piletska, E.; Guerreiro, A.; Ulbricht, M. Comparison of Thin-Layer and Bulk MIPs Synthesized by Photoinitiated in Situ Crosslinking Polymerization from the Same Reaction Mixtures. *J. Appl. Polym. Sci.* 2005, 98, 362–372, doi:10.1002/app.22112.
181. Lépinay, S.; Kham, K.; Millot, M.-C.; Carbonnier, B. In-Situ Polymerized Molecularly Imprinted Polymeric Thin Films Used as Sensing Layers in Surface Plasmon Resonance Sensors: Mini-Review Focused on 2010–2011. *Chem. Pap.* 2012, 66, 340–351, doi:10.2478/s11696-012-0134-6.
182. Shahhoseini, F.; Langille, E.A.; Azizi, A.; Bottaro, C.S. Thin Film Molecularly Imprinted Polymer (TF-MIP), a Selective and Single-Use Extraction Device for High-Throughput Analysis of Biological Samples. *Analyst* 2021, 146, 3157–3168, doi:10.1039/D0AN02228D.
183. Hudson, A.D.; Jamieson, O.; Crapnell, R.D.; Rurack, K.; Soares, T.C.C.; Mecozzi, F.; Laude, A.; Gruber, J.; Novakovic, K.; Peeters, M. Dual Detection of Nafcillin Using a Molecularly Imprinted Polymer-Based Platform Coupled to Thermal and Fluorescence Read-Out. *Mater. Adv.* 2021, 2, 5105–5115, doi:10.1039/D1MA00192B.
184. Tancharoen, C.; Sukjee, W.; Thepparit, C.; Jaimipuk, T.; Auewarakul, P.; Thitithanyanont, A.; Sangma, C. Electrochemical Biosensor Based on Surface Imprinting for Zika Virus Detection in Serum. *ACS Sensors* 2019, 4, 69–75, doi:10.1021/acssensors.8b00885.
185. Wang, Y.; Han, M.; Ye, X.; Wu, K.; Wu, T.; Li, C. Voltammetric Myoglobin Sensor Based on a Glassy Carbon Electrode Modified with a Composite Film Consisting of Carbon Nanotubes and a Molecularly Imprinted Polymerized Ionic Liquid. *Microchim. Acta* 2017, 184, 195–202, doi:10.1007/s00604-016-2005-2.
186. Huang, H.C.; Lin, C.I.; Joseph, A.K.; Lee, Y. Der Photo-Lithographically Impregnated and Molecularly Imprinted Polymer Thin Film for Biosensor Applications. *J. Chromatogr. A* 2004, 1027, 263–268, doi:10.1016/j.chroma.2003.08.106.
187. Tan, X.; Wu, J.; Hu, Q.; Li, X.; Li, P.; Yu, H.; Li, X.; Lei, F. An Electrochemical Sensor for the Determination of Phoxim Based on a Graphene Modified Electrode and Molecularly Imprinted Polymer. *Anal. Methods* 2015, 7, 4786–4792, doi:10.1039/C5AY00945F.
188. Aghoutane, Y.; Diouf, A.; Österlund, L.; Bouchikhi, B.; El Bari, N. Development of a Molecularly Imprinted Polymer Electrochemical Sensor and Its Application for Sensitive Detection and Determination of Malathion in Olive Fruits and Oils. *Bioelectrochemistry* 2020, 132, 107404, doi:10.1016/j.bioelechem.2019.107404.
189. Zhou, Q.; Sasaki, Y.; Ohshiro, K.; Fan, H.; Montagna, V.; Gonzato, C.; Haupt, K.; Minami, T. An Organic Transistor for the Selective Detection of Tropane Alkaloids Utilizing a Molecularly Imprinted Polymer. *J. Mater. Chem. B* 2022, 10, 6808–6815, doi:10.1039/D2TB01067D.
190. Völkle, J.; Kumpf, K.; Feldner, A.; Lieberzeit, P.; Fruhmann, P. Development of Conductive Molecularly Imprinted Polymers (CMIPs) for Limonene to Improve and Interconnect QCM and Chemiresistor Sensing. *Sensors Actuators B Chem.* 2022, 356, 131293, doi:10.1016/j.snb.2021.131293.

191. Haghdoost, S.; Arshad, U.; Mujahid, A.; Schranzhofer, L.; Lieberzeit, P.A. Development of a MIP-Based QCM Sensor for Selective Detection of Penicillins in Aqueous Media. *Chemosensors* 2021, 9, 362, doi:10.3390/chemosensors9120362.
192. Tai, D.-F.; Lin, C.-Y.; Wu, T.-Z.; Huang, J.-H.; Shu, P.-Y. Artificial Receptors in Serologic Tests for the Early Diagnosis of Dengue Virus Infection. *Clin. Chem.* 2006, 52, 1486–1491, doi:10.1373/clinchem.2005.064501.
193. Egli, S.N.; Butler, E.D.; Bottaro, C.S. Selective Extraction of Light Polycyclic Aromatic Hydrocarbons in Environmental Water Samples with Pseudo-Template Thin-Film Molecularly Imprinted Polymers. *Anal. Methods* 2015, 7, 2028–2035, doi:10.1039/c4ay02849j.
194. Aydın Urucu, O.; Beyler Çiğil, A.; Birtane, H.; Kök Yetimoğlu, E.; Kahraman, M.V. Selective Molecularly Imprinted Polymer for the Analysis of Chlorpyrifos in Water Samples. *J. Ind. Eng. Chem.* 2020, 87, 145–151, doi:10.1016/j.jiec.2020.03.025.
195. Lotierzo, M.; Henry, O.Y.; Piletsky, S.; Tothill, I.; Cullen, D.; Kania, M.; Hock, B.; Turner, A.P.. Surface Plasmon Resonance Sensor for Domoic Acid Based on Grafted Imprinted Polymer. *Biosens. Bioelectron.* 2004, 20, 145–152, doi:10.1016/j.bios.2004.01.032.
196. Cennamo, N.; D'Agostino, G.; Galatus, R.; Bibbò, L.; Pesavento, M.; Zeni, L. Sensors Based on Surface Plasmon Resonance in a Plastic Optical Fiber for the Detection of Trinitrotoluene. *Sensors Actuators B Chem.* 2013, 188, 221–226, doi:10.1016/j.snb.2013.07.005.
197. Shahhoseini, F.; Azizi, A.; Egli, S.N.; Bottaro, C.S. Single-Use Porous Thin Film Extraction with Gas Chromatography Atmospheric Pressure Chemical Ionization Tandem Mass Spectrometry for High-Throughput Analysis of 16 PAHs. *Talanta* 2020, 207, 120320, doi:10.1016/j.talanta.2019.120320.
198. Abu-Alsoud, G.F.; Bottaro, C.S. Porous Thin-Film Molecularly Imprinted Polymer Device for Simultaneous Determination of Phenol, Alkylphenol and Chlorophenol Compounds in Water. *Talanta* 2021, 223, 121727, doi:10.1016/j.talanta.2020.121727.
199. Boonsriwong, W.; Chunta, S.; Thepsimanon, N.; Singsanan, S.; Lieberzeit, P.A. Thin Film Plastic Antibody-Based Microplate Assay for Human Serum Albumin Determination. *Polymers (Basel)*. 2021, 13, 1763, doi:10.3390/polym13111763.
200. Piacham, T.; Josell, Å.; Arwin, H.; Prachayasittikul, V.; Ye, L. Molecularly Imprinted Polymer Thin Films on Quartz Crystal Microbalance Using a Surface Bound Photo-Radical Initiator. *Anal. Chim. Acta* 2005, 536, 191–196, doi:10.1016/j.aca.2004.12.067.
201. Mehdiinia, A.; Dadkhah, S.; Baradaran Kayyal, T.; Jabbari, A. Design of a Surface-Immobilized 4-Nitrophenol Molecularly Imprinted Polymer via Pre-Grafting Amino Functional Materials on Magnetic Nanoparticles. *J. Chromatogr. A* 2014, 1364, 12–19, doi:10.1016/j.chroma.2014.08.058.
202. Sharma, P.S.; Dabrowski, M.; D'Souza, F.; Kutner, W. Surface Development of Molecularly Imprinted Polymer Films to Enhance Sensing Signals. *TrAC - Trends Anal. Chem.* 2013, 51, 146–157, doi:10.1016/j.trac.2013.07.006

203. Sulitzky, C.; Rückert, B.; Hall, A.J.; Lanza, F.; Unger, K.; Sellergren, B. Grafting of Molecularly Imprinted Polymer Films on Silica Supports Containing Surface-Bound Free Radical Initiators. *Macromolecules* 2002, 35, 79–91, doi:10.1021/ma011303w.
204. Tian, H.; Liu, T.; Mu, G.; Chen, F.; He, M.; You, S.; Yang, M.; Li, Y.; Zhang, F. Rapid and Sensitive Determination of Trace Fluoroquinolone Antibiotics in Milk by Molecularly Imprinted Polymer-Coated Stainless Steel Sheet Electrospray Ionization Mass Spectrometry. *Talanta* 2020, 219, 121282, doi:10.1016/j.talanta.2020.121282.
205. Lowdon, J.W.; Eersels, K.; Rogosic, R.; Boonen, T.; Heidt, B.; Diliën, H.; van Grinsven, B.; Cleij, T.J. Surface Grafted Molecularly Imprinted Polymeric Receptor Layers for Thermal Detection of the New Psychoactive Substance 2-Methoxphenidine. *Sensors Actuators, A Phys.* 2019, 295, 586–595, doi:10.1016/j.sna.2019.06.029.
206. Yoshimi, Y.; Yagisawa, Y.; Yamaguchi, R.; Seki, M. Blood Heparin Sensor Made from a Paste Electrode of Graphite Particles Grafted with Molecularly Imprinted Polymer. *Sensors Actuators, B Chem.* 2018, 259, 455–462, doi:10.1016/j.snb.2017.12.084.
207. Patel, A.K.; Sharma, P.S.; Prasad, B.B. Electrochemical Sensor for Uric Acid Based on a Molecularly Imprinted Polymer Brush Grafted to Tetraethoxysilane Derived Sol-Gel Thin Film Graphite Electrode. *Mater. Sci. Eng. C* 2009, 29, 1545–1553, doi:10.1016/j.msec.2008.12.008.
208. Lee, H.Y.; S. Kim, B. Grafting of Molecularly Imprinted Polymers on Iniferter-Modified Carbon Nanotube. *Biosens. Bioelectron.* 2009, 25, 587–591, doi:10.1016/j.bios.2009.03.040.
209. Quaglia, M.; De Lorenzi, E.; Sulitzky, C.; Massolini, G.; Sellergren, B. Surface Initiated Molecularly Imprinted Polymer Films: A New Approach in Chiral Capillary Electrochromatography. *Analyst* 2001, 126, 1495–1498, doi:10.1039/b105401p.
210. Kim, D.-M.; Moon, J.-M.; Lee, W.-C.; Yoon, J.-H.; Choi, C.S.; Shim, Y.-B. A Potentiometric Non-Enzymatic Glucose Sensor Using a Molecularly Imprinted Layer Bonded on a Conducting Polymer. *Biosens. Bioelectron.* 2017, 91, 276–283, doi:10.1016/j.bios.2016.12.046.
211. Qin, L.; Shi, W.; Liu, W.; Yang, Y.; Liu, X.; Xu, B. Surface Molecularly Imprinted Polymers Grafted on Ordered Mesoporous Carbon Nanospheres for Fuel Desulfurization. *RSC Adv.* 2016, 6, 12504–12513, doi:10.1039/c5ra23582k.
212. Piletsky, S.A.; Matuschewski, H.; Schedler, U.; Wilpert, A.; Piletsky, E. V.; Thiele, T.A.; Ulbricht, M. Surface Functionalization of Porous Polypropylene Membranes with Molecularly Imprinted Polymers by Photograft Copolymerization in Water. *Macromolecules* 2000, 33, 3092–3098, doi:10.1021/ma991087f.
213. Gam-Derouich, S.; Nguyen, M.N.; Madani, A.; Maouche, N.; Lang, P.; Perruchot, C.; Chehimi, M.M. Aryl Diazonium Salt Surface Chemistry and ATRP for the Preparation of Molecularly Imprinted Polymer Grafts on Gold Substrates. In *Proceedings of the Surface and Interface Analysis*; John Wiley & Sons, Ltd, June 1 2010; Vol. 42, pp. 1050–1056.

214. Caldara, M.; Kulpa, J.; Lowdon, J.W.; Cleij, T.J.; Diliën, H.; Eersels, K.; Grinsven, B. van Recent Advances in Molecularly Imprinted Polymers for Glucose Monitoring: From Fundamental Research to Commercial Application. *Chemosensors* 2023, 11, 32, doi:10.3390/chemosensors11010032.
215. Cheong, W.J.; Yang, S.H.; Ali, F. Molecular Imprinted Polymers for Separation Science: A Review of Reviews. *J. Sep. Sci.* 2013, 36, 609–628, doi:10.1002/jssc.201200784.
216. Williams, P. The Sputtering Process and Sputtered Ion Emission. *Surf. Sci.* 1979, 90, 588–634, doi:10.1016/0039-6028(79)90363-7.
217. Grant, W.K.; Loomis, C.; Moore, J.J.; Olson, D.L.; Mishra, B.; Perry, A.J. Characterization of Hard Chromium Nitride Coatings Deposited by Cathodic Arc Vapour Deposition. *Surf. Coatings Technol.* 1996, 86–87, 788–796, doi:10.1016/s0257-8972(96)03071-x.
218. Dai, Z.R.; Pan, Z.W.; Wang, Z.L. Novel Nanostructures of Functional Oxides Synthesized by Thermal Evaporation. *Adv. Funct. Mater.* 2003, 13, 9–24, doi:10.1002/adfm.200390013.
219. Ince, G.O.; Armagan, E.; Erdogan, H.; Buyukserin, F.; Uzun, L.; Demirel, G. One-Dimensional Surface-Imprinted Polymeric Nanotubes for Specific Biorecognition by Initiated Chemical Vapour Deposition (ICVD). *ACS Appl. Mater. Interfaces* 2013, 5, 6447–6452, doi:10.1021/am401769r.
220. He, D.; Zhang, P.; Li, S.; Luo, H. A Novel Free-Standing CVD Graphene Platform Electrode Modified with AuPt Hybrid Nanoparticles and L-Cysteine for the Selective Determination of Epinephrine. *J. Electroanal. Chem.* 2018, 823, 678–687, doi:10.1016/j.jelechem.2018.07.022.
221. Delhaes, P. Chemical Vapour Deposition and Infiltration Processes of Carbon Materials. *Carbon N. Y.* 2002, 40, 641–657, doi:10.1016/S0008-6223(01)00195-6.
222. Zhang, Y.; Zhang, L.; Zhou, C. Review of Chemical Vapour Deposition of Graphene and Related Applications. *Acc. Chem. Res.* 2013, 46, 2329–2339, doi:10.1021/ar300203n.
223. Deshpande, A.D.; Harris-Hayes, M.; Schootman, M. Epidemiology of Diabetes and Diabetes-Related Complications. *Phys. Ther.* 2008, 88, 1254–1264, doi:10.2522/ptj.20080020.
224. Byun, D.; Jin, Y.; Kim, B.; Kee Lee, J.; Park, D. Photocatalytic TiO₂ Deposition by Chemical Vapour Deposition. *J. Hazard. Mater.* 2000, 73, 199–206, doi:10.1016/s0304-3894(99)00179-x.
225. Bradley, L.C.; Gupta, M. Microstructured Films Formed on Liquid Substrates via Initiated Chemical Vapour Deposition of Cross-Linked Polymers. *Langmuir* 2015, 31, 7999–8005, doi:10.1021/acs.langmuir.5b01663.
226. Dinata, A.A.; Rosyadi, A.M.; Hamid, S.; Zainul, R. Chemical Vapor Deposition: Process and Application. *INA-Rxiv* October 2018, doi:/10.31227/osf.io/yfeau

Preface to Chapter 6

Direct screen-printing of a mixture of graphitic ink and MIP particles to produce MIP-functionalized screen-printed electrodes (SPEs) is one of the most interesting mechanical deposition methods highlighted in **Chapter 5**. This method enables the creation of functionalized MIP-platforms with a cost-effective, reproducible, and easily scalable manufacturing process. Furthermore, electrodes are the most frequently used substrate in biosensors (e.g. glucometers) and work harmoniously with electrochemical transducers as well as other types of readouts. Using this manufacturing method for the production of MIP-modified electrodes opens up the possibility of using these platforms with a wide range of transducers and techniques.

Chapter 6 displays the application of this deposition technique using a mixture of ink and bulk MIP particles engineered towards the detection of glucose. This study results in the development of a MIP-coated screen-printed electrode (MIP-SPE) for glucose sensing. Thanks to the MIP-SPE sensor's design, the platform should be compatible with both electrochemical readout technology (electrochemical impedance spectroscopy) and the HTM technique. Lastly, the developed MIP-SPE sensor we will test the point-of-care efficacy of the sensor for non-invasive glucose detection by analysing its performance in glucose-spiked human urine samples using both impedimetric and HTM configurations. The potential combination of MIP-SPE sensors with an impedimetric readout configuration is particularly appealing due to the possibility of using it in combination with a handheld SPE connector and a commercial impedance analyser. In this way an effective dipstick sensor system is created. Such a system would allow for the non-invasive, single-shot analysis of the glucose presence in human urine samples. This further supports the high potential of the sensor for healthcare applications and brings MIP-based sensors one step closer to implementation in healthcare.

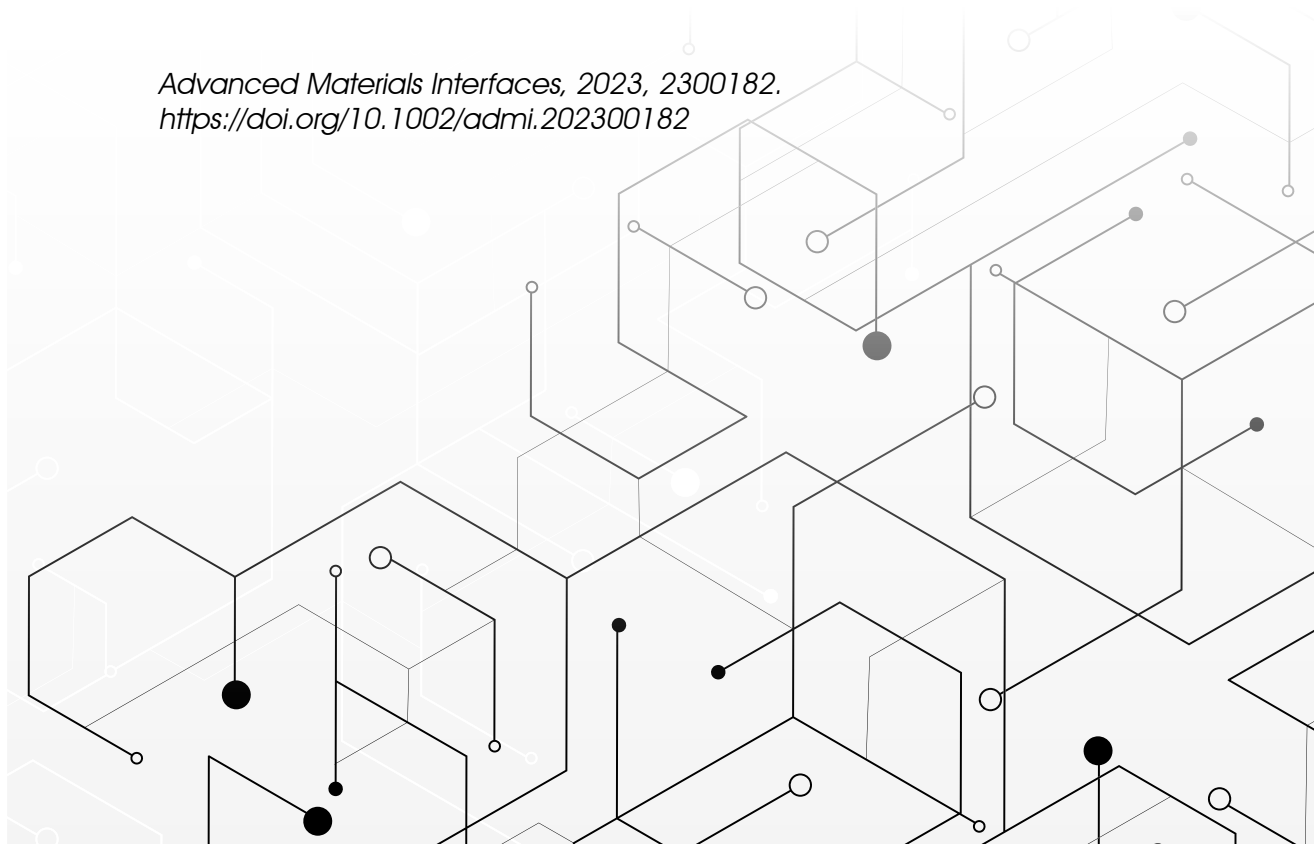
Chapter 6

Dipstick sensor based on molecularly imprinted polymer-coated screen-printed electrodes for the single-shot detection of glucose in urine samples - From fundamental study towards point-of-care application

Adapted from:

Caldara, M.*; Lowdon, J.W.; van Wissen, G.; Garcia-Miranda Ferrari, A.; Crapnell, R.D.; Cleij, T.J.; Diliën, H.; Banks, C.E.; Eersels, K; van Grinsven, B. Dipstick sensor based on molecularly imprinted polymer-coated screen-printed electrodes for the single-shot detection of glucose in urine samples- From fundamental study towards point-of-care application.

Advanced Materials Interfaces, 2023, 2300182.
<https://doi.org/10.1002/admi.202300182>



Abstract

Glucose biosensors play an important role in health care systems worldwide. Therefore, the field continues to attract significant attention leading to the development of innovative technologies. Due to their unique characteristics, Molecularly Imprinted Polymers (MIPs) represent a promising alternative to commercial enzymatic sensors. In this chapter, we present a low-cost and flexible MIP-based platform for glucose sensing by integrating MIP particles directly into screen-printed electrodes (SPEs). The sensor design allowed the detection of glucose via two different transducer principles, the so-called "heat-transfer method" (HTM) and electrochemical impedance spectroscopy (EIS). The sensitivity and selectivity of the sensor are demonstrated by comparing the responses obtained toward three different saccharides. Furthermore, the application potential of the MIP-SPE sensor is demonstrated by analysing the response in urine samples, showing a linear range of 14.38-330 μM with HTM and 1.37-330 μM with EIS. To bring the sensor closer to a real life application, a handheld dipstick sensor is developed, allowing the single-shot detection of glucose in urine using EIS. This chapter illustrates that the simplicity of the dipstick readout, coupled with the straightforward manufacturing process, opens up the possibility for mass production, making this platform a very attractive alternative to commercial glucose sensors.

Introduction

Diabetes (or Diabetes mellitus) is considered a global burden both in terms of health-related and economic costs. According to the WHO, the number of people suffering from diabetes rose worryingly from 108 million in 1980 to 422 million in 2014, and in 2019, the disease was the direct cause of 1.5 million fatalities.[1] Inevitably, the cost for diabetic care multiplied. The American Diabetes Association (ADA) estimated a 26% increase in the total cost of diagnosed diabetes from \$245 billion in 2012 to \$327 billion in 2017 the US only.[2] Diabetes is an incurable chronic disease that occurs when the pancreas does not produce enough insulin or when the body is not able to properly utilize the produced insulin.[3] The insulin-deficiency causes elevated levels of glucose in blood (also called hyperglycaemia) as well as in other body fluids.[4–6] Therefore, the easiest and fastest way for the diagnosis and monitoring of diabetes are accomplished via the use of sensors able to quantify the glucose levels in physiological fluids. Unsurprisingly, the first glucose biosensor was developed by Leland Clark over 60 years ago in order to tackle the disease by allowing its early diagnosis. As diabetes still represents a condition that can lead to serious long-term health problems, the development of novel glucose biosensors continues to be one of the top priorities globally.[7,8] Generally, the recognition elements utilized in most commercial glucose sensors are represented by enzymes such as glucose oxidase (GOx) or glucose-1-dehydrogenase (GDH).[8,9] Despite the fact that these enzymes have extensively proven their reliability for glucose sensing over the last decades, their main limitations reside in their relatively short long-term stability,[10,11] loss of activity at extreme pH[12] or reactivity towards other sugars (especially for GDH-based sensors).[13] For this reason, non-enzymatic glucose sensor have gained increasing attention from the scientific community in recent years.[14,15]

As was described in **Chapter 2**, a promising category of non-enzymatic recognition elements that could overcome the above-mentioned issues are molecularly imprinted polymers (MIP).[16,17] MIPs are artificially synthesized materials with tailor-made binding cavities complementary to the template molecule in shape, size and chemical functionalities; as such they are able to specifically and selectively bind to the target.[18] Some of the key advantages of these polymers are their high stability to extreme conditions, extremely long shelf life, and low-cost preparation methods.[19–21] MIPs have been successfully integrated into several platforms with the aim to detect a wide variety of targets, ranging from small organic molecules[22,23] to proteins,[24,25] viruses[26] and bacteria.[27,28] These features make MIPs ideal candidates as recognition elements in glucose biosensors and for the analysis in complex matrices, such as physiological fluids[29]. In order to develop a promising alternative to commercial sensors, the key features that a glucose biosensor needs to address are cost-effectiveness and possibility of mass production. In addition, these techniques should be minimally or non-invasive to create a commercial edge over the traditional glucose meters that require the collection of blood using a lancet device. In the past years, many MIP-based sensors have been developed for glucose detection (**Chapter 2**),[30,31] with most of them being MIP films polymerized onto a substrate[32–35] or platforms based on MIP micro particles embedded onto an adhesive layer (**Chapter 3**).[36,37] Even though such sensors showed promising results in terms of sensitivity and selectivity, the materials and procedures used to develop the platforms make the production process highly difficult to reproduce on a large scale and difficult to implement in a clinical setting.

This chapter focuses on the facile and up scalable fabrication of a MIP-modified screen-printed electrode for glucose detection and its potential for monitoring the glucose concentration in physiological samples. To this extent, MIP particles were prepared using a bulk polymerization approach

employing a procedure optimized in our previous work (**Chapter 3**),[36] the obtained particles were then mixed with carbon-graphitic ink and the mixture was screen-printed on top of the working electrode. This simple and straightforward procedure allowed the preparation of MIP-SPEs (**Figure 6.1a**) in a cost-effective and reproducible manner. Moreover, the design of the fabricated platform made it possible to use the sensor with two different transducer technologies (**Figure 6.1b and 6.1c**), the heat-transfer method (HTM) and electrochemical impedance spectroscopy (EIS). The MIP-SPE platform was characterized with Scanning Electron Microscopy (SEM) and Cyclic Voltammetry (CV) to assess morphological characteristic and electrochemical behaviour of the developed sensing platform. Subsequently, HTM and EIS rebinding analysis in buffer solutions confirmed the specificity of the platform when compared to the reference control. The selectivity of the developed platform was proven by comparing the thermal response of the platform to different structural analogues of the target. Finally, the response of the MIP-SPE platform to untreated urine samples, spiked with glucose, was assessed via HTM and EIS analysis. To bring the technology closer to a market-ready application, the EIS sensor was transformed into a dipstick technology for the single-shot detection of glucose in urine samples (**Figure 6.1c**). The results obtained in this chapter illustrate that it is possible to accurately measure the glucose concentration in urine in a fast manner, further emphasizing its potential use in diabetes diagnosis and management.

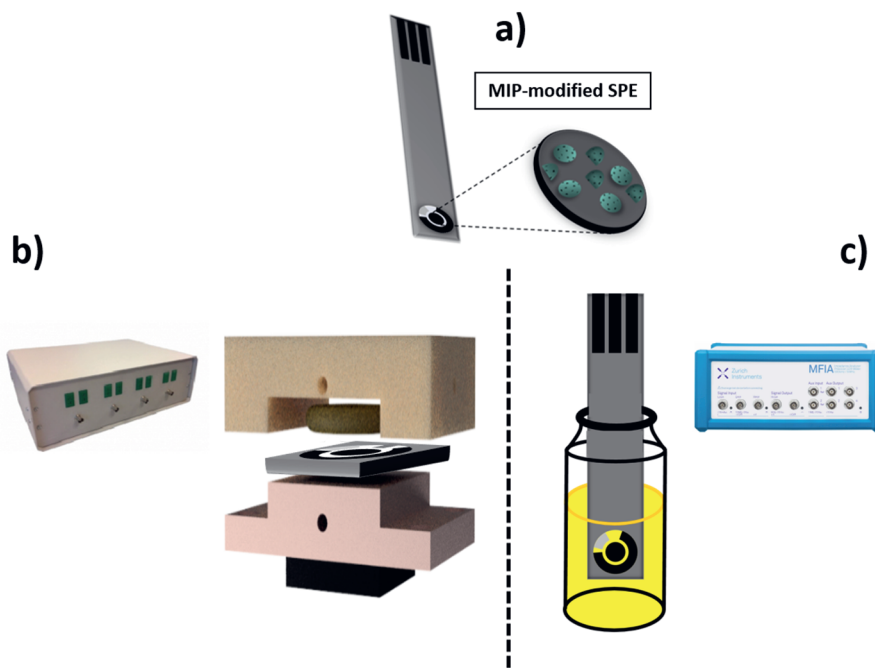


Figure 6.1 a) Design of the fabricated MIP-SPE. b) Heat-Transfer Method (HTM) setup and c) Electrochemical Impedance Spectroscopy (EIS) setup adopted for rebinding analysis using MIP-SPE as dipstick technology.

Materials and Methods

Materials

Stabilizers were removed from the monomer and cross-linker through filtration on aluminium oxide. Aluminium oxide ($\geq 99.7\%$), acrylamide ($\geq 99.9\%$), D-glucuronic acid ($\geq 98\%$), D-glucose ($\geq 99\%$), methanol (HPLC grade), acetic acid ($\geq 99.8\%$), dimethyl sulfoxide ($\geq 99.7\%$), potassium chloride (99%) potassium ferricyanide ($\geq 99\%$), potassium ferrocyanide trihydrate ($\geq 99\%$) were purchased from Fisher Scientific (Landsmeer, the Netherlands). Ethylene glycol dimethacrylate ($\geq 98\%$) and azobisisobutyronitrile ($\geq 98\%$) were purchased from Sigma Aldrich (Zwijndrecht, the Netherlands). Test strips for glucose analysis (Medi-Test) and Phosphate buffered saline (PBS) tablets 1X were obtained from VWR International BV (Amsterdam, the Netherlands). Milli-Q water ($18.2 \text{ M}\Omega \text{ cm}^{-1}$) or phosphate-buffer saline (PBS) were used to prepare solutions for rebinding studies.

Preparation of Molecularly Imprinted Polymers

Bulk molecularly imprinted polymers (MIPs) for the detection of glucose were synthesized through free radical polymerization, following a procedure reported in our previous work with slight modifications. (Chapter 3)[36] A dummy imprinting approach was employed using glucuronic acid as template to enhance the interaction with the functional monomer (acrylamide) during the imprinting process. In short, D-glucuronic acid (97 mg), acrylamide (282 mg), ethylene glycol dimethacrylate (EGDMA, 1.13 mL), and azobisisobutyronitrile (AIBN, 50 mg) were dissolved in dimethyl sulfoxide (DMSO, 6 mL). The pre-polymerization solution was degassed with N_2 for 15 min, and then the polymerization was performed at 65°C for 18 h. The bulk MIP was then ground and the obtained micro particles were dried at 65°C overnight. The removal of the template was achieved employing a previously described procedure.[36] A reference control (NIP) was prepared in parallel following the same procedure as per the MIP without the addition of the template.

Fabrication of the screen-printed macroelectrodes (SPEs) and glucose-MIPs bulk modified screen-printed macroelectrodes (MIP-SPEs)

Stencil designs with a microDEK 1760RS screen-printing machine (DEK, Weymouth, UK) were used for the production of the SPEs. For each of the screen-printed electrodes, a carbon-graphite ink formulation was first screen-printed onto a polyester flexible film (Autostat, $250 \mu\text{m}$ thickness). After that, the layer was cured at 60°C for 30 min in a box fan oven with extraction. Next, a silver/silver chloride (60:40) reference electrode was applied by screen-printing Ag/AgCl paste (Product Code: C2040308P3; Gwent Electronic Materials Ltd, UK) onto the plastic substrate. Then, this layer was cured at 60°C for 30 min in an oven. Finally, an insulating dielectric paste ink (Product Code: D2070423D5; Gwent Electronic Materials Ltd, UK) was printed to cover the connections and define the 3.1 mm diameter graphite working electrode. One more time, this layer was cured in the same conditions as the previous layers. After these steps, the SPE are ready to use and these platforms have been well characterized in previous works.[38–41]

The glucose-MIPs modified screen-printed macroelectrodes (MIP-SPEs) were made by modifying the carbon-graphitic ink via modification with glucose-MIPs. This was carried out using a weight percentage of M_P to M_I , where M_P is the mass of particulate (the mass of glucose-MIPs) and M_I is the total mass of the ink including the base graphitic ink and the mass of the particulate.[42–45] This was thoroughly mixed into the ink and screen-printed on top of the carbon-graphite working electrode. The equation

$(M_p/M_i) \times 100$ was used to formulate the 5% wt. MIP-SPEs. A 5% wt. of glucose-MIPs was used to ensure consistent printing of the analyte in the fabrication process and to test viability of the proposed system. The screen-printed electrodes used throughout this work had a connection length of 32 mm and average resistance of 2.16 ± 0.06 k Ω . [46]

Scanning Electron Microscope (SEM) and Cyclic Voltammetry (CV) characterization of Modified SPEs

In order to characterize the surface morphology of the modified screen-printed electrode, a bare SPE and a MIP-modified SPE were placed into 12 mm disks and after gold coating, the samples were imaged using a Scios Dualbeam scanning electron microscope (SEM). Cyclic voltammetry studies of bare SPE, NIP-SPE and MIP-SPE were performed using a PalmSens4 potentiostat (PalmSens BV, Utrecht, the Netherlands). CV scans were recorded at a potential range of -0.5 to 0.6 V in 0.01 M $[\text{Fe}(\text{CN})_6]^{3-/4-}$ (1:1) and 0.1 M KCl as electrolyte solution at a scan rate of 0.05 V/s.

Heat-Transfer Method (HTM) setup

The sensing platform used for the HTM rebinding studies has been described in previous works (**Chapter 4**). [47,48] Briefly, MIP-modified screen-printed electrodes were placed on a copper heat sink. The temperature of the sink, T_1 , was strictly controlled using a K-type thermocouple (TC Direct, Nederweert, The Netherlands), a power resistor (Farnell, Utrecht, The Netherlands) and a software-based PID controller ($P = 10$, $I = 8$, $D = 0$) in Labview (National Instruments, Austin, TX, USA). The electrode was exposed to the different analytes using an injection-moulded polycarbonate (PC) flow cell ($A = 28$ mm², $V = 110$ μL). A syringe pump was used to inject the studied samples at a rate of 0.250 mL/min for 5 min. To measure thermal changes at the solid-liquid interface, a second thermocouple monitored the temperature inside the flow cell, T_2 , at a constant inlet temperature of 37 °C. To stabilize the signal, phosphate-buffered saline (PBS) or human urine solution was used. Increasing concentrations (55.5 to 333 μM) of glucose solutions (or competitor) were gradually injected into the system. To stabilize the signal, a waiting time of 20 minutes was observed between each addition. Mean values and error bars presented in all the HTM analysis are obtained from the average of three measurements.

Electrochemical Impedance Spectroscopy (EIS) analysis

A MFIA impedance analyser (Zurich Instruments, Zurich, Switzerland) was used to measure the impedance changes. The impedance analyser was connected to the functionalized SPEs using a portable PalmSens SPE connector (PalmSens BV, Utrecht, the Netherlands). The sensing part of the modified screen-printed electrode was then inserted into vials containing 10 mL glucose solutions in PBS or untreated urine samples, ranging from 55.5 to 333 μM . Continuous frequency sweeps were taken at a low-frequency range from 10 Hz to 1 kHz at a test signal of 300 mV. Dose-response curves were obtained from the absolute impedance values at a single frequency at which the corresponding phase angle is 45 degrees. Mean values and error bars presented in all the EIS studies are obtained from the average of three measurements.

HTM and EIS analysis in urine samples

Human urine samples were collected from a healthy volunteer. The absence of glucose in the samples was confirmed using commercially available Medi-Test Glucose test strips. Increasing concentrations of

glucose (55.5 to 333 μM) in urine samples were then prepared and employed for the HTM and EIS rebinding analysis with no need of additional pre-treatment of the physiological sample.

Results and Discussion

SEM and CV characterization of functionalized MIP-SPE

The morphology of the functionalized part (working electrode) of the sensor was studied via Scanning Electron Microscopy (SEM) analysis (**Figure 6.2**).

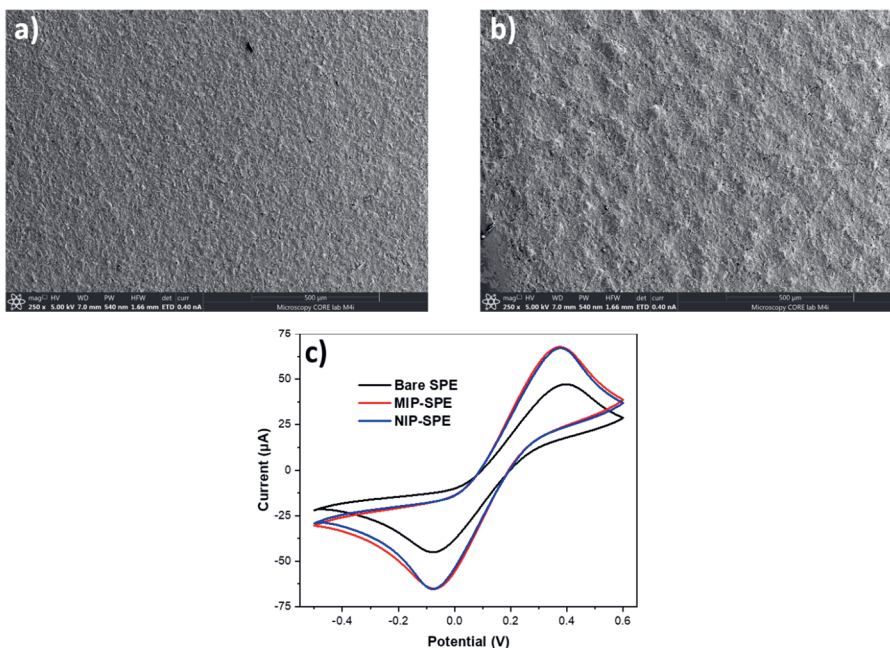


Figure 6.2 Characterization of the MIP-modified screen-printed electrodes. Scanning electron microscopy (SEM) images of working electrode of **a)** bare screen-printed electrode and **b)** screen-printed electrode modified with MIP particles (MIP-SPE). **c)** CV voltammograms of bare SPE, MIP-SPE and NIP-SPE.

When analysing the image obtained with the bare SPE, a flat and relatively smooth surface can be observed (**Figure 6.2a**). A different pattern is evident in the SEM image of MIP-SPE (**Figure 6.2b**). In fact, the modification of the electrode with graphitic ink and MIP micro particles can be clearly seen as the surface appears more rough and uneven when in presence of the polymer particles. The electrochemical behaviour of the functionalized SPEs was analysed by CV voltammetry using a $[\text{Fe}(\text{CN})_6]^{3-/4-}$ redox probe in KCl. In **Figure 6.2c**, cyclic voltammograms of MIP-SPE and NIP-SPE (red and blue lines) show increased oxidation and reduction peaks compared with those obtained for bare SPE (black line); the difference is attributed to the fabrication process of the modified SPEs, in which MIP-modified graphitic ink is screen-printed onto the working electrode. This results in an increased conductivity of the substrate due to the higher concentration of graphite in the WE. Another indication of the increased surface area in the modified electrodes is provided by the analysis of the oxidation

peaks of the different SPEs;[49] in fact, a shift from +0.4 to +0.37 V is observed when comparing the bare SPE with the MIP- and NIP-modified SPEs.

Heat-Transfer rebinding analysis in PBS

To scrutinize the rebinding efficiency of the MIP-modified SPEs thoroughly using the Heat-Transfer Method, the functionalized substrates were placed inside a flow cell at a stringently controlled temperature of 37 °C and upon injection of increasing concentrations of glucose in buffer solutions (PBS), the thermal variations at the solid-liquid interface were recorded and analysed (**Figure 6.3**).

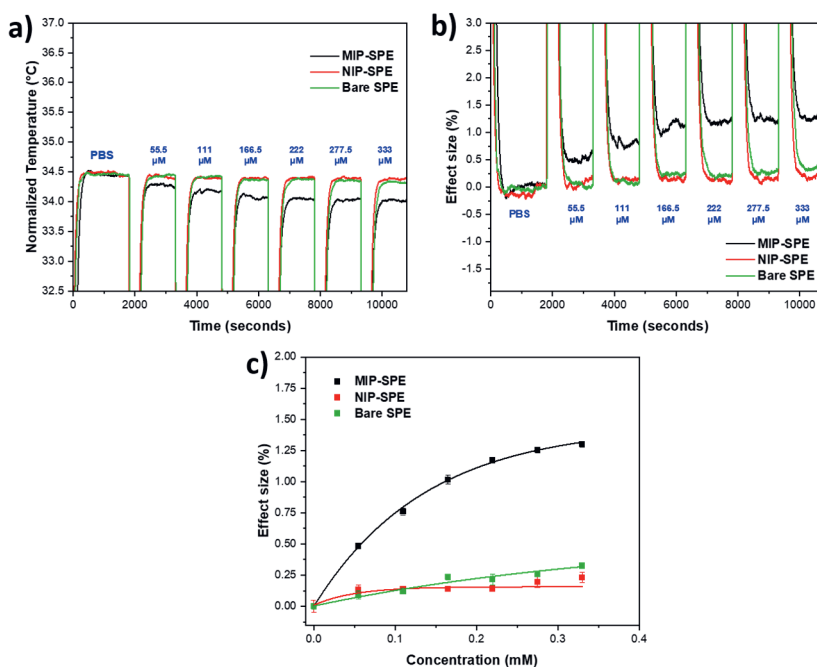


Figure 6.3 HTM rebinding analysis of MIP/NIP/Bare SPE after injection of glucose (55.5 to 333 μM). Analysis on time of **a)** Temperature and **b)** effect size changes upon injection of the analyte. **c)** Dose-response curves of MIP-SPE, NIP-SPE and Bare SPE.

In order to get a direct comparison with the NIP-functionalized SPE and bare SPE and therefore assess the specificity of the MIP-SPE over the two reference materials, the obtained temperature values were baselined and then transformed to effect size (%) values using an equation reported in previous works (**Chapter 3**) (**Figure 6.3b**).[36] The data show a clear distinction in the temperature profiles of MIP-SPE (black lines), NIP-SPE (red lines) and Bare SPE (green lines) from the first analyte injection. This difference is seen to increase with higher concentrations of glucose, proving the specificity of the MIP-sensor in the entire analysed range. Dose-response curves were constructed by plotting the effect size (%) values against the glucose concentration introduced inside the flow cell (**Figure 6.3c**). The dose-response curve obtained for the MIP-electrode shows a saturation trend commonly observed for

imprinted polymers coupled with HTM as readout technology. In fact, the measurement shows a clear response after the first injections, which then starts to plateau due to the saturation of the binding sites available for the binding. For this reason, the data was fit asymptotically with Origin, version 2021b (OriginLabs Corporation, Northampton, MA, USA) for MIP-SPE ($R^2= 0.9992$), NIP-SPE ($R^2= 0.6297$) and Bare SPE ($R^2=0.9632$).

Electrochemical Impedance Spectroscopy (EIS) rebinding analysis in PBS

To further prove the specificity of the MIP-SPE substrate and demonstrate its versatility in detecting glucose with different readout technologies, an EIS rebinding analysis in phosphate-buffered solution (used to mimic physiological samples) was carried out (**Figure 6.4**).

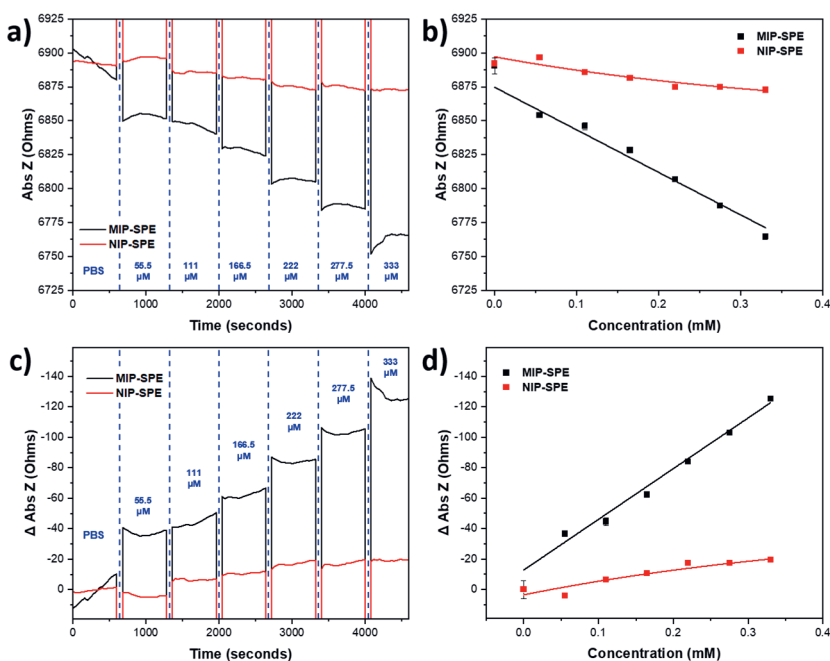


Figure 6.4 EIS rebinding analysis after injection of glucose (55.5 to 333 μM). Analysis on time of **a)** Absolute Z values and **b)** Delta Absolute Z at different concentrations of glucose. Dose-response curves for MIP-SPE and NIP-SPE of **c)** Absolute Z and **d)** Delta Absolute Z.

The analysis was carried out by connecting the functionalized SPEs to an impedance analyser with a commercially available SPE connector, demonstrating then the potential of the modified electrode as sensing element in handheld electrochemical devices. The measurement was recorded after simply inserting the sensing part of the functionalized electrode into a vial containing increasing concentration of target (55.5 to 333 μM). The obtained data show that MIP-SPE retains a high specificity when compared with NIP-SPE with a commercial electrochemical readout. A clear decrease in the absolute value of the impedance can be observed for the MIP-SPE after submerging it in the lowest concentration

of glucose (**Figures 6.4a and 6.4c**); in contrast, it can be seen that the NIP-SPE shows a negligible change in the impedance value upon exposure to glucose solutions. Dose-response curves were constructed after baselining the absolute impedance values for MIP- and NIP-SPE, and then plotting the changes ($\Delta \text{Abs } Z$) against the glucose concentrations used for the analysis (**Figure 6.4d**). The MIP-modified electrode shows a linear behaviour (black line, $R^2=0.9882$) with no evidence of saturation effects, suggesting that the sensor might be effective also at higher glucose concentrations when analysed in PBS samples; NIP-SPE (red line, $R^2=0.9114$) instead shows a diminished response that seems to plateau with higher glucose levels.

Selectivity studies of MIP-SPE

A key feature that needs to be evaluated for molecularly imprinted polymers and for biosensors in general is the selectivity of the sensor platform to a determined target over other competitors. To accurately assess the selectivity of the MIP-SPE substrate, the HTM response to three different saccharides was recorded and analysed (**Figure 6.5**).

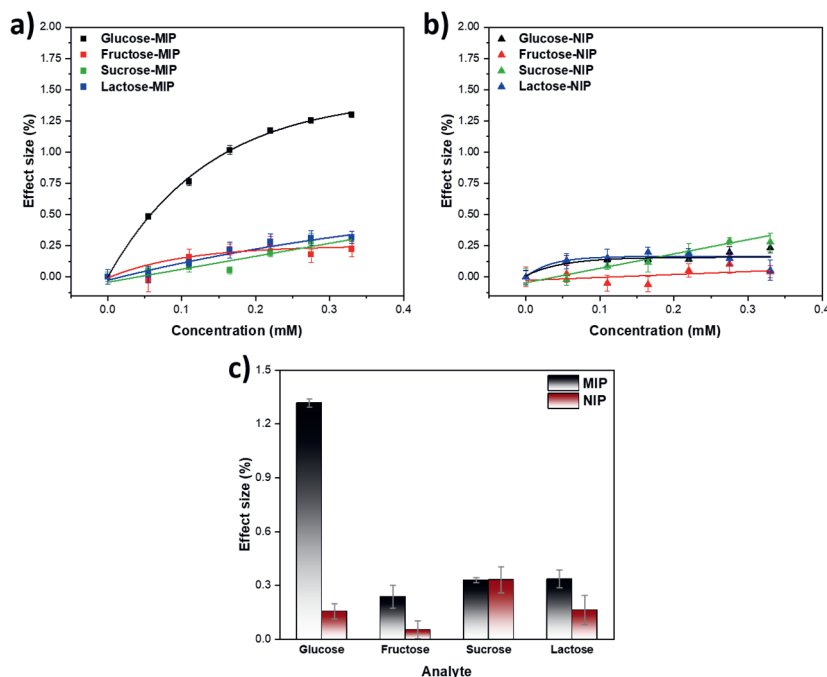


Figure 6.5 Selectivity studies via HTM analysis. Dose-response curves obtained after exposing **a)** MIP-SPE and **b)** NIP-SPE to increasing concentrations of three different saccharides. **c)** Analysis of the MIP-SPE/NIP-SPE response (%) after exposure to 0.33 mM of glucose, fructose, sucrose and lactose.

One of the tested molecules is fructose, a simple sugar with the same molecular formula as glucose ($C_6H_{12}O_6$) and, as such, the two molecules are classified as functional isomers. However, when analysing the structures of these two molecules, glucose is a six-membered ring, while fructose is a five-membered ring. Thus, it can be deduced that this structural difference is responsible for the clearly higher response of the sensor to glucose in comparison to fructose (**Figure 6.5c**). The other molecules tested (sucrose and lactose) instead are made up of two monosaccharides, and therefore are classified as disaccharides. It is important to highlight that both the molecules contain one glucose unit in their structure and as such are good indicator of the MIP selectivity. Despite this structural similarity, the developed MIP-SPE sensor exhibits high specificity (**Figures 6.5a and 6.5b**) and selectivity (**Figure 6.5c**) towards glucose over these molecules, thus suggesting that size and shape of the analysed disaccharides obstruct the potential interactions with the MIP-modified electrode.

Rebinding analysis in urine samples via HTM and EIS analysis

The potential applicability of the developed sensor for glucose detection in physiological samples was proven via HTM and EIS analysis of untreated urine samples spiked with the target.

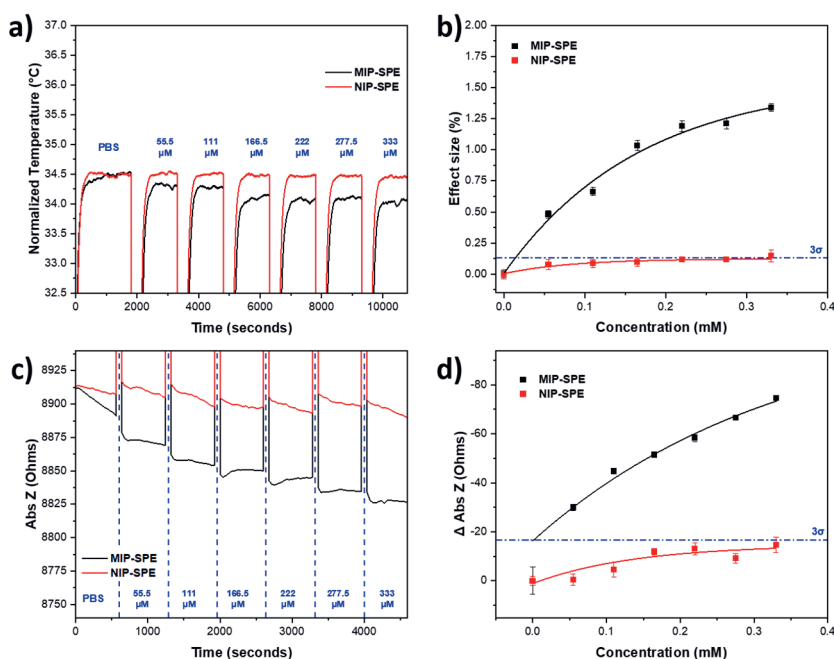


Figure 6.6 HTM and EIS rebinding analysis in human urine samples. Raw data obtained via a) HTM and c) EIS analysis after exposing the MIP-/NIP-modified SPE sensor to increasing concentration of glucose. Dose-response curves constructed from b) HTM and d) EIS measurements, the blue dashed lines indicates the calculated LoDs (3σ method).

From the raw data measurements obtained with the two different readout technologies it can be clearly observed a distinctive change for the MIP-SPE substrate, whereas NIP-SPE shows little to no response with both HTM and EIS (**Figures 6.6a and 6.6c**). Specifically, in the HTM analysis of the MIP-SPE, a decrease in temperature is observed after each injection of the glucose solutions due to the obstruction of the heat flow at the solid-liquid interface as a result of the interaction between the target and the cavities present in the polymer. The NIP-SPE signal, on the other hand, shows very little change after injections, thereby proving the specificity of the MIP sensor. To better highlight and compare the thermal response of MIP- and NIP-modified SPE, dose-response curves were constructed as indicated above (**Figure 6.6b**), and the data were fitted asymptotically for both MIP-SPE (black line, $R^2=0.9905$) and NIP-SPE (red line, $R^2=0.9356$).

Although HTM is commercially interesting due to its low-cost and user-friendly operating mechanism, its application in handheld single-shot analysis of urine samples, similar to a blood glucose meter, is cumbersome with the current equipment. Therefore, an EIS-based sensor was developed using a handheld commercial SPE connector and a commercial impedance analyser. This device can be used as a dipstick for non-invasive single-shot glucose detection in urine. The sensor was "dipped" in urine samples, spiked with the same concentrations analysed by the HTM method, therefore allowing a direct comparison between the two different data sets. The results show a clear decrease in the absolute value of the impedance upon exposure of the MIP-functionalized SPE to the lowest concentration of glucose, whereas the reference NIP-SPE shows a much smaller decrease. Furthermore, the change in impedance increases linearly when the MIP sensor is placed in contact with higher concentrations of glucose, thus demonstrating the reliability of the designed SPE for the quantitative analysis of glucose in complex matrices such as urine. To make interpretation of the impedance changes of MIP- and NIP-modified SPE during the rebinding experiments easier, dose-response curves for MIP-SPE (black line, $R^2=0.9861$) and NIP-SPE (red line, $R^2=0.8017$) were constructed in **Figure 6.6d**. When analysing the constructed curves with both the transducers (**Figure 6.6**), it is clear that the MIP-sensor can be successfully employed for both HTM and EIS analysis in a complex physiological matrix, such as urine. The sensitivity of the developed sensor in urine samples was assessed by calculating the limit of detection (LoD) from the dose-response curves of MIP-SPE (**Figures 6.6b and 6.6d**, black lines). The LoD was calculated using the three-sigma rule, (blue dashed line) corresponding to the maximum noise value of the signal throughout the measurement multiplied by three. The obtained y-values were then plotted (blue lines) and their intercept with the MIP-fits allowed the calculation of the two LoDs. The calculated LoDs were found to be $14.38 \mu\text{M}$ for the HTM and $1.37 \mu\text{M}$ for the EIS urinalysis. These results demonstrate the potential of MIP-SPE as low-cost, diagnostic device for the non-invasive diagnosis of diabetes in urine samples as the sensor proves its efficiency in the physiologically relevant regime. Moreover, when comparing **Figures 6.3 and 6.4** with **Figure 6.6**, it can be seen that the sensor's performance is not highly affected from complex matrices and therefore might be further developed for glucose detection in different body fluids.

Conclusions

In this chapter, we have successfully described an imprinted polymer for glucose detection using a free radical bulk polymerization. The prepared MIP particles were then employed as recognition element to fabricate a MIP-functionalized screen-printed electrode (MIP-SPE) sensor. The MIP-SPE sensor was fabricated by simple screen-printing a mixture of graphitic ink and MIP particles onto the working electrode of a standard carbon SPE. The sensor has demonstrated to be highly selective and is sensitive enough to allow both thermal and electrochemical quantification in urine samples in physiologically relevant concentrations. In terms of commercial application, the impedimetric sensor mainly stands out by the possibility of using it in combination with a handheld SPE connector and a commercial impedance analyser in a dipstick configuration. This would allow for the single-shot, non-invasive analysis of the glucose concentration in urine samples. The low-cost, disposable nature of the chips makes this possible, while the impedimetric sensor enables end-users to quickly get a result that can be easily quantified. In the current setup we used a benchtop impedance analyser but this can easily be replaced by a handheld model once implementation is complete. The combination with the easily scalable production process of the SPEs further emphasizes the commercial potential of the platform. Inter-sample variability has mainly shown to influence the baseline but not the relative response of the normalized MIP-NIP signal, allowing for easy and fast calibration of the sensor.

References Chapter 6

1. World Health Organization Diabetes Available online: <https://www.who.int/news-room/fact-sheets/detail/diabetes> (accessed on 24 October 2022).
2. Yang, W.; Dall, T.M.; Beronjia, K.; Lin, J.; Semilla, A.P.; Chakrabarti, R.; Hogan, P.F.; Petersen, M.P. Economic Costs of Diabetes in the U.S. in 2017. *Diabetes Care* 2018, 41, 917–928, doi:10.2337/dci18-0007.
3. Karamanou, M. Milestones in the History of Diabetes Mellitus: The Main Contributors. *World J. Diabetes* 2016, 7, 1, doi:10.4239/wjd.v7.i1.1.
4. Kap, Ö.; Kılıç, V.; Hardy, J.G.; Horzum, N. Smartphone-Based Colorimetric Detection Systems for Glucose Monitoring in the Diagnosis and Management of Diabetes. *Analyst* 2021, 146, 2784–2806, doi:10.1039/D0AN02031A.
5. Naik, A.R.; Zhou, Y.; Dey, A.A.; Arellano, D.L.G.; Okoroanyanwu, U.; Secor, E.B.; Hersam, M.C.; Morse, J.; Rothstein, J.P.; Carter, K.R.; et al. Printed Microfluidic Sweat Sensing Platform for Cortisol and Glucose Detection. *Lab on a Chip* 2022, 22, 156–169, doi:10.1039/D1LC00633A.
6. Wolkowicz, K.L.; Aiello, E.M.; Vargas, E.; Teymourian, H.; Tehrani, F.; Wang, J.; Pinsker, J.E.; Doyle, F.J.; Patti, M.E.; Laffel, L.M.; et al. A Review of Biomarkers in the Context of Type 1 Diabetes: Biological Sensing for Enhanced Glucose Control. *Bioeng. Transl. Med.* 2021, 6, e10201, doi:10.1002/btm2.10201.
7. Newman, J.D.; Turner, A.P.F. Home Blood Glucose Biosensors: A Commercial Perspective. *Biosens. Bioelectron.* 2005, 20, 2435–2453, doi:10.1016/j.bios.2004.11.012.
8. Zhang, Y.; Sun, J.; Liu, L.; Qiao, H. A Review of Biosensor Technology and Algorithms for Glucose Monitoring. *J. Diabetes Complications* 2021, 35, 107929, doi:10.1016/j.jdiacomp.2021.107929.
9. Hassan, M.H.; Vyas, C.; Grieve, B.; Bartolo, P. Recent Advances in Enzymatic and Non-Enzymatic Electrochemical Glucose Sensing. *Sensors* 2021, 21, 4672, doi:10.3390/s21144672.
10. Fan, H.-H.; Weng, W.-L.; Lee, C.-Y.; Liao, C.-N. Electrochemical Cycling-Induced Spiky Cu x O/Cu Nanowire Array for Glucose Sensing. *ACS Omega* 2019, 4, 12222–12229, doi:10.1021/acsomega.9b01730.
11. Petrulėvičienė, M.; Juodkazytė, J.; Savickaja, I.; Karpicz, R.; Morkvenaite-Vilkonciene, I.; Ramanavicius, A. BiVO₄-Based Coatings for Non-Enzymatic Photoelectrochemical Glucose Determination. *Journal of Electroanalytical Chemistry* 2022, 918, 116446, doi:10.1016/j.jelechem.2022.116446.
12. Hwang, D.-W.; Lee, S.; Seo, M.; Chung, T.D. Recent Advances in Electrochemical Non-Enzymatic Glucose Sensors – A Review. *Anal. Chim. Acta* 2018, 1033, 1–34, doi:10.1016/j.aca.2018.05.051.
13. Frias, J.P.; Lim, C.G.; Ellison, J.M.; Montandon, C.M. Review of Adverse Events Associated With False Glucose Readings Measured by GDH-PQQ-Based Glucose Test Strips in the Presence of Interfering Sugars. *Diabetes Care* 2010, 33, 728–729, doi:10.2337/dc09-1822.

14. Gorle, D.B.; Ponnada, S.; Kiai, M.S.; Nair, K.K.; Nowduri, A.; Swart, H.C.; Ang, E.H.; Nanda, K.K. Review on Recent Progress in Metal–Organic Framework-Based Materials for Fabricating Electrochemical Glucose Sensors. *J. Mater. Chem. B* 2021, 9, 7927–7954, doi:10.1039/D1TB01403J.
15. Wei, M.; Qiao, Y.; Zhao, H.; Liang, J.; Li, T.; Luo, Y.; Lu, S.; Shi, X.; Lu, W.; Sun, X. Electrochemical Non-Enzymatic Glucose Sensors: Recent Progress and Perspectives. *Chemical Communications* 2020, 56, 14553–14569, doi:10.1039/DOCC05650B.
16. Wackerlig, J.; Lieberzeit, P.A. Molecularly Imprinted Polymer Nanoparticles in Chemical Sensing – Synthesis, Characterisation and Application. *Sens. Actuators B Chem.* 2015, 207, 144–157, doi:10.1016/j.snb.2014.09.094.
17. Ahmad, O.S.; Bedwell, T.S.; Esen, C.; Garcia-Cruz, A.; Piletsky, S.A. Molecularly Imprinted Polymers in Electrochemical and Optical Sensors. *Trends Biotechnol.* 2019, 37, 294–309, doi:10.1016/j.tibtech.2018.08.009.
18. Pessagno, F.; Blair, M.; Muldoon, M.J.; Manesiotes, P. Molecularly Imprinted Polymers for (Thio)Urea Organocatalyst Recovery and Recycling. *ACS Appl. Polym. Mater.* 2022, 4, 7770–7777, doi:10.1021/acsapm.2c01308.
19. Chen, H.; Wu, F.; Xu, Y.; Liu, Y.; Song, L.; Chen, X.; He, Q.; Liu, W.; Han, Q.; Zhang, Z.; et al. Synthesis, Characterization, and Evaluation of Selective Molecularly Imprinted Polymers for the Fast Determination of Synthetic Cathinones. *RSC Adv.* 2021, 11, 29752–29761, doi:10.1039/D1RA01330K.
20. Kimani, M.; Kislenco, E.; Gawlitza, K.; Rurack, K. Fluorescent Molecularly Imprinted Polymer Particles for Glyphosate Detection Using Phase Transfer Agents. *Sci. Rep.* 2022, 12, 14151, doi:10.1038/s41598-022-16825-9.
21. Tabar, F.A.; Lowdon, J.W.; Caldara, M.; Cleij, T.J.; Wagner, P.; Diliën, H.; Eersels, K.; van Grinsven, B. Thermal Determination of Perfluoroalkyl Substances in Environmental Samples Employing a Molecularly Imprinted Polyacrylamide as a Receptor Layer. *Environ. Technol. Innov.* 2023, 29, 103021, doi:10.1016/j.eti.2023.103021.
22. Lowdon, J.W.; Eersels, K.; Arreguin-Campos, R.; Caldara, M.; Heidt, B.; Rogosic, R.; Jimenez-Monroy, K.L.; Cleij, T.J.; Diliën, H.; van Grinsven, B. A Molecularly Imprinted Polymer-Based Dye Displacement Assay for the Rapid Visual Detection of Amphetamine in Urine. *Molecules* 2020, 25, 5222, doi:10.3390/molecules25225222.
23. Ratautaite, V.; Brazys, E.; Ramanaviciene, A.; Ramanavicius, A. Electrochemical Sensors Based on L-Tryptophan Molecularly Imprinted Polypyrrole and Polyaniline. *Journal of Electroanalytical Chemistry* 2022, 917, 116389, doi:10.1016/j.jelechem.2022.116389.
24. Bereli, N.; Andaç, M.; Baydemir, G.; Say, R.; Galaev, I.Y.; Denizli, A. Protein Recognition via Ion-Coordinated Molecularly Imprinted Supermacroporous Cryogels. *J. Chromatogr A* 2008, 1190, 18–26, doi:10.1016/j.chroma.2008.02.110.
25. Çimen, D.; Bereli, N.; Günaydın, S.; Denizli, A. Molecular Imprinted Nanoparticle Assisted Surface Plasmon Resonance Biosensors for Detection of Thrombin. *Talanta* 2022, 246, 123484, doi:10.1016/j.talanta.2022.123484.

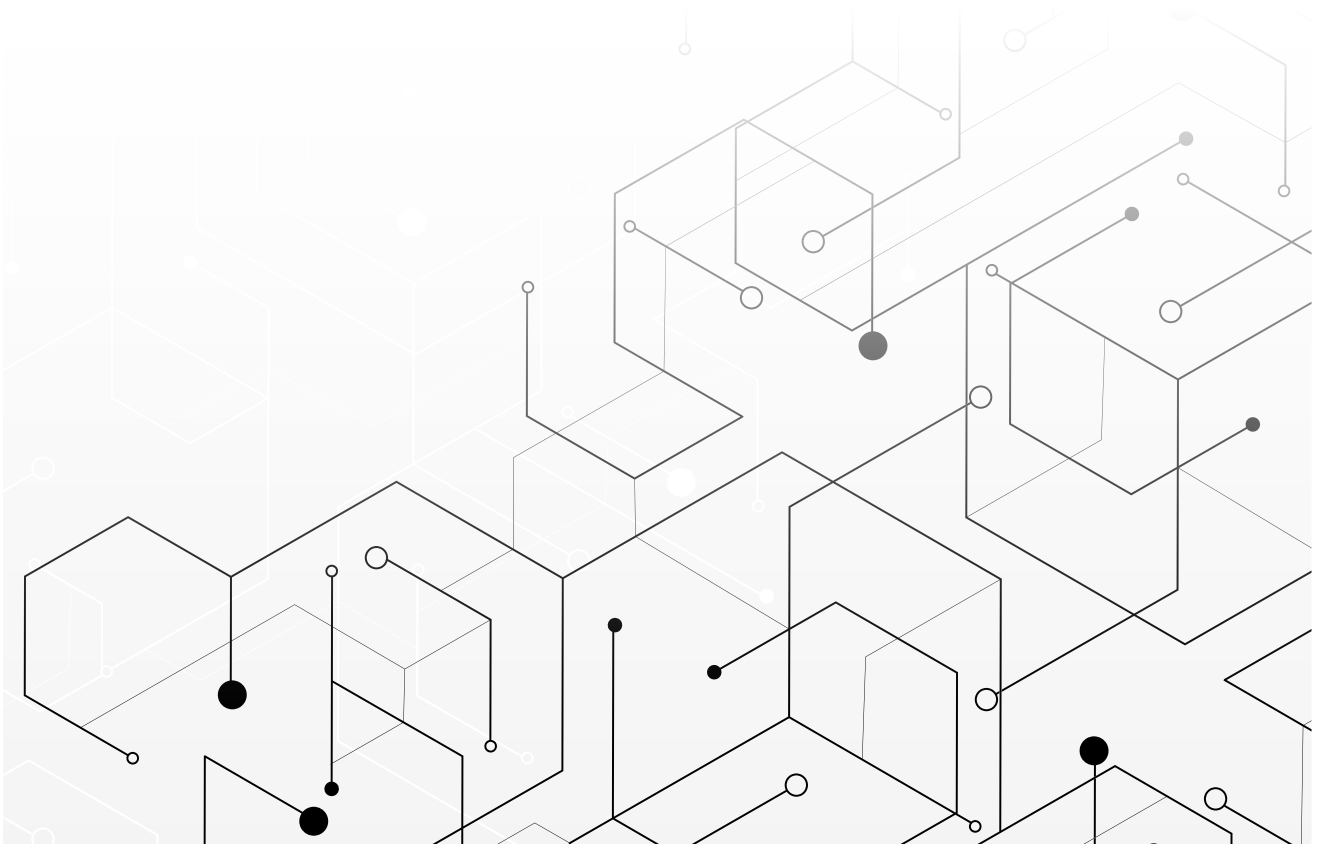
26. Birnbaumer, G.M.; Lieberzeit, P.A.; Richter, L.; Schirhagl, R.; Milnera, M.; Dickert, F.L.; Bailey, A.; Ertl, P. Detection of Viruses with Molecularly Imprinted Polymers Integrated on a Microfluidic Biochip Using Contact-Less Dielectric Microsensors. *Lab on a Chip* 2009, 9, 3549, doi:10.1039/b914738a.
27. Arreguin-Campos, R.; Eersels, K.; Lowdon, J.W.; Rogosic, R.; Heidt, B.; Caldara, M.; Jiménez-Monroy, K.L.; Diliën, H.; Cleij, T.J.; van Grinsven, B. Biomimetic Sensing of Escherichia Coli at the Solid-Liquid Interface: From Surface-Imprinted Polymer Synthesis toward Real Sample Sensing in Food Safety. *Microchemical Journal* 2021, 169, 106554, doi:10.1016/j.microc.2021.106554.
28. Bräuer, B.; Werner, M.; Baurecht, D.; Lieberzeit, P.A. Raman and Scanning Probe Microscopy for Differentiating Surface Imprints of E. Coli and B. Cereus. *J. Mater. Chem. B* 2022, 10, 6758–6767, doi:10.1039/D2TB00283C.
29. Pirzada, M.; Sehit, E.; Altintas, Z. Cancer Biomarker Detection in Human Serum Samples Using Nanoparticle Decorated Epitope-Mediated Hybrid MIP. *Biosens. Bioelectron.* 2020, 166, 112464, doi:10.1016/j.bios.2020.112464.
30. Sehit, E.; Drzazgowska, J.; Buchenau, D.; Yesildag, C.; Lensen, M.; Altintas, Z. Ultrasensitive Nonenzymatic Electrochemical Glucose Sensor Based on Gold Nanoparticles and Molecularly Imprinted Polymers. *Biosens. Bioelectron.* 2020, 165, 112432, doi:10.1016/j.bios.2020.112432.
31. Caldara, M.; Kulpa, J.; Lowdon, J.W.; Cleij, T.J.; Diliën, H.; Eersels, K.; Grinsven, B. van Recent Advances in Molecularly Imprinted Polymers for Glucose Monitoring: From Fundamental Research to Commercial Application. *Chemosensors* 2023, 11, 32, doi:10.3390/chemosensors11010032.
32. Cho, S.J.; Noh, H.-B.; Won, M.-S.; Cho, C.-H.; Kim, K.B.; Shim, Y.-B. A Selective Glucose Sensor Based on Direct Oxidation on a Bimetal Catalyst with a Molecular Imprinted Polymer. *Biosens. Bioelectron.* 2018, 99, 471–478, doi:10.1016/j.bios.2017.08.022.
33. Sehit, E.; Drzazgowska, J.; Buchenau, D.; Yesildag, C.; Lensen, M.; Altintas, Z. Ultrasensitive Nonenzymatic Electrochemical Glucose Sensor Based on Gold Nanoparticles and Molecularly Imprinted Polymers. *Biosens. Bioelectron.* 2020, 165, 112432, doi:10.1016/j.bios.2020.112432.
34. Karaman, C.; Karaman, O.; Atar, N.; Yola, M.L. A Molecularly Imprinted Electrochemical Biosensor Based on Hierarchical $\text{Ti}_2\text{Nb}_{10}\text{O}_{29}$ (TNO) for Glucose Detection. *Microchimica Acta* 2022, 189, 24, doi:10.1007/s00604-021-05128-x.
35. Diouf, A.; Bouchikhi, B.; el Bari, N. A Nonenzymatic Electrochemical Glucose Sensor Based on Molecularly Imprinted Polymer and Its Application in Measuring Saliva Glucose. *Materials Science and Engineering: C* 2019, 98, 1196–1209, doi:10.1016/j.msec.2019.01.001.
36. Caldara, M.; Lowdon, J.W.; Rogosic, R.; Arreguin-Campos, R.; Jimenez-Monroy, K.L.; Heidt, B.; Tschulik, K.; Cleij, T.J.; Diliën, H.; Eersels, K.; et al. Thermal Detection of Glucose in Urine Using a Molecularly Imprinted Polymer as a Recognition Element. *ACS Sens.* 2021, 6, 4515–4525, doi:10.1021/acssensors.1c02223.

37. Frigoli, M.; Lowdon, J.W.; Caldara, M.; Arreguin-Campos, R.; Sewall, J.; Cleij, T.J.; Diliën, H.; Eersels, K.; van Grinsven, B. Thermal Pycocyanin Sensor Based on Molecularly Imprinted Polymers for the Indirect Detection of *Pseudomonas Aeruginosa*. *ACS Sens.* 2023, doi:10.1021/acssensors.2c02345.
38. Galdino, F.E.; Foster, C.W.; Bonacin, J.A.; Banks, C.E. Exploring the Electrical Wiring of Screen-Printed Configurations Utilised in Electroanalysis. *Analytical Methods* 2015, 7, 1208–1214, doi:10.1039/C4AY02704C.
39. Metters, J.P.; Kadara, R.O.; Banks, C.E. New Directions in Screen Printed Electroanalytical Sensors: An Overview of Recent Developments. *Analyst* 2011, 136, 1067, doi:10.1039/c0an00894j.
40. Khorshed, A.A.; Khairy, M.; Banks, C.E. Electrochemical Determination of Antihypertensive Drugs by Employing Costless and Portable Unmodified Screen-Printed Electrodes. *Talanta* 2019, 198, 447–456, doi:10.1016/j.talanta.2019.01.117.
41. Khorshed, A.A.; Khairy, M.; Banks, C.E. Voltammetric Determination of Meclizine Antihistamine Drug Utilizing Graphite Screen-Printed Electrodes in Physiological Medium. *Journal of Electroanalytical Chemistry* 2018, 824, 39–44, doi:10.1016/j.jelechem.2018.07.029.
42. Hughes, J.P.; Blanco, F.D.; Banks, C.E.; Rowley-Neale, S.J. Mass-Producible 2D-WS 2 Bulk Modified Screen Printed Electrodes towards the Hydrogen Evolution Reaction. *RSC Adv.* 2019, 9, 25003–25011, doi:10.1039/C9RA05342E.
43. Adarakatti, P.S.; Mahanthappa, M.; Hughes, J.P.; Rowley-Neale, S.J.; Smith, G.C.; S, A.; Banks, C.E. MoS₂-Graphene-CuNi₂S₄ Nanocomposite an Efficient Electrocatalyst for the Hydrogen Evolution Reaction. *Int. J. Hydrogen Energy* 2019, 44, 16069–16078, doi:10.1016/j.ijhydene.2019.05.004.
44. Rowley-Neale, S.J.; Foster, C.W.; Smith, G.C.; Brownson, D.A.C.; Banks, C.E. Mass-Producible 2D-MoSe 2 Bulk Modified Screen-Printed Electrodes Provide Significant Electrocatalytic Performances towards the Hydrogen Evolution Reaction. *Sustain Energy Fuels* 2017, 1, 74–83, doi:10.1039/C6SE00115G.
45. Srinivasa, N.; Shreenivasa, L.; Adarakatti, P.S.; Hughes, J.P.; Rowley-Neale, S.J.; Banks, C.E.; Ashoka, S. In Situ Addition of Graphitic Carbon into a NiCo₂O₄/CoO Composite: Enhanced Catalysis toward the Oxygen Evolution Reaction. *RSC Adv.* 2019, 9, 24995–25002, doi:10.1039/C9RA05195C.
46. Whittingham, M.J.; Hurst, N.J.; Crapnell, R.D.; Garcia-Miranda Ferrari, A.; Blanco, E.; Davies, T.J.; Banks, C.E. Electrochemical Improvements Can Be Realized via Shortening the Length of Screen-Printed Electrochemical Platforms. *Anal. Chem.* 2021, 93, 16481–16488, doi:10.1021/acs.analchem.1c03601.
47. Caldara, M.; Lowdon, J.W.; Royackers, J.; Peeters, M.; Cleij, T.J.; Diliën, H.; Eersels, K.; van Grinsven, B. A Molecularly Imprinted Polymer-Based Thermal Sensor for the Selective Detection of Melamine in Milk Samples. *Foods* 2022, 11, 2906, doi:10.3390/foods11182906.
48. Arreguin-Campos, R.; Frigoli, M.; Caldara, M.; Crapnell, R.D.; Ferrari, A.G.-M.; Banks, C.E.; Cleij, T.J.; Diliën, H.; Eersels, K.; van Grinsven, B. Functionalized Screen-Printed Electrodes for the Thermal Detection of *Escherichia Coli* in Dairy Products. *Food Chem.* 2023, 404, 134653, doi:10.1016/j.foodchem.2022.134653.

49. Peeters, M.; van Grinsven, B.; Foster, C.; Cleij, T.; Banks, C. Introducing Thermal Wave Transport Analysis (TWTA): A Thermal Technique for Dopamine Detection by Screen-Printed Electrodes Functionalized with Molecularly Imprinted Polymer (MIP) Particles. *Molecules* 2016, 21, 552, doi:10.3390/molecules21050552.

Chapter 7

Conclusion and Outlook



The aim of this chapter is to synthesise, connect, and briefly analyse the findings from each chapter of the thesis, with an emphasis on the research questions addressed throughout the study.

The research presented in this thesis has demonstrated how synthetic receptors such as molecularly imprinted polymers (MIPs) can be employed as sensing elements in biosensor devices. In fact, a variety of fields can benefit from the many advantages that MIPs can bring for the detection of several biomarkers.[1] For example, modern healthcare industry could make use of MIPs in biosensor devices as an alternative to traditional biological recognition elements, such as enzymes and antibodies.[2] One of the key biomarkers in the healthcare sector is glucose. The monitoring of its levels is fundamental for the diagnosis and monitoring of diabetes, a disease affecting millions of people worldwide.[3] Commonly, early diagnosis and monitoring of this disease are achieved via testing the blood glucose with enzymatic-based test strips coupled with an electrochemical transducer. As previously mentioned, these enzymatic-based tests have proven to be very important in handling diabetes but they do have stability issues in challenging conditions and can suffer from degradation over time.[4] For this reason, the academic community have shifted their interest towards the development of innovative non-enzymatic alternatives. Although commercial non-enzymatic sensors are already emerging, MIPs-based sensors are also showing a lot of potential for the detection of glucose. This was the rationale for the literature review in **Chapter 2** on the advancements in MIP-based technologies for glucose monitoring. In this literature study, many MIP-based platforms have been critically evaluated and discussed from different points of view. Firstly, the different production methods employed for the synthesis of MIPs targeting glucose are discussed and summarized in order to identify the most promising approaches in terms of reliability as well as possibility of scaling up the fabrication process to an industrial scale. Different transducer technologies employed with MIP-platforms were then scrutinized and discussed. This has led to the identification of several promising MIP-based technologies, as well as the identification of some bottlenecks that still need to be addressed to reach the analytical market. In the following chapters of this thesis, we tried to build on the most promising approaches in previous research projects and overcome some of these bottlenecks to bring MIP-based glucose sensors closer to real-life applications.

After examining the glucose sensing field and, more specifically, the advancements and limitations of several MIP-based glucose sensors, the development of an innovative MIP-based thermal platform targeting glucose was presented in **Chapter 3**. In this chapter, different MIP compositions were tested in order to obtain a satisfactory glucose rebinding efficiency. After optimization of the imprinted polymer particles, these were integrated into a thermally conductive platform via a process of micro-contact deposition.[5] More specifically, a polyvinyl chloride (PVC) layer was spin coated onto a polished aluminium chip to obtain an Al-PVC substrate. Afterwards, the optimized MIP particles were then deposited onto the substrate by mechanical micro-contact to obtain a MIP-based thermally conductive platform. The thermal variations of the sensor platform after exposition to increasing glucose concentrations in buffer solutions were recorded and studied via HTM analysis and demonstrated a sensitivity well below the concentration regime in blood samples. Therefore, after an assessment of the MIP-HTM platform's selectivity, a real-life sample application was attained by analysing the response towards glucose in spiked human urine samples. The findings show that the sensor could provide a non-invasive, low-cost alternative to traditional enzyme-based methods for medical diagnostics. Furthermore, the sensor's sensitivity makes it fascinating to explore other potential applications, such as its use in food analysis or fermentation process monitoring.

The results achieved in glucose sensing illustrate that MIP-based sensors have proven to be effective tools for the detection of a wide variety of targets, making them potentially attractive in many fields of applications.[6] In **Chapter 4**, the production of a MIP-based platform for the detection of melamine was described. Melamine is a nitrogen-rich organic molecule often used as adulterant in milk and milk products,[7] is presented. This study was done to demonstrate that MIP-based thermal sensors can be used in a wide variety of application fields and not only healthcare. Therefore, a MIP-HTM sensor targeting melamine was developed using a similar fabrication method used in the previous chapter. Different MIP compositions were tested and the best MIP composition in terms of rebinding capabilities and specificity was employed as sensing element in a MIP-based platform. The sensing platform was fabricated using the same process employed in the previous chapter (micro-contact deposition of the MIP particles onto an Al-PVC layer). The sensitivity and selectivity of the platform was evaluated in CaCl_2 solutions with the HTM method. Finally, in order to prove the sensor's potential as tool for identifying illegal milk adulteration, the MIP-HTM platform was exposed to increasing concentrations of melamine in untreated milk samples. The sensitivity and linear range displayed in a challenging matrix such as milk, without any pre-treatment, demonstrated the potential of the developed platform in food safety analysis. This further confirms our initial hypothesis that MIPs are excellent alternatives to biological sensing elements that allow the resulting sensors to detect their target in matrices and environments where traditional sensors tend to fail. This opens up the possibility to further test the platform for different applications in the future.

The MIP-based sensor platforms introduced in the initial chapters of the thesis were prepared using a multi-step process in which different chemicals and machinery are necessary. Though the platforms have shown satisfying limits of detection in real-life samples, making them attractive alternatives to commercial analytical devices, the production process remains complex to translate into an industrial procedure. As a next step towards a more versatile and scalable procedure, in **Chapter 5** a literature review focusing on the different deposition methodologies for integrating MIPs into biosensor platforms is presented. To date, there is no single defined way for coupling a MIP with a specific transducer, with researchers employing a variety of methods. As a result, it is valuable to describe and distinguish the different ways in which MIPs can be deposited. Moreover, each approach, and possible modifications that can be carried out to integrate synthetic receptors for particular readout technologies, are highlighted and critically discussed from a commercial point of view. When analysing the different techniques employed, it is evident that the most valuable advancements in the area of receptor deposition will be those that allow the scaling, increased reproducibility, and eventual commercialization of synthetic receptors.

After studying the different deposition techniques reported in literature, a highly scalable, single step production process is employed to fabricate a MIP-functionalized screen-printed electrode for glucose detection. **Chapter 6** explores the possibility of integrating MIP particles onto a flexible electrode substrate by means of a direct screen-printing process. This process, described and discussed in **Chapter 5**, involves the screen-printing of a graphitic ink-MIP particles mixture directly onto a flexible substrate in order to form a MIP-modified screen-printed electrode (MIP-SPE). In **Chapter 6**, the sensitivity and selectivity towards glucose of the developed MIP-SPE platform was analysed in buffer solutions. Thanks to the sensor's design, the analysis were conducted with two different transducer technologies, the previously mentioned HTM as well as electrochemical impedance spectroscopy (EIS). Finally, the sensor's potential in healthcare diagnostics was demonstrated by means of HTM and EIS analysis in

urine samples at physiologically relevant concentrations. Moreover, when employing the platform with EIS as transducers, it could be used in combination with a handheld SPE connector, thus emphasizing the commercial potential of the sensor as single-shot, non-invasive tool for the determination of glucose in urine samples.

Overall, the research presented in **Chapters 3, 4, & 6** highlights the possibility of using MIPs as recognition elements in sensors for health and environmental applications. In this thesis MIPs were produced using a free-radical bulk polymerization process. Though this method is known to yield MIP particles in a low-cost and easily scalable manner, subsequent steps such as mechanical grinding and Soxhlet extraction make this production process slow and yields considerable polymeric waste. It is therefore recommended that future research efforts should be aimed at incorporating the newest trends in MIP synthesis in the sensor production process. This might overcome the disadvantages associated with bulk polymerizations. One can imagine using different MIP production methods, such as emulsion polymerization, precipitation polymerization, electro-polymerization or solid-phase MIP synthesis, as these involve easier and less cumbersome extraction processes and yield more homogenous particles.[8-10]

One of the benefits of MIPs in sensor devices is certainly their versatility in recognizing many different targets. In the future, innovative MIP-based platforms for other targets could be developed using similar production procedures presented in this thesis, in order to address emerging and pressing societal issues. For example, emerging clinical risks for public health, such as Per- and Poly-Fluorinated Alkyl Substances (PFAS) contaminations[11] or the pressing antimicrobial resistance[12] could be fought with the development of innovative MIP-biosensors for the detection of these targets in challenging matrices (soil and groundwater for PFAS, milk and other foodstuffs for antibiotics). Additional future studies should also investigate the possibility of utilizing different MIPs targeting diverse targets. This would allow the development of a multi-sensing platform and therefore critically enhance the real-life potential of MIP-based platforms. Another area that could be further explored is the employment of the developed MIP-platforms for glucose for the quantification of the sugar levels in different food products. It would be interesting to analyse the HTM or EIS responses of the MIP-based sensors when exposed to foods containing high level of sugar mixtures. Additionally, the developed MIP-technologies should be further tested and validated in a relevant environment in order to enhance the technology readiness level (TRL) and bring these sensors closer to commercialization. Innovative MIP-based glucose sensor could therefore be tested and validated in combination with traditional enzymatic sensors by healthcare professionals. These studies would allow researchers to understand possible areas of improvement for these sensors in order to bring them closer to commercialization and therefore to the end user. Similar validation studies could also be carried out with other MIP-based sensors for food safety and environmental applications by undertaking large in field testing analysis to evaluate reliability and possible drawbacks of the developed devices.

References Chapter 7

1. Crapnell, R.D.; Dempsey-Hibbert, N.C.; Peeters, M.; Tridente, A.; Banks, C.E. Molecularly Imprinted Polymer Based Electrochemical Biosensors: Overcoming the Challenges of Detecting Vital Biomarkers and Speeding up Diagnosis. *Talanta Open* 2020, 2, 100018, doi:10.1016/j.talo.2020.100018.
2. Scheller, F.W.; Yarman, A.; Bachmann, T.; Hirsch, T.; Kubick, S.; Renneberg, R.; Schumacher, S.; Wollenberger, U.; Teller, C.; Bier, F.F. Future of Biosensors: A Personal View. In *Advances in Biochemical Engineering/Biotechnology*; Springer Science and Business Media Deutschland GmbH, 2013; Vol. 140, pp. 1–28.
3. Vashist, S.K. Non-Invasive Glucose Monitoring Technology in Diabetes Management: A Review. *Anal. Chim. Acta* 2012, 750, 16–27, doi:10.1016/j.aca.2012.03.043.
4. Harris, J.M.; Reyes, C.; Lopez, G.P. Common Causes of Glucose Oxidase Instability in In Vivo Biosensing: A Brief Review. *J. Diabetes Sci. Technol.* 2013, 7, 1030–1038, doi:10.1177/193229681300700428.
5. Vandenryt, T.; van Grinsven, B.; Eersels, K.; Cornelis, P.; Kholwadia, S.; Cleij, T.; Thoelen, R.; De Ceuninck, W.; Peeters, M.; Wagner, P. Single-Shot Detection of Neurotransmitters in Whole-Blood Samples by Means of the Heat-Transfer Method in Combination with Synthetic Receptors. *Sensors* 2017, 17, 2701, doi:10.3390/s17122701.
6. Mahony, J.O.; Nolan, K.; Smyth, M.R.; Mizaikoff, B. Molecularly Imprinted Polymers—Potential and Challenges in Analytical Chemistry. *Anal. Chim. Acta* 2005, 534, 31–39, doi:10.1016/j.aca.2004.07.043.
7. Ritota, M.; Manzi, P. Melamine Detection in Milk and Dairy Products: Traditional Analytical Methods and Recent Developments. *Food Anal. Methods* 2018, 11, 128–147, doi:10.1007/s12161-017-0984-1.
8. Haupt, K. Molecularly Imprinted Polymers: The next Generation. *Anal. Chem.* 2003, 75, 376-A.
9. Zhang, H. Molecularly Imprinted Nanoparticles for Biomedical Applications. *Adv. Mater.* 2020, 32, 1806328, doi:10.1002/adma.201806328.
10. Poma, A.; Turner, A.P.F.; Piletsky, S.A. Advances in the Manufacture of MIP Nanoparticles. *Trends Biotechnol.* 2010, 28, 629–637, doi:10.1016/j.tibtech.2010.08.006.
11. Rodriguez, K.L.; Hwang, J.-H.; Esfahani, A.R.; Sadmani, A.H.M.A.; Lee, W.H. Recent Developments of PFAS-Detecting Sensors and Future Direction: A Review. *Micromachines* 2020, 11, 667, doi:10.3390/mi11070667.
12. Tse Sum Bui, B.; Auroy, T.; Haupt, K. Fighting Antibiotic-Resistant Bacteria: Promising Strategies Orchestrated by Molecularly Imprinted Polymers. *Angew. Chemie* 2022, 134, e202106493, doi:10.1002/ange.202106493.

Summary

This thesis investigates the employment of an innovative class of polymeric materials, the so-called molecularly imprinted polymers (MIPs) as synthetic recognition elements in in sensor arrays. These synthetic receptors have emerged as synthetic alternatives to biological sensing elements that are traditionally used in biosensing. MIPs have several advantages including their ability to detect various target molecules in challenging conditions and thus providing a viable option in biosensor development to natural receptors (e.g. antibodies or enzymes).

In **Chapter 1**, an introduction to biosensors is provided, followed by a discussion of the two main categories of biological sensing elements, namely natural and synthetic receptors. After a short overview of molecularly imprinted polymers (MIPs), a type of synthetic recognition element, and their potential incorporation into biosensor platforms, a comparison with their natural counterparts is presented.

Chapter 2 seeks to categorize and evaluate new developments in MIPs as recognition elements for glucose detection. This chapter critically examines the crucial field of glucose biosensing by comparing traditional devices based on enzymes capable of selectively oxidizing and thus detecting blood glucose with potential alternatives that use MIPs as synthetic receptor elements instead. To this end, the various manufacturing techniques and transducers used in the development and testing of MIP-based sensors for glucose detection are summarized and critically examined from a commercial standpoint. As a result, several published works were identified as potential starting points for the development of commercially viable MIP-based biosensors for glucose sensing and, more specifically, diabetes diagnosis and monitoring.

In **Chapter 3**, MIPs for glucose detection were synthesized, optimized, and characterized using different techniques, with the best MIP composition being used as sensing element in a thermally conductive layer. The MIP-based platform was manufactured by micro-contact stamping MIP particles onto an aluminium adhesive layer (Al-PVC), and its thermal response to increasing concentrations of glucose and other saccharides was investigated using a novel, low-cost transducer technology known as the Heat-Transfer Method, or HTM. The HTM results collected showed adequate sensitivity and selectivity towards glucose in buffer solutions. Finally, the platform demonstrated its real-world application for detecting glucose in human urine samples.

Chapter 4 investigates the possibility of using the same fabrication method used in the previous chapter to construct a MIP-HTM sensor for food safety analysis. A MIP targeting melamine, an adulterant molecule frequently found in milk products, was synthesized and optimized for this purpose. The optimized MIP particles were then deposited onto an Al-PVC layer as previously described, and the MIP-platform's HTM response after exposure to increasing concentrations of melamine was recorded and analysed. The sensor's sensitivity and selectivity were tested in CaCl_2 solutions to simulate milk samples. An HTM rebinding analysis of melamine was performed using untreated milk samples to demonstrate the promising potential of the developed MIP-based sensor for food safety analysis. The sensor displayed a limit of detection that was more than three times lower than the molecule's set legal limit in milk, demonstrating the platform's potential for identifying melamine-adulterated milk samples.

Chapter 5 dives into the various techniques used by researchers around the world for the deposition of imprinted polymers in sensor applications. This review categorizes deposition methods into mechanical, electrochemical, chemical, and vacuum deposition, and analyses and discusses the benefits and drawbacks of each method. In addition, a reflection on the most appropriate methods for mass production is made, emphasizing promising approaches reported in literature as well as the missing steps to the commercialization of MIP-based biosensors.

In **Chapter 6**, the emphasis is shifted to the possibility of fabricating a MIP-based platform for glucose sensing using a more appropriate large-scale deposition technique capable of producing MIP-based sensors in a single step, automated process. To reach this goal, a glucose sensing platform is manufactured by screen printing a mixture of MIP particles and graphitic ink resulting in a MIP-functionalized screen-printed electrode. (MIP-SPE). The sensor's design allowed for glucose rebinding analysis using two distinct readout technologies, the HTM method and electrochemical impedance spectroscopy. (EIS). Furthermore, the EIS configuration demonstrated the ability to use the MIP-SPE sensor as a dipstick sensor, highlighting the platform's potential for healthcare applications. In conclusion, the HTM and EIS responses of the sensor in untreated human urine samples indicated a practical application in the diagnosis and monitoring of glucose levels in diabetic patients.

Finally, in **Chapter 7**, the thesis' findings are critically examined and discussed, as well as a future outlook on the various potential improvements that could be explored in the MIP-sensing field in the coming years in order to achieve the first MIP-based commercial product in the analytical market.

**Development of Molecularly Imprinted
Polymer-based sensing platforms for health
and environmental applications**

-

**Ontwikkeling van detectieplatforms op
basis van Molecularly Imprinted Polymers
voor gezondheids en milieutoepassingen**

Summary (in Dutch)

In dit proefschrift wordt het gebruik van zogenaamde molecularly imprinted polymers (MIPs) als synthetische receptoren in biosensors onderzocht. Traditioneel worden biologische receptoren zoals antilichamen en enzyme gebruikt als receptor in biosensoren maar MIPs hebben voordelen ten opzicht van hun natuurlijke tegenhangers: ze zijn in staat om in extreme omstandigheden hun target te binden. In deze thesis wordt getracht om MIP sensoren dichter naar een tastbare toepassing te brengen.

In **Chapter 1** wordt een inleiding tot biosensoren gegeven, gevolgd door een bespreking van de twee belangrijkste categorieën detectie-elementen, namelijk natuurlijke en synthetische receptoren. Hierbij wordt uitgelegd hoe MIPs een voordeel kunnen bieden ten opzichte van bioreceptoren en in welk toepassingsveld ze een toegevoegde waarde kunnen bieden.

In **Chapter 2** wordt een van deze toepassingsvelden nader onderzocht. Aan de hand van een uitgebreide literatuurstudie wordt nagegaan in welke mate het al mogelijk is om MIPs te gebruiken als receptor in glucose sensoren. Traditionele gluco meters maken gebruik van enzymen die glucose oxideren, hetgeen leidt tot een electrochemisch signaal. Deze sensoren zijn snel, goedkoop en makkelijk te gebruiken en zijn daarom ook een commercieel succesverhaal gebleken in diabetes management. Maar ze hebben ook nadelen waardoor niet-enzymatische alternatieven ontwikkeld worden. MIP sensoren zijn hier een voorbeeld van. Dit academisch veld wordt in deze studie samengevat en er wordt geanalyseerd welke MIP synthese aanpak het meest veelbelovend is en hoe ze best in sensoren worden verwerkt. De uitkomst van deze analyse vormt het uitgangspunt van de studie in hoofdstuk 3.

In **Chapter 3** werd een MIP sensor ontwikkeld voor het detecteren van glucose in urine stalen. Hiertoe werden MIPs gesynthetiseerd, geoptimaliseerd en gekarakteriseerd. Het beste recept werd gebruikt om MIPs te produceren die fungeerden als receptor element in een thermische biosensor. De MIP deeltjes werden daartoe in een PVC laag gestempeld. Vervolgens werden de MIP-gebaseerde sensor chips blootgesteld aan toenemende concentraties glucoses (en andere suikers). De experimenten in hoofdstuk 3 dat het selectief binden van glucose aan de MIPs leidt tot een verandering van de thermische weerstand van de chip, een effect dat kan gebruikt worden om MIPs in klinisch relevante concentraties te detecteren in biologische stalen (urine).

In **Chapter 4** wordt nagegaan of het MIP-HTM platform ook gebruikt kan worden in ander toepassingsvelden voor de detectie van andere moleculen. Hiertoe werd een vergelijkbare sensor gemaakt voor het opsporen van melamine in melkproducten. In de zuivelindustrie wordt het proteïnegehalte van producten gemeten als onderdeel van de kwaliteitscontrole. Melamine kan deze testen om de tuin leiden waardoor het lijkt dat de producten rijk zijn aan proteïnen terwijl dat niet het geval is. Daarnaast is melamine ook schadelijk van de gezondheid. Een sensor die dit kan opsporen, zou dus van grote waarden kunnen zijn in het kader van voedselveiligheid. Hiertoe werden MIPs ontwikkeld en in een sensor geïntegreerd op een vergelijkbare manier als voor de glucose sensor in het vorige hoofdstuk. HTM werd opnieuw als thermische uitlezing gebruikt en na metingen in zowel calcium buffer als melk werd vastgesteld dat de sensor wel degelijk in staat is om snel en eenvoudig de aanwezigheid van melamine vast te stellen in melk. Traditionele biosensoren kunnen dergelijke analyse enkel uitvoeren na voorbehandeling van de stalen, de MIP HTM sensor kan dit meteen in volle melk. Een enorm voordeel dat de mogelijkheid opent voor additioneel onderzoek naar andere toepassingsgebieden.

In **Chapter 5** wordt nagegaan of de MIP HTM sensor op een andere manier zou kunnen worden vervaardigd waardoor deze ook geschikt is voor massaproductie. Daartoe werd een literatuurstudie uitgevoerd naar een van de voornaamste struikelblokken in het commercialiseren van MIPs: het produceren van chips met een homogene hoeveelheid aan MIPs. Hiertoe werd een literatuurstudie uitgevoerd naar verschillende methoden om MIPs af te zetten op sensor chips. De meest veelbelovende methoden worden hierbij uitgelicht en van naderbij onderzocht.

In **Chapter 6** wordt de kennis uit de literatuurstudie in het vorige hoofdstuk, in de praktijk gebracht. Een van de meest veelbelovende depositiemethoden is immers het mengen van MIPs met een ink om dit mengsel vervolgens door zeefdrukken (screen printen) in een dunne laag met een welbepaald patroon af te zetten op de sensor chips. In dit hoofdstuk werden de eerder ontwikkelde glucose MIPs op deze manier afgezet op aluminium chips voor de detectie van glucose met behulp van zowel HTM als impedantie. Vooral de combinatie met impedantie is hierbij interessant omdat het een commerciële technologie betreft die gecombineerd kan worden met de massa productie van screen-printed electrodes (SPEs) en adapters die toelaten deze SPEs als dipsticks te gebruiken. Bovendien zijn impedantie analyzers doorgaans handheld waardoor MIP sensoren weer een stukje dichterbij komen bij implementatie in de gezondheidszorg, het originele doel van de thesis.

Ten slotte worden in **Chapter 7** de bevindingen van het proefschrift kritisch onderzocht en besproken, alsmede een toekomstperspectief voor de verschillende potentiële verbeteringen die de komende jaren op het gebied van MIP-sensoren kunnen worden onderzocht om te komen tot het eerste op MIP gebaseerde commerciële product op de analytische markt.

Impact

The first chapters of this thesis have primarily concentrated on the scientific advancements of molecularly imprinted polymers (MIPs) and MIPs-based sensor platforms. However, it is also critical to emphasize the impact of the presented findings on the healthcare and food safety sectors and society in general. The research findings presented look into various methodologies that could be used to develop sensitive, low-cost and user-friendly MIP-based sensors to address a variety of societal issues.

Glucose, for example, is a crucial biomarker for global healthcare systems that millions of diabetic patients monitor on a daily basis.[1,2] Diabetes is a worldwide condition that can have devastating consequences if undiagnosed or untreated. This condition is tracked by analysing blood glucose levels using easily accessible enzymatic-based assays (**Figure 1**). Though these devices are considered the holy grail of biosensors, MIP-platforms can overcome some disadvantages associated with enzymatic stability in specific conditions.



Figure 1 Representation of a commercial enzymatic glucose sensor used to measure blood glucose.[3]

Therefore, in **Chapter 3**, a study on the development, optimization, and analysis of a low-cost, non-invasive MIP-based glucose platform coupled with an innovative readout technology, as well as a proof-of-concept in human urine samples, is presented. Urine is advantageous over blood analysis as it can be obtained through non-invasive sampling, while retaining high correlation with glucose blood levels.[3,4] It also lowers the threshold for e.g. children that suffer from diabetes but might be scared of the Lancet device and are too young for having a continuous monitoring implant. Furthermore, MIP-based sensing might offer a non-enzymatic alternative that allows for measuring in challenging circumstances in e.g. low-income countries where sensor stability is an issue.

Another societal problem that could benefit from the advantageous properties of MIPs in biosensor arrays is food safety analysis.[5] Food safety describes the circumstances and routines that maintain food quality in order to avoid contamination and food-borne illnesses. Melamine, a nitrogen-rich organic molecule, has infamously received global attention in the last two decades for its improper use in milk and milk products. The adulteration of milk products with melamine in order to falsify the

protein content of these foods resulted in a 2008 incident in China in which over 50000 infants were hospitalized and diagnosed with melamine-related urinary stones.[6] As a result, regulators around the globe have set a melamine limit of 2.5 mg/kg in dairy products[6] Sensors that enable low-cost routine screening of dairy products would enable consumers and industrial stakeholders at various points along the dairy production value chain to detect melamine adulteration quickly, This in turn would considerably reduce its negative effects on public healthcare systems. The results presented in **Chapter 4** aim to show how a low-cost MIP-based sensor coupled with an appropriate readout technology can detect adulterated milk products in a regulatory regime, offering a very promising tool for both end-users and the food industry.

Scalability of the manufacturing process is a critical aspect of biosensor platforms that must be addressed in order for them to reach the market and thus the end user. In reality, many MIP-based research works still struggle with this translation, resulting in a limited availability of MIP-products for the end user. After a literature study presented in **Chapter 5** on the different deposition methods used to integrate MIP in sensing platforms, the research study described in **Chapter 6** focuses on the development of a MIP-based glucose platform using a one-step, easily scalable production process. The platform's results show that the manufacturing process produced a MIP-based sensor capable of detecting glucose in human urine samples, demonstrating its potential as alternative for commercial glucose test strips.

In the work presented in **Chapter 6**, we attempted to demonstrate how a screen-printed MIP-based electrode can be used for the non-invasive detection of glucose in human urine samples. The aim of this study was to optimise the deposition methods used in **Chapter 3** and, above all, to demonstrate the potential of the modified electrode in the diagnosis and monitoring of diabetes. However, after the publication of this study, we were contacted by BASF Vegetable Seeds to try to implement our MIP-based SPE sensor for another type of application of great commercial and social importance. The platform developed in **Chapter 6** could in fact be a perfect tool for detecting glucose in food samples, such as tomatoes. As already mentioned, traditional enzymatic devices using glucose oxidase (GOx) show a decrease in stability and activity at acidic pH.[7] Considering that several published works report pH ranges in tomatoes between 3.9 and 4.9,[8,9] this would inevitably hamper the accuracy and stability of measurements. Therefore, in order to successfully and reliably analyse the glucose content in different tomato types, a different enzymatic assay (e.g. glucose hexokinase) or a non-enzymatic sensor must be used. Therefore, the MIP-SPE platform realised in **Chapter 6** could be used for the fast and reliable detection of sugar in tomatoes and many other food samples, thus showing the wide commercial and societal potential of this work.

The research works presented on this thesis provide additional knowledge on the MIP-sensing field whilst focusing on societal needs. For this reason, in this works, real-life sample applications have been demonstrated by analysing the content of the different analysed targets (glucose and melamine) in untreated relevant matrices, such as human urine and milk samples. Notwithstanding, other characteristics of the developed platforms still need to be evaluated and optimized in order to move these technologies even closer to commercialisation and thus to the end-user. For this reason, these findings have been showcased and discussed with many international experts in the sensing field in different international conferences. More specifically, these works have been presented at the following events:
2022 Material Research Society Spring Meeting (Honolulu, May 2022), Engineering of Functional

Interfaces 2022 Meeting (Maastricht, July 2022), 9th Kurt Schwabe symposium (Graz, July 2022), American Chemical Society Fall 2022 Meeting (Chicago, August 2022) and at NWO Chains 2022 conference (Veldhoven, September 2022).

Despite the fact that MIPs have many benefits as compared to their natural counterparts, it is essential to note that they do not represent a commercial alternative in the analytical market at this moment, and thus for the end user. Since their discovery, the MIP-sensing field has seen many advances in terms of sensitivity and selectivity. However, some important aspects still remain unaddressed before this product can reach the market. Several promising MIP-based products have emerged in recent years; for example, a company called MIP Discovery[10] recently commercialized nanoMIPs for the detection of COVID-19 and illicit drugs. The company Affinise[11] has also created and commercialized other MIP-based extraction products. Furthermore, other businesses and start-ups, such as SixthWave Innovations Inc.,[12] Sensip-dx,[13] or Affinomer,[14] are getting involved in and concentrating on the use of MIPs for target detection and extraction. This growing commercial interest indicates that it is only a matter of time before MIP-based technologies are going to make a significant impact in the healthcare market and aid in the battle against current and future societal challenges. During the course of this thesis, I started to collaborate with several of these companies to ensure that the chance that our sensors could once reach the market and actually impact society is maximized.

References Impact paragraph

1. Shrivastava, S.R.; Shrivastava, P.S.; Ramasamy, J. Role of Self-Care in Management of Diabetes Mellitus. *J. Diabetes Metab. Disord.* 2013, 12, 14, doi:10.1186/2251-6581-12-14.
2. van Enter, B.J.; von Hauff, E. Challenges and Perspectives in Continuous Glucose Monitoring. *Chem. Commun.* 2018, 54, 5032–5045, doi:10.1039/C8CC01678J.
3. Chen, J.; Guo, H.; Yuan, S.; Qu, C.; Mao, T.; Qiu, S.; Li, W.; Wang, X.; Cai, M.; Sun, H.; et al. Efficacy of Urinary Glucose for Diabetes Screening: A Reconsideration. *Acta Diabetol.* 2019, 56, 45–53, doi:10.1007/s00592-018-1212-1.
4. Morris, L.R.; McGee, J.A.; Kitabchi, A.E. Correlation between Plasma and Urine Glucose in Diabetes. *Ann. Intern. Med.* 1981, 94, 469–471, doi:10.7326/0003-4819-94-4-469.
5. Cao, Y.; Feng, T.; Xu, J.; Xue, C. Recent Advances of Molecularly Imprinted Polymer-Based Sensors in the Detection of Food Safety Hazard Factors. *Biosens. Bioelectron.* 2019, 141, 111447, doi:10.1016/j.bios.2019.111447.
6. Li, Q.; Song, P.; Wen, J. Melamine and Food Safety: A 10-Year Review. *Curr. Opin. Food Sci.* 2019, 30, 79–84, doi:10.1016/j.cofs.2019.05.008.
7. Hwang, D.-W.; Lee, S.; Seo, M.; Chung, T.D. Recent Advances in Electrochemical Non-Enzymatic Glucose Sensors – A Review. *Anal. Chim. Acta* 2018, 1033, 1–34, doi:10.1016/j.aca.2018.05.051.
8. Davies, J.N.; Hobson, G.E. The Constituents of Tomato Fruit — the Influence of Environment, Nutrition, and Genotype. *C R C Crit. Rev. Food Sci. Nutr.* 1981, 15, 205–280, doi:10.1080/10408398109527317.
9. Petró-Turza, M. Flavor of Tomato and Tomato Products. *Food Rev. Int.* 1986, 2, 309–351, doi:10.1080/87559128609540802.
10. We Design Recognition. - MIP Discovery Available online: <https://mipdiscovery.com/> (accessed on 6 April 2023).
11. Ready-to-Use Kits SPE and MIPs - Affinisep Available online: <https://www.affinisep.com/products/ready-to-use-kits-spe-and-mips/> (accessed on 6 April 2023).
12. MIPs – Sixth Wave Innovations Inc. Available online: <https://sixthwave.com/mips/> (accessed on 6 April 2023).
13. Sensip-Dx | Food Quality Available online: <https://www.sensipdx.com/> (accessed on 6 April 2023).
14. Affinomer Available online: <https://affinomer.com/> (accessed on 6 April 2023).

Curriculum Vitae

Manlio Caldara obtained a master's degree cum laude in pharmacy from the University of Camerino, Italy, in 2019. During his studies, he participated in different research projects focused on the fields of organic synthesis and biological evaluation of novel small organic molecules as antibacterial and LpxC inhibitors antibiotics. Since March 2020, he has started his Ph.D. appointment at the Sensor Engineering Department at Maastricht University. His research interests include the synthesis of functional polymeric materials as recognition elements in chemical/biological sensors, chemical and electrochemical readout technologies, and the development of novel sensing technologies that can be used for healthcare and environmental applications.

List of Publications

Included in this thesis:

- **Caldara, M.***; Kulpa, J.; Lowdon, J.W.; Cleij, T.J.; Diliën, H.; Eersels, K.; van Grinsven, B. Recent Advances in Molecularly Imprinted Polymers for Glucose Monitoring: From Fundamental Research to Commercial Application. *Chemosensors* 2023, *11*, 32. <https://doi.org/10.3390/chemosensors11010032>
- **Caldara, M.***; Lowdon, J. W., Rogosic, R., Arreguin-Campos, R., Jimenez-Monroy, K. L., Heidt, B., Tschulik, K., Cleij, T. J., Diliën, H., Eersels, K., & van Grinsven, B. Thermal Detection of Glucose in Urine Using a Molecularly Imprinted Polymer as a Recognition Element. *ACS Sensors* 2021, *6*(12), 4515–4525. <https://doi.org/10.1021/acssensors.1c02223>
- **Caldara, M.***; Lowdon, J.W.; Royakkers, J.; Peeters, M.; Cleij, T.J.; Diliën, H.; Eersels, K.; van Grinsven, B. A Molecularly Imprinted Polymer-Based Thermal Sensor for the Selective Detection of Melamine in Milk Samples. *Foods* 2022, *11*(18), 2906. <https://doi.org/10.3390/foods11182906>
- **Caldara, M.**; van Wissen, G.; Cleij, T.J.; Diliën, H.; van Grinsven, B.; Eersels, K.; Lowdon, J.W.* Deposition Methods for the Integration of Molecularly Imprinted Polymers (MIPs) in Sensor Applications. *Advanced Sensor Research* 2023, 2200059. <https://doi.org/10.1002/adsr.202200059>
- **Caldara, M.***; Lowdon, J.W.; van Wissen, G.; Garcia-Miranda Ferrari, A.; Crapnell, R.D.; Cleij, T.J.; Diliën, H.; Banks, C.E.; Eersels, K.; van Grinsven, B. Dipstick sensor based on molecularly imprinted polymer-coated screen-printed electrodes for the single-shot detection of glucose in urine samples - From fundamental study towards point-of-care application. *Advanced Materials Interfaces*, 2023, 2300182. <https://doi.org/10.1002/admi.202300182>

Co-author (not part of this thesis):

- Arreguin-Campos, R.*; Frigoli, M.; **Caldara, M.**; Crapnell, R.D.; Ferrari, A.G.-M.; Banks, C.E.; Cleij, T.J.; Diliën, H.; Eersels, K.; van Grinsven, B. Functionalized Screen-Printed Electrodes for the Thermal Detection of Escherichia Coli in Dairy Products. *Food Chem.* 2023, *404*, 134653, doi:10.1016/j.foodchem.2022.134653.
- Tabar, F.A.*; Lowdon, J.W.; **Caldara, M.**; Cleij, T.J.; Wagner, P.; Diliën, H.; Eersels, K.; van Grinsven, B. Thermal Determination of Perfluoroalkyl Substances in Environmental Samples Employing a Molecularly Imprinted Polyacrylamide as a Receptor Layer. *Environ. Technol. Innov.* 2023, *29*, 103021, doi:10.1016/j.eti.2023.103021.
- Frigoli, M.*; Lowdon, J.W.; **Caldara, M.**; Arreguin-Campos, R.; Sewall, J.; Cleij, T.J.; Diliën, H.; Eersels, K.; van Grinsven, B. Thermal Pyocyanin Sensor Based on Molecularly Imprinted Polymers for the Indirect Detection of Pseudomonas Aeruginosa. *ACS Sensors* 2023, doi:10.1021/acssensors.2c02345.
- Lowdon, J.W.*; Ishikura, H.; Kvernenes, M.K.; **Caldara, M.**; Cleij, T.J.; van Grinsven, B.; Eersels, K.; Diliën, H. Identifying Potential Machine Learning Algorithms for the Simulation of Binding Affinities to Molecularly Imprinted Polymers. *Computation* 2021, *9*, 103, doi:10.3390/computation9100103.

- Arreguin-Campos, R.; Eersels, K.*; Lowdon, J.W.; Rogosic, R.; Heidt, B.; **Caldara, M.**; Jiménez-Monroy, K.L.; Diliën, H.; Cleij, T.J.; van Grinsven, B. Biomimetic Sensing of Escherichia Coli at the Solid-Liquid Interface: From Surface-Imprinted Polymer Synthesis toward Real Sample Sensing in Food Safety. *Microchem. J.* 2021, 169, 106554, doi:10.1016/j.microc.2021.106554.
- Rogosic, R.*; Heidt, B.; Passariello-Jansen, J.; Bjornor, S.; Bonni, S.; Dimech, D.; Arreguin-Campos, R.; Lowdon, J.; Jimenez Monroy, K.L.; **Caldara, M.**; Eersels, K.; van Grinsven, B.; Cleij, T.J.; Diliën, H. Modular Science Kit as a Support Platform for STEM Learning in Primary and Secondary School. *J. Chem. Educ.* 2021, 98, 439–444, doi:10.1021/acs.jchemed.0c01115.
- Lowdon, J.W.*; Eersels, K.; Arreguin-Campos, R.; Caldara, M.; Heidt, B.; Rogosic, R.; Jimenez-Monroy, K.L.; Cleij, T.J.; Diliën, H.; van Grinsven, B. A Molecularly Imprinted Polymer-Based Dye Displacement Assay for the Rapid Visual Detection of Amphetamine in Urine. *Molecules* 2020, 25, 5222, doi:10.3390/molecules25225222.
- Hoff, K.; Mielniczuk, S.; Agoglitta, O.; Iorio, M.T.; **Caldara, M.**; Bülbül, E.F.; Melesina, J.; Sippl, W.; Holl, R.* Synthesis and Biological Evaluation of Triazolyl-Substituted Benzyloxyacetohydroxamic Acids as LpxC Inhibitors. *Bioorganic Med. Chem.* 2020, 28, 115529, doi:10.1016/j.bmc.2020.115529.

